The Institute of Paper Chemistry

Appleton, Wisconsin

Doctor's Dissertation

The Influence of Temperature Test Frequency and Moisture Sorption on the Viscoelastic Moduli of Cellulose

Bernard J. Berger

June, 1988

THE INFLUENCE OF TEMPERATURE TEST FREQUENCY AND MOISTURE SORPTION ON THE VISCOELASTIC MODULI OF CELLULOSE

A thesis submitted by

Bernard J. Berger

B.S. 1983, Western Michigan University

M.S. 1985, Lawrence University

in partial fulfillment of the requirements
of The Institute of Paper Chemistry
for the degree of Doctor of Philosophy
from Lawrence University
Appleton, Wisconsin

June, 1988

TABLE OF CONTENTS

ABSTRACT

Three ultrasonic techniques (30-60 Hz) were used to measure viscoelastic parameters for several papers and cellophanes as a function of temperature and moisture. Mass specific viscoelastic modulus and loss tangent measurements were made under equilibrium and nonequilibrium moisture conditions. The study was unique in measuring moisture and temperature in a nonequilibrium moisture environment. Temperature measurements are important in helping to compensate for sample temperature changes caused by heat of sorption or evaporative cooling. When compared at equal moistures and temperatures, modulus and loss tangent data obtained under nonequilibrium moisture conditions were identical to those at equilibrium. This result is contrary to previously published data, where transient increases in loss tangent and decreases in modulus were found in wool and cellulose to accompany sorptive and desorptive conditions. A low frequency (1 Hz) cyclic loading technique was also employed to measure the modulus and loss tangent of samples in transient moisture states. The published transient minimums in modulus were again absent. However, the transient loss tangent maximums reported previously were found in all samples undergoing sorption and desorption. Between the temperatures of 25 and 85°C linear moisture-specific modulus and temperature-specific modulus relations were found for all samples over the moisture range studied. These linear relations simplify the calculations required to convert on-line ultrasonic modulus measurements to a common temperature-moisture basis. Ultrasonic and low frequency data obtained in the present study under equilibrium moisture conditions are compared to previously published data. The influence of moisture, temperature, and frequency on the measured viscoelastic parameters are discussed in terms of thermal relaxation processes. Data obtained during moisture sorption and desorption are also discussed in relation to the published transient decreases in modulus and increases in loss tangent.

INTRODUCTION

It is possible to nondestructively measure elastic moduli of paper using ultrasonic techniques. These measurements are important in that elastic moduli are fundamental mechanical parameters and have been found to relate to many end-use strength properties such as tensile strength[1] and compressive strength.[2] The techniques are in the stage of development where they can now be used to acquire data on-line.[3] This is a dramatic breakthrough in that such techniques make real time mechanical integrity evaluation possible. No longer will the paper maker have to wait for hours while samples from the already manufactured reel are conditioned and tested to determine in retrospect whether mechanical properties are adequate.

However, with new technologies come new challenges. It is a well known fact that elastic moduli of paper and other viscoelastic polymers are affected by moisture and temperature. Also, these variables can fluctuate considerably near the reel of the paper machine where on-line ultrasonic readings are taken. Therefore, in order for ultrasonic data to be of practical use they must be converted to a standard temperature-moisture condition. Very little data are available relating the effects of moisture and temperature to the ultrasonic moduli, especially at temperatures typically encountered on-line.

The above situation may be complicated further by nonequilibrium moisture effects. Evidence from several sources suggests that a transient decrease in modulus and a transient increase in loss tangent occur in cellulose during non-equilibrium moisture conditions.[27,47,66,67,69] Similar phenomena are reported in wool.[57-65,68,69] In other words, paper undergoing sorption or desorption will

have a lower modulus and a higher loss tangent at a given moisture content relative to an identical sample, at the same temperature and moisture content, under equilibrium moisture conditions. Such an effect would be important to on-line modulus conversions, because sample moisture at the reel is not at equilibrium.

The objective of this thesis is twofold; to obtain a larger data base in an attempt to more thoroughly understand moisture-temperature-modulus relations under equilibrium conditions and to study the reported transient decrease in modulus and/or increase in loss tangent accompanying nonequilibrium moisture conditions. The nondestructive ultrasonic techniques developed at the IPC and a low frequency mechanical cycling technique were utilized in this study.

BACKGROUND AND LITERATURE REVIEW

Some background information is presented to ensure that the reader is familiar with the pertinent literature and terminology. In order to accomplish this task, the text is divided into three major parts: a review of viscoelasticity and thermal transition theory, an equilibrium literature review, and a nonequilibrium literature review.

VISCOELASTICITY AND THERMAL TRANSITIONS

Paper is a viscoelastic material and has properties between those of an elastic solid and those of a viscous liquid. At small strains, stress and strain are related linearly. This means that the total strain in a sample is a linear combination of the separate strain responses to all of the previously applied stresses. Unlike elastic solids, viscoelastic solids have a time dependent strain response when stressed, and the strain in a sample depends not only on the stress but also on the time at which the stress is applied.

Insight concerning viscoelastic behavior can be obtained by considering the molecular level. The noncrystalline regions of polymers can be thought of as having a distribution of molecular conformations. Within conformations, a range of energy states exists. These ranges are small, however, compared to the energy barriers between conformations, which are much greater than kT (k = Boltzman's constant, T = absolute temperature). When a sample is subjected to a small stress, shifts in the energy states proportional to the stress occur. Those states favored by the stress decrease in energy, while the states not conforming well to the stress shift to higher energy levels. These shifts, within the potential wells of conformations, are very rapid and comprise the elastic

response of the sample. They also result in a shift between conformations toward the ones with more favorable energy states. This redistribution takes time, however. In order for a conformational change to occur, sufficient energy from random thermal motion must be absorbed to surmount the potential barrier that exists between conformations. The redistribution between conformations following a step stress change occurs at an exponentially decreasing rate. Ward, using Eyring's absolute rate theory,[4] showed that the relaxation time, τ, for this redistribution between two conformations is related to the absolute temperature, T, and the smaller of the two free energy differences, G2, between the conformation states, and the activated states at the top of the energy barrier by a constant A (see Fig. 1).

$$1/\tau = A\ell^{-\Delta G2/kT} \tag{1}$$

Making plausible assumptions concerning the activated and conformation states, Eq. (1) can be approximated as:[5]

$$1/\tau \approx 2\nu\ell^{-Vo/kT} \tag{2}$$

where the activation energy, Vo, is the height of the energy barrier and ν is the frequency of the molecular vibration responsible for the escape from the potential well. In summary, when a viscoelastic solid is stressed, an instantaneous elastic strain response due to energy shifts within conformations is followed by a time dependent strain resulting from changes between conformations. The rate of interconformational changes depends exponentially on the temperature of the sample and the activation energy of the molecular relaxation.

For a linear viscoelastic solid, sinusoidal loading produces a sinusoidal strain response. However, because of the time dependency of conformational

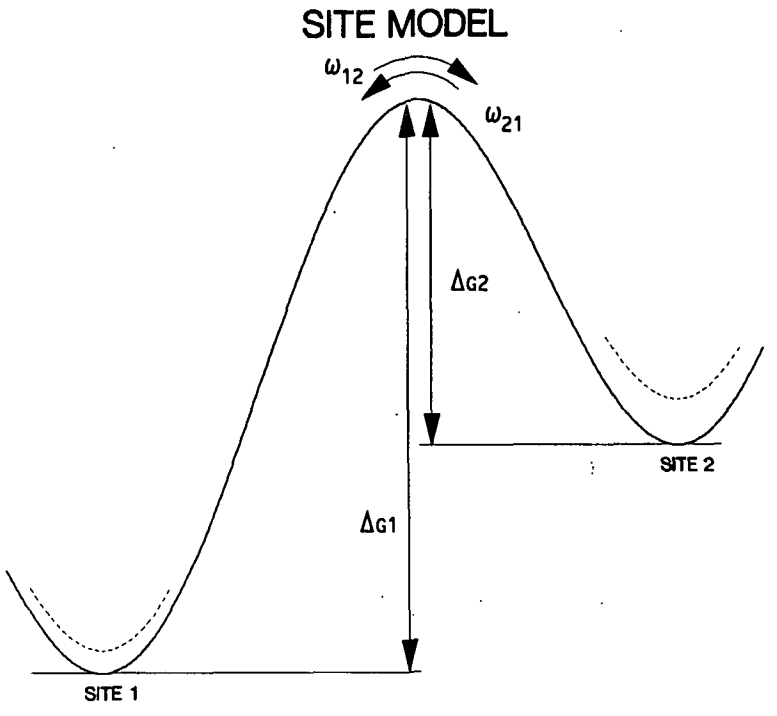

Figure 1. A model of the energy barrier between molecular sites in a hypothetical polymer.

changes, the strain will lag the stress by a certain angle depending on the frequency. Therefore:

$$\varepsilon(t) = \varepsilon_o \sin\omega t + \varepsilon_s \tag{3}$$

$$\sigma(t) = \sigma_o \sin(\omega t+\delta) + \sigma_s \tag{4}$$

where ε_o is the strain amplitude, ε_s the strain offset, δ_o the stress amplitude, σ_s the stress offset, ω the angular frequency, t the time, and δ the phase lag. Expanding Eq. (4)

$$\sigma(t) = \sigma_o \sin\omega t\cos\delta + \sigma_o \cos\omega t\sin\delta + \sigma_s \tag{5}$$

Thus, the stress consists of two components, one in phase and one out of phase with the strain. If we define

$$E' = (\sigma_o/\epsilon_o)\cos\delta = \text{storage modulus} \quad (6)$$

and

$$E'' = (\sigma_o/\epsilon_o)\sin\delta = \text{loss modulus} \quad (7)$$

then

$$\sigma(t) = \epsilon_o E'\sin\omega t + \epsilon_o E''\cos\omega t + \sigma_s \quad (8)$$

Straining a viscoelastic sample requires energy. Some of this energy is recovered when the strain is released, while some of the energy is lost to the system, usually in the form of heat. For later discussions it will be useful to define a parameter, S, which is a relative measure of the energy stored at maximum strain (see Fig. 2).

$$S = 1/2(\sigma_{\epsilon max} - \sigma_{\epsilon min})(\epsilon_{max} - \epsilon_{min})$$
$$= 1/2(2\sigma_o\cos\delta)(2\epsilon_o) \quad (9)$$

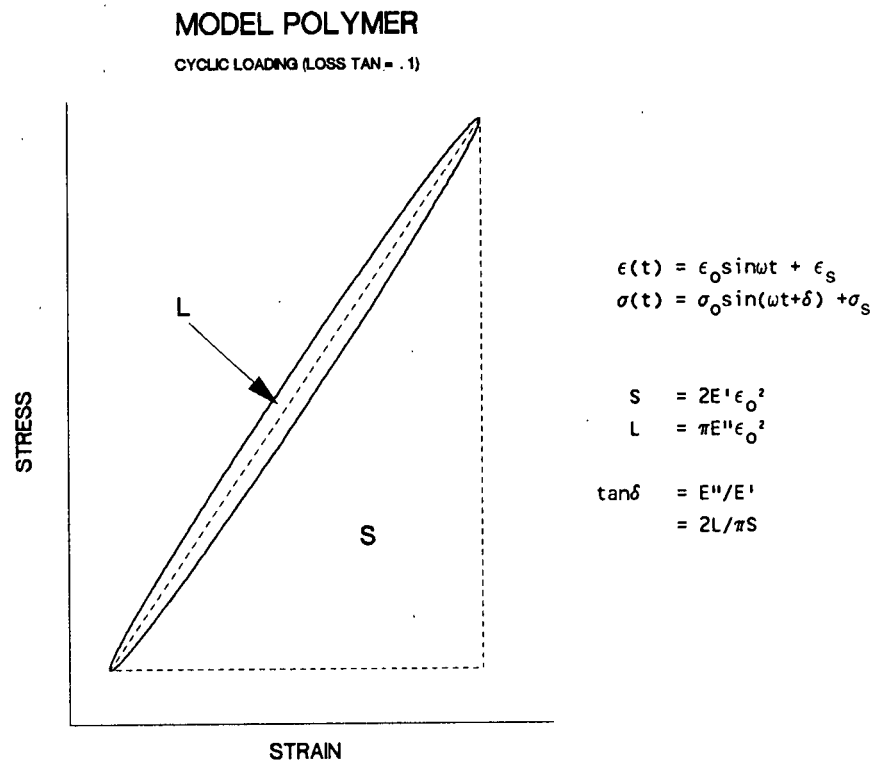

Figure 2. A model of the stress-strain relation in a viscoelastic material loaded sinusoidally.

where $\sigma_{\varepsilon max}$ and $\sigma_{\varepsilon min}$ are the stresses at ε_{max} and ε_{min}, respectively. Using Eq. (6), Eq. (9) can be written as:

$$S = 2E'\varepsilon_o^2 \tag{10}$$

If δ is not zero, some energy is dissipated during each cycle. This energy, L, is calculated as:

$$\begin{aligned} L &= \oint \sigma d\varepsilon \\ &= \int_0^{2\pi/\omega} [\varepsilon_o(E'\sin\omega t + E''\cos\omega t)\omega\varepsilon_o\cos\delta t]dt \\ &= \pi E''\varepsilon_o^2 \end{aligned} \tag{11}$$

The fact that E' appears in the solution for the energy stored in a cycle, while E" appears in the dissipated energy solution explains the choice of storage and loss modulus for the respective names. Storage modulus is usually considerably larger than the loss modulus and is often simply referred to as the modulus, E.

The tangent of the phase lag (loss tangent) is also discussed quite frequently in conjunction with dynamic mechanical tests. It is defined as the ratio of the loss to the storage modulus.

$$\tan\delta = E''/E' \tag{12}$$

Notice that tanδ can be expressed in terms of the previously defined parameters, L and S.

$$\begin{aligned} L/S &= \pi E''\varepsilon_o^2/2E'\varepsilon_o^2 \\ &= (\pi/2)\tan\delta \end{aligned} \tag{13}$$

In a perfectly elastic solid, δ and hence $\tan\delta$, E", and L are all zero. Note that during subsequent discussions, parameters akin to the modulus, such as stiffness and rigidity, are mentioned quite frequently as are those similar to loss tangent, such as logarithmic decrement, loss angle, damping, and internal friction. Keep in mind that what is said about one parameter applies equally to the related parameters, at least qualitatively.

It is important to remember that E', E", and δ are functions of test frequency. Frequency effects are most easily understood by considering a single pronounced transition. If test frequency is much greater than $1/\tau$ the time dependent relaxation won't be able to keep up, stress and strain will be in phase, δ will be small, and a large "unrelaxed" storage modulus will result. Stress and strain are again in phase and δ small at frequencies far below $1/\tau$ where the relaxation has plenty of time to occur. In this case, however, the occurrence of the relaxation will result in a lower "relaxed" storage modulus. In both of these cases, the material responds elastically. At intermediate frequencies on the order of $1/\tau$, the phase angle between the strain and the stress will go through a maximum, storage modulus will have intermediate values, and loss modulus and loss tangent will also go through maxima. This can be seen in Fig. 3 for a single relaxation modeled using a standard linear solid.[4]

The frequency of maximum loss tangent, f_o is approximately equal to $1/\tau$. If Eq. (2) is valid, then f_o is a function of temperature, and an Arrhenius plot of $\ln(f_o)$ vs. $1/T$ should result in a straight line with a slope of $-Vo/k$. Notice that the change in f_o with T depends upon the activation energy, and that the temperature of a high activation energy relaxation is less sensitive to frequency than a low activation energy relaxation. The relationship between frequency (time) and temperature therefore allows thermal transitions to be

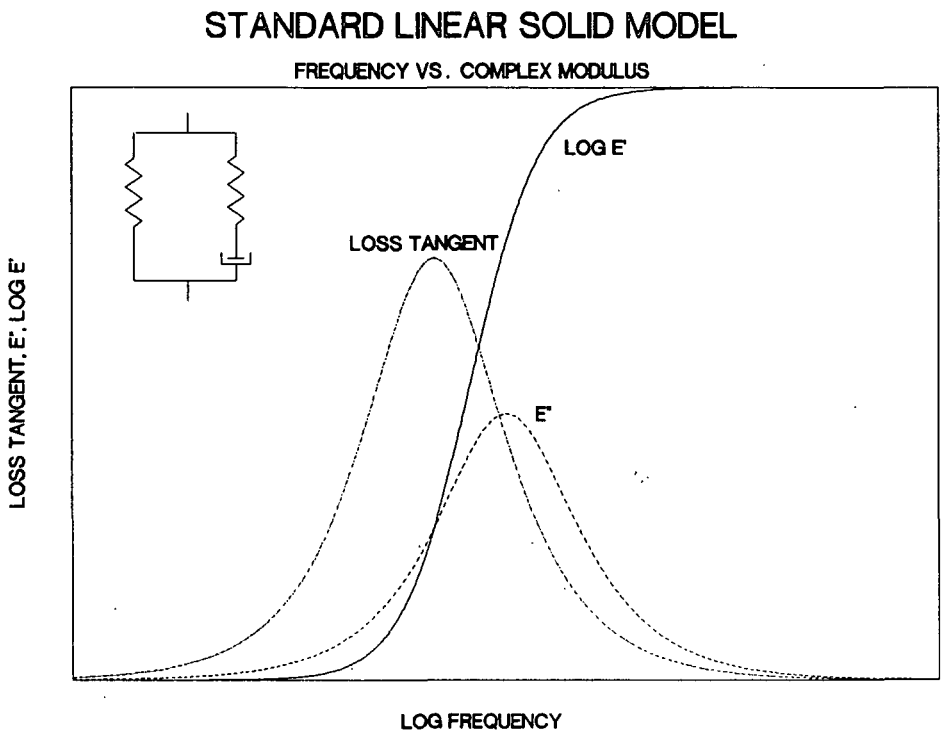

Figure 3. Loss tangent, loss modulus, and log storage modulus-log frequency relations showing a single thermal relaxation of a viscoelastic material modeled as a standard linear solid.

observed by varying the temperature at a constant frequency. Of course, in polymers there is usually more than one thermal transition, each with its own activation energy. Actually, individual transitions also have a limited distribution of activation energies. This means that loss tangent-frequency plots can result in several broad peaks that may overlap. Figure 4 shows an Arrhenius curve for a hypothetical polymer with two transitions. The higher temperature transition also has the higher activation energy as is indicated by its larger slope. Measurements conducted at temperatures well to the right of a transition line are not influenced by that relaxation, while those well to the left are influenced to the fullest extent. In the vicinity of the line, measurements are partially affected by the transition. The convergence of transition lines at higher frequencies can also be noted. This leads to increased

overlap in loss tangent-frequency plots and eventually to a frequency at which individual peaks can no longer be resolved. As 1/T approaches zero, f_o's extrapolate to frequencies of 10^{13}-10^{14} Hz. These frequencies correspond to the molecular vibrations of the transitions, are in the infrared range, and are far above most normal test frequencies.

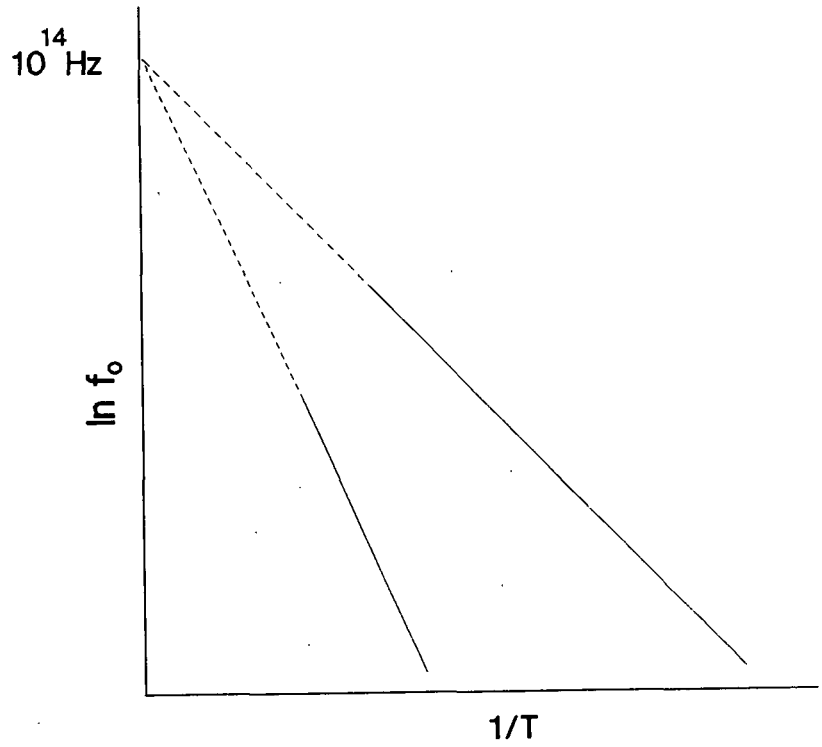

Figure 4. A hypothetical Arrhenius plot for a viscoelastic material with two thermal relaxations.

From the above discussion, the importance of stating test frequency when reporting moduli and loss tangent values is quite apparent. Often, moduli data in the literature are not accompanied by a frequency. At low frequencies modulus can be obtained by calculating the initial slope of a stress-strain curve. If frequency effects are considered at all, modulus is stated as being an increasing function of strain rate and strain rate data accompany moduli values.

This is not entirely correct, however. Modulus appears to increase with strain rate only because secant lines are usually drawn at constant strains, and hence, the effective time used to calculate the modulus becomes lower at higher strain rates. A more accurate statement would be that secant modulus increases with decreasing times at which the modulus is obtained. To be complete, strain rate as well as the strain amplitude used to calculate the modulus should be given so that an equivalent test frequency can be determined. It is important to realize that a ramp loading technique results in a distribution of frequencies which depend upon the strain amplitude used in the modulus calculation.

Moisture generally "plasticizes" thermal transitions in hydrophilic polymers. It does this by penetrating into the noncrystalline regions and increasing the free volume of the structure. This tends to reduce the activation energies of transitions, move them to lower temperatures, and increase their relaxation intensities. Hydrophilic polymers such as nylon[6] and cellulose[7] can, however, be "antiplasticized"[8] by moisture. In these cases, water transforms a secondary transition into a higher temperature, higher activation energy transition by attaching to the polymer segment responsible for the transition, and hindering its motion. Water therefore diminishes the low temperature relaxation as it augments that of the higher energy, higher temperature segment-water complex relaxation. As moisture is increased, the higher temperature, water induced transition responds as a typically plasticized relaxation, moving to lower temperatures and increasing in magnitude.

EQUILIBRIUM MOISTURE REVIEW FOR CELLULOSE

Thermal relaxations in cellulose and in cellulose-water systems have been studied extensively. A broad, low-temperature relaxation in dry cellulose,

named the γ transition, has been measured with mechanical,[7,9-12] dielectric,[12-19] NMR,[14,20] and piezoelectric[13] techniques. The γ relaxation is a secondary transition. This means that its motion is localized to small segments of the polymer chain; it has a relatively low activation energy, it is observed at low temperatures, and it is comparatively weak. For experiments conducted at 1 Hz the γ relaxation occurs in dry cellulose at about -95°C, with reported activation energies ranging from 9-13 kcal/mole.[7,12-14,17,19] At an ultrasonic frequency of 60 kHz this corresponds to a transition temperature of approximately -10°C if an activation energy of 12 kcal/mole is assumed. The factors that contribute to the scatter in observed γ relaxation temperature and activation energy include the testing of different materials (wood, paper, cellulose I, cellulose II, etc.), the use of different conventions in defining the location of the relaxation (loss tangent maximum vs. the maximum in loss modulus or dielectric loss), and the differing amounts of residual moisture in samples. Moisture content is probably the most crucial of the above-mentioned parameters. Due to the intensely hydrophilic nature of cellulose, it is difficult to obtain or even define dry cellulose. Data reported as dry may actually contain small amounts of residual water. As will be discussed in greater detail later on, this moisture decreases the magnitude of the transition and shifts it to a lower temperature.

Many investigators suggest that the γ transition results from a hindered rotation of the methylol side groups ($-CH_2OH$) in the disordered regions of cellulose.[7,11,13,14,17,19] Evidence to support this view comes from several areas. Mikhailov, Artukhov, and Shevelev[14] documented the γ transition in wood, cellulose, and cellulose derivatives, but found no transition to occur in xylan where the methylol group is absent. This work has subsequently been supported

by Norimoto and Yamada[17] and Handa, Fukuoka, Yoshizawa, and Kanamoto.[19] They found the transition to occur in cellulose and mannan where the methylol group is present, but not in xylan. Bradley and Carr[7] found the transition in cellophane and amylose, but not in dextran. This is consistent with the hypothesis, since dextran contains primarily 1,6-glucosidic linkages, and hence, the methylol group at C6 is absent. Bradley and Carr's work with amylose, as well as similar work performed by Nishinari and Fukada[13] helps to discount the other popular theory that assigns the γ transition to conformational changes in the glucopyranose rings. They found the γ transition to occur in amylose where only the chair form exists in the ordinary state. The relatively small activation energy of this transition also makes a cooperative ring interconversion theory seem doubtful.[7]

In addition to the γ relaxation, a high temperature, high activation energy α relaxation is present in dry cellulose. This transition is very strong and is usually, loosely referred to as a glass transition, T_g, in the non-crystalline region. The temperature of the relaxation is thought to be around 230°C.[7,21-24] However, at these temperatures, changes occurring in samples as a result of pyrolitic degradation[21] and/or autocrosslinking[22] make direct determinations difficult. Comparison of published data is also hampered by the fact that different methods are used to define the transition. Finally, differing amounts of hemicelluloses and lignins in samples as well as different types and crystallinities of cellulose can lead to variability in the reported α transition temperatures. The activation energy for the α transition in cellulose is very large. Bradley and Carr[7] give an estimate of 75 kcal/mole for the activation energy in the less ordered regions of cellophane. A higher activation energy of 105 kcal/mole was calculated by Salmen[24] for the softening temperature

of a dry NSSC-paper sample. Salmen defines the softening temperature as the location along the $\ln(E/E_o)$ *vs.* temperature curve where the slope is a maximum. E_o refers to the Young's modulus at 20°C.

A large activation energy causes transition location to be fairly insensitive to frequency. For this reason, reporting the frequency at which the α transition is measured is not as critical as reporting the γ transition frequency. A very large change in test frequency will, however, cause measurable changes in this location. For example, an α transition of 230°C at 1 Hz is equivalent to a temperature of around 245°C at 50 kHz when an activation energy of 75 kcal/mole is used. However, it should be remembered that unlike the more localized secondary transitions, the use of a constant activation energy Arrhenius-type equation with time-temperature equivalence techniques is questionable for glass transitions in polymers. This is due to the fact that the large scale segmental motion accompanying glass transitions usually results in a temperature dependent activation energy.[4] Although not insignificant, changes in the α transition due to test frequency are usually overwhelmed by the far larger effects of sample moisture content.

Moisture has profound influences on the thermal transitions of cellulose. The low temperature behavior is a classic example of antiplasticization by water. Small amounts of water decrease the intensity of the γ peak[7,11,13,15] and generate a new peak,[7,10,11,13,15] called the β relaxation. Because of its close relationship with the γ transition, the β transition is considered by several investigators[7,11,17] to be due to the hindered rotation of the methylol side groups containing hydrogen bound water ($-CH_2OH--H_2O$). As water sorbs onto these side groups, rotational movement is restricted. This results in structural stabilization of the polymer, an attenuation of the γ transition, and an

intensification of the higher temperature β transition. Due to the longer relaxation time of the (CH_2)-OH--H_2O as opposed to the (CH_2)-OH motion the β relaxation is at a higher temperature (around -70°C at 1 Hz and 7.3% moisture in cellophane) and has a higher activation energy (about 16.5 kcal/mole[7] in cellophane with 7.3% moisture) than the γ relaxation. At a moisture content corresponding to approximately one water molecule per methylol group in the non-crystalline region, the γ relaxation disappears, and the β relaxation remains as the only secondary transition.[7] As previously indicated, measurements made at frequency-temperature combinations between the γ and β relaxations demonstrate that water addition can actually increase the stiffness of cellulose.[7,9-11]

The quantitative effects that water has on the α transition in cellulose are more difficult to ascertain. Water plasticizes this transition by increasing free volume. This lowers the activation energy and hence the transition temperature of the relaxation and increases its intensity. At moderate moisture contents, the low-temperature flank of the α relaxation begins to have significant influence on room-temperature experiments.[7] This results in the well known increase in sensitivity of the room-temperature physical properties of cellulose to moisture at contents above about 5%.[25] Salmen and Back[26] saw this as a decrease in the softening temperature, T_s, of kraft sack paper from 65 to -25°C with an increase in moisture from 7 to 15%. It should be emphasized that T_s is not equivalent to T_g as it is defined in this thesis (maximum in loss tangent). Their T_s, defined as a maximum in $d(E/\rho)/dT$ or $d(E/\rho)/dM$, where M equals moisture and T equals temperature, is closer to the onset rather than the peak of the α transition. It does, however, give an approximate idea of the shifts expected in the transition temperature with changing moisture. These researchers also give an indication of the importance of sample crystallinity.

Moisture affects the noncrystalline regions of cellulose. At equivalent RH's the noncrystalline regions of high and low crystallinity samples have identical moisture contents. However, when different crystallinity samples are compared at equivalent overall moisture contents, the moisture must be more locally concentrated in the noncrystalline regions of the more highly crystalline sample. T_g and T_s of high crystallinity paper therefore tend to be lowered a greater amount than T_g and T_s of less ordered samples when compared at equal moisture contents, but are lowered the same amount if compared at equal RH's. Finally, the importance of the hemicelluloses and lignin must again be mentioned. Goring[21] showed the softening temperature of a variety of lignins and hemicelluloses to be affected a great deal more by moisture than that of cellulose. The effect of moisture on the α transition temperature should therefore depend not only on cellulose crystallinity but on hemicellulose and lignin content as well.

NONEQUILIBRIUM MOISTURE REVIEW

Before discussing the transient decrease in modulus and/or increase in loss tangent that accompanies sorption and desorption, the seemingly related phenomenon of accelerated creep, which occurs under cyclic humidity conditions, will be discussed briefly. The discussion is pursued in this fashion because the accelerated creep phenomenon is more widely accepted and work in this area generally predates that of studies concerned with transient decreases in modulus and increases in loss tangent.

Accelerated Creep

Figure 5 shows an example of the creep that occurs in paper subjected to a compressive load. This figure, and all others in the NONEQUILIBRIUM REVIEW section, has been traced from the originally published graph. Notice that paper

creeps far more in a cyclic humidity (35-90-35-90 ...% RH) relative to a high humidity (90% R.H.) environment. This greater creep under cyclic moisture conditions has led to the use of the term "accelerated creep" when describing this phenomenon. The term "mechanosorptive effect" is also often used. Accelerated creep occurs in many cellulosic materials including wood,[27-37] wood based boards,[38-41] and paper.[42-47] Several reviews on this subject can be found in the literature.[27,48,49] The following is a summary of the characteristics of the phenomenon.

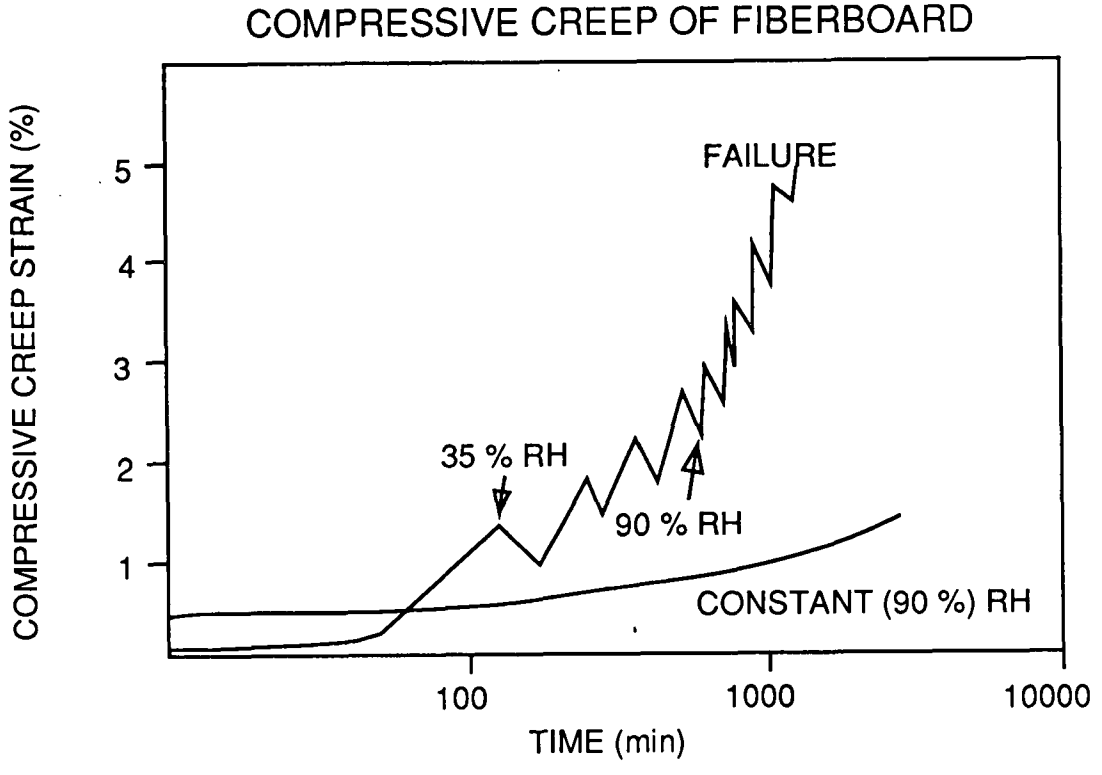

Figure 5. Compressive creep-time data for a fiberboard sample under constant (90% RH) and cyclic (35-90%) conditions (Byrd[42]).

The magnitude of the moisture change, and not its rate, is the most important factor governing the overall deformation of the sample.[29] High sorption and desorption rates lead to high creep rates, but the overall deformation depends primarily upon the size of the moisture step. For example, changing the

moisture content of a sample very slowly from 4-10-4% would result in the same total creep as more rapid moisture changes over the same moisture range.

The mechanosorptive effect appears to be coupled with dimensional changes occurring as a result of moisture change. In wood species where cell walls are prone to collapse during drying, a larger mechanosorptive effect is reported.[29] Also, prefreezing of wood, which minimizes dimensional changes in the kiln drying operation, results in a reduction of accelerated creep.[51,52]

Steady-state moisture diffusion through samples does not cause accelerated creep. This was demonstrated in a compressive creep experiment utilizing a solid rectangular block of wood that had a bored out cylindrical core.[33] When air in the core was maintained at 30% RH and that surrounding the block at 90% RH, a condition of steady-state diffusion of moisture toward the core was set up. In this case the creep was similar to that found when the block was at a uniformly high or low moisture content (i.e., core and surrounding air at identical RH's). However, when the moisture in the sample was changed by either increasing the core RH to 90% or decreasing the outside RH to 30% a dramatic increase in creep was observed. Similar results have been found in hardboard bending experiments.[27] Therefore, any theory relying solely on diffusion to describe the mechanosorptive effect must be inadequate.

Accelerated creep occurs in many basic loading modes including shear, tension, and compression as well as more complex modes such as bending and torsion. However, all test modes do not appear to be affected to the same degree. For example, wood samples subjected to compression loads along the grain creep more than those in tension along the grain when loaded at equivalent percentages of the ultimate short term load.[29]

Accelerated creep occurs on both sorption and desorption. In order to see this most clearly, the dimensional changes caused strictly by swelling or shrinkage must be accounted for. For example, the measured compressive creep accompanying sorption is equal to the actual creep minus the dimensional changes caused by the swelling of the sample. If this swelling is appreciable compared to the actual compressive creep, the measured creep might appear to decrease even though the actual creep is increasing.

The removal of the load after accelerated creep causes immediate and delayed recovery of dimensions, similar in magnitude to those which would occur after a normal creep test, where moisture has been held constant. However, a far greater recovery, consisting of the bulk of the creep caused by the mechano-sorptive effect, can be realized if sample moisture is cycled in the unloaded state.[30] It appears that some portion of the sample "remembers" its original shape. This memory can be "erased" if the sample temperature is increased to 50-65°C before unloading.[35]

In addition to increased creep, moisture cycling under load can lead to failure at low loads. In these cases, the creep at failure is far greater than breaking strains obtained under equilibrium moisture conditions. Also, tensile stiffness, measured by the initial slope of a stress-strain curve, decreases during accelerated creep, gradually dropping by 20-30% prior to failure.[44]

The mechanosorptive effect appears to occur not only in wood and wood based products but in wool[53] and concrete[54] as well. Plasticizers other than water, capable of swelling samples can also result in the mechanosorptive effect in polymers.[55]

No completely satisfactory explanation describing all of the characteristics of the mechanosorptive effect is presently available. Two schools of thought employ (1) increased molecular mobility and (2) stress gradients as primary factors affecting creep during nonequilibrium moisture conditions. Many theories discuss the importance of diffusion and/or stress gradients.[56,57] However, the fact that steady-state diffusion does not result in accelerated creep shows that steady-state stress gradients alone are not the principal factors. In order to produce the mechanosorptive effect, nonsteady-state conditions are required.

Takemura[37] describes the phenomena in terms of molecular mobility concepts. He attributes the increased rate of stress relaxation accompanying sorption to time-dependent volumetric changes. For example, as a sample loses moisture, molecular voids are formed in areas where water molecules had previously been located. In an effort to move to more energetically favorable positions, neighboring polymer chains rearrange, attempting to close up these voids. This is a time dependent process, however, during which molecular mobility passes through a maximum. It seems, therefore, that sorption and desorption rate should be important in a molecular mobility-type concept. In order to minimize accelerated creep, the time required for moisture change during cycling should be small relative to the time needed for the above-mentioned molecular rearrangements. The same arguments should also hold for transient decreases in modulus and increases in loss tangent. During sorption and desorption, the time dependent molecular reorganizations in the polymer would make it more compliable and more "lossy" when subjected to a load.

Transient Decrease in Modulus (Increase in Loss Tangent)

As previously mentioned, certain published data indicate that a transient decrease in modulus accompanies sorption and desorption.[27,58-63,68] Concurrent with this decrease in modulus is a transient increase in loss tangent.[47,58,64,66,69] Modulus and loss tangent measurements are somewhat different from creep tests in that they are made in the linear viscoelastic regime. Creep can also be linear but is more likely to be nonlinear or plastic.

In order to facilitate reporting of the results, two definitions are introduced to clarify the meaning of a transient "decrease" in modulus or "increase" in loss tangent. If data obtained under changing moisture conditions are compared with equilibrium data at the same moisture content and are found to have a lower modulus and/or higher loss tangent, they are defined as exhibiting a transient decrease in modulus and/or increase in loss tangent:

$$\%\ T_{\text{decrease in E}} = 100(E_{\text{equ.}} - E_{\text{trans.}})/E_{\text{equ.}} \tag{14}$$

$$\%\ T_{\text{increase in tan}\delta} = 100(\tan\delta_{\text{equ.}} - \tan\delta_{\text{trans.}})/\tan\delta_{\text{equ.}} \tag{15}$$

Unfortunately, in many studies, the sample moisture content during sorption or desorption is not reported. Also, even when moisture is measured and reported during rapid moisture changes, equilibrium moisture-modulus (or tanδ) relationships are often not available. Therefore, in many cases, direct comparisons of nonequilibrium-equilibrium data at identical moistures are impossible. However, the existence of transient-equilibrium differences can be inferred from the fact that transient overshoots in loss tangent and/or undershoots in modulus are often reported. These overshoots occur even though moisture generally increases or decreases continuously with time. Loss tangent overshoots and modulus undershoots are defined as transient maxima or minima to

distinguish them from the transient increases or decreases described earlier. Different definitions are required for sorptive,

$$\% T_{maximum} \text{ in } \tan\delta = 100(\tan\delta_{max.} - \tan\delta_{final})/\tan\delta_{final} \quad (16)$$

$$\% T_{minimum} \text{ in } E = 100(E_{final} - E_{min.})/E_{final} \quad (17)$$

and desorptive data:

$$\% T_{maximum} \text{ in } \tan\delta = 100(\tan\delta_{max.} - \tan\delta_{init.})/\tan\delta_{init.} \quad (18)$$

$$\% T_{minimum} \text{ in } E = 100(E_{init.} - E_{min.})/E_{init.} \quad (19)$$

Protein

A short description of the structure of hair and wool fibers enables the moisture-modulus interactions to be more thoroughly understood. This description can be compared and contrasted to a later discussion of cellulose morphology. Wool and hair are examples of proteinaceous fibers. Wool fibers are highly accessible to water (≈ 80%). This water is hydrogen-bonded to carbonyl (-C=O) groups in the main chain as well as active groups in the side chains.[70] They are also extensible up to 65%.[64] In an unstretched condition, molecules in wool fibers are held in a folded form by internal cross-links. However, as the fibers are strained, the molecules unfold and the crystalline structure changes from that of α-keratin to that of β-keratin.

An early study of wool in a changing moisture environment was a torsion study performed by Mackay and Downes.[58] Utilizing Merino wool fibers (wet diameter 30 μm) and a freely oscillating torsion pendulum (period 17-33 seconds, angular shear strain amplitude ≈ 2%), they observed large transient minima in the torsional rigidity of fibers undergoing sorption. They also demonstrated that these minima could not be explained by the fiber diameter changes accompanying sorption. For a large sorption (0-94% RH), torsional rigidity fell so

low as to be temporarily unmeasurable. The minimum in rigidity corresponded to the time that gains in sample moisture were essentially complete. This occurred long before rigidity reached an equilibrium value. Figure 6 shows the effect that the rate of moisture change had on the minimum found in rigidity. In this figure, the normalized rigidity is plotted vs. the square root of the time after humidity is changed from 0-61% RH at several rates (denoted as A, B, C, and D). Sample regain, defined as water weight divided by oven dry weight, accompanying sorption is also shown. Notice the increased size of the minimum as the sorption rate increases. Notice also the changes in rigidity that occur long after moisture uptake is essentially complete. Fibers undergoing desorption also exhibited a transient decrease in rigidity. Unlike sorption, however, transient modulus minima were not found. Measurements of internal friction showed transient maxima on sorption. When initially dry samples were placed in an environment of 65% RH, rapid sorption was accompanied by transient maxima in internal friction as large as 100%. Desorption damping data were not reported.

Shortly after the work of Mackay and Downes, Nordon[59] performed similar work with 45 μm wet diameter Corriedale wool fibers and a forced oscillation torsion pendulum operated at frequencies between 10 and 100 Hz and angular shear strain amplitudes of around 0.03%. Using forced oscillation allows a greater frequency range to be employed as well as smaller oscillation amplitudes. Torsional rigidity was measured during sorption for a variety of step changes in RH. In most cases a transient minimum in rigidity was observed. Also, the magnitude of the humidity change appeared to have little effect on the size of the minima. In fact, small step changes at low humidities produced the largest transient minima in rigidity relative to the overall equilibrium changes. Typical results are shown in Fig. 7. Here transient minima for sorption steps

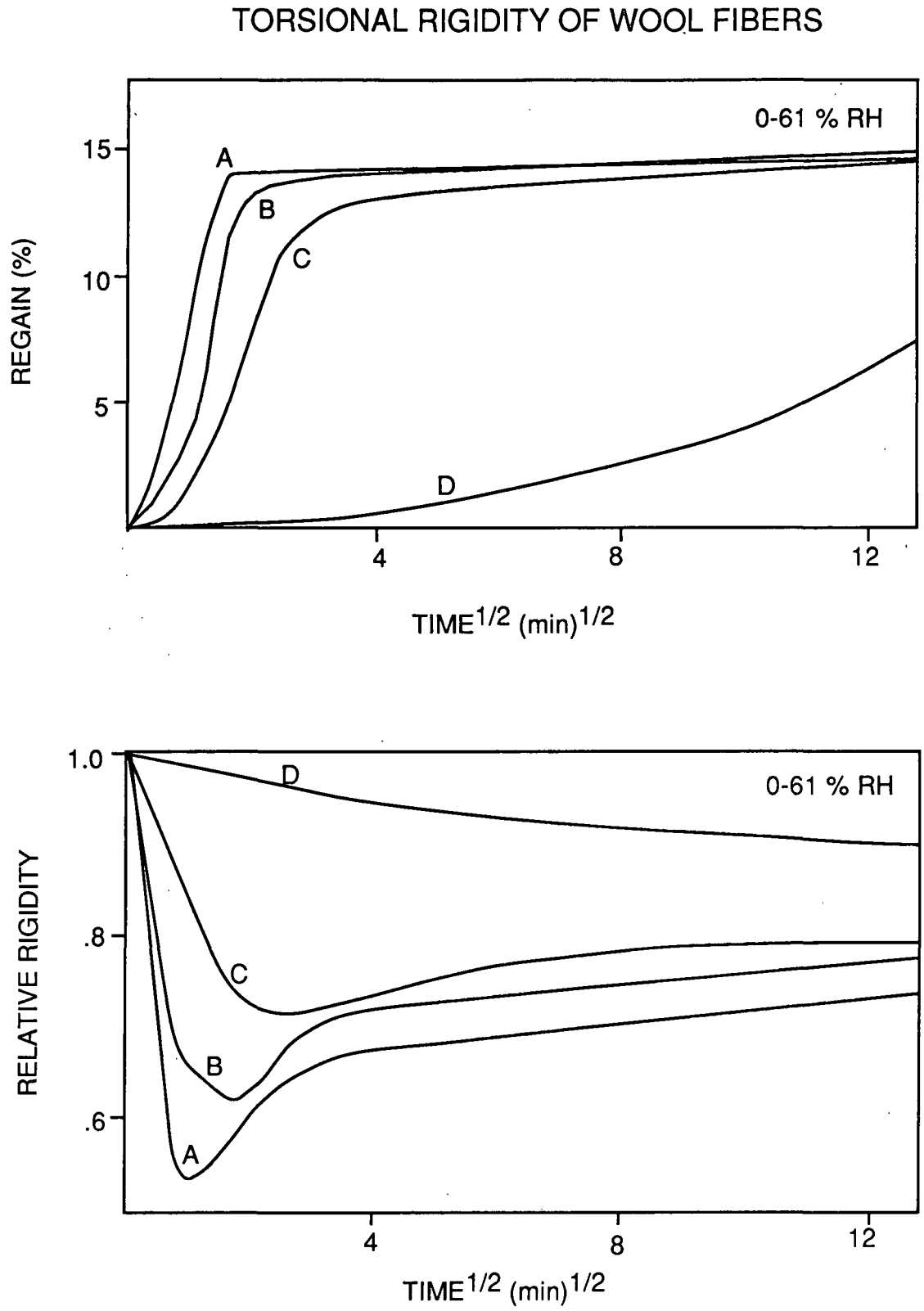

Figure 6. Regain and torsional rigidity-time data for wool fibers sorbing between 0-61% RH at various rates (Mackay and Downes[58]).

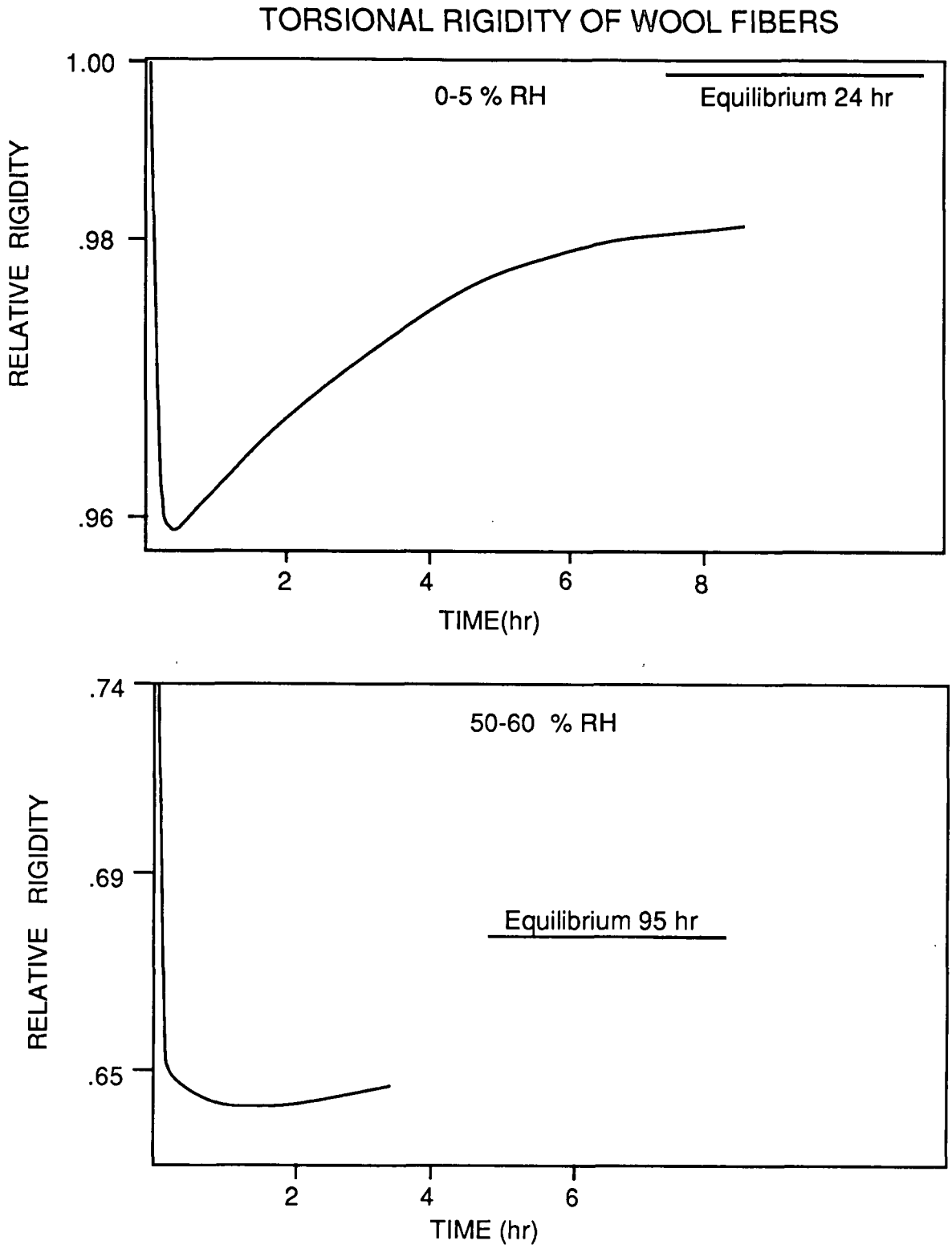

Figure 7. Torsional rigidity-time data for wool fibers sorbing between 0-5 and 50-60% RH (Nordon[59]).

of 0-5 and 50-60% RH were both found to be around 4%. The minimum looks more dramatic in the 0-5% RH case, however, because of the far smaller equilibrium change in rigidity accompanying this sorption step. In any case, the transient minima in rigidity measured by Nordon were considerably smaller than the ones found by Mackay and Downes, usually being less than 5%. To determine the importance of diameter, Nordon subjected a 30 μm diameter Merino wool fiber (as used by Mackay and Downes), a 45 μm diameter Corriedale wool fiber, and an 80 μm diameter human hair to the same large sorption step from 0-90% RH. The large transient minimum in rigidity reported by Mackay and Downes was found to occur in the 30 μm fiber, the 45 μm fiber exhibited only a small minimum, and no minimum was measured in the hair. Nordon also attributed some of the difference in the size of the minima to the smaller oscillation amplitude used in his study. No desorption or damping data were published.

Effects similar to those seen by Nordon in torsion were reported about this time in stress relaxation studies of wool fibers held in tension.[60-63] Transient minima in the longitudinal stress of wool fibers held under small axial tensile strains (≈ 1.5%) were found by Haly and Feughelman to accompany sorption.[62] As was the case in the torsion study of Nordon, these minima were found to be 5% or less. In contrast to Nordon's study, however, and similar to the work of Mackay and Downes, the minima produced became greater as the magnitude of the humidity step was increased as shown in Fig. 8.

Recently, a dynamic sinusoidal extension technique, where fibers are mounted in loop form between a fixed and vibrating rod (axial strain amplitude 0.01%, fixed extension 0.6%, frequency 116 Hz), has been used by Danilatos and Postle[64] to study horse hair and wool fibers during sorption. They found transient maxima in loss angle of around 20% when horse hair samples initially at

53% RH were submerged in water. These maxima coincided with the completion of swelling as shown in Fig. 9. It can be noted from this figure that the loss angle maximum was not accompanied by a transient minimum in modulus. Loss angle maxima were smaller or nonexistent when sorption in wool fibers was induced by step humidity changes (Fig. 10). Transient minima in modulus accompanying sorption were again absent (Fig. 11). Danilatos and Postle[65] also tested wool fibers axially during desorption and found no transient minima in modulus values or maxima in loss tangents (Fig. 12 and 13). Notice that although modulus and loss tangent values are affected considerably by the initial strain offset, the qualitative effects of desorption are similar. Unfortunately, equilibrium-nonequilibrium differences could not be determined from these studies.

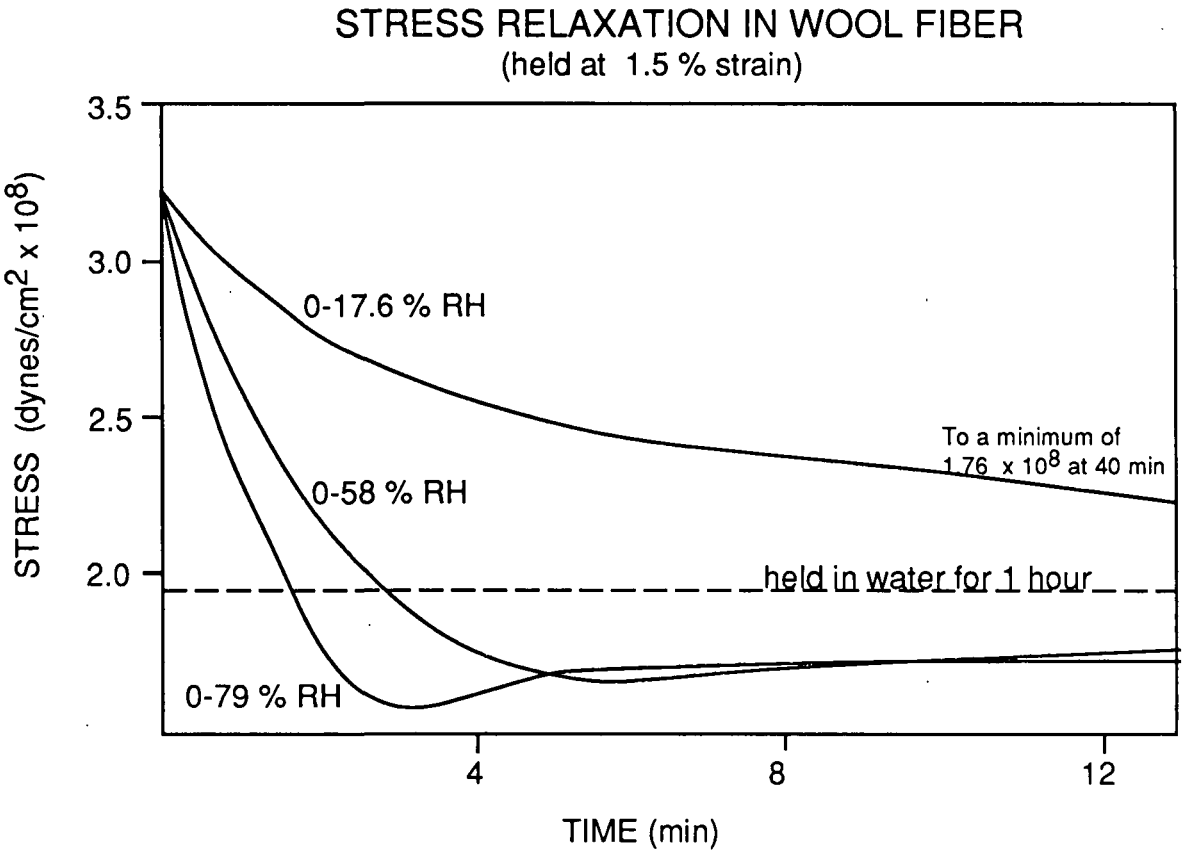

Figure 8. Stress relaxation-time data for wool fibers held at 1.5% strain and undergoing various sorptions from initially dry states (Haly and Feughelman[62]).

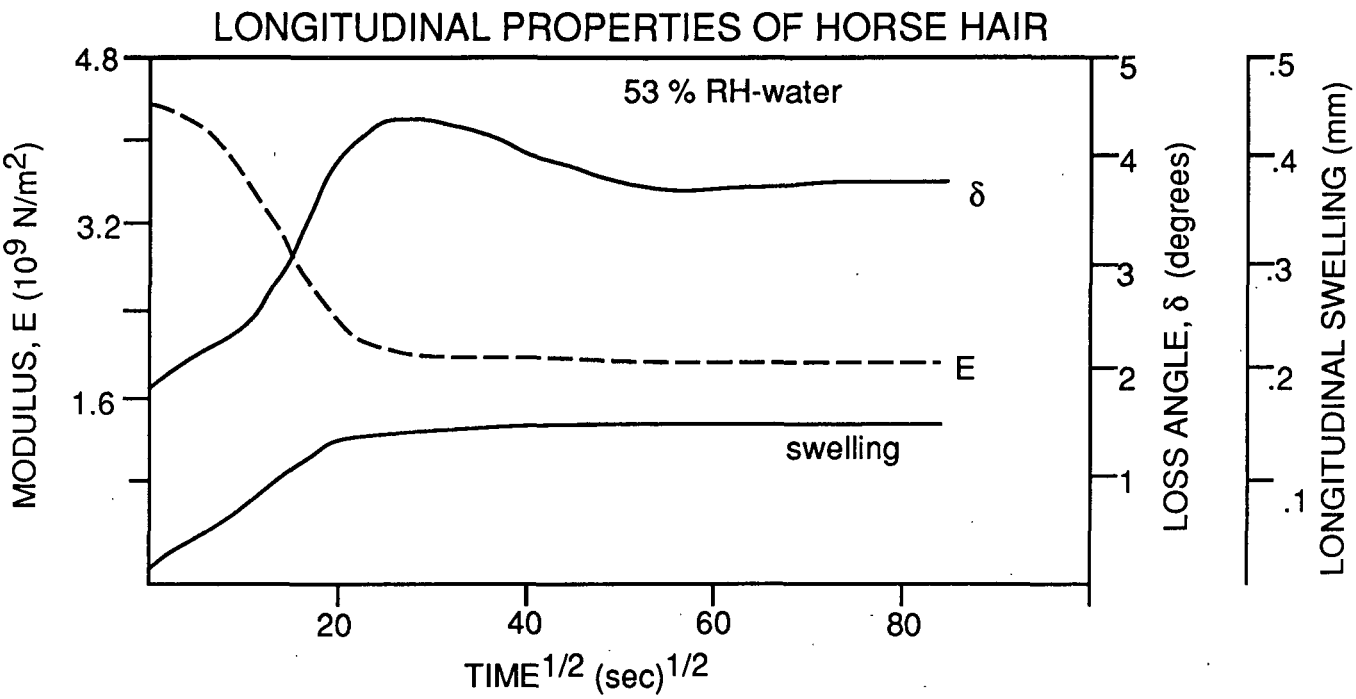

Figure 9. Longitudinal loss angle, swelling, and modulus-time data for horse hair submerged in water (Danilatos and Postle[64]).

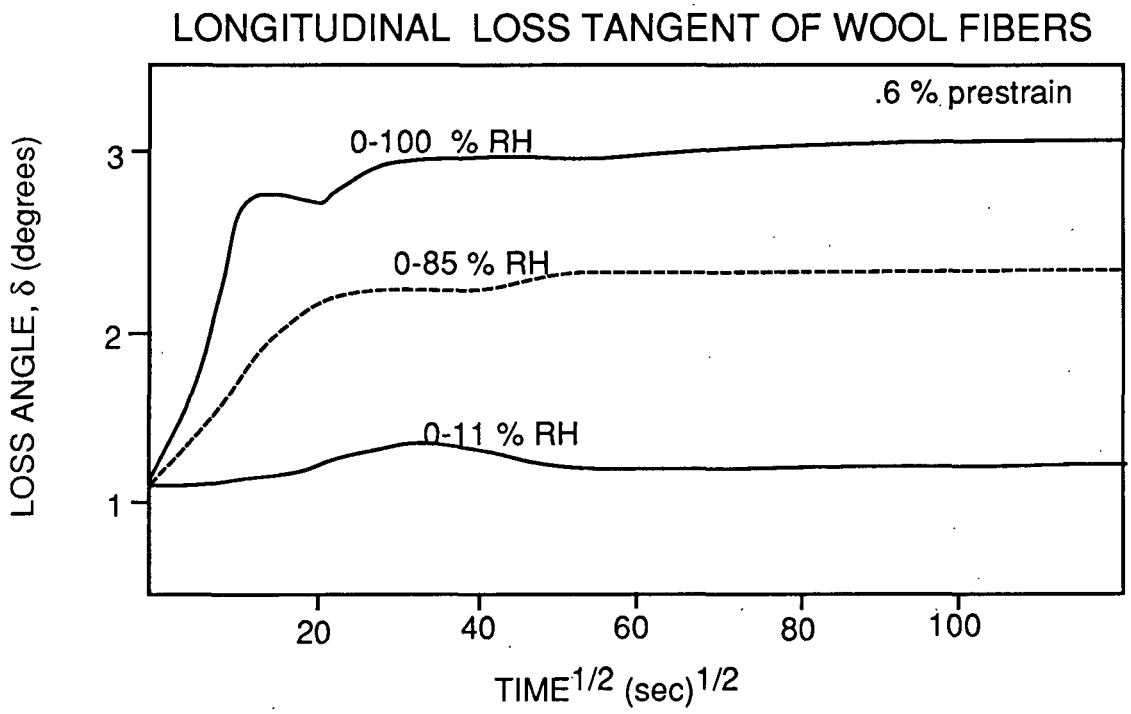

Figure 10. Longitudinal loss angle-time data for wool fibers undergoing various sorptions from initially dry states (Danilatos and Postle[64]).

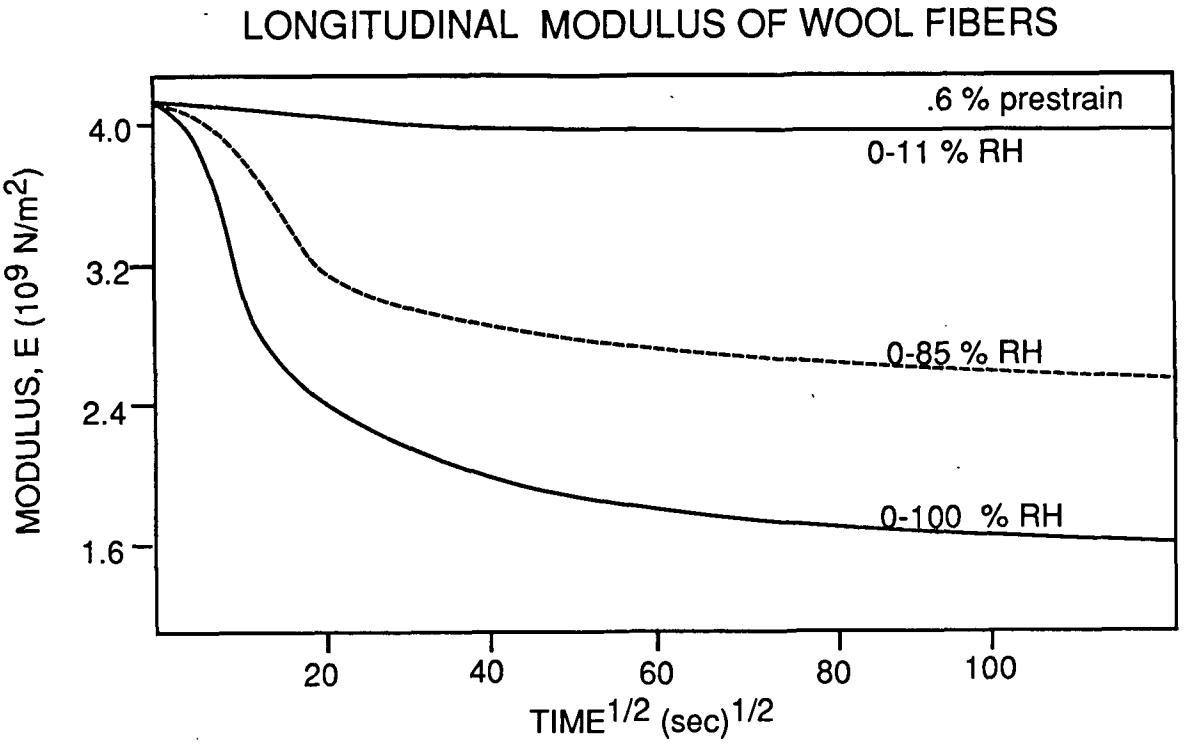

Figure 11. Longitudinal modulus-time data for wool fibers undergoing various sorptions from initially dry states (Danilatos and Postle[64]).

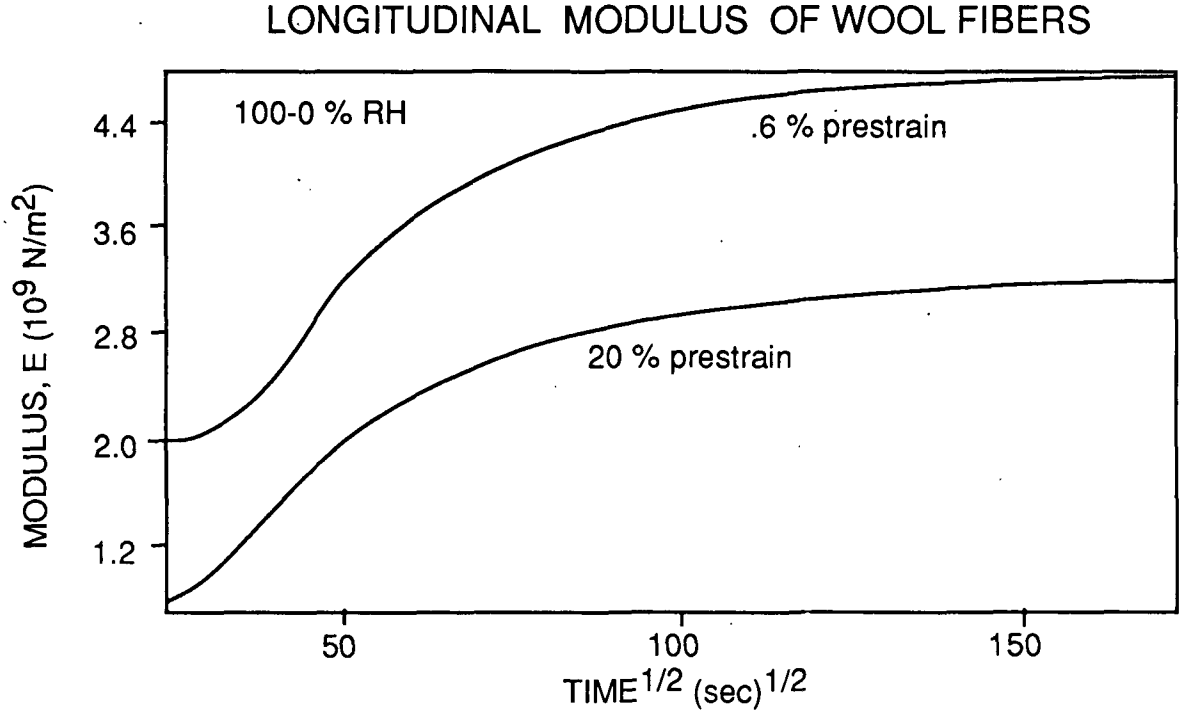

Figure 12. Longitudinal modulus-time data for wool fibers undergoing desorption from 100-0% RH (Danilatos and Postle[65]).

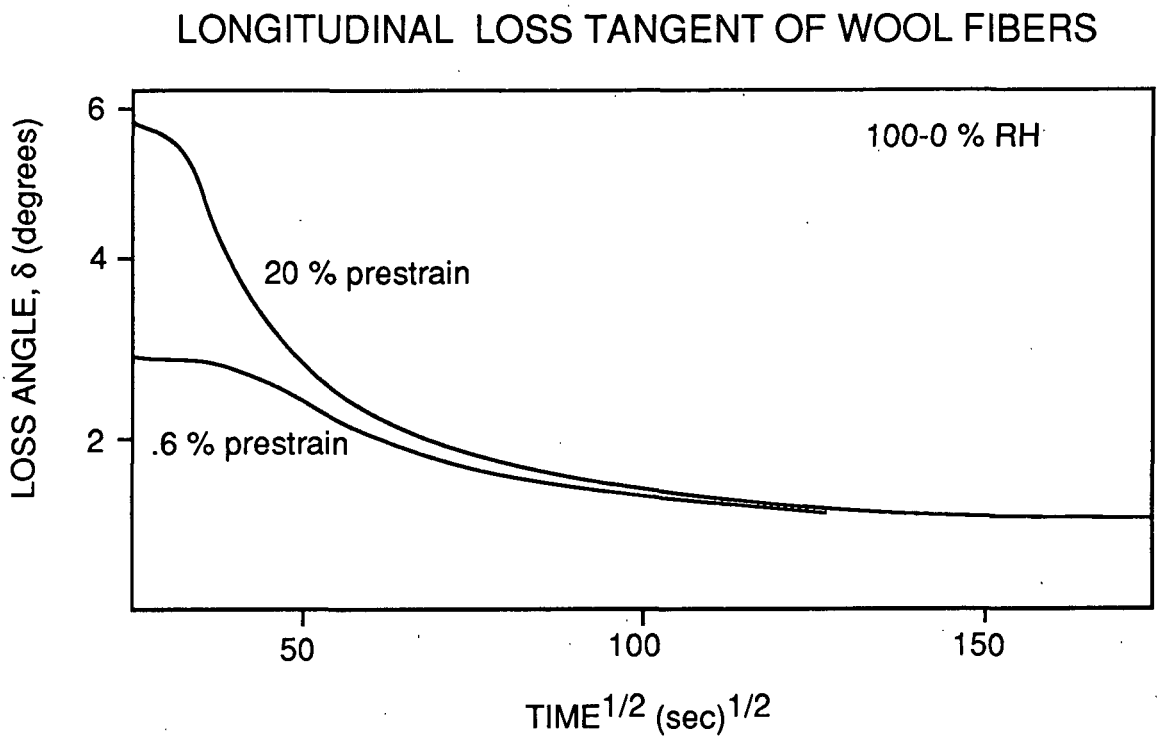

Figure 13. Longitudinal loss angle-time data for wool fibers undergoing desorption from 100-0% RH (Danilatos and Postle[65]).

Cellulose

Cellulosic materials are more crystalline, and therefore, less accessible to water than wool. However, the accessibility is still quite high, being around 40% in cotton and around 67% in viscose rayon.[70] Cellulosic fibers are also less extensible than wool fibers and usually have ultimate elongations of less than 5%. This is a result of their layered structure in which the largely crystalline fibrils are wound helically around the fiber axis. The angle of wind for the majority of the fibrils is quite low relative to the fiber axis so that the crystalline regions are aligned nearly axially. Water in cellulosic materials hydrogen bonds primarily to hydroxyl groups.

Transient maxima in loss tangent as well as minima and decreases in modulus have been reported in cellulosic materials undergoing sorption and desorption.

For example, using a freely oscillating torsion pendulum, De Ruvo, Lundberg, Martin-Lof, and Soremark[47] found a transient maximum in the logarithmic decrement of about 25% when testing 15 μm diameter sulfate fibers undergoing sorption induced by an increase in RH from 10-22% (Fig. 14). A typical sorption curve for a similar RH change is also included in Fig. 14. Rigidities and desorption log decrement values were not reported.

Kubat and Lindbergson[66] used thin strips (14 cm long, 1.5 cm wide) and a torsion pendulum in free oscillation (frequency of 0.1-1 Hz, strain amplitude ≈ 0.01%) in their measurements of the effects of moisture change on dynamic in-plane shear modulus. They tested a variety of polymer-plasticizer combinations [including paper-water, paper-ammonia, cellophane-water, cellophane-ammonia, gelatin-water, nylon 66-water, cellulose acetate-acetone, poly(vinyl) acetate-acetone, rubber hydrochloride-chloroform, and polystyrene-benzene] and found transient maxima in loss tangent as large as 100% accompanying both sorption and desorption. Results for paper and cellophane with water and ammonia acting as plasticizers are shown in Fig. 15. The samples in this figure were initially at 65% RH. They were then placed in a chamber and exposed to a vacuum for around 10 minutes. At this point water or ammonia was introduced into the system and the sorption from 0-70% RH or 0-200 torr ammonia was begun. When using the above technique, the equilibrium dry loss tangent values were not known and hence, the X-axis of the left hand portion of Fig. 15 begins approximately 1000 seconds after sorption is initiated. It can be noted, however, that even after 10^4 seconds, when the majority of the sorption process was undoubtedly complete, the loss tangent was still changing. At 10^5 seconds a vacuum was drawn, desorption occurred, and an initial transient loss tangent maximum resulted. A considerable amount of time elapsed before the loss tangent decreased below the

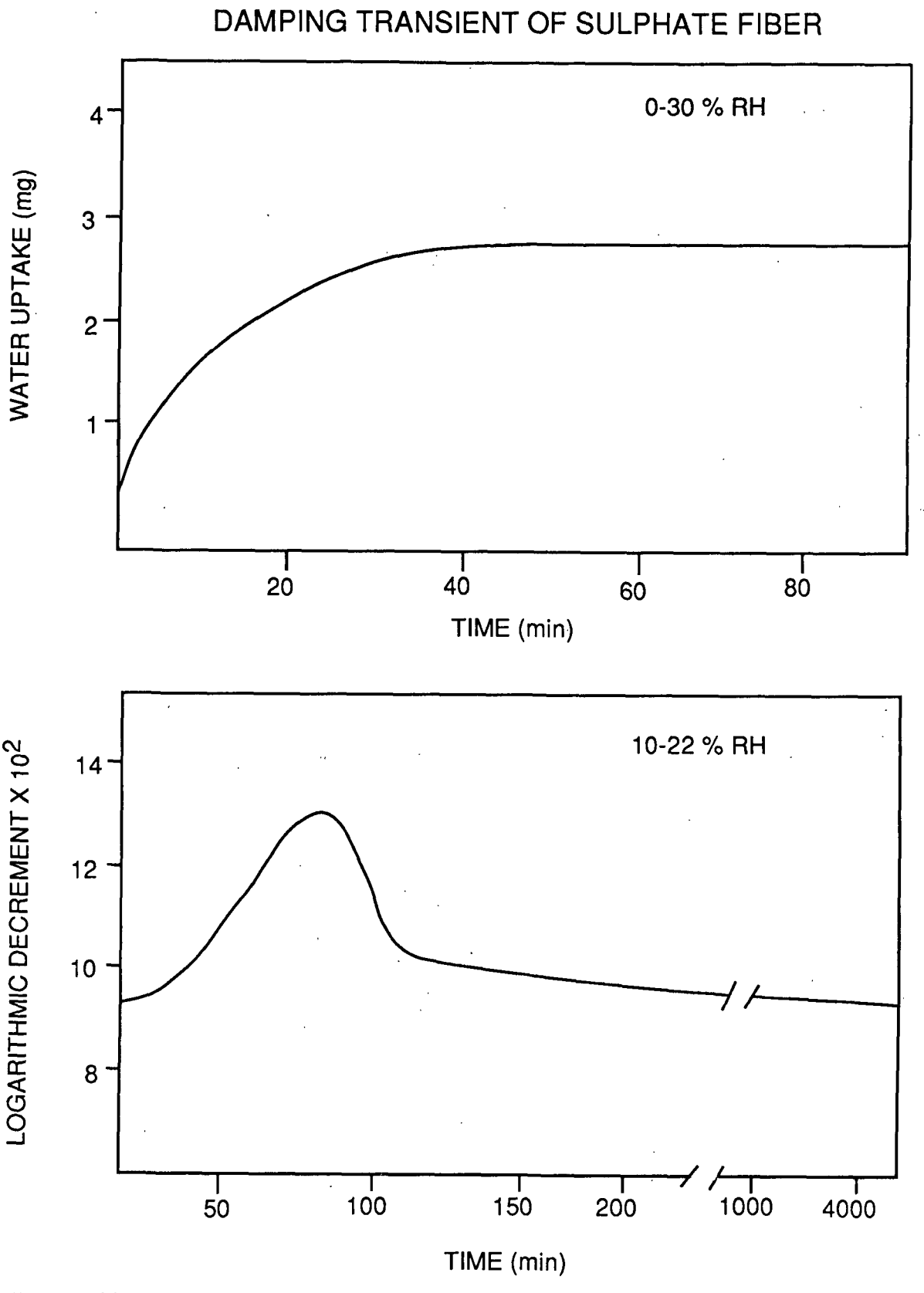

Figure 14. Logarithmic decrement and regain-time data for sulfate fibers undergoing sorption (DeRuvo, Lundberg, Martin-Lof, and Soremark[47]).

initial value, and changes occurred up to 72 hours even though desorption had long been completed. The results of the study are taken by the authors to demonstrate that the occurrence of a transient loss tangent maximum during moisture change is a general phenomenon as it was found in all of the polymer-plasticizer systems tested. A more detailed report by these authors, considering just the paper-water system,[67] showed that although transient maxima in torsional loss tangent of approximately 100% were created whenever sample moisture was changed, no transient minima occurred in shear modulus values. They also found strain offsets between $\approx 10^{-3}$-10^{-1}% to have no influence on the damping behavior.

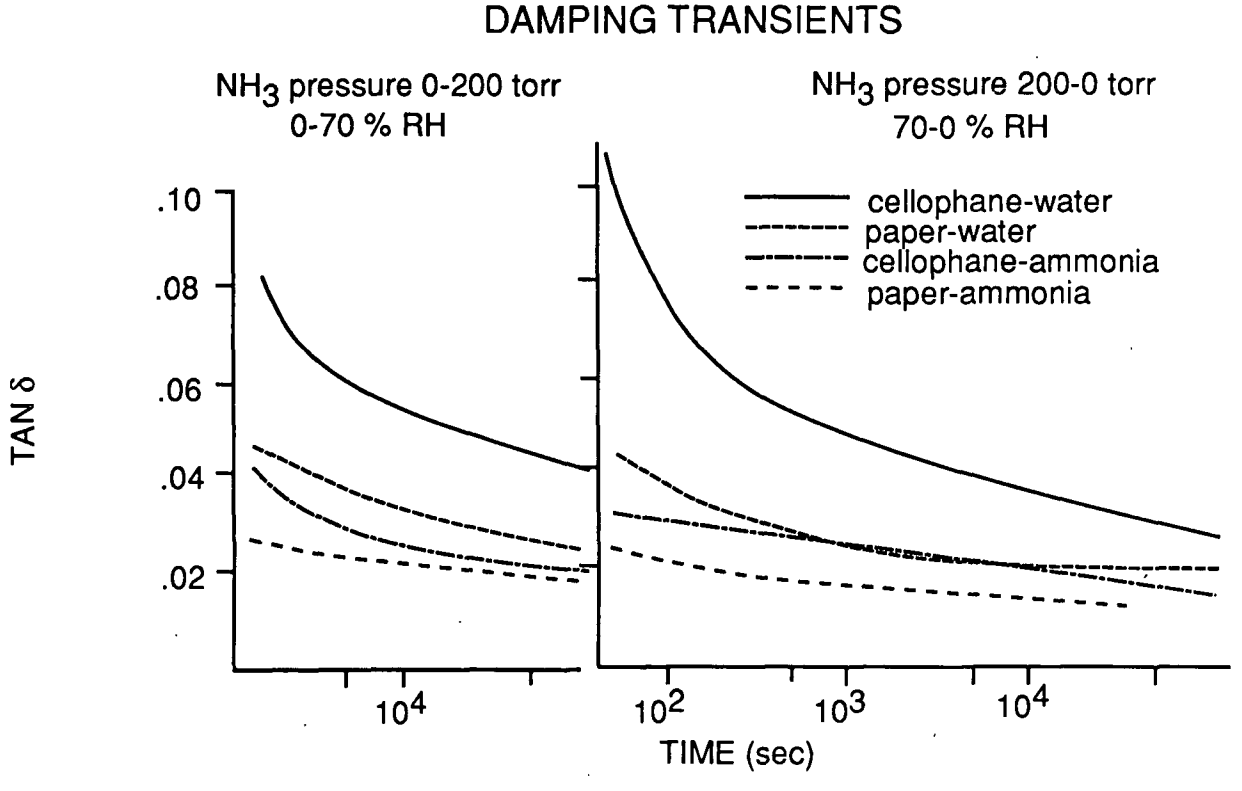

Figure 15. Torsional loss tangent-time data for cellophane and paper strips after step changes in vapor pressure of moisture or ammonia (Kubat and Lindbergson[66]).

Transient decreases as well as minima in tensile stiffness were found, however, by Back, Salmen, and Richardson[27] when testing kraft sack paper during sorption and desorption. Tensile stiffness, obtained by measuring the initial slope of a stress strain curve, can be seen plotted vs. the square root of time in Fig. 16 and 17. The dashed line in these figures represents averages of stiffness data obtained under equilibrium moisture conditions, and does not pertain to the horizontal time scale. They are comparisons, at equivalent moisture contents, to nonequilibrium data. Nonequilibrium data are obtained by removing samples from an initial environment and placing them in a different RH environment. The samples are then allowed to sorb or desorb for a given amount of time before they are clamped in the tensile tester and strained at a rate of 0.83% per second. Moisture content-time relations are obtained by observing the weight of similar samples as a function of sorption time. The solid lines in Fig. 16 and 17 are assumed to be composites of many such tests at several times, however, raw data were not published along with the figures. As can be seen, nonequilibrium tensile stiffnesses are lower than equilibrium values throughout the duration of the measurements. Notice also the lack of convergence of equilibrium and sorption data after 20 minutes even though the majority of the moisture change is accomplished in the first ten minutes. This time lag in the recoverability of stiffness is similar to several of the results discussed earlier.[58,59,62] The shallow minimum in stiffness accompanying sorption is also quite similar to the results previously discussed as having been found by Nordon[59] using a torsion pendulum and by Feughelman, Haly, and Robinson[60-62] in stress relaxation studies. The dramatic thing about this study, however, is the initial transient decrease in tensile stiffness on desorption. This minimum has not been reported previously. The desorption rigidity values reported by Mackay

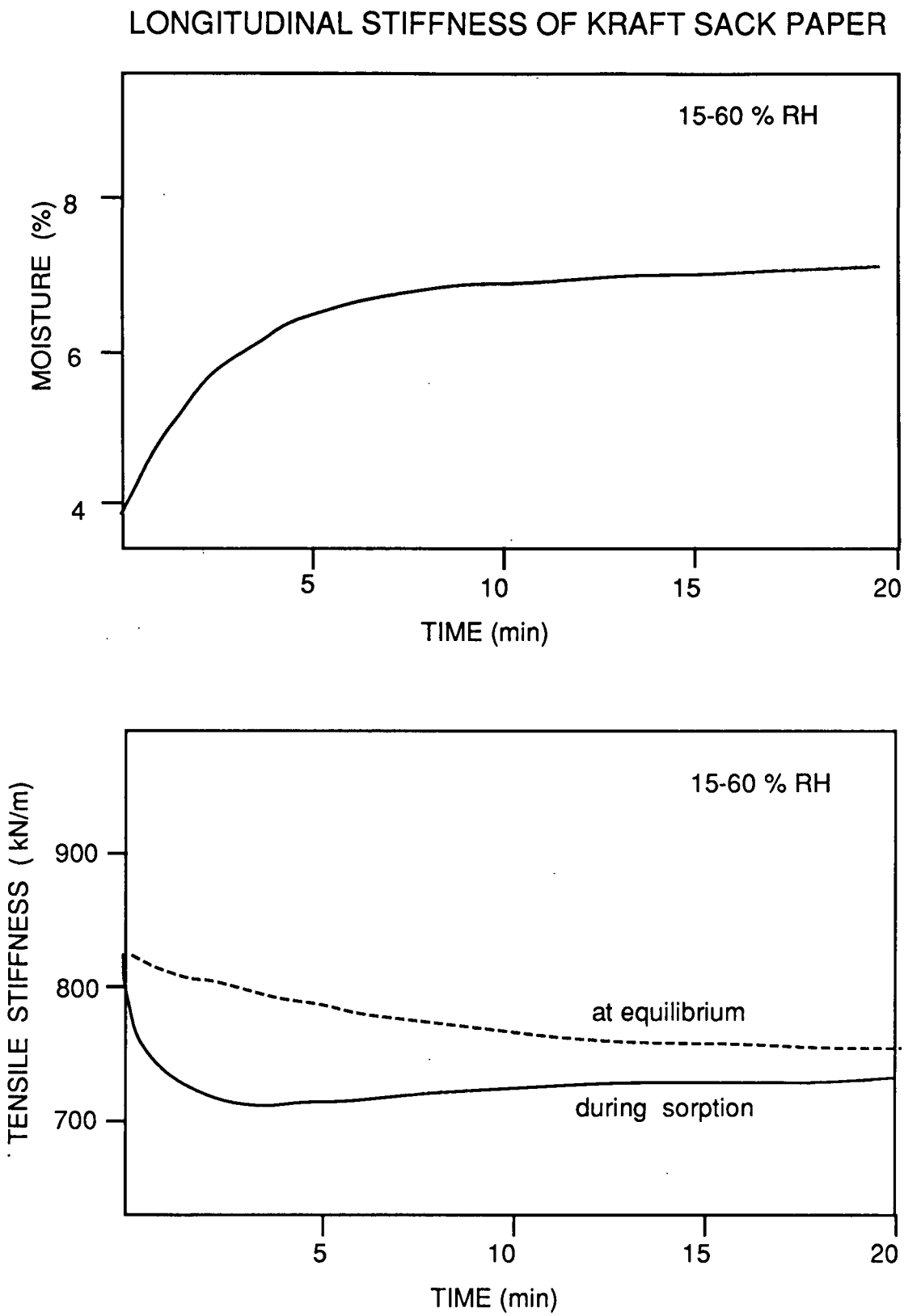

Figure 16. Tensile stiffness and moisture change-time data for kraft sack paper undergoing sorption from 15-60% RH (Back, Salmen, and Richardson[27]).

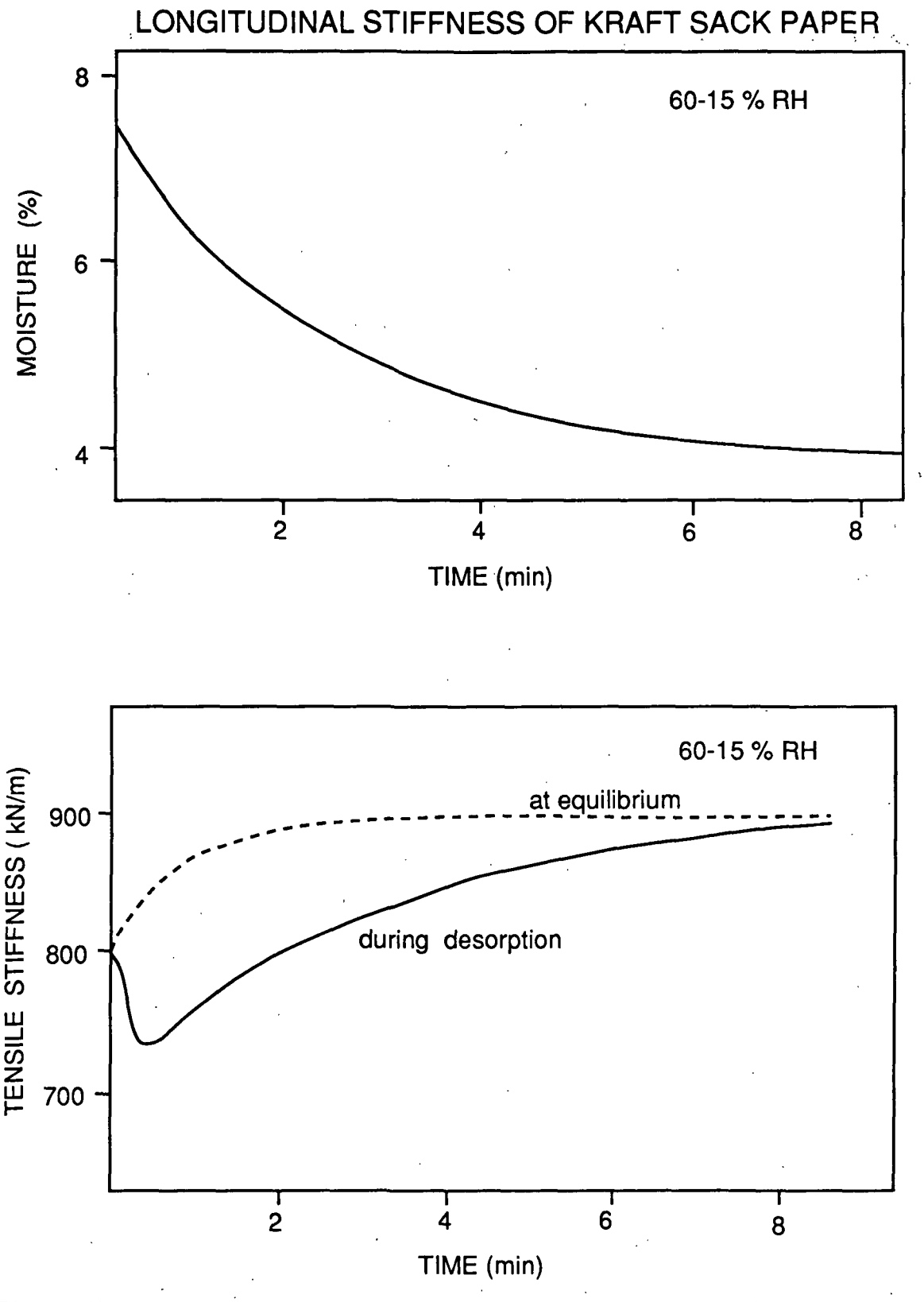

Figure 17. Tensile stiffness and moisture change-time data for kraft sack paper undergoing desorption from 60-15% RH (Back, Salmen, and Richardson[27]).

and Downes, although exhibiting transient decreases, did not indicate transient minima.

A dielectric study of Algie's,[68] using a test frequency of 1592 Hz to test Corriedale wool fibers in the transverse direction, provides evidence of increased molecular mobility during nonequilibrium moisture conditions. Large transient maxima were found to occur in the real part of the dielectric constant of samples undergoing small sorptions from initially dry conditions (Fig. 18). Larger sorption steps resulted in smaller maxima. Although the dissimilarities between dielectric and mechanical tests might be expected to lead to different results, dielectric data are qualitatively very similar in appearance to that from Nordon's torsion study, the major difference being the far larger maxima occurring in the dielectric measurements.

A final piece of evidence for increased molecular mobility during moisture change comes from an NMR study of cotton and wool by Shishoo and Lundell.[69] They argue that the broad peak half width of the proton absorption curve is a measure of matrix rigidity and show that this half width exhibits a minimum during sorption. The shape of their broad peak half width vs. time curve accompanying sorption in cotton is again quite similar to curves already described for measures of sample stiffness, passing through a slight minimum before increasing to a final equilibrium value (Fig. 19). Note that wool fibers did not exhibit this minimum.

It is apparent, from the above discussion, that a wide range of transient loss tangent maxima and modulus minima have been reported in cellulose and wool samples undergoing sorption and desorption. Some of the data are contradictory and must somehow be rationalized before definite statements concerning the transient effects of moisture change on mechanical properties can be made. A more

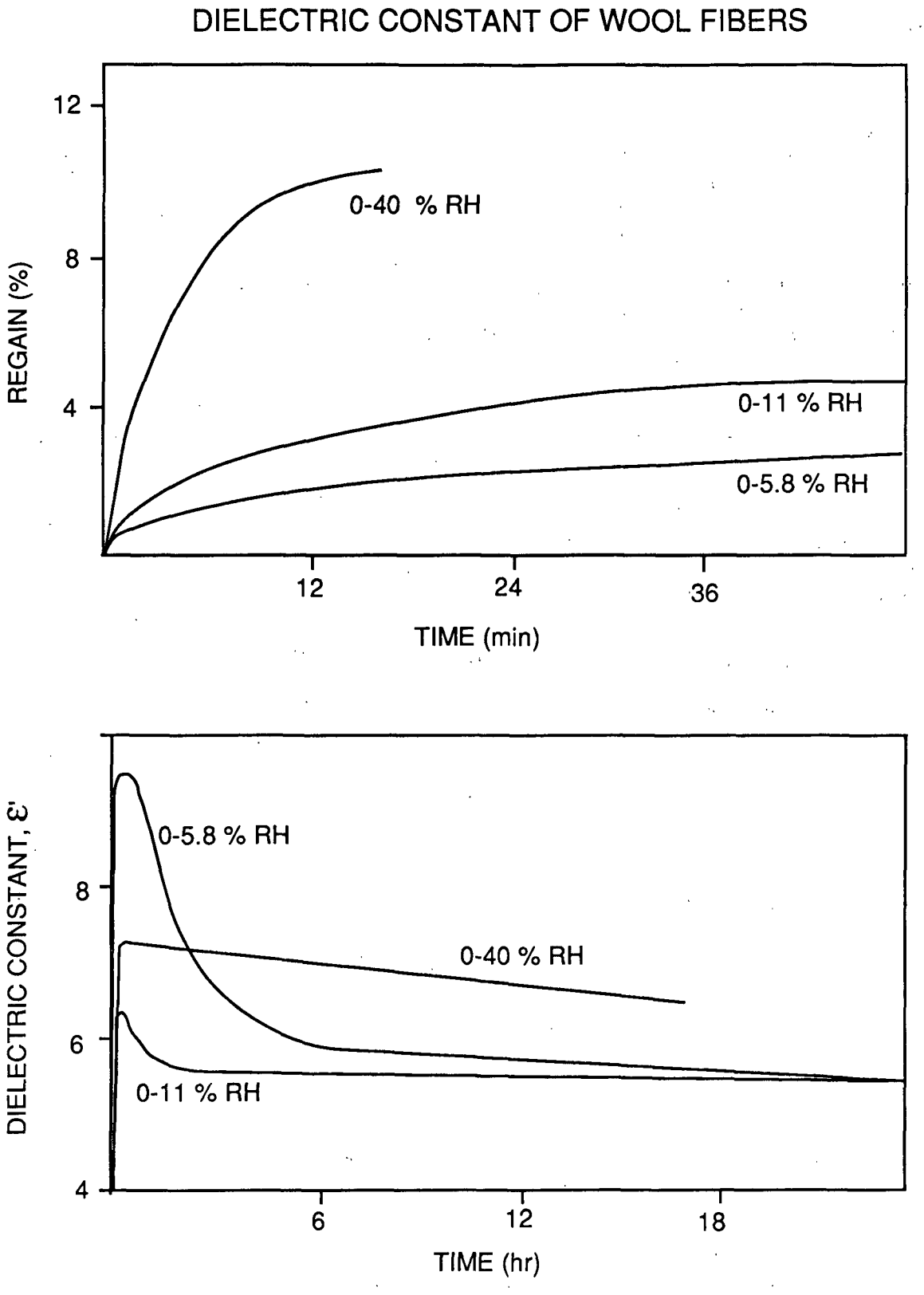

Figure 18. Dielectric constant and regain-time data for wool fibers undergoing various sorptions from initially dry states (Algie[68]).

complete understanding of these transient moisture phenomena is critical to the on-line application of ultrasound techniques, especially with regard to moisture compensation. Additional knowledge of moisture-temperature-ultrasonic modulus relations under equilibrium conditions is also desirable. The ultrasonic techniques developed at the IPC appear to be ideal for research in this area. The techniques are nondestructive, operate at low strain amplitudes, and can acquire data rapidly. For these reasons, they will be employed in modulus and loss tangent testing of cellulosic materials at various temperatures and under various equilibrium and nonequilibrium moisture conditions. A low frequency dynamic sinusoidal tensile technique is used for additional comparisons. The present study will help to clarify the importance and/or existence of transient moisture effects on paper mechanical properties measured in the linear regime.

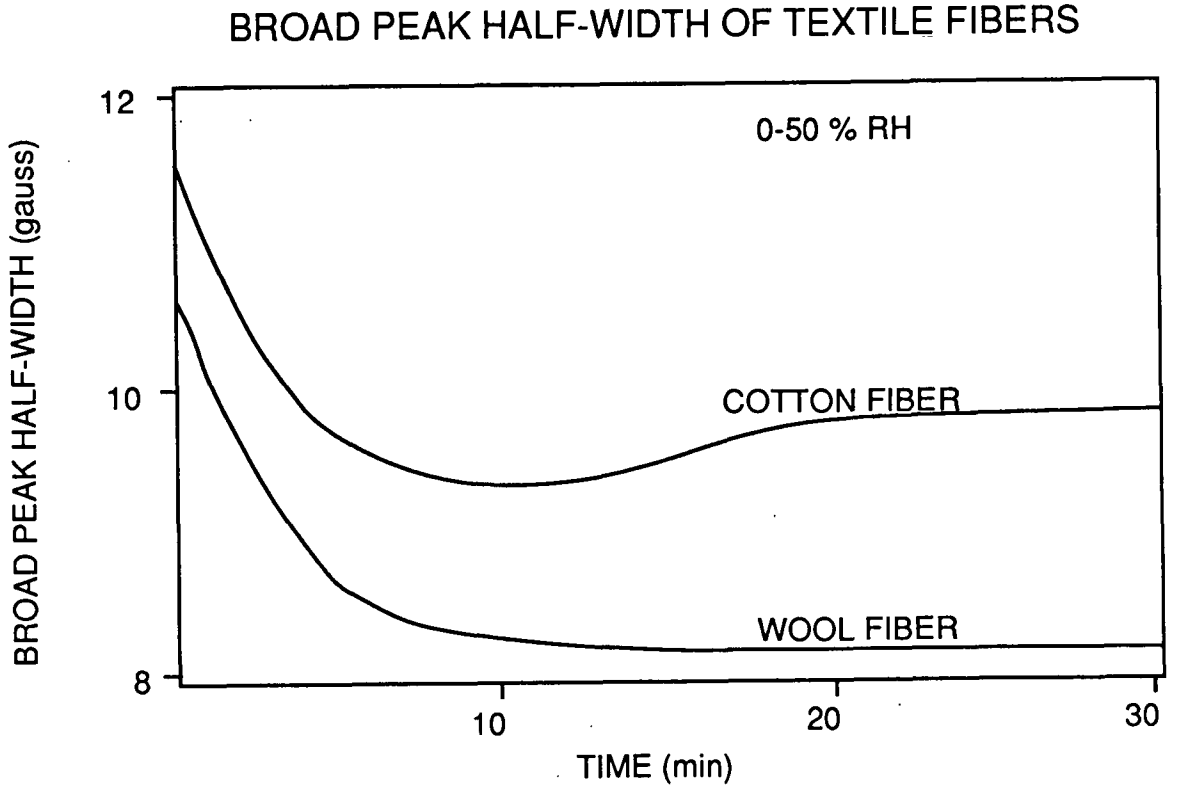

Figure 19. Broad peak half-width-time data for cotton and wool fibers undergoing sorption from 0-50% RH (Shishoo and Lundell[69]).

EXPERIMENTAL

ULTRASONIC PROCEDURES

Resonance and time-of-flight techniques were used to measure viscoelastic parameters of cellulosic materials at ultrasonic frequencies. Several commercial samples were tested including two different cellophanes, typing paper, blotter stock, an alkaline made bond paper, and two different basis weight linerboards. Although samples were chosen somewhat arbitrarily, an effort was made to include a wide variety of materials. For example, cellophane has a lower overall crystallinity than the linerboards which in turn are less crystalline than the bleached papers, as indicated by equilibrium moisture contents. Cellophane samples also differ from the others by the lack of a fibrous network, a difference in crystalline structure, and a far higher density. Blotter stock, on the other hand, is bulky, has a low modulus and is relatively square (low in-plane anisotropy ratio). Different samples also sorbed and desorbed at various rates depending upon their thickness and the openness of their structure.

The ultrasonic techniques employed in this study are complementary. For example, shear modulus measurements are possible with the time-of-flight technique but not with the strip resonance technique. Conversely, loss tangent measurements can only be made using the strip resonance technique. The range of possible sample sizes tested with each technique is also different. This allowed the various effects of sample size to be more thoroughly investigated. Other dissimilarities, which led to additional insight regarding moisture-temperature-modulus relationships, will become more apparent as the discussion proceeds.

The operation and theory of the resonance apparatus were initially described by Pankonin and Habeger[9] and are outlined below. The basic approach, which is diagrammed as a part of Fig. 20, is to determine the mass specific modulus (E/ρ) and the loss tangent ($\tan\delta$) from the frequency dependence of the standing wave vibrations in a narrow strip. The strip is coupled between a pair of ceramic piezoelectric transducers; one transducer is excited with a sinusoidal voltage; and the resulting signal at the other transducer is measured as a function of frequency. The transducers are 5 x 5 mm squares of a 2 mm thick sheet of a lead zirconate titanate ceramic (Edo Western EC-65 PZT) cut from a larger sheet using a carborundum wheel. The dimensions of the transducers were chosen to be small enough to ensure that their resonances are over 200 kHz and well above the upper range (100 kHz) of the lock-in amplifier. The piezoelectric is polarized in the thickness direction with the top and bottom surfaces acting as electrodes. The shield and active leads of a miniature coaxial cable are soldered to opposite electrodes of the transducers to provide electrical contact and physical support. Each cable is threaded through an oversized hole in an aluminum block. The cable is held in the block and acoustically isolated from the block with a silicone potting compound. The aluminum blocks are mounted on a track which allows the transducer separation to be adjusted.

Test samples are typically cut with a razor blade to lengths of 3-6 cm and widths of approximately 2 mm. Samples cut to these dimensions are easy to work with and produce fundamental and first harmonic resonance frequencies well within the range of the lock-in amplifier. Lengths as great as 20 cm and widths as wide as the transducers (5 mm) were tested without any major problems. However, long, narrow strips are difficult to handle and can crimp easily. In the present study, an effort was made to choose lengths that resulted in first

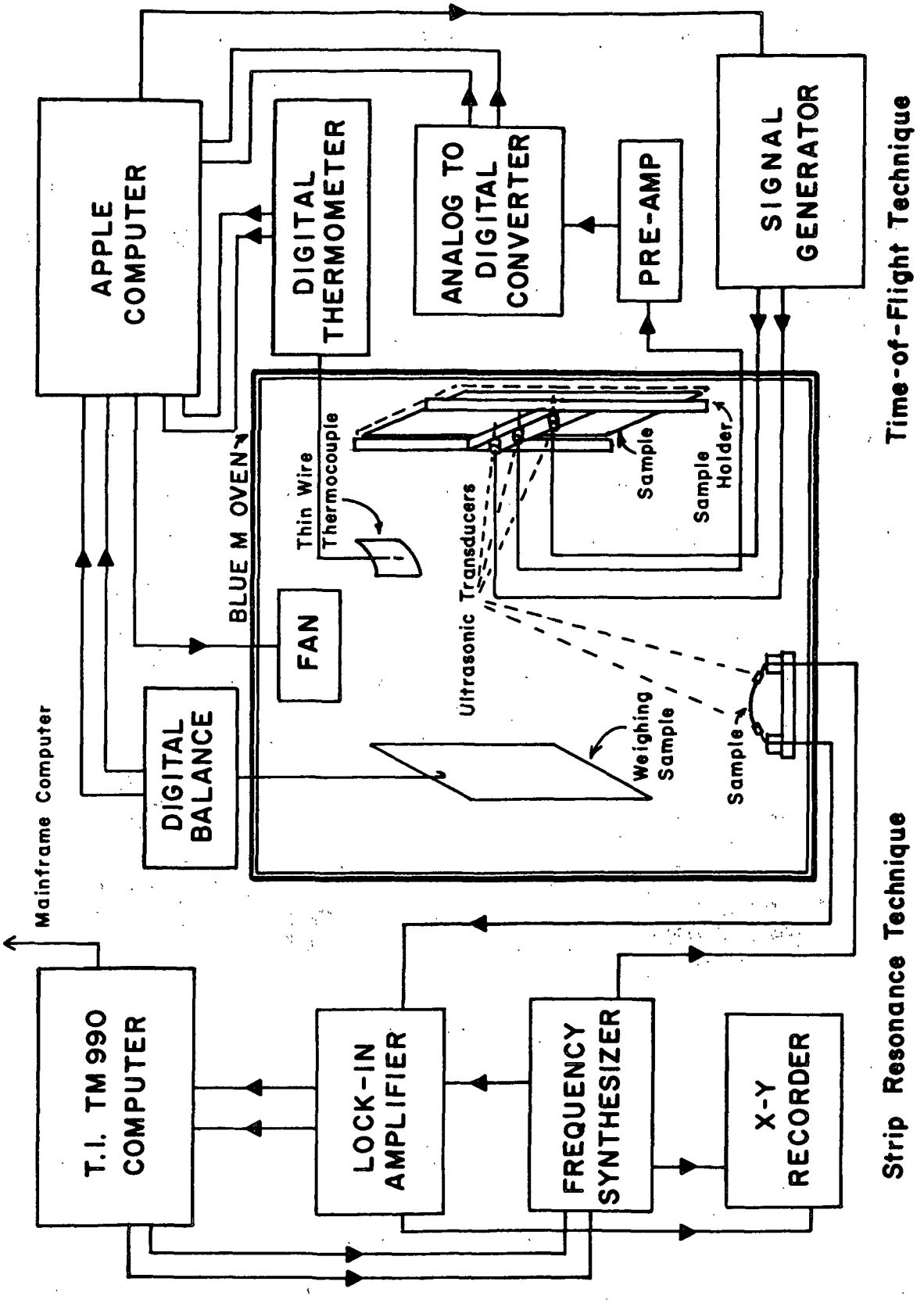

Figure 20. A schematic of the resonant and time-of-flight experiments enclosed in the variable humidity oven.

harmonic resonance peaks near 60 kHz when measured at 22°C and 50% RH. Samples are glued between the transducers using a thin layer of adhesive. The choice of adhesive depends upon the conditions of the test. Ideal adhesives resist heat and moisture, are viscous enough during application to limit wicking into the sample, and clean up readily after the completion of a test. A cyanoacrylate adhesive manufactured by Loctite Co. and designed to resist thermal cycling was used for all runs reported in this thesis. A picture of two samples with their mounting assembly is shown in Fig. 21. It can be noted from the figure that samples are bowed slightly between transducers. This simplifies the gluing operation. Bowing also minimizes the possibility of tensile stresses being set up in the samples during moisture change.

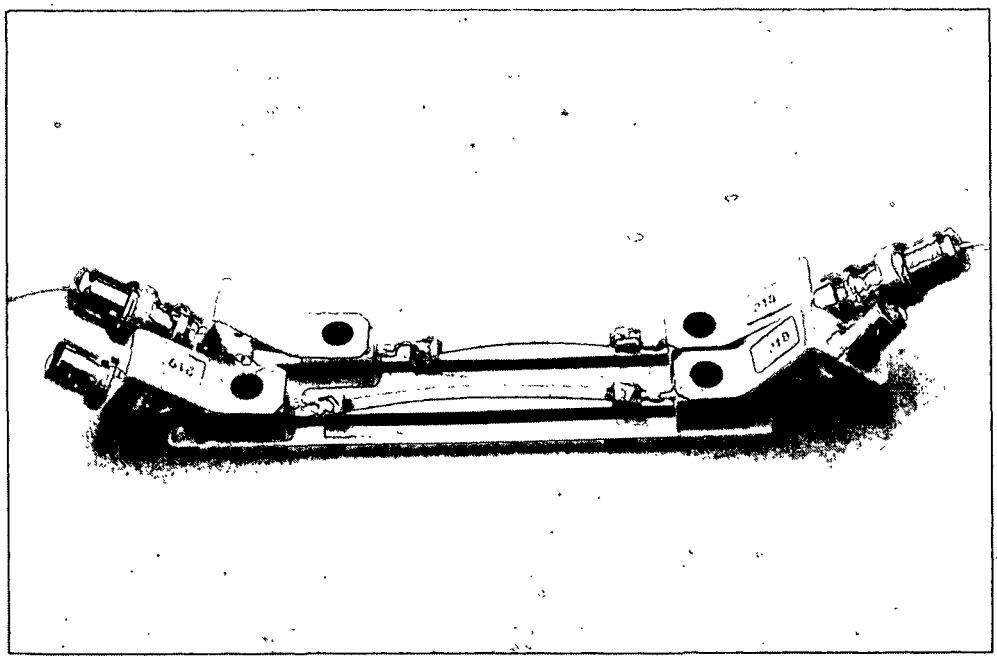

Figure 21. A close-up of the strip resonance assembly.

The transmitter excitation signal is generated by a Hewlett Packard 3325A Frequency Synthesizer. The frequency and amplitude of the synthesizer output are controlled by a Texas Instruments 9900 Microcomputer over an I.E.E.E. bus.

The sinusoidal voltage across the transmitter causes it to expand in the transverse direction exciting longitudinal vibrations in the sample. These vibrations are converted to an electrical signal by the transducer at the other end of the sample. The signal then goes to an Ithaco 393 Lock-In Amplifier which functions as a narrow band-pass filter and amplifier at the frequency generated by the synthesizer. Finally, the output of the lock-in is routed to an analog to digital converter in the microcomputer and to the Y-axis of a Hewlett Packard 7045A X-Y recorder. The X-axis of the plotter is connected to an analog output from the synthesizer that is proportional to the frequency.

When the frequency of the synthesizer is swept, the X-Y plotter generates a graph of the lock-in amplitude vs. frequency. If the sample is properly attached to the transducers, the graph contains sharp, regularly-spaced resonance peaks. Typical spectra from well-bonded and poorly bonded samples are presented in Fig. 22 and 23, respectively. As can be seen from Fig. 22, the shapes of the peaks and their locations are used to calculate the sample loss tangent and mass specific Young's modulus. It is crucial therefore, to have test specimens well bonded to the transducers. Mass specific Young's modulus is equal to $[2\ell_s f_{max}/(m+1)]^2$, where m is the order of the harmonic, ℓ_s is the sample length, and f_{max} is the frequency of the resonance peak. The loss tangent equals $\Delta f/f_{max}$ where Δf is the frequency width of the peak at $1/\sqrt{2}$ of the maximum amplitude (see Appendix I). Notice the double peak at the fundamental resonance in Fig. 23. The use of this peak would lead to erroneous modulus and loss tangent calculations.

By adjusting the sample length and concentrating on different harmonics, the frequency range of the experiment can be extended from 10 to 100 kHz. In the present study, the first harmonic was used for all data acquisition. Once

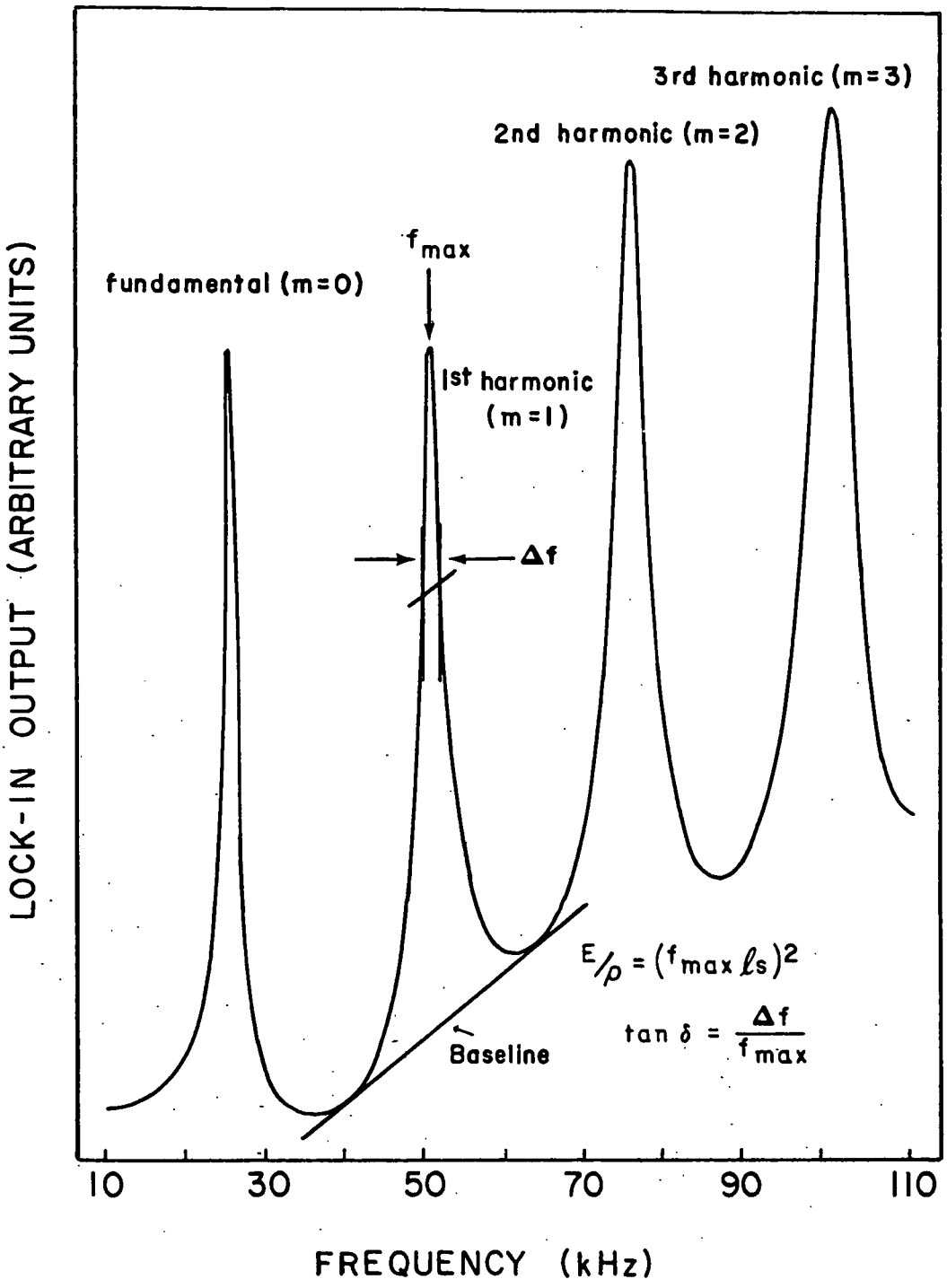

Figure 22. An X-Y plotter trace of the lock-in amplifier response as a function of frequency for a well bonded sample (the methods used for modulus and loss tangent calculations are demonstrated on the first harmonic peak).

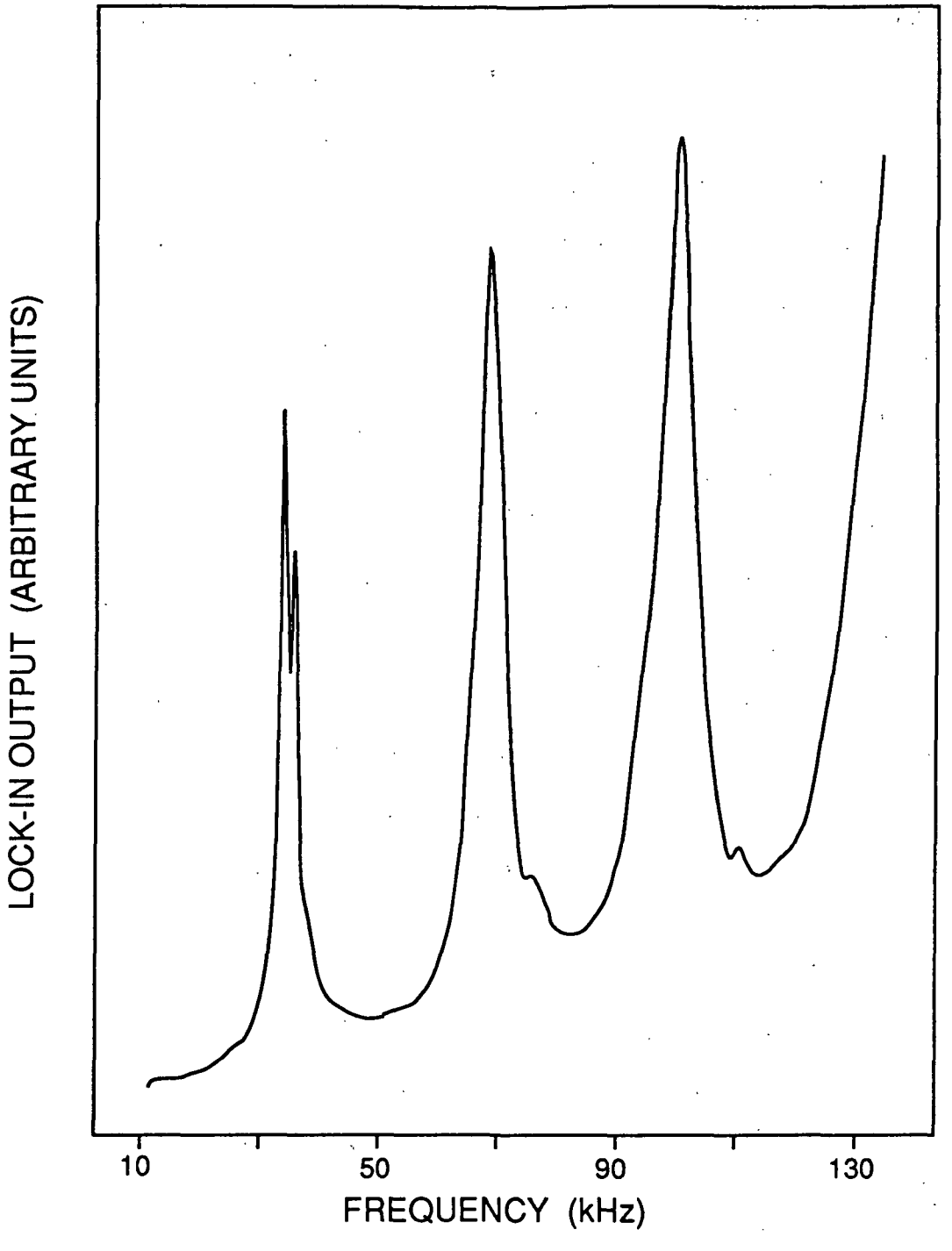

Figure 23. An X-Y plotter trace of the lock-in amplifier response as a function of frequency for a poorly bonded sample.

proper sample coupling is demonstrated by a well-formed spectrum, operation of the synthesizer is controlled by the microcomputer. A program supervises a sequence of synthesizer frequencies and lock-in output readings which allows the calculation of E/ρ and $\tan\delta$. The optimization routine used to calculate these values was slightly different than the one described earlier.[9] A modified routine was required for the present study because the old routine was inadequate in keeping up with the movement of the loss peaks that accompanies rapid moisture changes. The new program first establishes a base line by searching for the minima on each side of the peak and using an average of their amplitudes. All subsequent amplitudes are taken relative to this baseline. The maximum of the peak is then found within ± 25 Hz. Finally, the peak width is found by measuring the response at two frequencies, 200 Hz apart, near the $1/\sqrt{2}$ height on both sides of the peak. A linear interpolation is then used to calculate the frequency at the $1/\sqrt{2}$ height on each side, and these two frequencies determine Δf. Details of the new program, which is written in Power Basic, can be found in Appendix II. The new program requires approximately 5 seconds to obtain a modulus and loss tangent. The time required with the old program was closer to 20 seconds. The fact that old and new routines produce identical results during equilibrium tests is a good indication of the equivalence of the two techniques. Through the use of operator input parameters, data can also be averaged, and acquisition speed and time between tests can be changed. After modulus and loss tangent calculations are complete, values can be periodically printed to a terminal and/or sent to a mainframe computer.

Since the value of the sample length is used to calculate the strip mass specific modulus, length variance with moisture and temperature must be considered. Dimensional changes of cellulose with temperature are small[71] and are

ignored. However, there is a significant linear[42] dependence of length on moisture, and an appropriate correction must be made. Corrections were performed by measuring sample lengths at 18 and 92% RH and room-temperature using a Neenah multiple specimen paper expansimiter.[72] This device permits the lengths to be measured accurately under small loads. Sample moisture content, defined in the present study as the weight of water divided by the total weight, was then calculated at 18 and 92% RH and a linear relation between length and moisture change determined. This relation was unaffected by further humidity cycling, although a general shrinkage resulted, which in some samples (especially MD cellophane), was as large as 1.5%. Shrinkage accompanying moisture cycling is typical[73] and is a result of the relaxation of dried-in stresses. It appeared to be essentially complete after three or four cycles from 18-92% RH. Necessary adjustments to E/ρ data due to length changes were therefore performed at the completion of a run.

The time-of-flight technique is a modification of a two-transducer method described elsewhere.[74] That apparatus translated one transducer in order to achieve time-of-flight measurements at two different separations. Because of the difficulties in manipulating transducers in an environmental chamber, an apparatus with three stationary transducers was used for this temperature-moisture dependence study. The three-transducer method is also diagrammed in Fig. 20 and briefly discussed below, with emphasis on the special considerations encountered with fixed transducers.

As with the two-transducer time-of-flight method, piezoelectric bender transducers are used. They are mounted in-line to a rigid frame. The frame is of open construction so that air can circulate freely around the sample. The outer two transducers act as transmitters and the inner one as a receiver. The

receiver is 30 mm from one transmitter and 60 mm from the other. The mounting frame is part of a larger assembly designed to clamp the sample vertically between the transducers and neoprene backings. The clamping pressure can be adjusted by changing the length of a spring which holds the transducers to the backings. A picture of this frame is shown in Fig. 24.

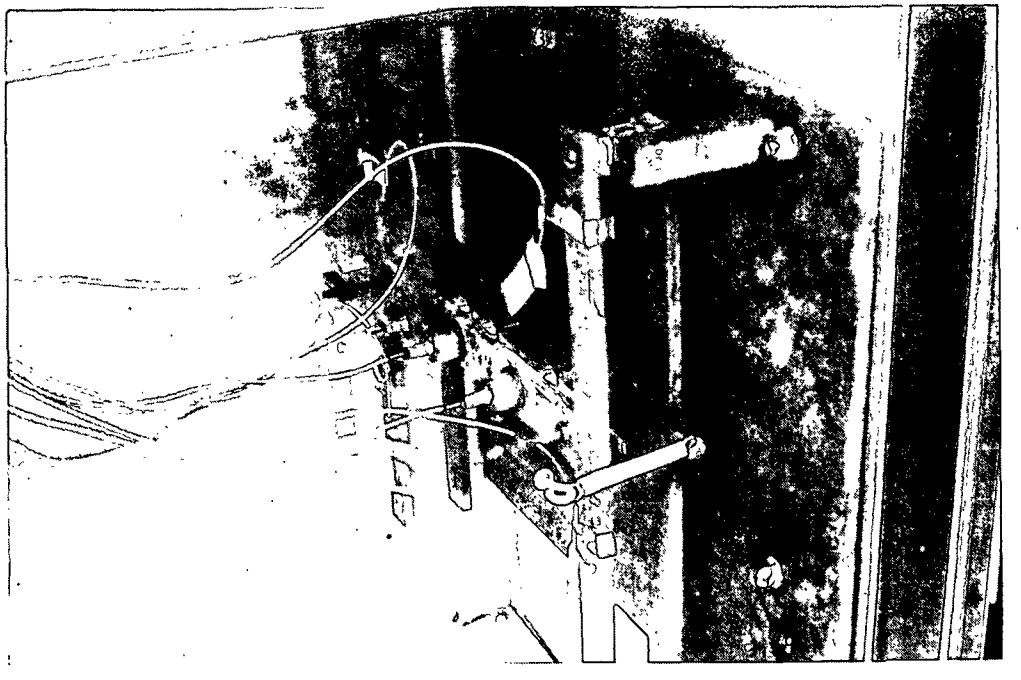

Figure 24. A close-up of the time-of-flight frame assembly.

During operation, the measurement starts with a pulse from an Apple II Plus Computer. This triggers a signal generator to send a one-cycle, 80 kHz electrical pulse to the transmitter nearest to the receiver. The transmitter oscillates in the plane of the paper. If the transducers are aligned so that this oscillation is parallel to their separation, a longitudinal plate wave is generated in the sheet and is detected by the receiver. If oscillation is perpendicular to transducer separation, a shear wave results. In either case, the received signal is amplified by a Panametrics 505AE Preamplifier, sent to a

Biomation 805 Transient Recorder for analog-to-digital conversion, and transferred to the Apple for data analysis. Next, the far transmitter is excited and the data gathering process is repeated. The resulting signals are roughly sinusoidal waves with initial dead times.

The Apple determines a time-of-flight difference between the signals from the near and far transmitters by finding the maximum in the cross-correlation function of the first half-cycles. The initial step in the cross-correlation procedure is to apply a time shift to the far transmitter signal. Unless overridden by the operator, a default, dependent upon the test mode, is used to determine the magnitude of this initial time shift. The program then multiplies each data point from the near wave (up to the end of the first half-cycle) by the equivalent data point from the shifted wave and sums the values to obtain a cross-correlation function for this particular offset. The far wave is then shifted in time by an additional increment and another cross-correlation calculation is made. This procedure is repeated until a maximum cross-correlation function is found (i.e., when the near and far half-cycles line up). Finally, in order to determine a time-of-flight velocity, the difference in the distances between the transducer spacings is divided by the offset time required to produce the maximum cross-correlation function. The cross-correlation procedure has the advantage of using the first half-cycles in their entirety to calculate the velocity rather than just a point on these cycles. Signal-to-noise ratio is improved by taking multiple near and far signals and programming the computer to perform digital signal averaging.

When narrow strips are tested with the bender transducers aligned for longitudinal wave generation, the velocity squared is equal to the mass specific Young's modulus, E/ρ. However, if sheets whose width is large compared to the

wavelength of sound are tested, the velocity squared is a mass specific planar stiffness, C/ρ. The planar stiffness, C, is equal to $E/(1-\nu_{12}\nu_{21})$, where the ν_{ij}'s are the in-plane Poisson ratios. If the transducers are oriented for shear waves, the velocity squared in the extended sheet is G/ρ, where G is the in-plane shear modulus. In comparison with the two-transducer approach, this technique is handicapped in that measurement of an accurate velocity depends on matching the transmitter transducers and their coupling to the sample. Therefore, absolute values are somewhat in question, but relative variations generated by moisture and temperature changes are valid.

In order to get a feel for variations in mass specific modulus and loss tangent values measured using these techniques, linerboard samples were tested at 50% RH and 23°C. The cross direction longitudinal results from tests on ten samples are shown in Table 1. Standard deviations in mass specific modulus calculated on a percent basis were typically around 5% from spot to spot on a given sample or between samples, regardless of the technique used. Larger deviations in loss tangent data can be noted and are indicative of the difficulty in making these types of measurements. It must be emphasized that much of the deviation in measurements is due to variations between samples. When a single sample is used for an entire run, measured modulus and loss tangent standard deviations are smaller. Table 1 can also be used to compare average mass specific modulus values from different techniques. The average cross direction mass specific Young's modulus calculated using the strip resonance technique is seen to be around 4% lower than values obtained from strip time-of-flight measurements. This result is typical. Strip resonance data were usually between 5 and 10% lower than strip time-of-flight data. Reasons for the differences are not well understood. The questionable validity of the absolute values

obtained with the three transducer time-of-flight technique has already been mentioned. Also, imperfect sample transducer coupling may lead to decreased modulus values. It is believed that reduced coupling occurs in the strip resonance samples during moisture cycling as they attempt to expand and contract near the transducer-sample interface but are held rigidly in place by the adhesive. Slight increases in loss tangent and decreases in mass specific modulus were often found to accompany moisture cycling. However, these changes were usually small, somewhat erratic, and therefore difficult to quantify. Finally, the lower frequencies employed when using the strip resonance technique (30-60 kHz) would tend to result in slightly lower mass specific modulus values relative to time-of-flight technique (60 or 80 kHz) values.

Table 1. Typical % deviations in ultrasonic data[a] measured at 50% RH, 23°C.

Technique[b]	Mode[c]	Harmonic	V_o^2 $(km/sec)^2$	S.D. (%)	Tanδ	S.D. (%)
B	CDL	--	5.01	± 4	--	--
C	CDL	--	3.56	± 6	--	--
A	CDL	Fund.	3.43	± 3	0.0350	± 7
A	CDL	1st	3.50	± 1	0.0345	± 8
A	CDL	2nd	3.45	± 5	0.0347	± 16
A	CDL	3rd	3.32	± 4	0.0355	± 19
A	CDL	4th	3.39	± 2	0.0348	± 6

[a]Commercial linerboard; basis weight 69 lb/1000 ft^2 (337 g/m^2); thickness 480 μm; ten samples averaged.
[b]A: Strip resonance.
B: Sheet time-of-flight.
C: Strip time-of-flight.
[c]CDL: Cross machine direction longitudinal.

A 28% difference between strip and sheet time-of-flight squared velocities can also be noted. As mentioned earlier, squared velocities measured in sheets should be greater than those obtained in strips by a factor of $1/(1-\nu_{21}\nu_{12})$. Squared velocities in sheets are expected to be approximately 10% greater than those in strips if an average value of 0.3 is used for the Poisson ratio. However, in order to explain the 25% difference, the sample would have to have an unrealistically high average Poisson ratio of 0.5. Figure 25 shows additional squared velocity data obtained by cutting various samples to narrower and narrower widths. Data are normalized for ease of comparison. High caliper samples are noticeably damaged as sample width is decreased and resulting continuous decreases in squared velocities occur. Low caliper samples, however, where damage due to cutting is not apparent, reach a plateau region where strip squared velocities remain around 20% lower than original sheet squared velocities. Further decreases in sample width have no apparent effect on values obtained. Therefore, damage due to sample cutting appears to be by itself, an inadequate explanation for the inordinately large differences seen between strip and sheet velocities.

Oven

In order to study the effects of moisture on the ultrasonic moduli at a variety of temperatures, a modified Blue M Model CF Temperature/Humidity Chamber was used. A schematic of the humidity control system is shown in Fig. 26. The air temperature in this oven can be controlled at any value between ambient and 105°C. Relative humidity depends on the temperature in a cooling bath at the bottom of the chamber. Bath temperature is determined by the temperature and flow rate of water into the bath, the level of the bath, and the heat supplied to the bath water by a submerged heating element. The bath level is fixed by

adjusting the height of an overflow pipe, while a valve controls the flow rate into the oven. Cooling water is supplied by a 70 gallon insulated tank of ice-water. The water flows by gravity from the tank into the oven bath where it is heated. It eventually flows out the overflow pipe and into a 2 gallon holding tank. In an effort to minimize the water and cooling demand of the system, a recirculating pump periodically returns this water to the ice tank. A special fan, which can be switched rapidly on and off by an Apple computer, is installed at the top of the chamber. The fan vigorously forces air past the bath and ensures that humidity and temperature are uniform throughout the chamber.

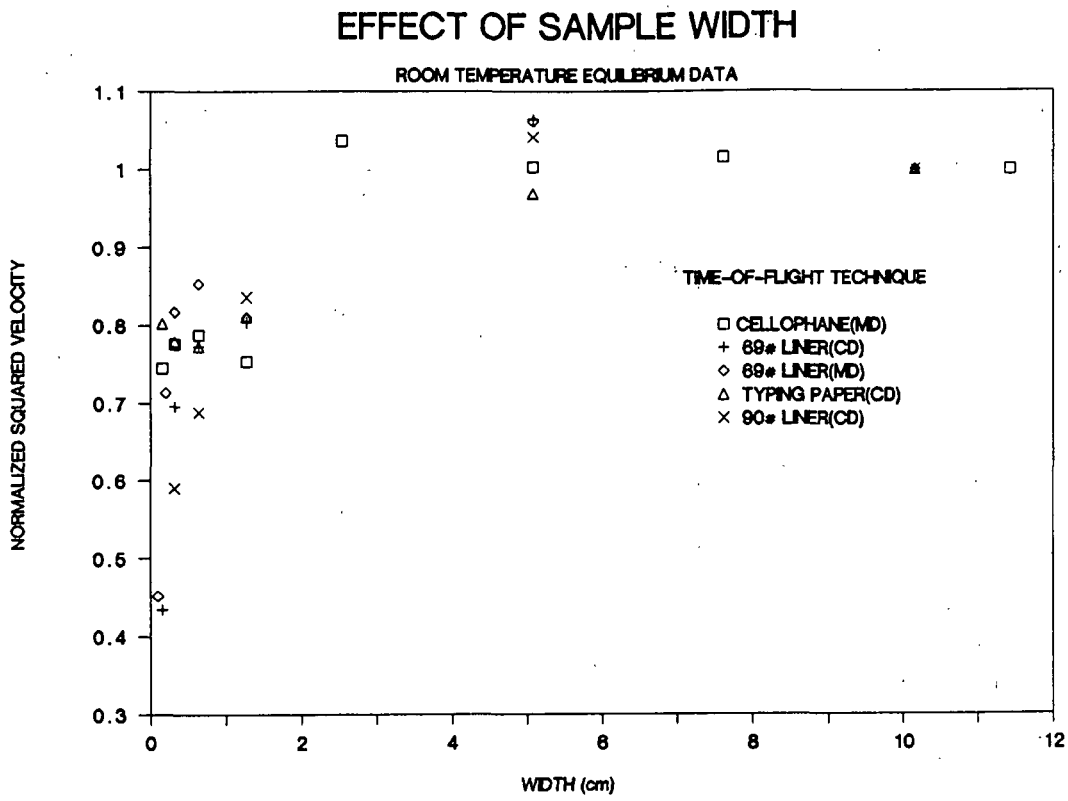

Figure 25. Time-of-flight normalized squared velocity-sample width data for various samples.

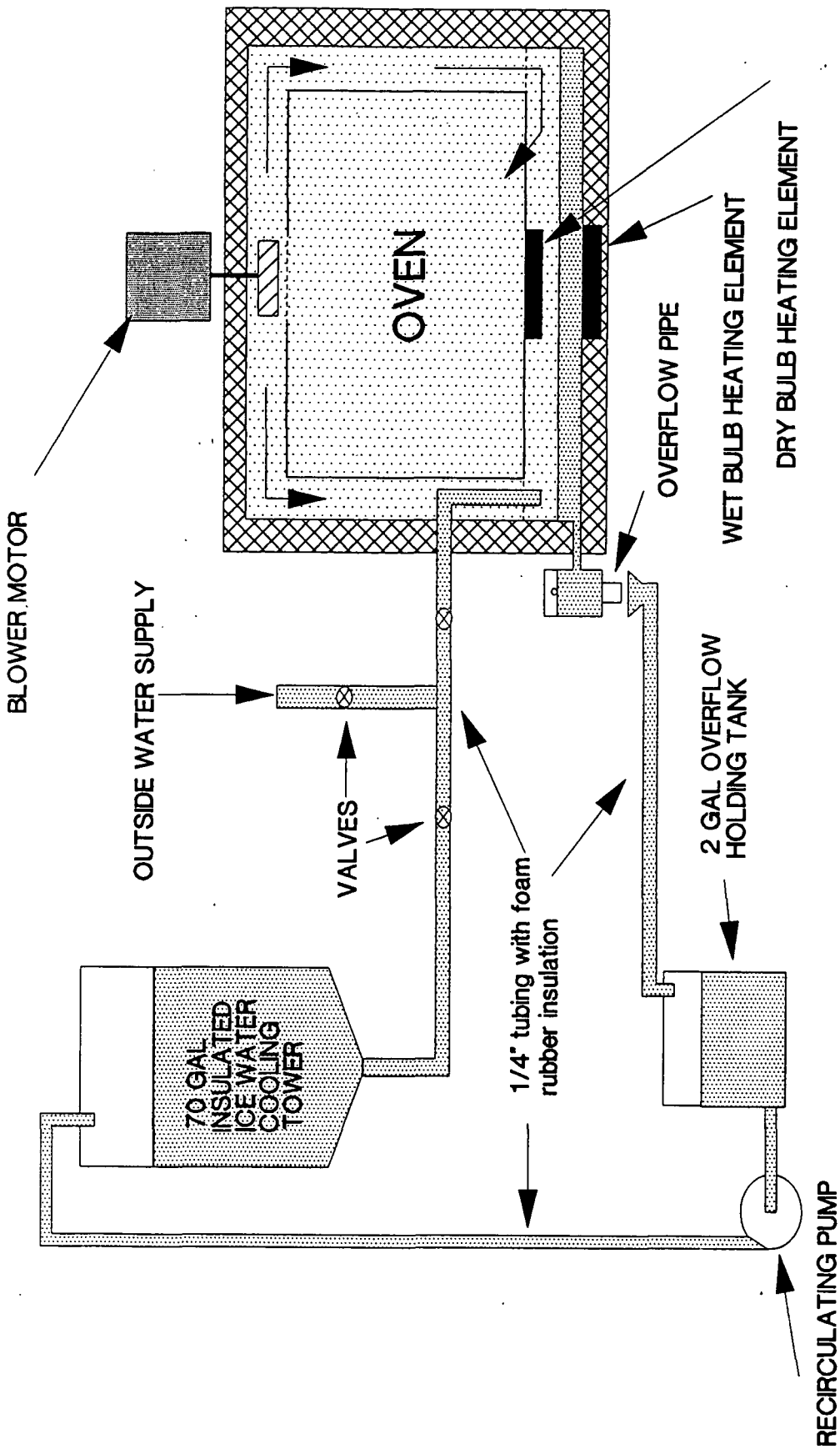

Figure 26. A schematic of the oven humidity system.

Moisture content is determined by weighing a sample similar to the one being tested with a Mettler PE 360 Balance that is capable of weighing hanging objects. The balance is isolated from oven vibrations by placing it on a platform which is cantilevered above the oven from a cement wall. A thin wire sample holder attaches to the bottom of the balance and extends through a small hole into the oven. A heating lamp is aimed at the hole to ensure that there is no condensation on the sample holder where oven and room air meet. The digital interface existing between the balance and the Apple allows the computer to obtain sample weight at any time by stopping the fan and reading the balance. Moisture content can later be calculated from the oven-dry weight (12 hours at 105°C) of the weighed sample. The use of such a technique for moisture calculation was made viable by the fact that oven conditions were not severe enough to cause the type of degradation that might lead to changes in the oven-dry weight of samples over the extended time periods of the runs.

Originally, the sample weighed for moisture determinations was also used for velocity measurements. This was made possible through the use of a stepping motor capable of lifting the transducers off the sheet during weighing. In a typical weighing sequence the motor would first lift the transducers from the sheet. The fan would then be shut off and turbulence allowed to die down for four seconds. After weighing was complete the transducer would again be brought into contact with the sample and the fan turned on. This method was abandoned, however, due to the relatively large amounts of scatter it produced in the time-of-flight data. Changes in coupling caused by the transducers seating into the sample differently after each weight determination were believed to be the primary reason for the lack of reproducibility. Fortunately, turbulent conditions in the oven made sample location unimportant with regard to moisture content or

rate of moisture change. This result was inferred by placing the strip resonance assembly at various locations in the oven and measuring the rate of mass specific modulus change during sorptive and desorptive conditions. The rate of modulus change was found to be independent of the assembly location in the oven, allowing a separate weighing and testing strategy to be adopted and resulting in less scatter.

Temperature is measured using a Fluke 2170A Digital Thermometer and 75 μm diameter copper-constantan thermocouples. There is a digital interface between this thermometer and the Apple computer. Samples tested for temperature are approximately 3 cm square. As was the case for moisture measurements, the temperature of a sample identical (except for size) to the one being tested is measured. This is accomplished by prying the layers of a sample apart and imbedding a thermocouple. When samples tested are too thin to separate into layers the thermocouple is sandwiched between two samples and the edges sealed with masking tape. In this way the temperature on the inside of the sample is measured. It should also be noted that the diameters of the thermocouples, being quite small, have very little heat capacity and respond rapidly to temperature changes. When a room temperature thermocouple is clasped between the thumb and forefinger, temperature rises are complete within five seconds. As will be seen, rapid thermocouple response is very important during transient moisture runs.

Equilibrium Data Acquisition

A typical equilibrium run, where temperature is constant and moisture changes slowly, proceeds as follows. The dry bulb heating element is adjusted to obtain the desired air temperature. When the oven reaches this temperature, the valve controlling the flow of the cooling water is fully opened, allowing a

maximum amount of cooling water to flow through the system. This produces the minimum possible relative humidity in the oven at the given air temperature and bath depth. After stabilizing the oven for an hour, the flow control valve is closed. This causes the water in the cooling bath to slowly heat up and the relative humidity in the oven to increase. Depending upon the air temperature in the oven and the depth of the bath, this heating period can take from several hours to a day. Eventually the bath temperature reaches a maximum and the sample moisture content attains its maximum value. Due to a slow loss of moisture from the system, water in the bath continues to evaporate. As the bath dries up, the relative humidity begins to fall and a moisture content that is close to the one obtained originally at maximum flow rate of cooling water is approached. In this manner, the samples are slowly cycled from dry to wet to dry. In order to stabilize the sample by relieving dried-in stresses, the oven is cycled in this manner two times before actual testing is begun. This also helps to seat transducers firmly into the sample.

During a typical equilibrium cycle, data are taken approximately every 20 minutes. The sample temperature and mass, the frequency of the strip resonance, the peak width of the resonance, and the time-of-flight velocity are all regularly measured. These measurements are used to calculate the equilibrium moisture dependence of the sample loss tangent and mass specific modulus during sorption and desorption. After a cycle is complete, additional cycles at the same temperature can be performed, or the temperature can be altered and different modulus *vs.* moisture data generated. Although time between data acquisition points is typically 20 minutes during equilibrium tests, the Apple program affords the operator a great deal of flexibility in adjusting this or a number of other test parameters. For example, preliminary tests were performed

in order to verify that data obtained in a slowly changing moisture environment were, in fact, identical to data obtained under more stable conditions. This was done by monitoring samples as they slowly desorbed moisture. After desorption was essentially complete, testing was continued for 48 hours to determine whether any additional changes in moduli values would occur. In order to minimize the amount of data acquired, the program was set up to make measurements less frequently as run time proceeded. No additional changes in moduli were observed, indicating that the slowly changing moisture environment (where air and bath temperatures are different) closely approximated equilibrium conditions (where air and bath temperatures are identical).

The program used to control the time-of-flight technique is written in Apple Basic and can be found in Appendix III. It was initially designed for equilibrium testing but was modified considerably so that it could be used for transient moisture tests as well.

Transient Data Acquisition

In order to produce humidity conditions resulting in rapid sample moisture changes, different techniques are required to control the oven. Similar to equilibrium data acquisition, the dry bulb heating element is first adjusted to obtain the desired air temperature. Also, the flow control valve is again held open. In the desorption transient case, however, the overflow pipe is removed resulting in a minimum bath depth. These procedures minimize the average dwell time of water in the system and lead to a minimum bath temperature. This in turn produces the minimum possible moisture condition at the given air temperature. Once the system is stabilized a sorption run can be started.

Sorption runs are begun by closing the flow control valve. Three base-line data points are then acquired, using the time-of-flight technique, while water in the cooling bath drains. As the third data point is being obtained drainage from the system becomes negligible and the overflow pipe is inserted. Immediately following the acquisition of the third data point, three liters of heated water are poured into the bath. This produces an increase in oven RH and results in rapid sample sorption. The rate and magnitude of the sorption depend upon the temperature of the heated water, the air temperature of the oven, and the type of sample being tested. For most runs, water heated to a temperature identical to that of the oven air was used. As the fan effectively agitates the air in the oven chamber, the majority of the sorption is complete in less than 20 minutes. During a transient moisture run, data are obtained approximately every 25 seconds with the time-of-flight technique and every 5 seconds using strip resonance. If five ultrasonic signals are averaged instead of the 25 typically used, the time required for time-of-flight data acquisition can be lowered to around 15 seconds.

At the completion of a sorption run, a desorption run can be made. Desorption runs are started by removing the overflow pipe and beginning data acquisition. Three base-line data points are again obtained while water drains from the system. After the third point is obtained, the flow control valve is completely opened allowing ice water to enter the bath and desorption to occur. As was the case for sorption, desorption is quite rapid, becoming essentially complete in less than 30 minutes. When following the described procedures, sorption is slightly faster than desorption. However, in either case, transient runs of thirty minutes are usually adequate to encompass the majority of the moisture changes.

Several difficulties are encountered and must be considered when attempting to use the present system to measure mass specific modulus in a changing humidity environment. Because the sample moisture is changing very rapidly, less averaging is possible. This, of course, leads to a certain and unavoidable amount of increased data scatter. Another problem can arise from the fact that simultaneous moisture and mass specific modulus measurements are not possible. In order to handle this problem and maintain simplicity in the computer program, the moisture content at the time of modulus measurement is estimated using previous moisture measurements to calculate a rate of moisture change, and then extrapolating ahead in time. Sample size is also an important variable to consider when transient moisture runs are made. Sorption and desorption rates increase slightly as samples are cut to smaller dimensions. The size of the sample used to obtain weight determinations must therefore be identical to the one being measured ultrasonically. If the two differ, erroneous moisture contents can be paired with measured mass specific modulus values. In many instances, multiple samples must be weighed in order to increase the accuracy of the moisture measurement. This is especially true when strips rather than sheets are tested. In these cases, care must be taken to ensure that samples being weighed are adequately spaced (1-2 cm). If small samples are placed too closely to one another, air flow around samples becomes restricted and they begin to sorb and desorb as a single, large sample rather than as small, individual ones. Weight determinations were therefore made using a holder designed to provide plenty of separation.

LOW FREQUENCY PROCEDURES

Cyclic loading tests were used to obtain mass specific modulus and loss tangent data at low frequencies. As previously discussed, because paper is a

viscoelastic solid, a stress-strain hysteresis loop occurs during cyclic loading (Fig. 2). For small strains the area contained within this loop, L, as well as the area below the loop, S, determine the loss tangent [Eq. (13)], whereas the slope of the loop is a measure of the storage modulus.

Cyclic tests were performed using a 200 lb load cell and an 1122 series tensile tester manufactured by Instron. An extensiometer manufactured by Instron (catalog No. 2630-D13) was used to measure deformation. The tensile tester contains a load cycling unit which allows the sample to be cycled in tension between two different loads. The load limits are independently adjustable so that a variety of different cyclic strain amplitudes as well as initial strain offsets are possible. Load limits, and hence the resulting strains, can be varied at any time but were usually held constant within a given run. With this testing device, the sample is subjected to a constant rate of deformation. This rate is governed by the crosshead speed and is also adjustable. As was the case with the load limits, crosshead speed was not changed within runs but was varied between runs. Within a run, the test frequency, strain amplitude, and strain offset are determined by the dimensions and modulus of the sample, the crosshead speed, and the loads cycled between. Therefore, changes in modulus resulting from sorption and desorption cause changes to occur in frequency, strain amplitude, and strain offset. Loading and unloading using a constant rate of deformation also results in a roughly triangular rather than a sinusoidal loading scheme. The consequences of these and other problems inherent to the experimental setup will be discussed later in the thesis.

Samples at various moisture contents were sealed in plastic bags before testing. Due to the impracticality of attaching the extensiometer directly to the sample inside the plastic bag, it actually measures the deformation between

3 mm diameter brass rods which are rigidly connected through the use of specially designed attachments to the flat plates of the Instron 200 pound screw-type plate clamps. A picture of the clamping assembly is shown in Fig. 27. Deformation between the plate clamps is assumed identical to sample deformation. However, past studies have shown that plate clamps can lead to sample slippage and subsequently to erroneous modulus and loss tangent calculations. Line clamps deliver better results.[75] Because the screw-type clamps were easier to use and could be outfitted more readily with the required brass rod attachments, preliminary tests were performed to compare the two types of clamps. No measurable differences in loss tangent and mass specific modulus data were found between line and plate clamps when testing linerboard samples under equilibrium, sorptive, and desorptive conditions and at strain amplitudes less than 0.15%. These results indicated that the use of plate clamps in the present study was reasonable. This is not a surprising result considering that small loads were used in an attempt to remain in the linear regime, and clamp slippage problems were therefore not expected. Samples were cut shorter than the bags and clamped so that the bags were not in tension during the cyclic tests. In order to ensure that the plastic bags had no influence on the results obtained, loss tangent and mass specific modulus values were obtained with and without bags for several linerboard samples under equilibrium moisture conditions and at strain amplitudes less than 0.15%. Again, no measurable differences were observed.

The tensile tester load and deformation outputs are direct current voltage signals obtained from a programming unit located in the back of the control console. These signals are sent to a 12 bit, 16 channel analog to digital converter (Dash-16 manufactured by Metra Byte Corp.) located in a PC. The personal computer along with developed software allow these digital signals to

be used in conjunction with a number of inputted parameters to calculate mass specific modulus, loss tangent, cyclic frequency, strain amplitude, and initial strain offset as a function of time. The main portion of the software, written in Turbo Pascal, can be found in Appendix IV. The basic strategy is briefly discussed below.

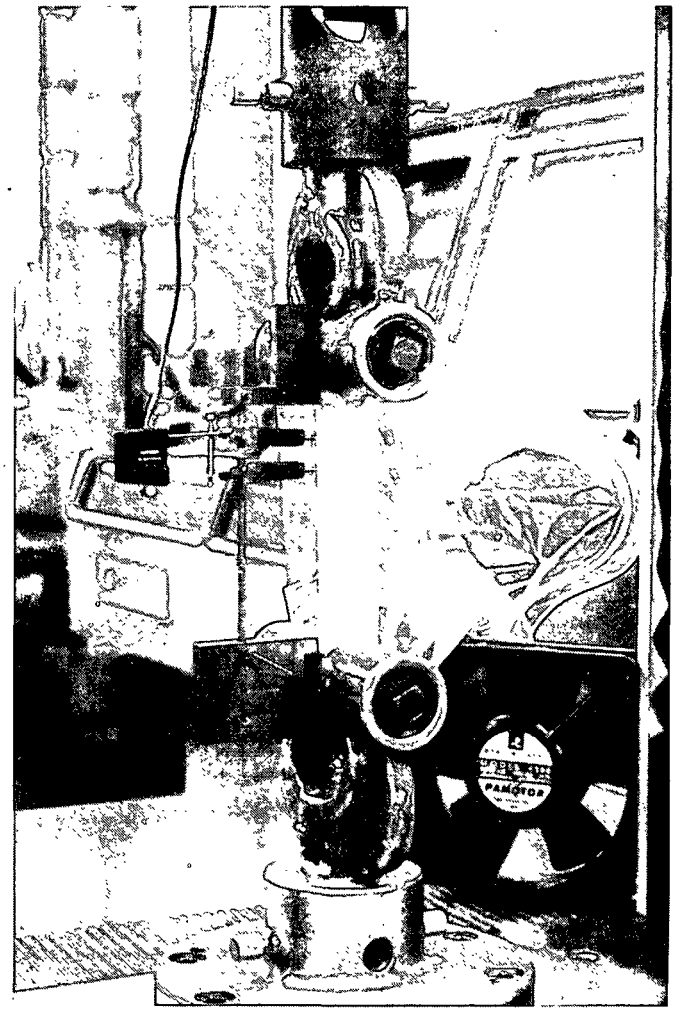

Figure 27. A picture of the Instron clamp assembly.

Adjustable input parameters include the sample name, length, basis weight and width, the full scale load and deformation, the crosshead speed, the estimated elongation, the number of crosshead cycles averaged per data point, the number of data points within a run, the gain of the analog-to-digital converter, and the number of raw data signals per cycle for loss tangent and mass specific modulus calculations. All data reported in this thesis were obtained using 500 raw data signals per cycle and were averages of three cycles per data point. Preliminary tests showed these values to be a good compromise between data quality and test speed. The acquisition of a data point starts with the alternate conversions of raw load and deformation signals by the A/D converter. The rate that conversions are performed is proportional to the test frequency which, in turn, is equal to the crosshead speed divided by four times the strain amplitude. After enough raw data for four complete cycles have been obtained, A/D conversions are terminated and analysis begins. The program first finds the maximum and minimum loads and calculates an average load, l_a. It then begins searching the raw data for the location in the load-deformation cycle where the load crosses l_a from below (i.e., where the load and deformation are both increasing). All raw data before this point are thrown out. The above technique is required because the program has no control over the tensile tester, and the location in the load-deformation cycle at which raw data acquisition begins varies. Starting from this location is critical for calculating tanδ in a changing moisture environment. In order to simplify calculations, as discussed in Appendix V, the first raw data point used is the crossover load, l_1. Data before the initial crossover point can't be used, and in some cases, may include close to a full cycle. This explains the reason for gathering raw data from four complete cycles when only three cycles are used in the calculations. Once the crossover load has been found, actual mass specific modulus and

loss tangent values can be determined. The crossover load along with the immediately preceding, e_o, and succeeding, e_2, deformation points are used to calculate an area under the load-deformation curve.

$$a_1 = (e_2 - e_o)l_1$$

The next area under the curve is:

$$a_2 = (e_4 - e_2)l_3$$

where l_3, the next load and e_4, the next deformation are used. This area is then added to the first area. In this manner, all the individual areas obtained in going around the load-deformation cycle three times are calculated until the load again crosses over l_a:

$$a_t = \sum_{i=1}^{n} (e_{i+2} - e_i)l_{i+1}$$

The deformation before this crossover load is then used in conjunction with the initial deformation and l_a to obtain a final area,

$$a_f = (e_o - e_{last-1})l_a$$

and close up the loop. All of these areas are then summed to obtain a total area, A_t:

$$A_t = a_t + a_f$$

Notice from Fig. 2 that the areas obtained on the down slope of the load-deformation cycle are negative. Also, because three cycles are averaged, A_t is nearly three times the L calculated previously. The small difference between A_t and L caused by the lack of loop closure is discussed later. When going around

the cycle three times, the maximum and minimum deformations, e_{max} and e_{min}, are also found. The two loads on either side of these deformations are then averaged to obtain the load at maximum and minimum deformation (l_{emax} and l_{emin}). Finally, loss tangent and mass specific modulus are calculated as follows:

$$\text{Tan}\delta = 4A_t/3[\pi(l_{emax}-l_{emin})(e_{max}-e_{min})] \tag{17}$$

$$E/\rho = (l_{emax}-l_{emin})\text{length}/[\text{width}(e_{max}-e_{min})\text{basis weight}] \tag{18}$$

Transient Data Acquisition

During an experimental run the sample is clamped in the Instron and cyclic loading is begun. Initially, slight changes in the size and location of the stress-strain hysteresis loop will occur due to the effects of work hardening and sample creep. The magnitude of these changes depends primarily on the strain amplitude and offset. A study by Kubat, Nyborg, and Steenberg[76] gives an indication of just how stringent the strain amplitude and offset requirements are, in order to ensure that work hardening is negligible. They found a strain amplitude of 0.075% and an offset of 0.17% to result in little or no change in the CD modulus and specific damping values of kraft paper when cycled at 0.5 Hz and 45% RH. Slight increases were, however, found at 85% RH. Figures 28 and 29 show cyclic loading MD mass specific modulus and MD loss tangent results obtained in the present study for a typing paper tested at a frequency of 0.2 Hz, a strain amplitude of 0.085%, a strain offset of 0.2%, and a relative humidity of 50%. In this case the seemingly small strain amplitude produced work hardening effects resulting in appreciable increases in mass specific modulus and decreases in loss tangent.

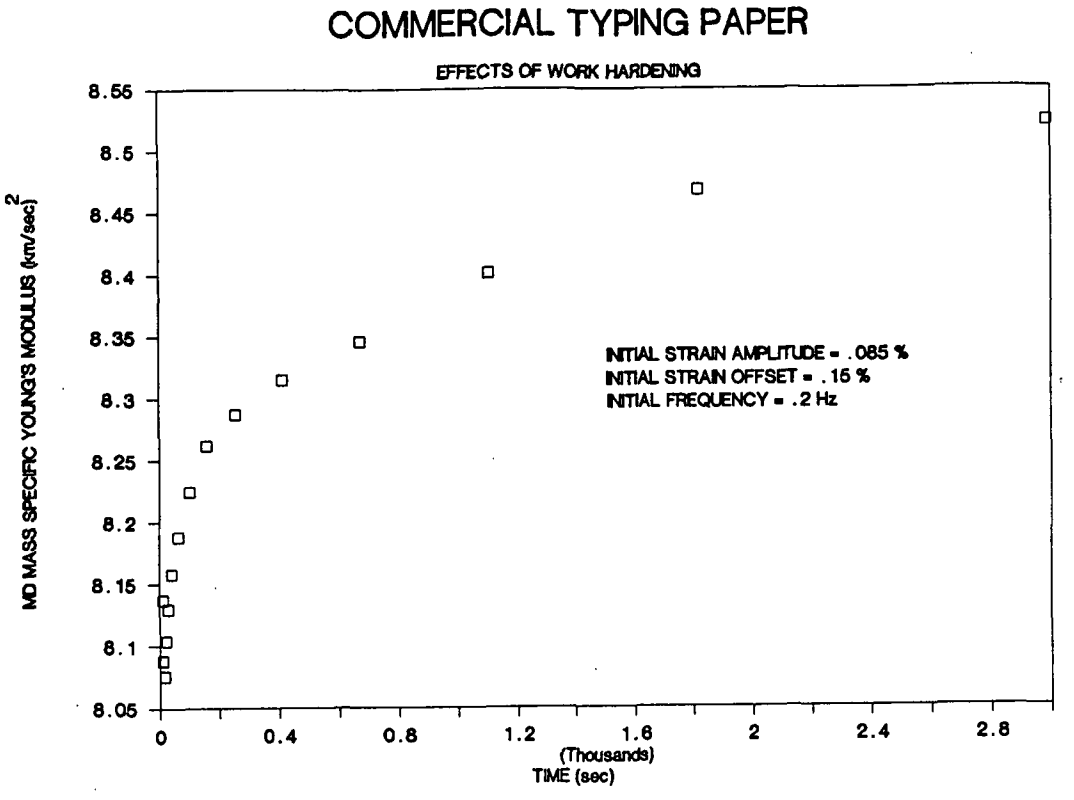

Figure 28. Typical MD mass specific Young's modulus-time data for commercial typing paper showing work hardening effects.

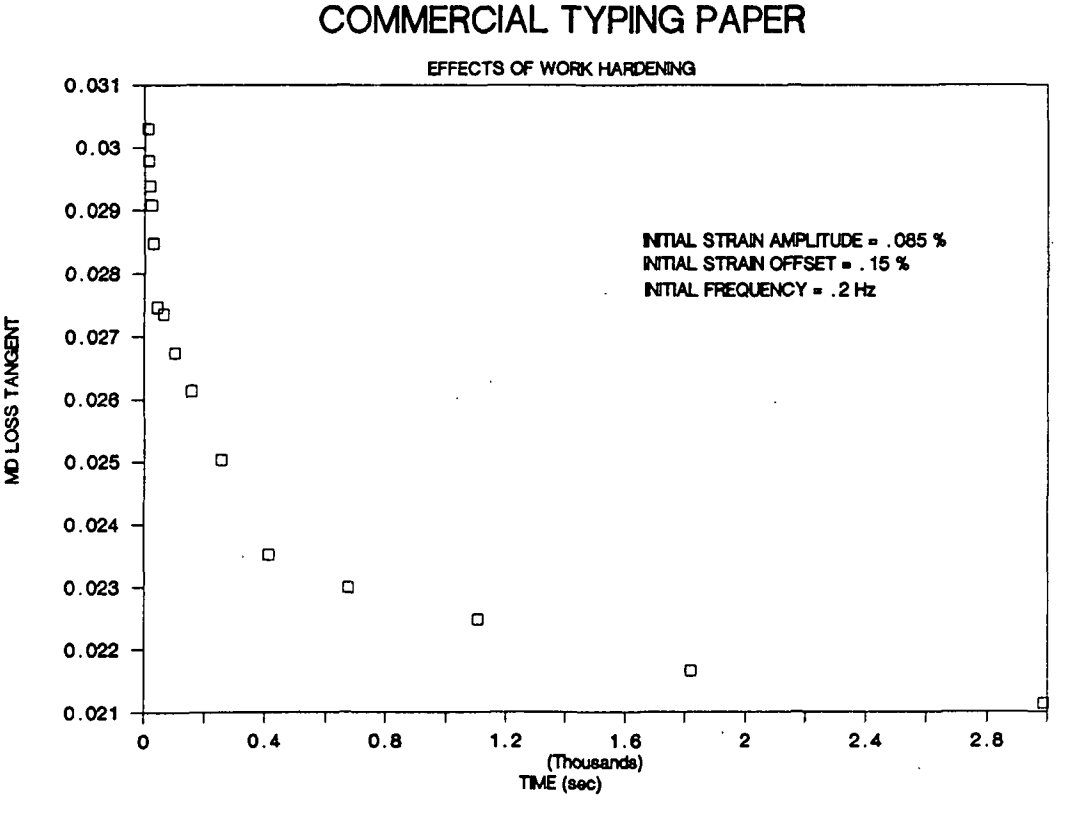

Figure 29. Typical MD loss tangent-time data for commercial typing paper showing work hardening effects.

Work by Rigdahl and Salmen[77] also shows that even at very low strain amplitudes, where work hardening effects are no longer significant, modulus and loss tangent values are a function of strain amplitude, modulus increasing and loss tangent decreasing as strain amplitude is decreased. Therefore, in order to make meaningful modulus and loss tangent determinations, measurements should be performed at several low strain amplitudes, where work hardening effects are negligible and data are extrapolated back to zero strain. This allows all data to be compared on a common basis. An extrapolation technique could not be used in the present study, since testing at a variety of low strain amplitudes is very difficult. Also, moisture is constantly changing throughout a transient run, so that testing at a multitude of strain amplitudes within the run is impractical. A test method could be envisioned wherein a sample would be tested in a given run at one strain amplitude, reconditioned, and subsequently tested at other strain amplitudes. However, such a technique would require the exact duplication of the environmental conditions of a run, identical sample clamping, and the insurance that sample properties were not altered during previous runs. Of course, these restrictions are unrealistic. In fact, difficulties encountered in positioning samples in the test jaws are believed to be the major factor resulting in the fairly high variability of loss tangent and mass specific modulus values obtained between runs using this technique. It must be emphasized again, however, that the primary purpose of this low frequency study was to determine the relative changes accompanying sorption and desorption. In an attempt to minimize work hardening effects, the lowest practical strain offsets and amplitudes were used. These were governed primarily by the sample type and dimensions. Strain amplitudes between 0.025 and 0.05% were usually the smallest that could be employed. Even though work hardening effects at these low strains

usually tended to be small relative to the changes produced by sorption or desorption, work hardening was appreciable in some cases (Fig. 28 and 29).

Providing that the strains are quite small and work hardening unimportant, a repeatable stress-strain loop is set up in the sample within a few load cycles. After attainment of a repeatable loop, a transient moisture run can be started by opening the plastic bag and blowing air on the sample with a fan. Depending upon the initial moisture content of the sample and the relative humidity in the surrounding air, the sample moisture will either increase or decrease. Changes in measured values (mass specific modulus, loss tangent, test frequency, strain amplitude, strain offset) due to sorption or desorption are measured and stored automatically by the computer. The initial data acquisition speed depends primarily upon the test frequency and can be as rapid as every 5 seconds for a 1 Hz test. However, in order to limit the amount of data, they are acquired less frequently as the run proceeds according to the equation,

$$t = \ell^{1+0.5(P)} \tag{19}$$

where t is the time in seconds at which the raw data acquisition is begun for data point P, relative to the start of the run. Initially, data is usually not obtained rapidly enough to satisfy Eq. (19). This is especially true when the test frequency is lowered or the number of cycles averaged per data point is increased. In these cases, acquisition of the raw data needed to determine the next data point is initiated immediately following calculation of the previous data point.

As was indicated previously, several problems are encountered when using an Instron 1122 tensile tester along with a cyclic loading technique to follow loss tangent and mass specific modulus changes during rapid sorption or desorption.

One problem with this technique, regardless of the equipment used, is the lack of loop closure that occurs when moisture changes cause rapid alterations in sample properties relative to test frequency. Htun, De Ruvo, and Fellers[78] have already speculated on the importance of this phenomenon. A mathematical analysis of the problem can be found in Appendix V. Here it is shown, using a reasonable, generalized definition of tanδ, that if lack of closure is not pronounced (drift in ε per cycle $<$ 1/4 the width of the loop at its midpoint) the effects it has on loss tangent are negligible and can be ignored. Of course, testing using a higher frequency will always help to minimize the anomalous effects caused by lack of closure. However, because the tensile tester used was not designed to make dynamic cyclic tests, anomalously large tanδ values are generated at higher frequencies. This loss tangent increase is believed to be an artifact because it occurs in brass foil strips which are thought to be highly elastic and should therefore not exhibit a measurable loss tangent. The loss tangent was found to increase by approximately 0.02 for every 1 Hz increase in frequency. A possible explanation for this increase involves the response time of the strain gage. If the dc strain signal were to lag the load signal by about 0.003 second, an increase in the loss tangent similar to the one measured would result. The consequences of this effect, as well as the means by which it can be corrected for, are discussed more thoroughly in Appendix VI. Inertial effects also become important at higher frequencies but are not significant below 1 Hz, and were generally ignored in the present study (see Appendix VII).

The loss tangent calculations and the analyses of loop closure, inertia, and strain gage-load cell response time difference assume a sinusoidal loading scheme. As indicated previously, sinusoidal loading is not possible with the tensile tester. Instead, it produces a rounded triangular wave form. This

wave, although predominantly a sine wave at the same fundamental frequency, has higher order harmonic terms. To see this more clearly, the triangle wave can be written as a Fourier series:

$$f(t) = (8k/\pi^2)\{[\sin(\pi t/T)]/1^2 - [\sin(3\pi t/T)]/3^2 + [\sin(5\pi t/T)]/5^2 + -...\} \quad (20)$$

where 2T is the period and k the amplitude. From Eq. (20) it can be seen that the relative importance of the harmonics drops off rapidly. The magnitude of the first harmonic is 11% when compared to the fundamental frequency whereas the second and third harmonics are even less significant, being 4 and 2% of the fundamental, respectively. Also, in order for the tensile tester to load the sample in a truly triangular fashion, an infinite amount of acceleration would be required as the crosshead direction is reversed. This is not possible in a real application so the actual wave is somewhat rounded at its peaks and troughs. Because it is at these points where the harmonics are most important in affecting the wave shape, the actual contribution of the harmonics is even less than that calculated above, and was therefore ignored. Nevertheless, loss "factor" rather than loss tangent is discussed to keep in mind that a true loss tangent at one frequency is not being obtained.

The cyclic loading technique, although having the above-mentioned problems, seems to give reasonable results if its limitations are realized and its deficiencies accounted for where possible. An indication of this is the low value of loss tangent obtained when testing thin brass strips ($\tan\delta \approx 0.005$, where f is extrapolated to zero). This is very close to zero, the value to be expected if the strips were completely elastic. The loss tangent values for paper and cellophane, measured using this technique, are also in the same range as those obtained with other low frequency devices.[7,78,84]

A final drawback to this experiment is the fact that although mass specific modulus and loss factor values are recorded, sample moisture content is not measured during the nonequilibrium moisture runs. The technique is therefore only valuable in looking for transient maxima in loss tangent or minima in modulus. The absence of these maxima or minima does not exclude the possibility of equilibrium-nonequilibrium differences.

RESULTS

ULTRASONIC TESTS

Equilibrium Data

The Blue M oven was used in conjunction with the ultrasonic techniques to make mass specific modulus measurements on cellophane and a variety of papers in a temperature and moisture regime representative of conditions at the dry end of a paper machine. Equilibrium strip resonance results for a 38 μm thick unplasticized cellophane film, made by BCL Cellophane and designated as 550 P00, are presented in Fig. 30. Notice that in this range the moisture dependence of the mass specific modulus is nearly linear. Also, temperature changes are equivalent to uniform horizontal shifts in the mass specific modulus plots, and the magnitude of the shift is proportional to the temperature difference. This permits the construction of the master curve presented in Fig. 31 for the cellophane at 55°C. If care is taken not to exceed the range of the experiments, mass specific moduli plots at other temperatures can be generated by shifting the master curve -0.088% moisture for every degree centigrade above 55°C.

As described in the experimental procedures section, equilibrium oven moduli were obtained through slow sorption and desorption. However, no significant moisture-mass specific modulus hysteresis was observed. The equivalence of sorption and desorption moduli, shown in Fig. 30, is representative of results obtained with other samples as well. The lack of an equilibrium moisture-modulus hysteresis was reported previously from load-elongation experiments by Higgins[78] and Salmen and Back.[26] The present study extends this observation to higher frequency experiments. Also, since ultrasonic tests are nondestructive

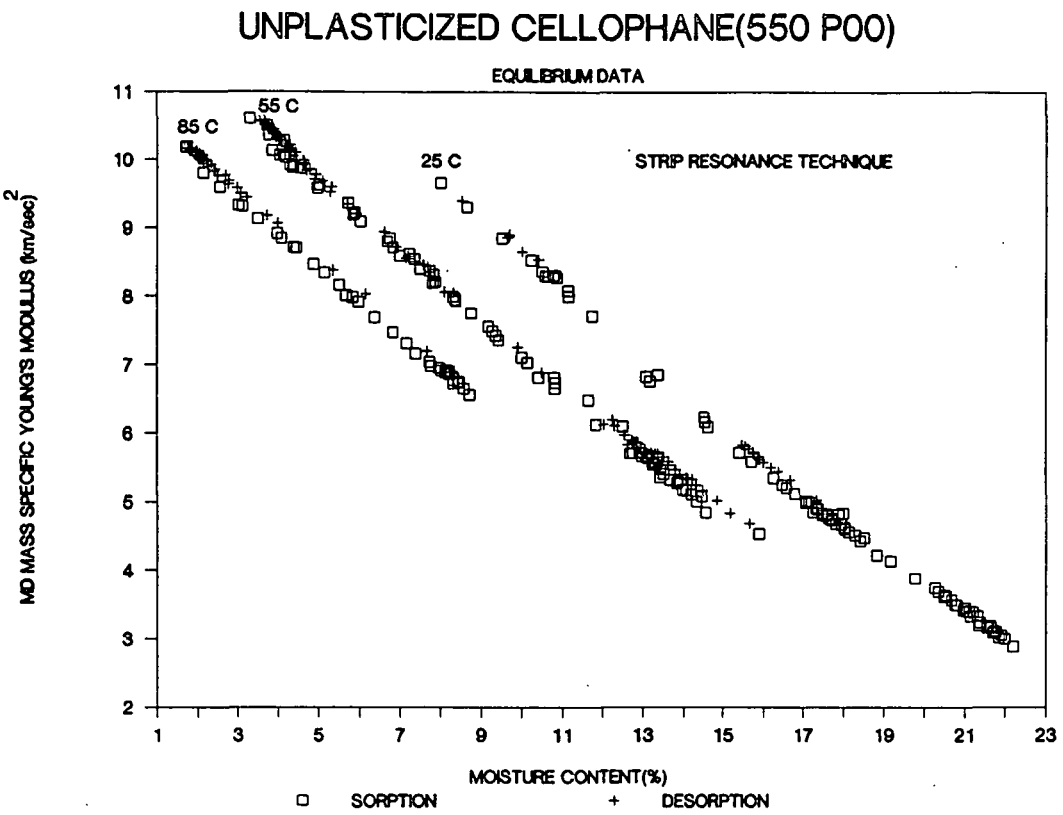

Figure 30. Strip resonance moisture-temperature-mass specific MD Young's modulus for 550-P00 cellophane.

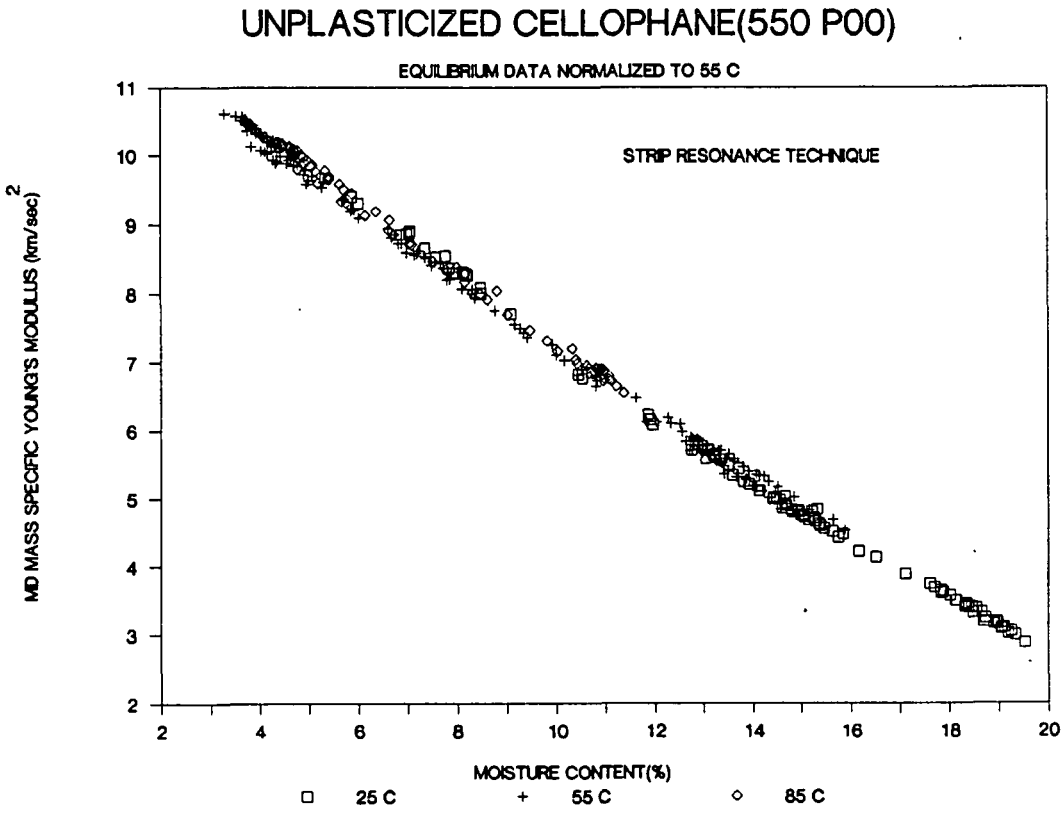

Figure 31. The 55°C moisture-MD mass specific Young's modulus master curve for 550-P00 cellophane.

and a single sample is used over the entire range, scatter due to sample variability is minimized, and the conclusion is made with more confidence. The lack of a moisture-modulus hysteresis is interesting in that hysteresis is observed in the dielectric measurements of Dusoiu.[80] In his microwave permittivity study, a moisture-dielectric constant hysteresis loop was found indicating that water is on average bonded differently in sorption and desorption at the same moisture content. The absence of a moisture-modulus hysteresis seems to indicate that the mobility of water molecules are of lesser importance to mechanical compliance.

The linear dependence of mass specific modulus on temperature and moisture, which was shown in Fig. 30 and 31 for cellophane, was observed for all other samples, when tested in this regime. The results are presented in Table 2 in terms of regression coefficients for the least squares fit to linear relations of the form, $V^2 = \beta_M(M-M_o) + \beta_T(T-T_o) + V_o^2$. The symbol M represents the percent moisture content; M_o is the percent moisture content at 50% RH arrived at through sorption; T is the temperature; and T_o is 25°C. The least squares regression coefficients are represented by β_M, β_T, and V_o^2. To facilitate the discussion, the runs in Table 2 are numbered in the order they were performed. A run consists of a series of equilibrium and transient tests on the same sample. In a typical run, equilibrium data at 25°C are obtained through a series of slow sorptions and desorptions. These tests are followed by several additional tests under transient moisture conditions. The oven temperature is then increased and the same procedure is followed at 55°C and finally at 85°C. However, because the temperature and moisture conditions in the oven were found to cause no permanent changes in sample properties, the order of the tests was arbitrary. The order in which the runs were performed was also unimportant

Table 2. Moisture-temperature-modulus regression analysis from present study.

Run[a]-Sample[b]-Technique[c]	Mode[d]	S_y^e $(km/sec)^2$	r^2	V_o^2 $(km/sec)^2$	β_M/V_o^2 $(1/\%)$	β_T/V_o^2 $(1/°C)$	β_M/β_T $(°C/\%)$	M_o (%)
2-I-B	Shear	0.11	0.976	3.21	-0.067	-0.0070	9.6	10.2
2-I-A	MDL	0.17	0.992	9.74	-0.062	-0.0063	9.9	10.2
11-I-A	MDL	0.18	0.995	8.52	-0.057	-0.0050	11.3	10.3
15-II-A	MDL	0.12	0.995	8.57	-0.072	-0.0061	11.8	10.2
7-III-B	Shear	0.07	0.980	3.52	-0.064	-0.0049	13.1	6.4
7-III-A	MDL	0.11	0.993	11.30	-0.051	-0.0041	12.5	6.4
8-III-B	Shear	0.08	0.984	3.43	-0.061	-0.0053	11.4	6.4
8-III-A	MDL	0.11	0.996	11.38	-0.051	-0.0042	12.2	6.4
9-III-B	Shear	0.05	0.996	3.43	-0.069	-0.0052	13.3	6.4
9-III-A	MDL	0.14	0.993	11.23	-0.052	-0.0040	12.8	6.4
10-III-B	Shear	0.09	0.988	3.83	-0.058	-0.0048	12.0	6.4
10-III-A	MDL	0.08	0.998	12.15	-0.044	-0.0033	13.5	6.4
13-IV-C	MDL	0.06	0.987	4.77	-0.056	-0.0039	14.3	6.2
13-IV-A	MDL	0.04	0.992	4.47	-0.053	-0.0044	12.1	6.2
14-IV-C	MDL	0.06	0.990	4.65	-0.057	-0.0038	14.8	6.2
14-IV-A	MDL	0.05	0.987	4.25	-0.053	-0.0041	12.9	6.2
3-V-B	Shear	0.05	0.972	2.65	-0.042	-0.0047	9.1	7.7
3-V-A	MDL	0.10	0.991	10.33	-0.042	-0.0045	9.2	7.7
5-V-B	Shear	0.03	0.992	2.35	-0.055	-0.0043	12.9	7.7
5-V-A	MDL	0.12	0.991	9.44	-0.052	-0.0045	11.6	7.7
6-V-B	Shear	0.03	0.996	2.67	-0.056	-0.0045	12.6	7.7
6-V-A	MDL	0.11	0.993	9.66	-0.047	-0.0038	12.2	7.7
12-V-A	CDL	0.03	0.995	3.89	-0.059	-0.0049	12.0	7.7
12-V-A	MDL	0.03	0.994	10.39	-0.041	-0.0033	12.4	7.7
4-VI-B	Shear	0.05	0.985	3.02	-0.055	-0.0049	11.4	7.4
4-VI-A	MDL	0.09	0.990	7.81	-0.044	-0.0051	8.7	7.4
1-VII-B	MDL	0.18	0.976	9.77	-0.057	-0.0045	12.9	6.7
1-VII-A	MDL	0.15	0.961	7.20	-0.057	-0.0058	9.8	6.7

[a]Relative order or runs.
[b]I: 550 POO (unplasticized cellophane); b.w. 55 g/m^2; thickness 38 μm; BCL.
II: PUDO-134 (unplasticizied cellophane); b.w. 55 g/m^2; thickness 38 μm; Du Pont.
III: Commercial typing paper; basis weight 75 g/m^2; thickness 100 μm.
IV: Commercial blotter stock; basis weight 256 g/m^2; thickness 600 μm.
V: Commercial linerboard; basis weight 26 $lb/1000\ ft^2$ (127 g/m^2); thickness 240 μm.
VI: Commercial linerboard; basis weight 90 $lb/1000\ ft^2$ (439 g/m^2); thickness 660 μm.
VII: Commercial bleached kraft; basis weight 86 g/m^2; thickness 190 μm.
[c]A: Strip resonance (1st harmonic).
B: Sheet time of flight.
C: Strip time of flight.
[d]MDL: Machine direction longitudinal.
CDL: Cross machine direction longitudinal.
[e]Standard error in the Y estimate.

except for the fact that the transducers used with the time-of-flight technique were replaced after run 12. The new transducers were ≈ 1.3 mm long, 3 mm wide, and were operated at a frequency of 80 kHz. The older transducers were the same length, but were ≈ 6 mm wide and were operated at 60 kHz. Also, small refinements in experimental techniques were continuously being made using the experience gained with each run. Latter runs may therefore be of slightly higher quality. In each run (excluding 11 and 15), two samples, cut from the same sheet, were tested; one with the time-of-flight and one with the strip resonance technique. Comparing coefficients within runs gives the reader a feeling for the consistency of results between ultrasonic techniques as well as the importance of the test mode. Notice that multiple runs are presented for typing paper, linerboard, blotter stock, and BCL cellophane. Comparisons between runs can therefore be used to give an idea of the variability within and between samples and an indication of the repeatability of the test techniques.

In addition to the consistently large values for the squared correlation coefficients (r^2), there are other interesting observations to be made in Table 2. Notice that the longitudinal mass specific modulus of linerboard in the MD is significantly less affected by temperature and moisture than the CD specific longitudinal moduli. This results in an increased anisotropy ratio (MD/CD) at higher moistures and temperatures. Also, although there is some variation between runs, within runs BCL cellophane, linerboard, and typing paper all exhibit a shear mode which is more environmentally sensitive than the longitudinal mode. The greater stability in MD longitudinal mass specific modulus is presumably a result of the greater concentration of stresses in crystalline regions during propagation of this mode as discussed later. Another observation is that the values of β_M and β_T are positively correlated in such a way that β_M/β_T (the

temperature rise in degrees centigrade that causes a mass specific modulus change equal to that produced by a one percent moisture increase) is remarkably independent of the sample tested and the mode propagated. The average value of β_M/β_T for all runs is 11.8°C/%, with a standard deviation of 1.6°C/%. A final observation is made concerning the consistency between results obtained with the different ultrasonic techniques. It can be noted from runs 1, 13, and 14, where similar modes were tested, that β_M/β_T is considerably greater when tested with the time-of-flight technique. The reasons for this difference are not known.

The range of sample moisture contents that can be obtained in the oven depends on the temperature. The maximum and minimum moistures measured at each temperature are listed in Table 3 for all samples. Temperatures and moistures at the reel of a paper machine, where on-line ultrasonic measurements are made, usually fall within the extremes listed in this table. The existence of the linear moisture-mass specific modulus and temperature-mass specific modulus relationships, cited in Table 2, is therefore fortunate, since by measuring sample mass specific modulus, temperature, and moisture on-machine and applying linear correction factors, the mass specific modulus at a standard environmental condition can be calculated.

Table 3. Measured moisture ranges from present study.

Sample[a]	ΔM at 25°C (%)	ΔM at 55°C (%)	ΔM at 85°C (%)
I	8-22	3-16	2-9
II	8-14	2-12	1-8
III	5-14	2-9	1-6
IV	6-12	3-11	1-6
V	6-16	4-11	2-8
VI	9-16	5-13	3-9
VII	9-14	4-10	2-7

[a]Same designation as Table 2.

Transient Data

Figure 32 shows the change in sample moisture content during a typical group of nonequilibrium runs. In this case, commercial blotter stock was tested at ≈ 55°C. The figure consists of three sorption and three desorption runs. To facilitate the discussion, these runs are collectively called run T14 as they are part of the larger run 14. Note from Fig. 32 that the runs can be replicated quite accurately. Note also the fact that the majority of moisture changes are complete within the first five minutes. As might be expected, the rate of moisture change generally becomes greater as sample size is decreased, basis weight lowered, and oven air temperature raised. Although not readily apparent from the figure, the experimental procedures caused sorption rates to be generally higher than desorption rates as discussed previously.

Figure 33 shows the changes in MD mass specific Young's modulus in run T14 as measured using the strip time-of-flight technique. These modulus data are highly reproducible between tests as might be expected considering the previously discussed moisture results. The expected increase in mass specific modulus during desorption and decrease upon sorption can also be noted. Similar data were obtained using the strip resonance technique as shown in Fig. 34. Strip resonance mass specific modulus values, however, as was previously discussed, are typically around 10% lower than ones obtained with the strip time-of-flight technique.

The largest difference between equilibrium and transient mass specific modulus data was found to be a result of transient changes in sample temperature. As a sample sorbs moisture it heats up. This rise in temperature comes from the heat of sorption of the water vapor with cellulose and is equal to the heat of condensation of the water vapor plus the heat of sorption of the

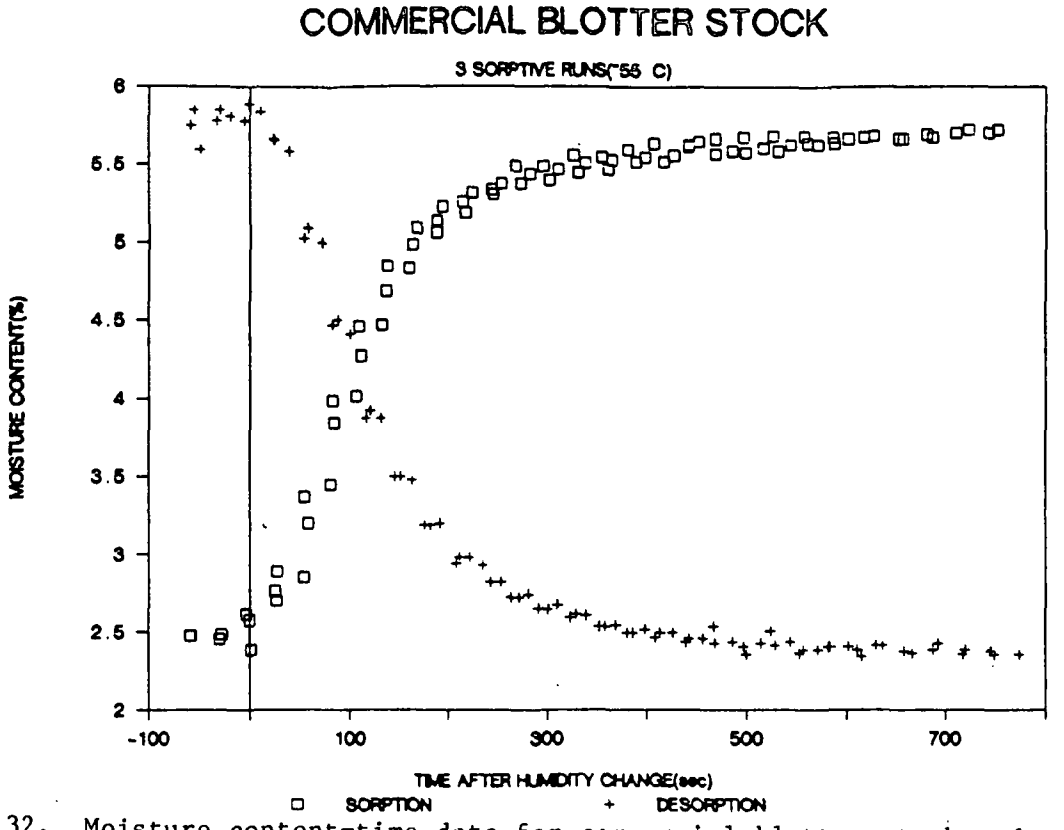

Figure 32. Moisture content-time data for commercial blotter stock undergoing sorption and desorption.

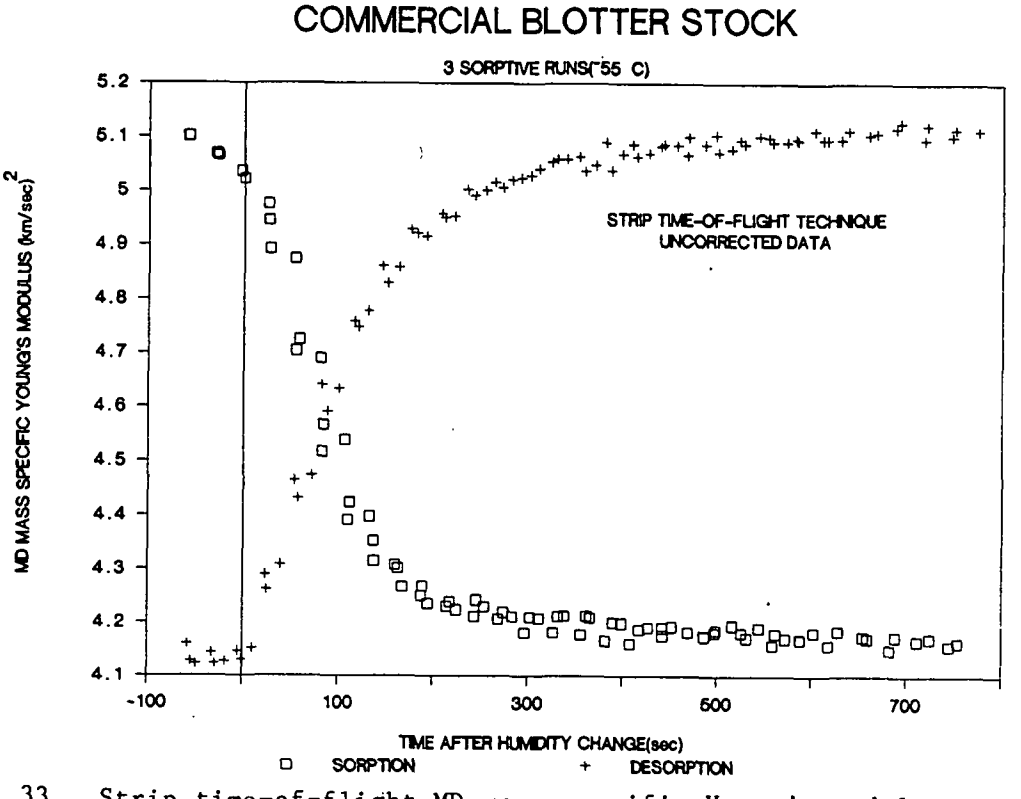

Figure 33. Strip time-of-flight MD mass specific Young's modulus-time data for commercial blotter stock undergoing sorption from 2.5-6% and desorption from 6-2.5% moisture.

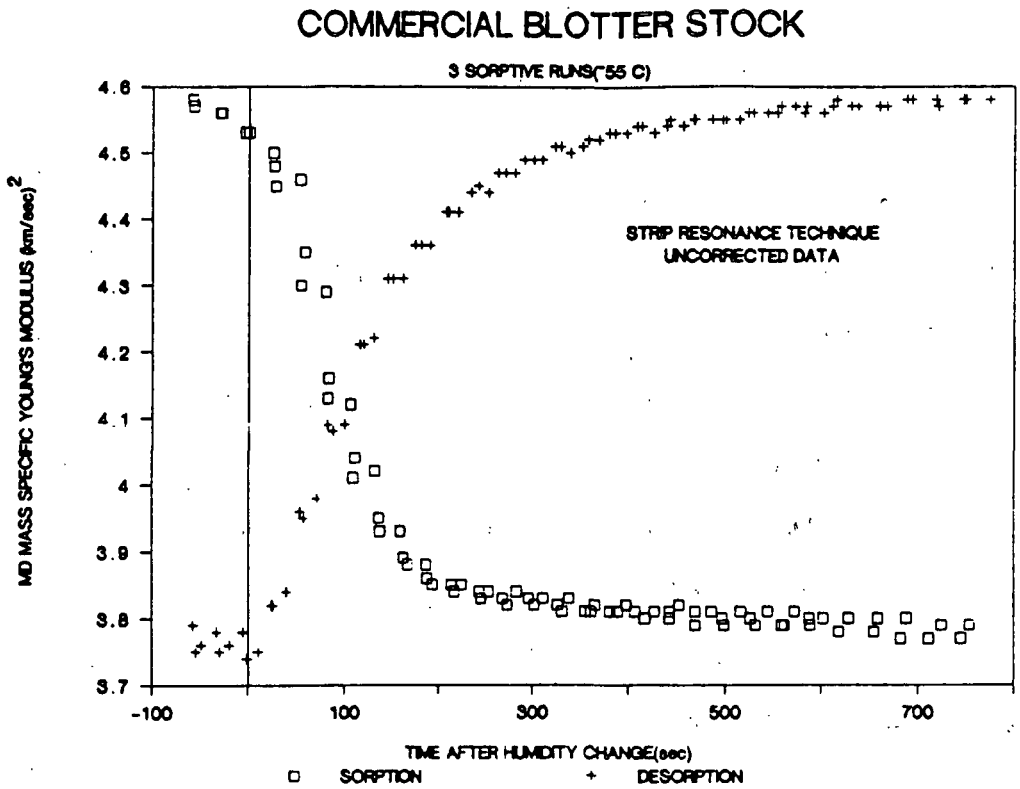

Figure 34. Strip resonance MD mass specific Young's modulus-time data for commercial blotter paper undergoing sorption from 2.5-6% and desorption from 6-2.5% moisture.

water with cellulose. Conversely, as samples desorb, evaporative cooling occurs. Figure 35 shows a typical example of temperature changes accompanying nonequilibrium moisture conditions. These data are again from run T14. The maximum temperature change occurs after about two minutes and is seen to be around 5°C. Also, the time at which the maximum temperature change occurs coincides quite well with the maximum rate of moisture change, the temperature maximum due to sorption slightly preceding the minimum caused by desorption. The difference between the sorption and desorption rate that typically accompanies transient moisture runs in the oven can be seen most clearly in these time-temperature graphs. It was found that the magnitude of the temperature change depends primarily on the rate of moisture change, and to a lesser extent on the

type of sample, the initial moisture content, and the air flow around the sample. Changes in sample temperatures in the oven accompanying moisture changes ranged from zero (equilibrium case) to around 8°C. Higher oven temperatures usually resulted in larger temperature transients, presumably because initial moisture contents were inherently lower and sorption rates higher. Similar transients have been measured in newsprint and linerboard using an infrared technique.[81] Even larger temperature drops were measured (up to 17°C) when samples were placed in a small chamber[9] and a vacuum drawn. The larger transient decrease in this case results from an increased desorption rate and a greater thermal isolation of the sample. Such large transient temperature changes are by no means extraordinary. Transient temperature excursions accompanying moisture changes in wool and have been reported as high as 40°C.[70]

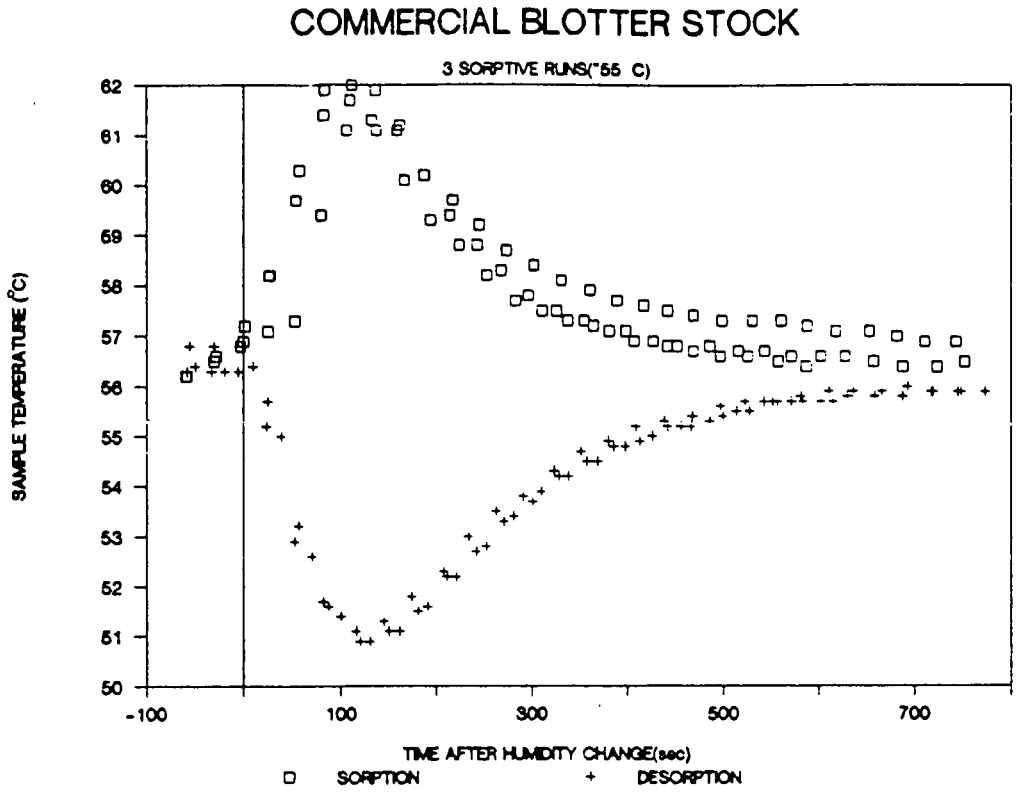

Figure 35. Temperature-time data for commercial blotter stock undergoing sorption and desorption.

It is apparent from Fig. 30 and Table 2 that the mass specific modulus of cellulosic materials is dependent upon sample temperature. Therefore, in order to determine modulus values at a constant temperature during rapid moisture changes, compensations must be made for temperature changes caused by evaporative cooling or heat of sorption. A simple way of correcting transient values to a standard temperature is to assume that samples are approximately uniform in temperature and to use the equilibrium temperature-mass specific modulus data from Table 2. By combining temperatures acquired during nonequilibrium moisture runs with known equilibrium temperature-mass specific modulus relationships, changes in mass specific modulus caused by transient temperature variations can be compensated for. Figure 36 shows uncorrected data from Fig. 34 and data standardized to 55°C. The rates of mass specific modulus change can be seen to be slightly higher in the uncorrected data. Correction of Fig. 33 data gives a similar result. The effects of temperature corrections can also be made apparent by plotting mass specific modulus values against moisture. This is shown in Fig. 37 for uncorrected strip resonance mass specific modulus values from run T14, and in Fig. 38 for temperature corrected data. Figures 37 and 38 also contain transient moisture data from run 14 at 25 and 85°C, as well as equilibrium data at all three temperatures. Several interesting observations can be made concerning these figures. First, note the moisture-mass specific modulus hysteresis loops in Fig. 37 apparent at all temperatures for nonequilibrium data not corrected for transient changes in temperature. These loops are similar to those presented previously in a conductivity study of filter paper undergoing sorption and desorption.[82] In that study, the loop was assumed to be due to the moisture induced temperature changes, and conductivity differences were used to calculate seemingly reasonable temperature changes. Fortunately, sample temperatures were measured in the present study and could be

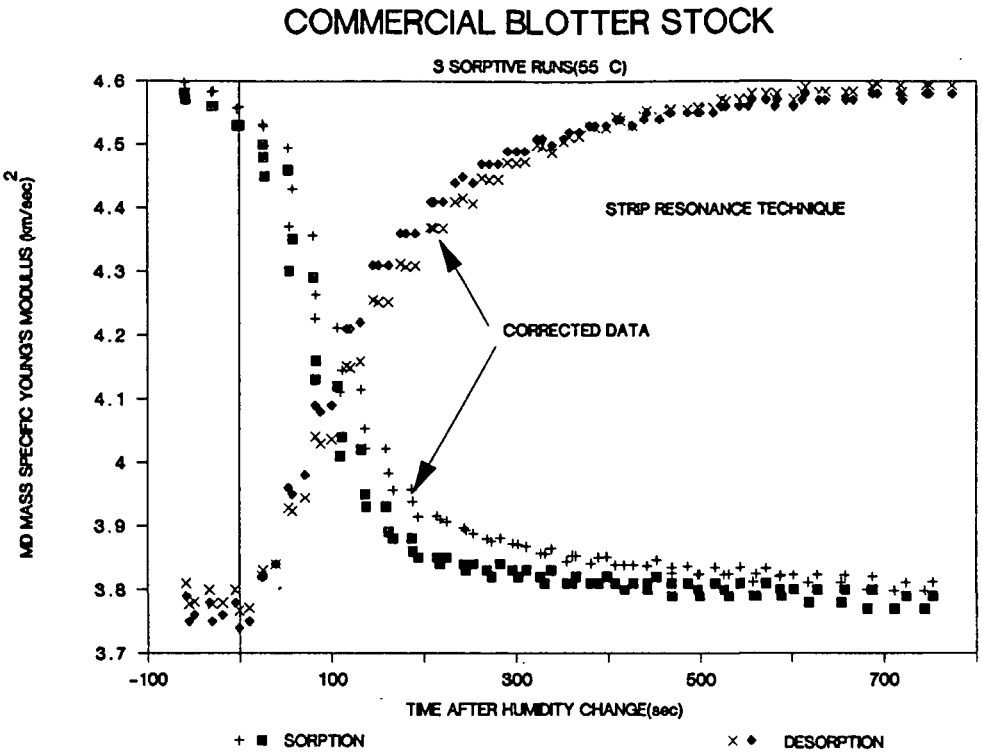

Figure 36. Strip resonance MD mass specific Young's modulus-time data (corrected for temperature) for commercial blotter stock undergoing sorption and desorption.

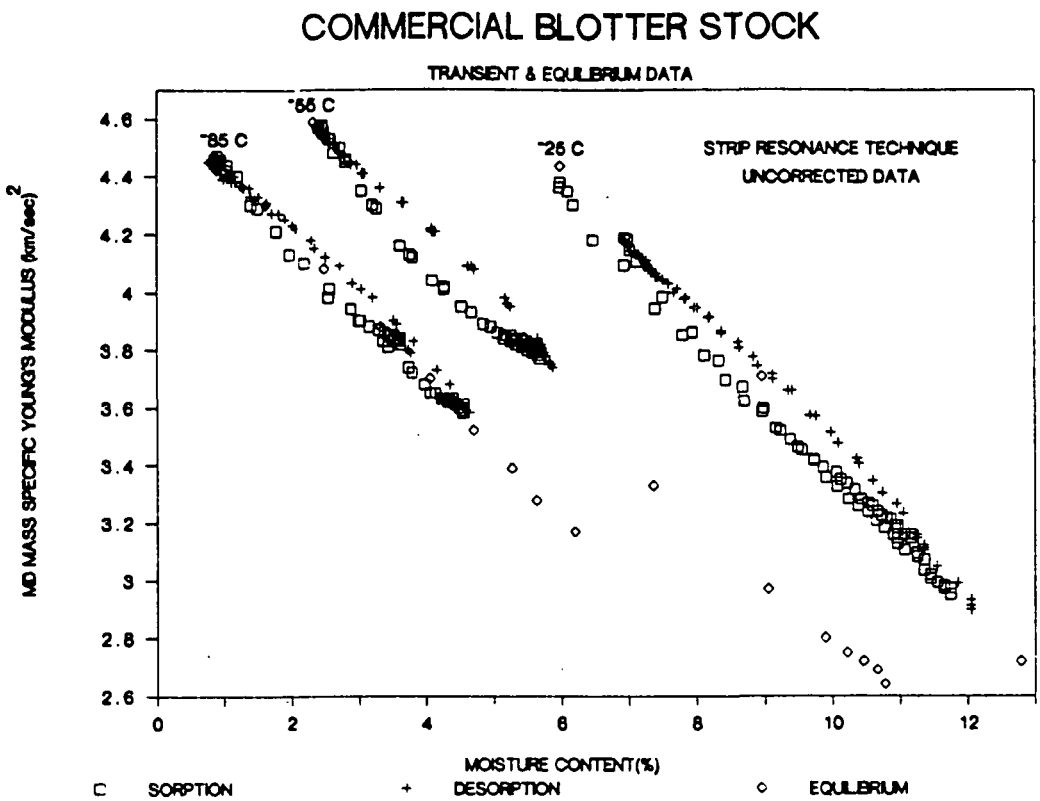

Figure 37. Strip resonance MD mass specific Young's modulus-temperature-moisture data for commercial blotter stock under equilibrium and transient moisture conditions.

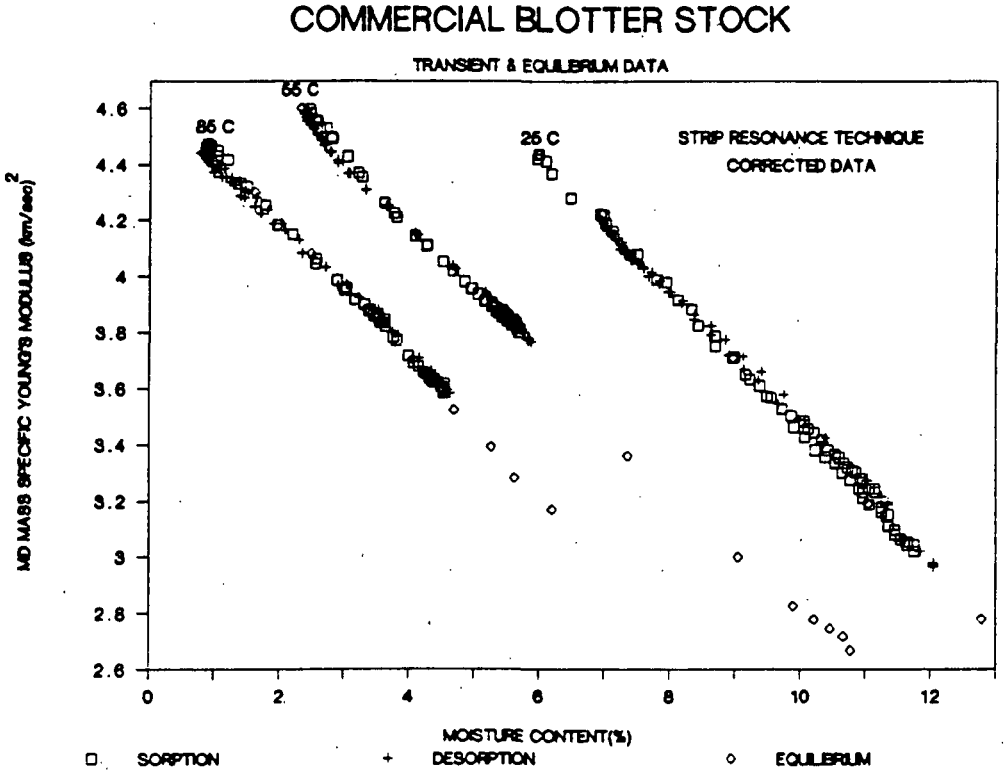

Figure 38. Strip resonance MD mass specific Young's modulus-temperature-moisture data (corrected for temperature) for commercial blotter stock under equilibrium and transient moisture conditions.

used to verify that the loops were, in fact, due to transient temperature changes. They are seen in Fig. 38 to disappear when temperature corrections have been made. Figure 38 also shows the nonequilibrium data to be identical to those obtained under equilibrium conditions. This equilibrium-transient data equivalence was found for all samples, regardless of the mode tested or the technique used. For example, Fig. 39 shows an equilibrium-transient equivalence for cellophane (run 11) tested longitudinally in the MD using the strip resonance technique, while Fig. 40 shows the equivalence in linerboard data (run 6) tested in shear. Notice the larger scatter in the shear data. This is most likely due to the fact that these data were obtained in an earlier run where experimental techniques had not yet been fully developed. In any case, if temperature variations are accounted for, there is no transient increase or decrease in ultrasonically measured mass specific modulus during rapid moisture

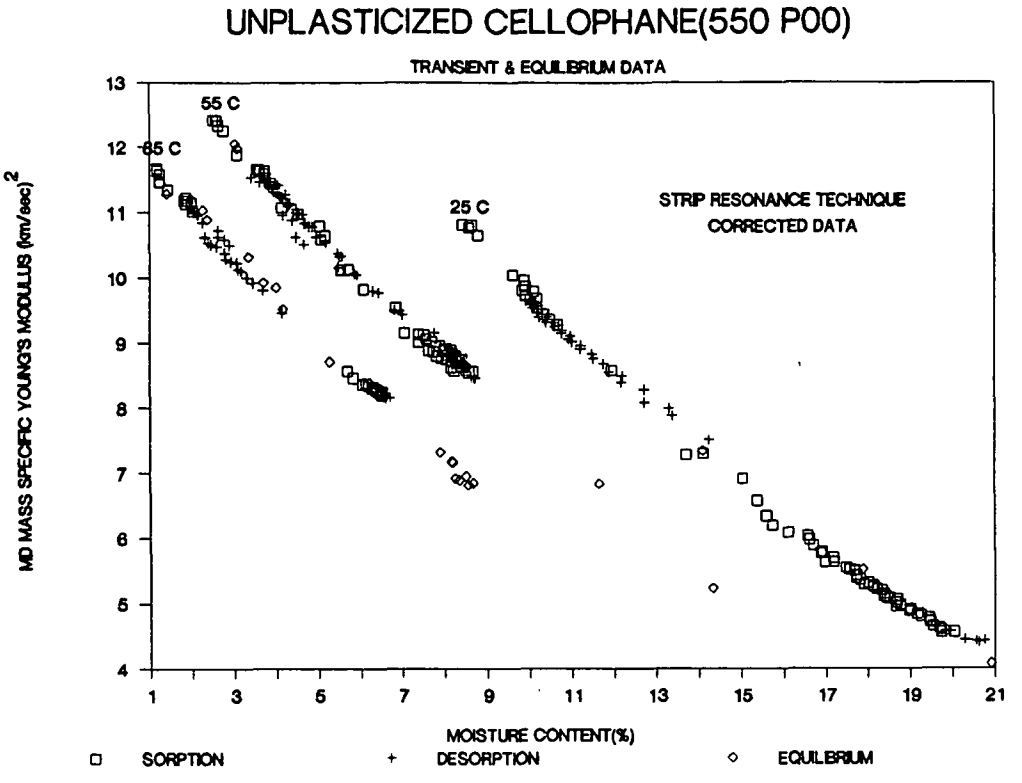

Figure 39. Strip resonance MD mass specific Young's modulus-temperature-moisture data (corrected for temperature) for commercial cellophane under equilibrium and transient moisture conditions.

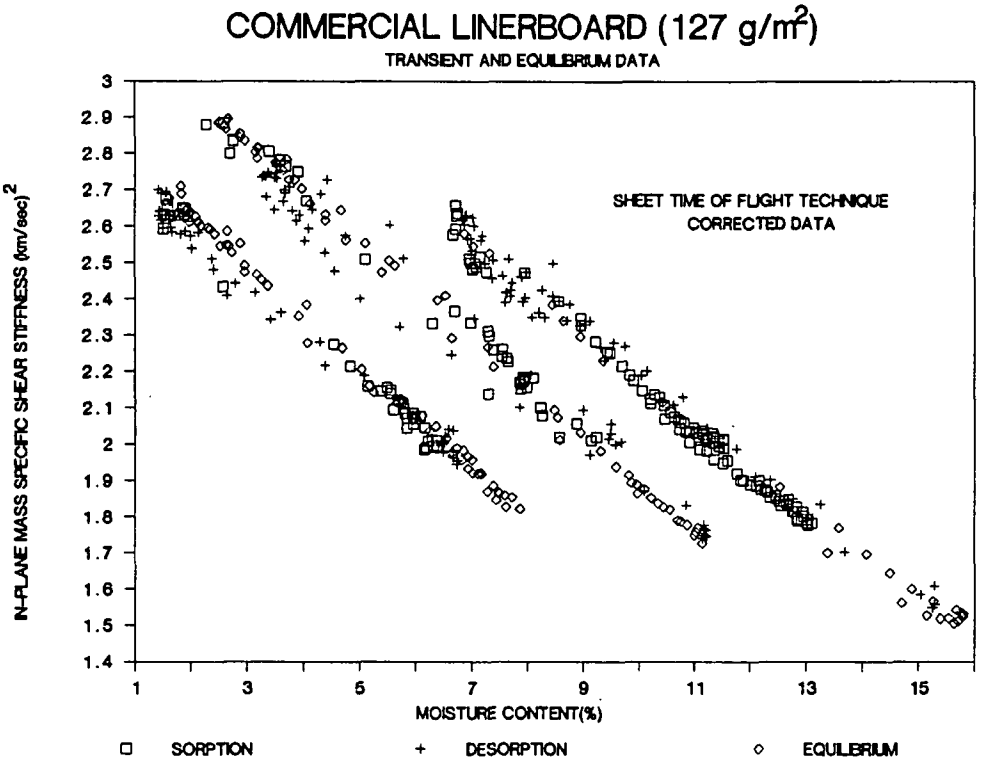

Figure 40. Sheet time-of-flight in-plane mass specific shear stiffness-temperature-moisture data (corrected for temperature) for commercial linerboard under equilibrium and transient moisture conditions.

changes! One final note can be made concerning the data in Fig. 37-40. Equilibrium data are seen to encompass a larger moisture range at each test temperature. This results from the fact that bath temperature during sorptive runs doesn't become as high as it does in equilibrium runs. Some of the heating value of the water poured in at the beginning of a sorptive run is required to heat the metal portions of the bath and any remaining water.

Loss tangent values accompanying run 14 are plotted in Fig. 41. They are seen to increase very rapidly during sorption while a more gradual decrease occurs with desorption. Note also the slight maximum that appears to occur in sorption values. The difference in the rate of change of loss tangent between sorption and desorption as well as the slight maximum with sorption are probably the result of sample temperature changes. However, temperature corrections for loss tangents vary with moisture and are not as easily determined as those for moduli. This can be better understood by viewing Fig. 42 where equilibrium moisture-MD loss tangent data from run 14 at 25, 55, and 85°C are shown. Notice that the loss tangent appears fairly insensitive to temperature over this range. The reason for this insensitivity is that at these temperatures ultrasonic loss tangent data are passing through a trough located between the β and α transitions as described later. Figure 43 shows the equilibrium data from Fig. 42 along with sorptive and desorptive data at all three temperatures. In order to retain clarity in the graph, temperature separation of sorptive and desorptive data is not shown. Notice that the sorptive data appear slightly higher than the desorptive data. However, data scatter makes it difficult to draw definite conclusions. If any differences do exist between these sorptive, desorptive, and equilibrium loss tangent data they are certainly quite small. Data in Fig. 42 and 43 are typical of all loss tangent data. Although some samples show a

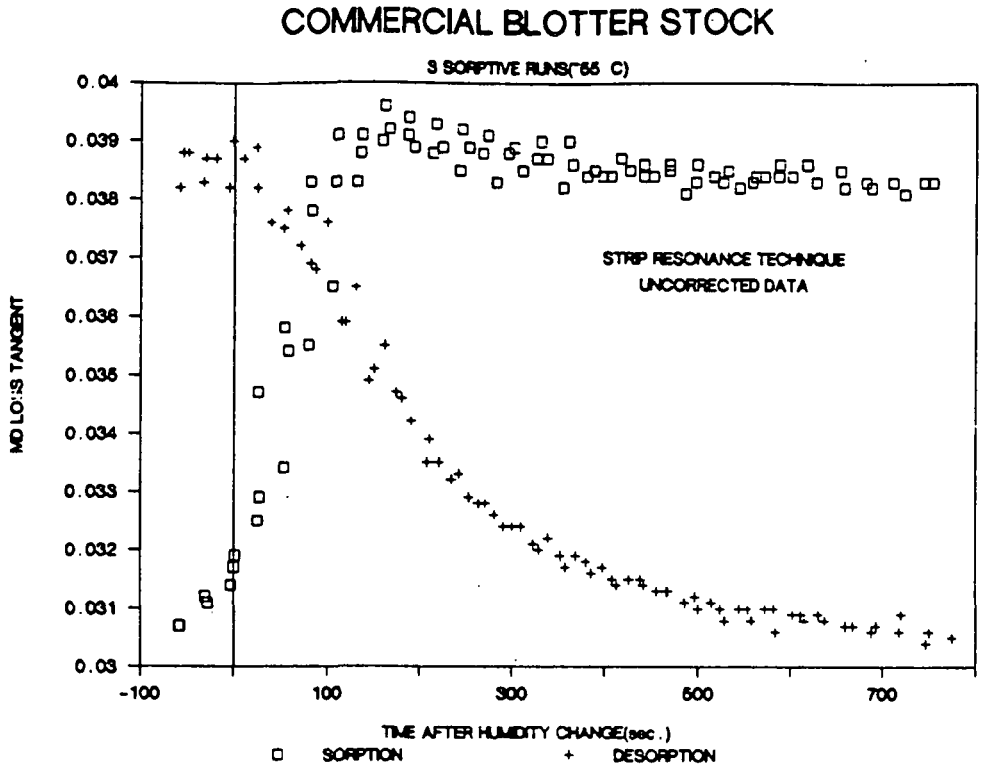

Figure 41. Strip resonance MD loss tangent-time data for commercial blotter stock undergoing sorption from 2.5-6% and desorption from 6-2.5% moisture.

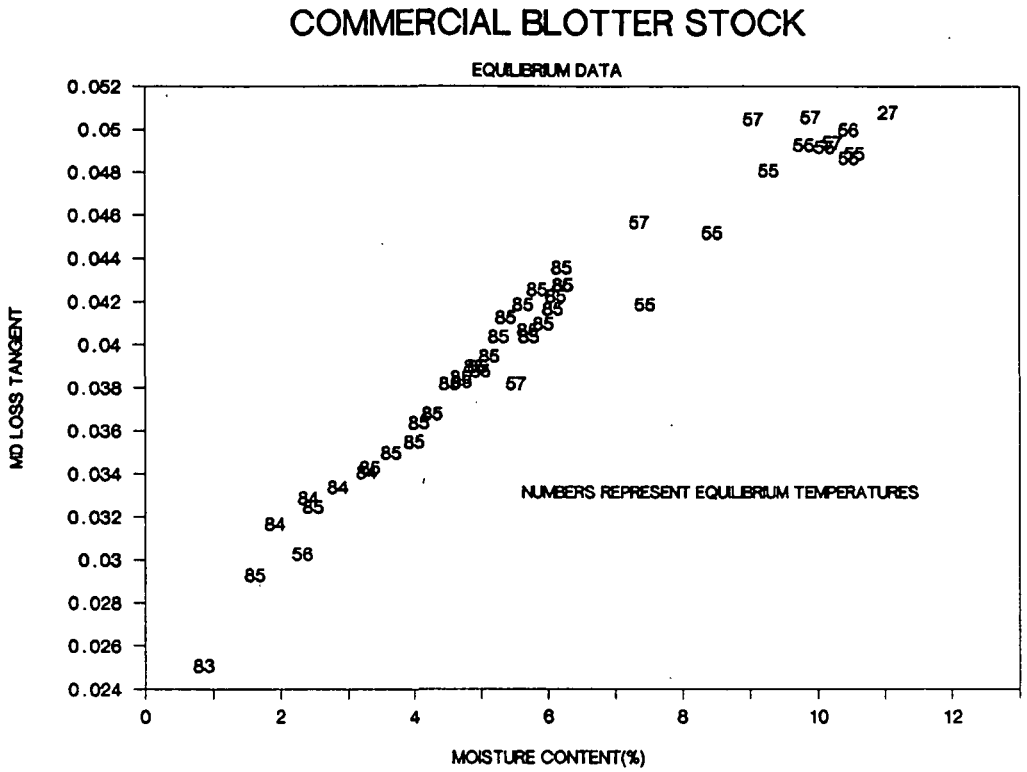

Figure 42. Strip resonance moisture-temperature-MD loss tangent data for commercial blotter stock.

greater temperature sensitivity, little or no transient increases in loss tangent were observed.

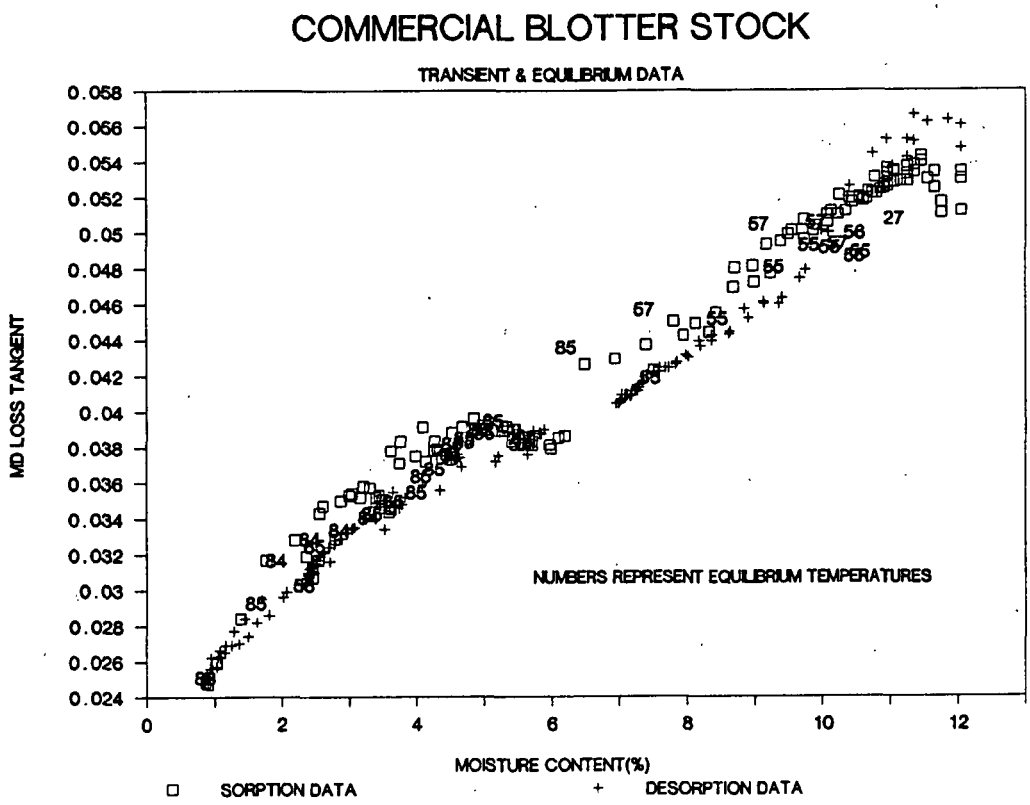

Figure 43. Strip resonance moisture-temperature-MD loss tangent data for commercial blotter stock under equilibrium and transient moisture conditions.

In order to investigate the effect of longitudinal loading on the transient phenomenon, experiments were conducted on strip resonance samples loaded axially. Samples were loaded by clamping the mounting track in a vertical position, loosening the lower aluminum block allowing it to slide along the track, and hanging a weight over the block. Tensile loads applied to the samples in this fashion ranged from 15-30% of the ultimate breaking load measured at room temperature and 50% RH. Transient and equilibrium runs were conducted between 25 and 85°C on two typing paper samples, three cellophane samples, and a bleached kraft sample. Loading resulted in accelerated creep as evidenced by

failure in several of the samples after repeated moisture cycling. Creep was also accompanied by slow decreases in apparent modulus of up to 20% prior to failure. These modulus decreases are similar to those reported previously by Gunderson and Considine.[44] Not all of the measured modulus decrease is real, however, some of it being due to length increases which are not monitored, and hence can't be corrected for. It is impossible, therefore, to know how much of the modulus decrease is actual, and how much is due to an increasing sample length. Nevertheless, the facts that modulus decreases are accompanied by loss tangent increases and loss tangent measurements are independent of length indicate that at least some of the modulus decrease is real. The above modulus decreases and loss tangent increases are the result of many moisture cycles (5-20). Within a given cycle, drifts in values were small and transient moisture conditions could therefore be analyzed without the complicating effects of creep. Sample loading did not produce any measurable differences between nonequilibrium and equilibrium data. These results are the same as in the unloaded case and indicate that the application of a static tensile load is unimportant to the transient phenomenon.

LOW FREQUENCY TESTS

Transient Data

An obvious difference between the above-mentioned ultrasonic study and most of the nonequilibrium literature data is the higher test frequencies and lower strain amplitudes used to measure modulus and loss tangent. It was felt that these differences might be responsible for the seemingly contradictory equilibrium-nonequilibium results obtained ultrasonically when compared with those acquired using low frequency techniques. Low frequency measurements were therefore made during changing moisture conditions in an attempt to duplicate

previously reported results, especially those of Back, Salmen, and Richardson[27] and Kubat and Lindbergson.[66] Most runs were made at a frequency of around 1 Hz in order to minimize the corrections required for lack of loop closure. Typical mass specific modulus results accompanying desorption are shown in Fig. 44 and 45 for blotter stock and typing paper, respectively. Initial strain amplitudes and offsets are also included in these figures. In most cases, the minimum practical strains were used. Notice that the mass specific modulus of typing paper increases at a more rapid rate than that of the blotter stock. This is presumably a result of the more rapid desorption occurring in the thinner typing paper sample. Of more importance to the present study, however, is that in both cases mass specific modulus continuously increases as desorption proceeds. The initial minimum in modulus seen by Back, Salmen, and Richardson was not found. Figures 46 and 47 show similar mass specific modulus data for sorption. Again, changes occur more rapidly with typing paper. Notice the slight mass specific modulus minimum that appears to accompany sorption. This minimum is similar to those found by others[27,59-62] during sorption. It is not known, however, whether the minimum is due to the temperature rise caused by heat of sorption, is a result of work hardening, or is, in fact, a real effect.

Loss factor data accompanying Fig. 44-47 are shown in Fig. 48-51. As can be noted, maxima in loss factor typically accompany desorption. These maxima in loss factor were also prevalent with sorption data. The magnitude of the maxima on sorption and desorption varied between samples, but the maxima were usually quite significant. These transient maxima in loss factor are similar to those reported previously by Danilatos and Postle[64,65] and De Ruvo, Lundberg, Martin-Lof, and Soremark.[47] Figures 44-51 are typical of the results found for all samples tested in the Instron, which included MD and CD tests of blotter stock, typing paper, cellophane, and various basis weight linerboards.

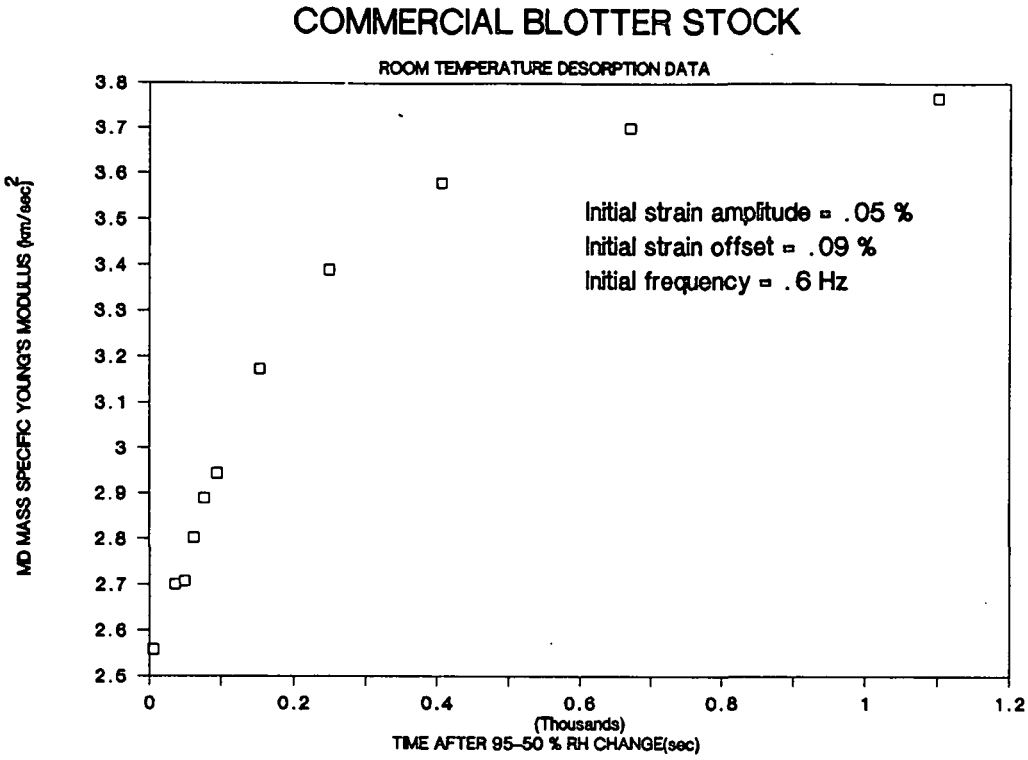

Figure 44. Low frequency MD mass specific Young's modulus-time data for commercial blotter stock undergoing desorption from 10-6% moisture.

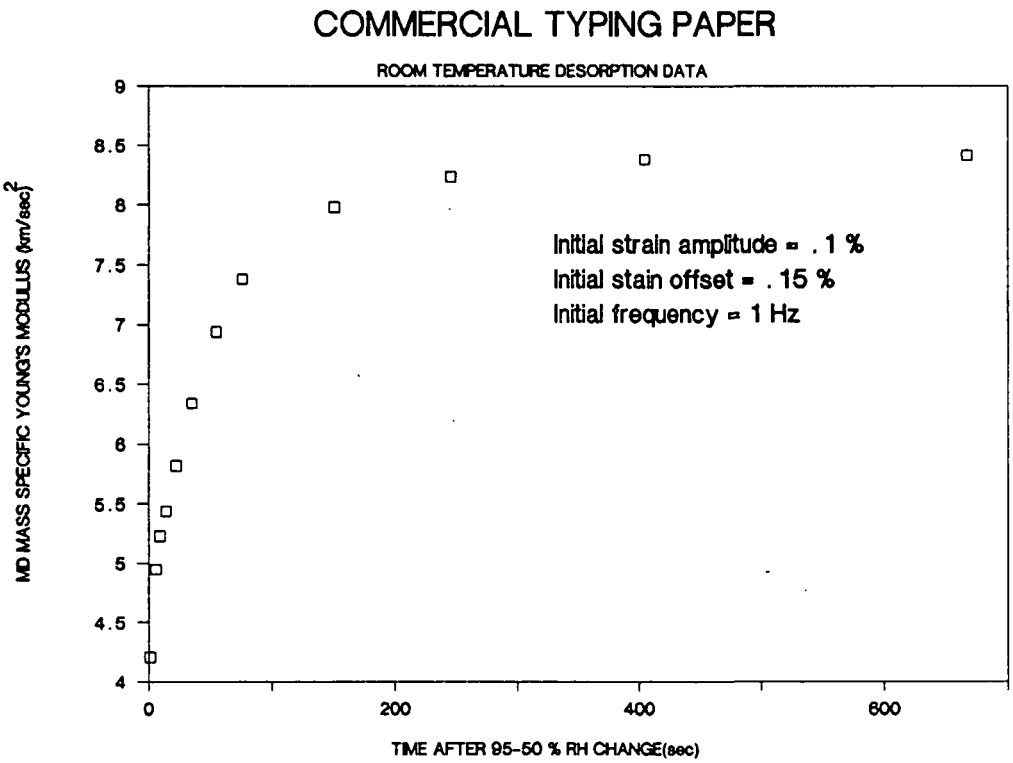

Figure 45. Low frequency MD mass specific Young's modulus-time data for commercial typing paper undergoing desorption from 12.1-6.2% moisture.

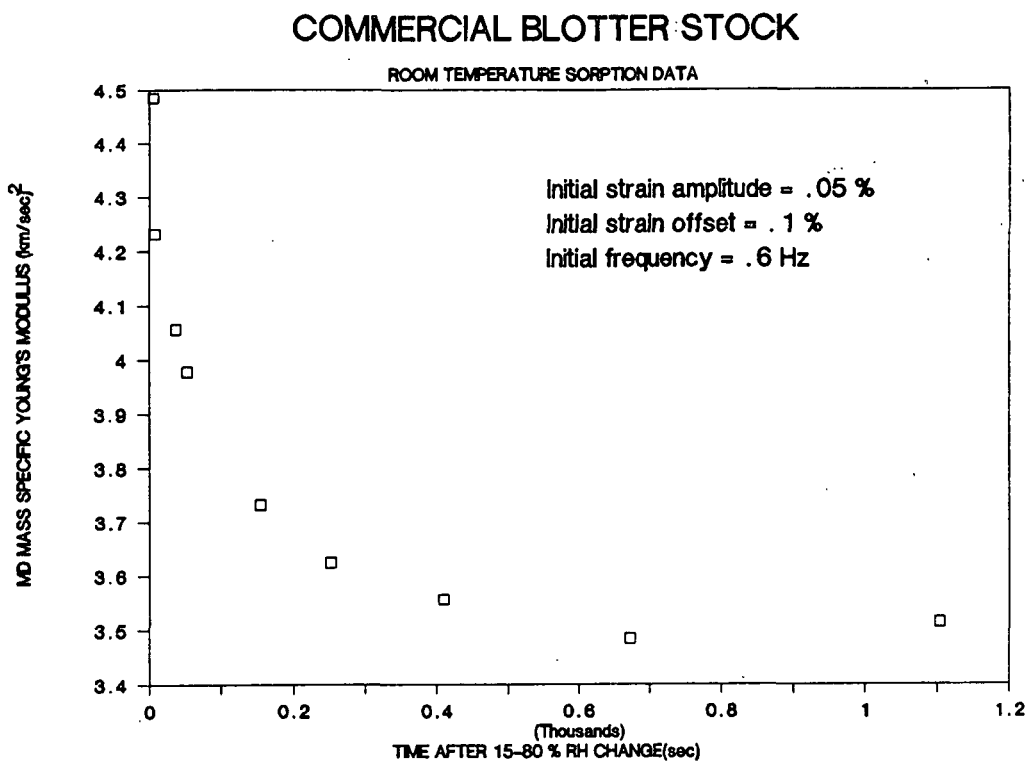

Figure 46. Low frequency MD mass specific Young's modulus-time data for commercial blotter stock undergoing sorption from 3.8-7.3% moisture.

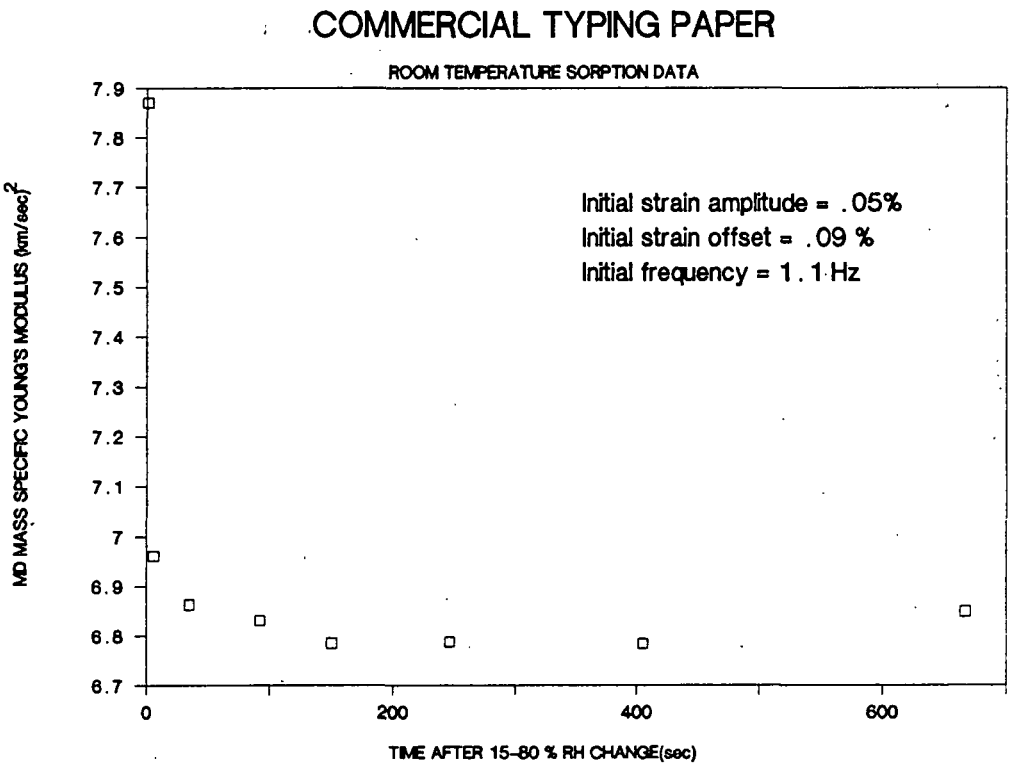

Figure 47. Low frequency MD mass specific Young's modulus-time data for commercial typing paper undergoing sorption from 3.9-7.9% moisture.

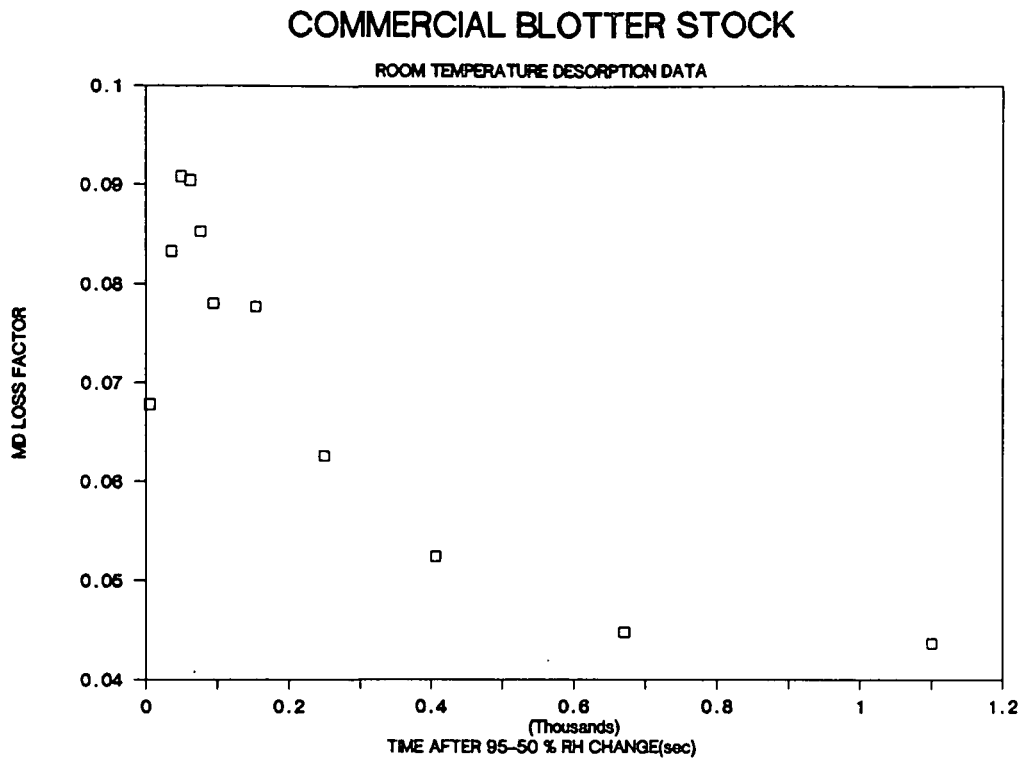

Figure 48. Low frequency MD loss factor-time data for commercial blotter stock undergoing desorption from 10-6% moisture.

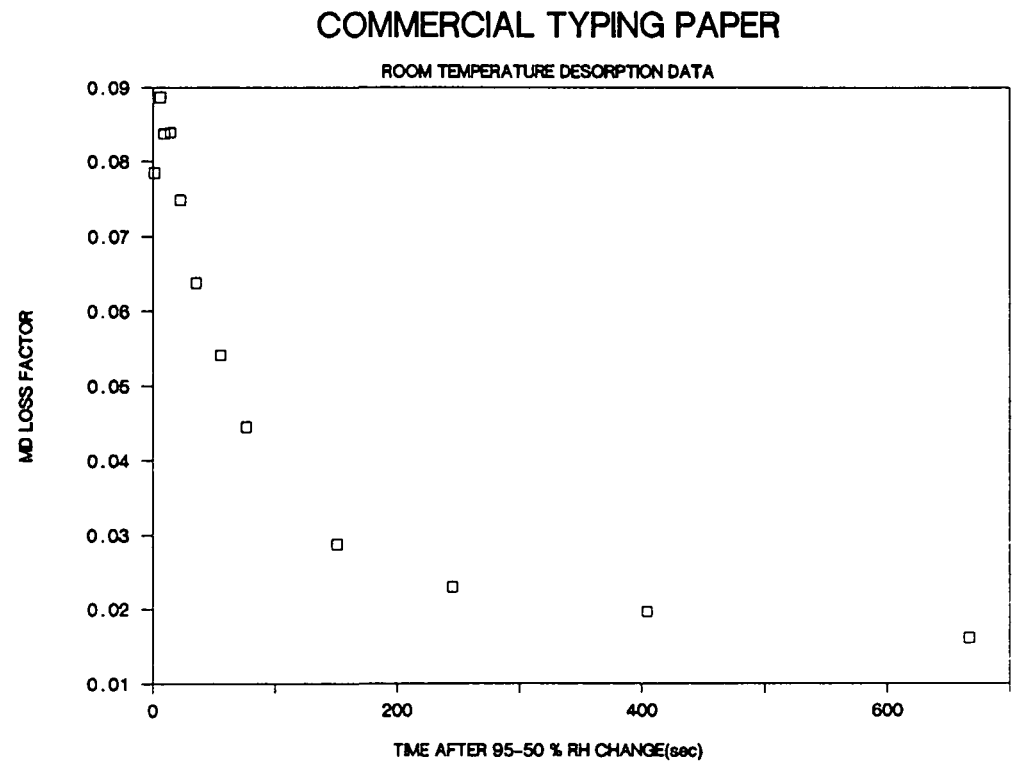

Figure 49. Low frequency MD loss factor-time data for commercial typing paper undergoing desorption from 12.1-6.2% moisture.

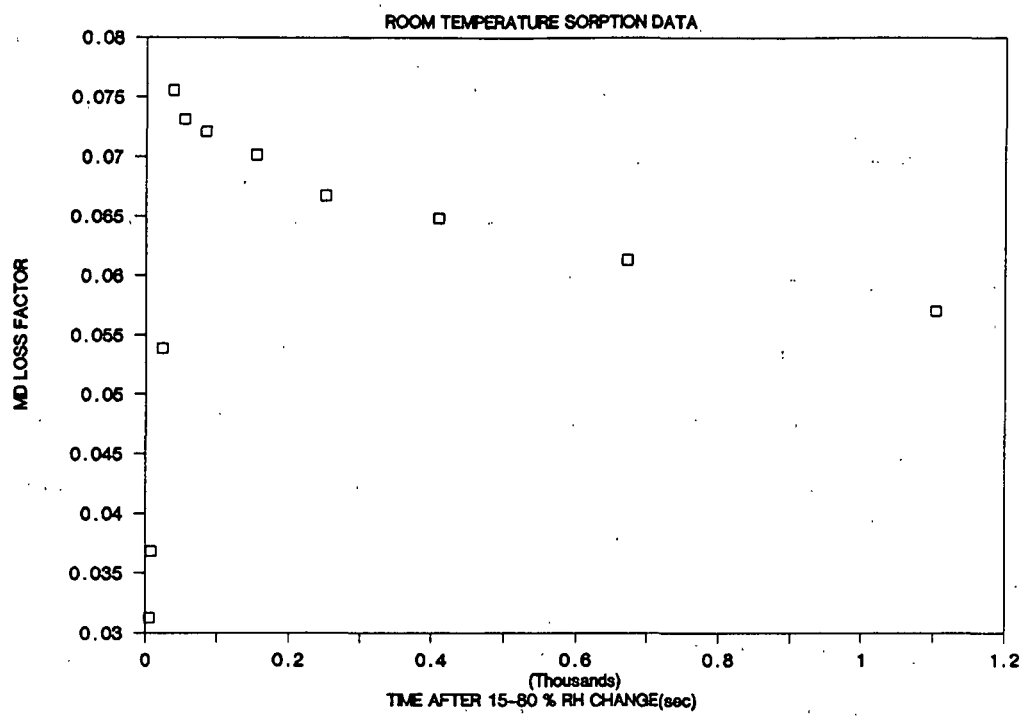

Figure 50. Low frequency MD loss factor-time data for commercial blotter stock undergoing sorption from 3.8-7.3% moisture.

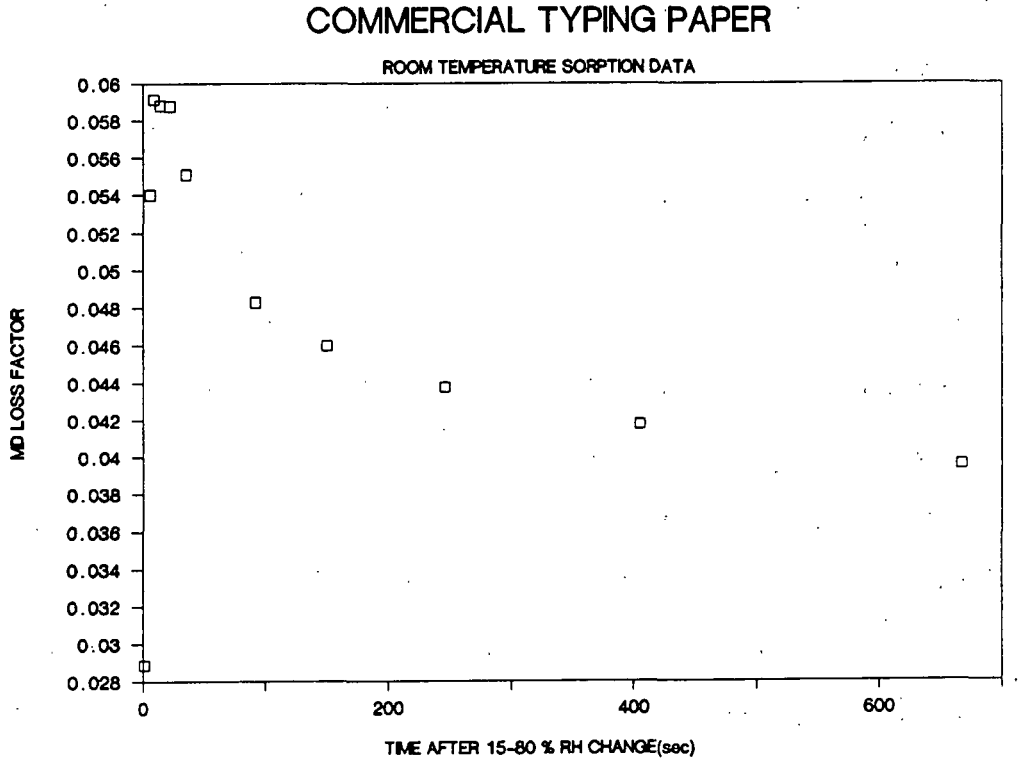

Figure 51. Low frequency MD loss factor-time data for commercial typing paper undergoing sorption from 3.9-7.9% moisture.

Strain amplitude was varied in several tests in an effort to determine whether linear-nonlinear differences were important. Increasing the strain amplitude had no measurable effect on the shapes of the mass specific modulus and loss factor vs. time curves over the ranges investigated (0.025-0.125% = maximum strain amplitude). Typical data are shown in Fig. 52-54. Unfortunately, a larger strain amplitude range was not possible. At low strain amplitudes the system was limited by the sensitivity of the load cell, while work hardening effects became prohibitively large at amplitudes much greater than 0.125%.

Equilibrium Data

The difficulties in obtaining absolute mass specific moduli values using the present Instron technique have already been noted. Errors are due primarily to inaccuracies in aligning and clamping samples in the test jaws as well as to work hardening effects. Nevertheless, an attempt was made to compare low frequency moduli and their moisture sensitivities with ultrasonic data obtained from similar samples. As previously mentioned, sample moistures could not be measured during the sorptive and desorptive runs. Moisture contents were, however, measured at the beginning and end of each run. Initial and final moistures for the runs shown in Fig. 44-47 were, respectively, measured as 10 and 6% (blotter stock desorption), 12.1 and 6.2% (typing paper desorption), 3.8 and 7.3% (blotter stock sorption), and 3.9 and 7.9% (typing paper sorption). These moistures, along with the relevant moduli, were used to obtain β_M/V_o^2 values of 0.075 and 0.083% for blotter stock and 0.040 and 0.085% for typing paper when using sorption and desorption data for the respective calculations. The large difference in the β_M/V_o^2 values (0.040% vs. 0.085%) obtained for typing paper when using desorption as opposed to sorption data is believed to be due to a substantial amount of work hardening occurring in the desorption run.

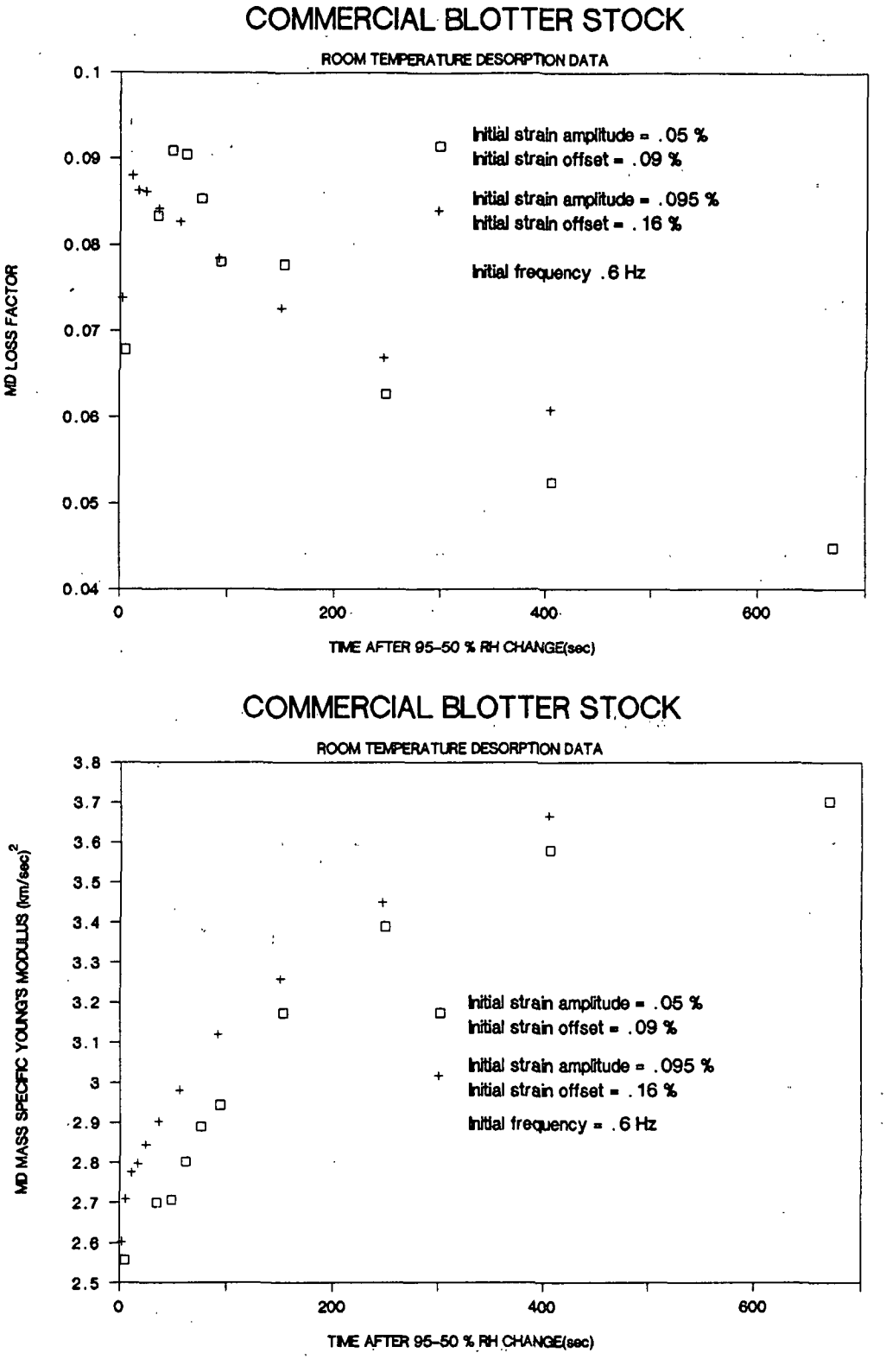

Figure 52. Low frequency MD loss factor and mass specific Young's modulus-time data for commercial blotter stock undergoing desorption (showing the effect of strain amplitude and offset).

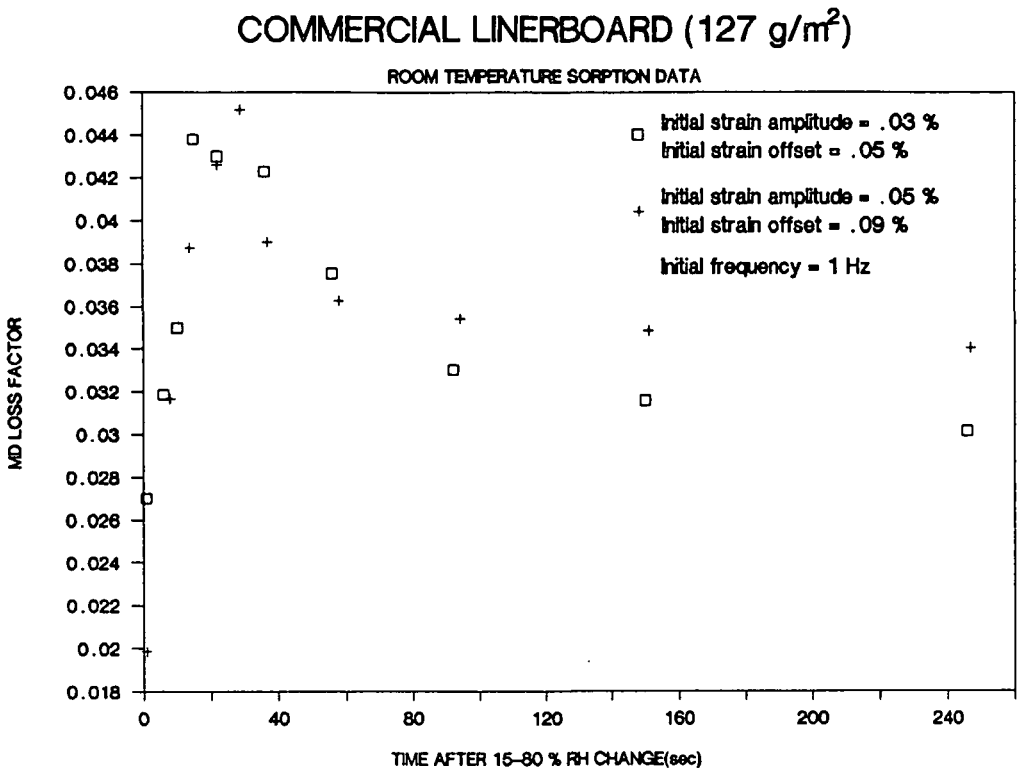

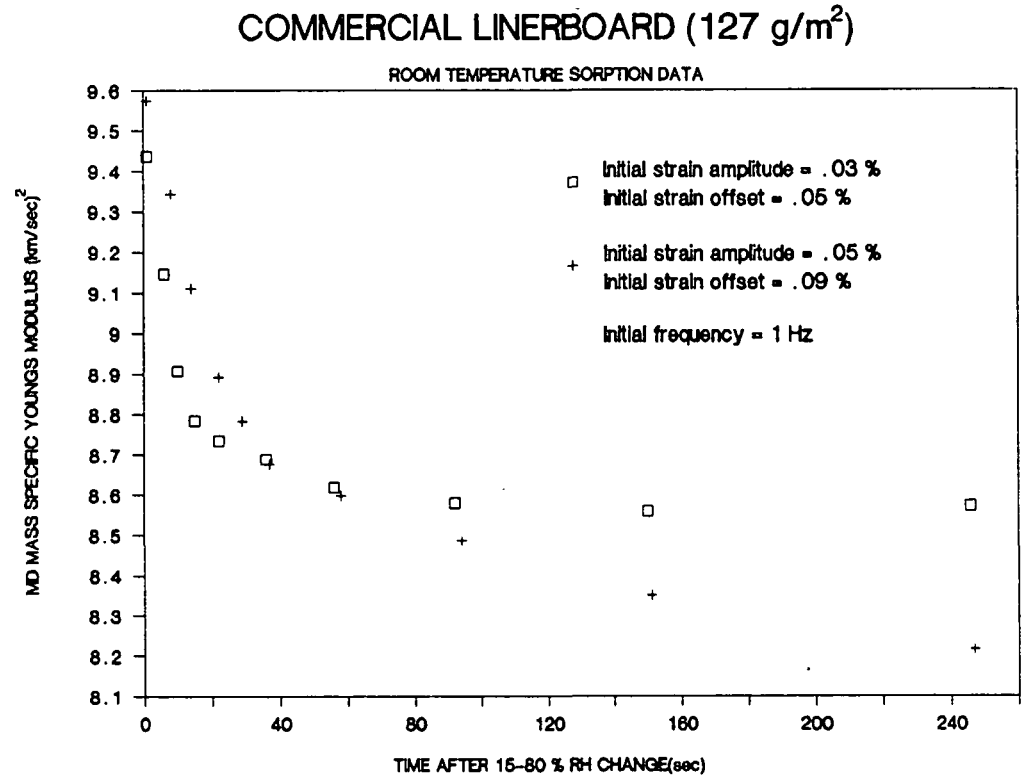

Figure 53. Low frequency MD loss factor and mass specific Young's modulus-time data for commercial linerboard undergoing sorption (showing the effect of strain amplitude and offset).

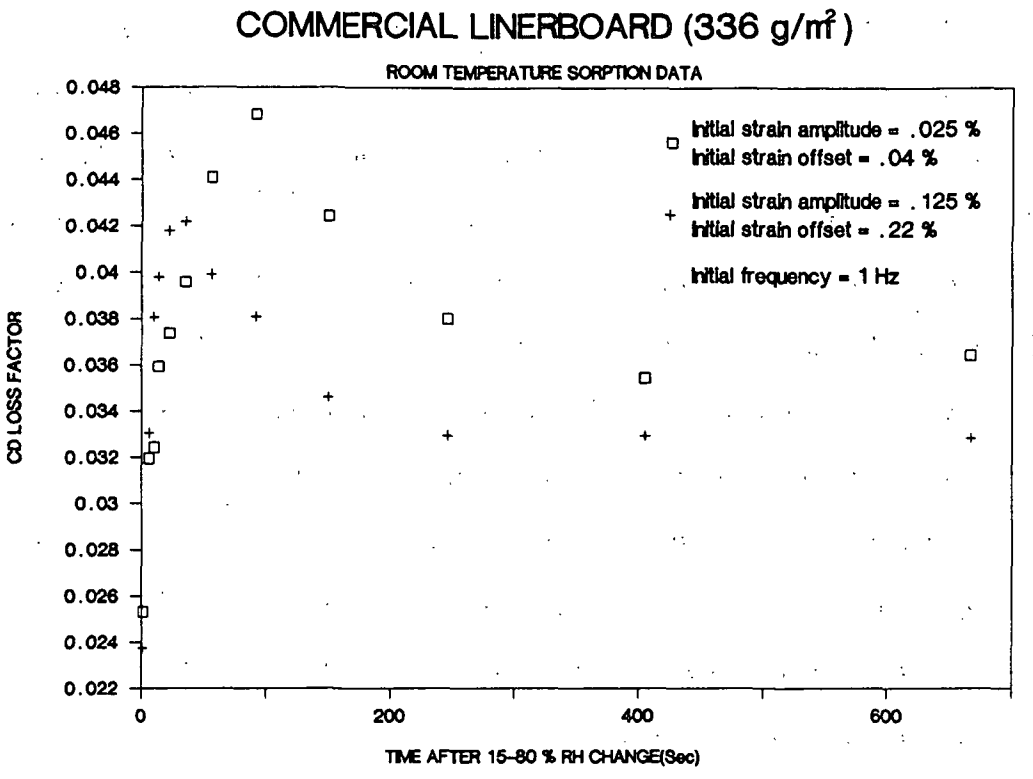

Figure 54. Low frequency CD loss factor-time data for commercial linerboard undergoing sorption (showing the effect of strain amplitude and offset).

Final mass specific modulus values from this run are unrealistically high, and are even higher than the initial sorption data obtained at a much lower moisture. This conclusion is also supported by the loss factor data. Final values from the typing paper desorption run are considerably lower than those from the sorption run even though the final moisture contents of the two samples are fairly close. Work hardening is expected to be greater in the case of desorption because the sample is at a higher moisture throughout most of the run. Work hardening didn't appear to be a problem in the blotter stock runs, however, as evidenced by the similarity of the sorption and desorption β_M/V_o^2 values as well as the fact that final loss factor values are much closer. The greater amount of work hardening that occurred in the typing paper desorption run is not surprising, considering that the initial strain offset and amplitude

were about twice as high in this case as those used in the typing paper sorption run and in the blotter stock runs. Using the initial mass specific modulus-moisture data from the sorption and desorption runs to calculate β_M/V_o^2 is therefore probably more appropriate as it eliminates work hardening effects. This produced a β_M/V_o^2 of 0.085% for blotter stock and 0.065% for typing paper. These slopes are higher than those obtained ultrasonically (see Table 2). The reasons for these differences are discussed in the next section. Table 2 regression data can also be used to calculate the difference between ultrasonic and Instron mass specific modulus data. At the standard moistures and temperatures defined in this table, the MD mass specific Young's modulus for blotter stock and typing paper measured ultrasonically are about 4.5 and 11.3 $(km/sec)^2$, respectively. Using initial data from the Instron sorption and desorption runs from Fig. 44-47 to obtain moisture-mass specific modulus relationships, low frequency mass specific modulus values of 3.7 and 6.8 $(km/sec)^2$ are calculated. Thus, a drop in mass specific modulus of approximately 20% for blotter stock and 40% for typing paper is seen when going from ultrasonic to Instron frequencies. These values encompass the 25% figure typically found for such frequency shifts at room temperature. Considering the previously mentioned difficulties in obtaining accurate mass specific modulus values with both the high and low frequency techniques used in the present study, the drops obtained in mass specific modulus (20 and 40%) appear reasonable.

DISCUSSION

EQUILIBRIUM

It must be emphasized that even though ultrasonic mass specific moduli vary linearly with moisture and temperature over the range available in the oven, linear variance of modulus with environment is not a universal property of cellulosic materials. At the oven conditions, moisture and temperature primarily alter the mechanical compliance of cellulose through their influence on the low temperature flank of a single transition, namely the α relaxation. Over the limited range experienced in the oven, this happens to lead to linear moisture-mass specific modulus and temperature-mass specific modulus behavior. At lower temperatures, however, complex interactions between environmental conditions and secondary transitions result in large deviations from linearity. Figure 55 is an illustration of the more general behavior of cellulose. Here, data from the Du Pont PUDO-134 cellophane obtained with the strip resonance technique in a low temperature environmental chamber[9] are extended by resonant strip measurements made in the oven. The oven data are represented by lines calculated from Table 2, run 15 regression coefficients at the five moisture contents measured in the low-temperature study. Notice particularly how mass specific modulus data at each moisture level intersect the curve for the "dry" sample at different temperatures along the curves shown in Fig. 55. The moist-dry crossovers range from room temperature for a moisture content of 2.4% to 200°K at 11% and are a manifestation of the antiplasticizing effect of water on the secondary relaxations in cellulose. At temperatures below the β relaxation, repression of γ relaxation by water leads to an increase in mass specific modulus. At higher temperatures, the β relaxation and the onset of the α relaxation

are encountered, and moisture has the more common consequence of decreasing the modulus.

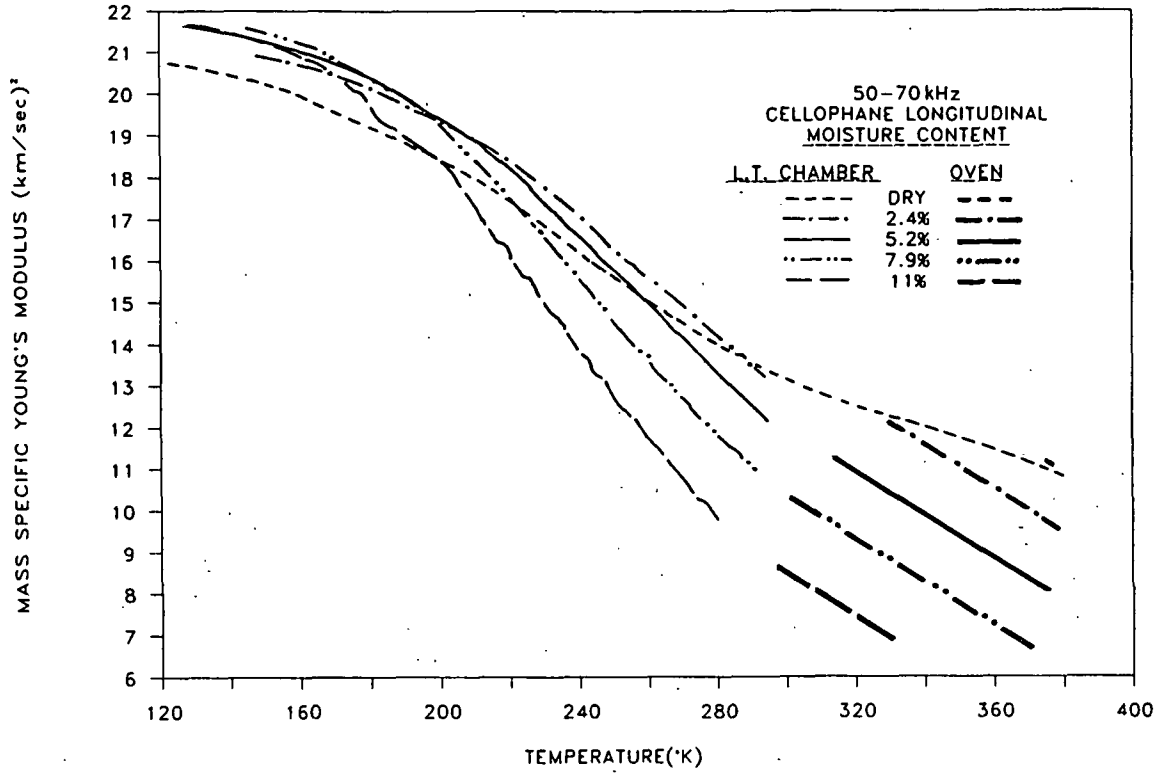

Figure 55. Strip resonance moisture-temperature-MD mass specific Young's modulus data for PUDO-134 cellophane over an extended temperature range.

Additional insight into moisture-temperature-modulus relationships can be obtained by studying the loss tangent vs. inverse absolute temperature curves in Fig. 56. As was Fig. 55, this is a composite of data taken in the low-temperature chamber and in the oven. In order to get the oven loss tangents to coincide with the low-temperature data, the loss tangents measured in the oven were uniformly decreased by 0.008. This resulted in similar values at the two moisture-temperature conditions common to both studies (378°K - 0% moisture, 298°K - 7.9% moisture). It is speculated that artificially high oven loss tangents result from the transducer-sample coupling degradation that occurs when the humidity of the oven is cycled in an attempt to stabilize the sample, as

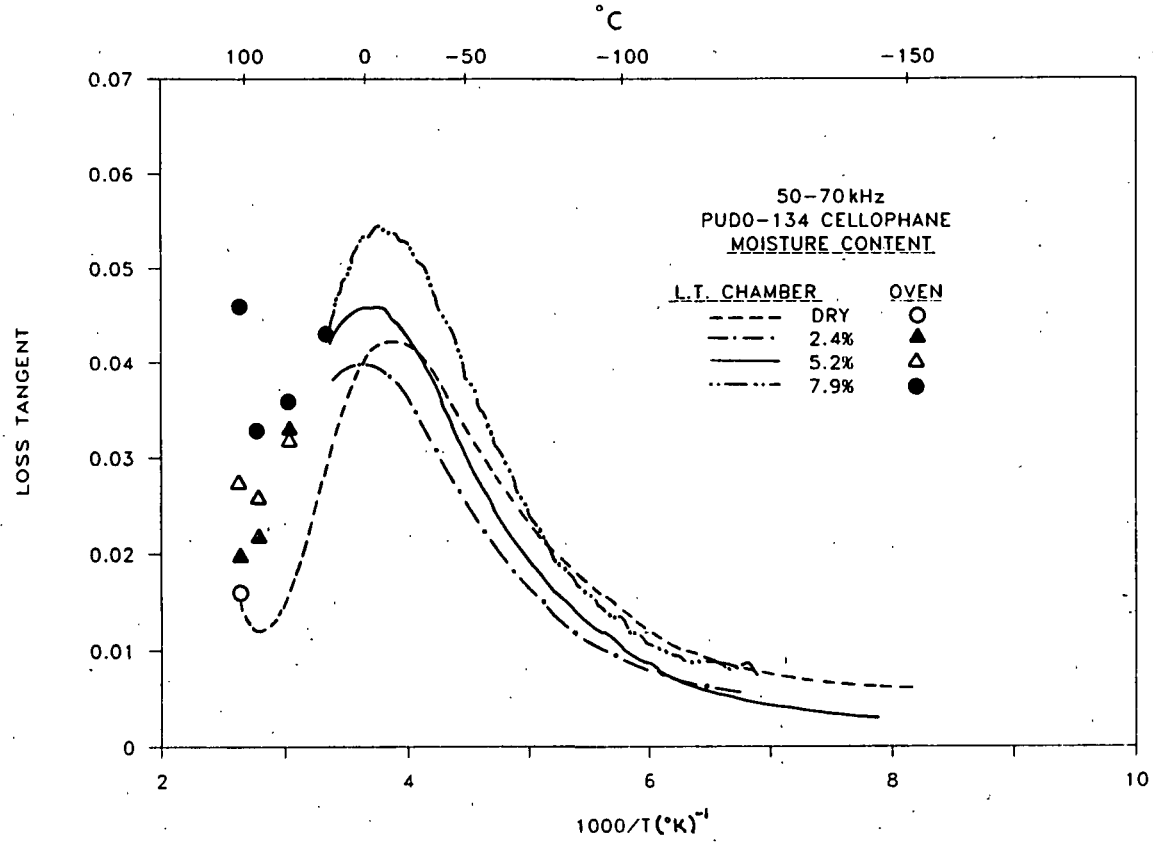

Figure 56. Strip resonance moisture-temperature-MD loss tangent data for PUDO-134 cellophane over an extended temperature range.

described earlier. Increases in loss tangent determinations are routinely observed when samples are moisture cycled. Since the low-temperature chamber was not cycled after sample bonding, it is assumed that it yields the more reliable absolute values of loss tangent. Notice the tanδ curve in Fig. 56 for the dry cellophane. Here, the γ relaxation produces a distinct peak at about -10°C. Addition of the first moisture increments decreases the intensity of this peak and shifts it up to a temperature of around 0°C. Further moisture additions increase the peak height and move it to lower temperatures. These results are understood in terms of the antiplasticization of the γ relaxation by water. The water first converts the γ transition to a higher temperature β

transition and then effectively plasticizes the β transition. Separate maxima are not observed for these relaxations, since their overlap causes them to be too close to be resolved at ultrasonic frequencies. The dry loss tangent data in Fig. 56 also contain evidence for the α relaxation. This is seen as an upturn in the loss tangent curve above room temperature. The onset of this transition is steadily enhanced by moisture addition.

Since ultrasonic mass specific modulus measurements are conducted at higher frequencies than the standard mechanical tests, they experience the secondary transitions at higher temperatures and find them more closely spaced in temperature. This is demonstrated by comparing Fig. 56 with the loss tangent data for a 25 μm thick unplasticized cellophane at 11 Hz published by Bradley and Carr.[7] Their cellophane, PUDO-193, was also obtained from Du Pont and differs from the Fig. 56 sample in thickness. Their Fig. 1 is reproduced as Fig. 57. In this figure at 2.8% moisture, separate peaks are generated by the β and γ transitions. At 4.1 and 7.3% moistures the γ transition is eclipsed by the β transition, while at 0.34% moisture γ dominates and β is barely discernible. As mentioned earlier, differences between low and high frequency data arise because the β relaxation has a higher activation energy than the γ relaxation, and the two are therefore too close in temperature to be displayed as distinct peaks at ultrasonic frequencies. Unlike the lower temperature transitions, the α relaxation has a much larger activation energy, and its onset temperature is not very sensitive to frequency.

Dry loss tangent data from Fig. 56 and 57 can be used to determine an activation energy for the γ transition. The peak is seen to shift from -80 to -10°C when going from 11 Hz to 60 kHz. This results in a calculated activation energy of around 12 kcal/mole. A rough estimate of the activation energy for the α

transition can also be obtained from dry data (assuming temperature shifts of troughs are similar to those of peaks). At ultrasonic frequencies the onset of the α transition occurs at around 90°C. The corresponding onset for the Bradley and Carr data is more difficult to determine but appears to occur around 60 or 70°C, resulting in a calculated activation energy between 70 and 105 kcal/mole.

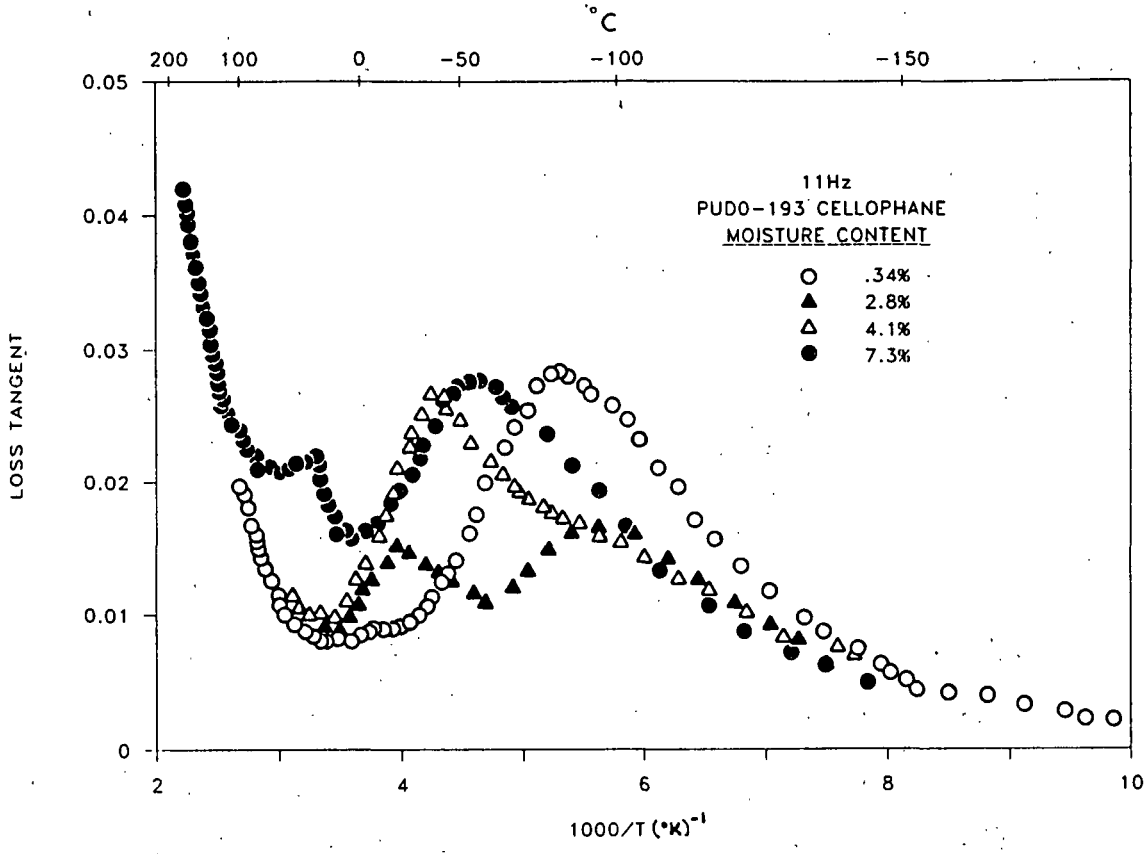

Figure 57. A reproduction of the low frequency moisture-temperature-MD loss tangent data for PUDO-193 cellophane (Bradley and Carr[7]).

A time-temperature superposition argument can be used to rationalize the differences in mass specific modulus values obtained using ultrasonic and lower frequency techniques. The mass specific modulus of dry cellophane (PUDO-134) measured ultrasonically at room temperature (295°K) and 60 kHz is approximately 13.5 $(km/sec)^2$. If the density of PUDO-193 and PUDO-134 cellophanes are assumed

similar (1.45 g/cm^3), then the use of data obtained by Bradley and Carr[7] at 295°K and 11 Hz results in a calculated mass specific modulus of approximately 10 (km/sec)^2. As previously mentioned, this decrease of approximately 25% is typical of the observed modulus changes in cellulose when shifting from ultrasonic to load-elongation frequencies. When compared at an equivalent temperature, however, results are much closer. If an activation energy of 12 kcal/mole for the γ relaxation is used, ultrasonic data at room temperature are equivalent to 11 Hz data at 210°K. At this temperature, the low frequency mass specific modulus is approximately 13.8 (km/sec)^2, a value much closer to the 13.5 (km/sec)^2 measured using the strip resonance technique.

In addition to the present study, other reports of the effects of moisture on the room temperature ultrasonic mass specific modulus of paper are available. These results, along with some published low frequency moisture-moduli data, are summarized in Table 4. For the sake of comparison, literature data with moistures above 20% were not used. An attempt was also made to express all results in terms of the parameters described for Table 2. This led to some difficulties, however. To start with, there was no straightforward way of determining the appropriate r^2 values for some of the studies. This is because raw data were not always available, and r^2 had to be estimated using representative points taken from published curves. These correlation coefficients, which are placed in parentheses, have limited statistical significance but do give an indication of the linearity of data. Also, M_o, the moisture content at 50% RH, was not always presented, and some M_o numbers were estimated from known values of similar papers. Finally, since density was not always reported, modulus rather than mass specific modulus was listed for the low frequency work and a different moisture sensitivity parameter, β_{M1} calculated. However, as density

Table 4. Room temperature moisture-modulus regression analysis (published data).

Sample[a]	Mode[b]	Frequency[c] (kHz)	r^2	E_o^2 ($d/cm^2 \times 10^{10}$)	β_{M1}/E_o^2 (1/%)	ΔM (%)	M_o[d] (%)
VIII	MDL	Low	{0.990}	4.15	-0.071	2-18	{7.70}
IX	MDL	Low	{0.999}	6.07	-0.065	4-14	{7.70}
IX	CDL	Low	{0.994}	2.89	-0.071	4-14	{7.70}
X	MDL	Low	{0.998}	5.28	-0.065	4-14	{7.70}
X	CDL	Low	{0.995}	2.10	-0.076	4-14	{7.70}
XI	HSL	0.2	0.992	2.45	-0.073	0-12	6.95
XII	HSL	Low	0.981	6.35	-0.053	4-17	6.89
XIII	MDL	Low	{0.941}	4.40	-0.050	0-20	{7.70}
XIV	MDL	Low	0.997	4.71	-0.063	3-14	6.24
XIV	MDL	57	0.994	6.27	-0.045	3-14	6.24
				V_o^2 $(km/sec)^2$	β_M/V_o^2 (1/%)		
XIV	MDL	57	0.990	9.83	-0.043	3-14	6.24
XIV	CDL	57	0.994	6.92	-0.047	3-14	6.24
XIV	Shear	57	0.996	2.90	-0.048	3-14	6.24
XV	MDL	5	{0.995}	11.09	-0.041	0-20	{7.70}
XV	CDL	5	{0.993}	4.19	-0.044	0-20	{7.70}
XVI	HSL	10	{0.918}	6.19	-0.011	4-18	{6.95}
XVII	MDL	60	0.994	10.99	-0.041	5-12	7.75
XVII	CDL	60	0.991	4.24	-0.052	5-12	7.75
XVII	Shear	60	0.985	2.63	-0.044	5-12	7.75

[a] VIII: Kraft eucalypt.[79]
IX: Lake States linerboard.[83]
X: Southern linerboard.[83]
XI: Bleached sulfite (215 g/m^2; 256 µm).[84]
XII: Softwood alpha (56 g/m^2; 75 µm).[85]
XIII: Kraft sack (105 g/m^2; 182 µm).[26]
XIV: Bond (75 g/m^2; 112 µm).[86]
XV: Kraft linerboard (186 g/m^2).[87]
XVI: Bleached sulfite (60 g/m^2).[1]
XVII: Linerboard (337 g/m^2; 527 µm).[88]

[b] MDL: Machine direction longitudinal.
CDL: Cross machine direction longitudinal.
HSL: Handsheet longitudinal.

[c] Low: (Initial slope of stress-strain curves).

[d] { }: Estimated.

is not overly sensitive to moisture at contents less than 20%, β_M/V_o^2 is approximately equal to β_{M1}/E_o^2 and meaningful comparisons of the relative moisture dependence of modulus and mass specific modulus at different frequencies can be made. To illustrate this, the ultrasonic data from sample XIV are presented in both forms. Notice that the relative sensitivities of modulus to moisture (β_M/V_o^2 = -0.043/% and β_{M1}/E_o^2 = -0.045/%), are nearly equal. The slight difference indicates that the measured density decreased slightly with increased moisture over this range. Sample XIV is also the only sample for which modulus is listed at both a low and high frequency. Again, notice the 25% difference observed between ultrasonic and load-elongation measurements.

From the high r^2 values in Table 4, it appears that linear relationships are appropriate characterizations of high and low frequency room temperature moisture-modulus measurements. However, as might be expected, results extending to higher moisture levels conform better to an exponential dependence of modulus to moisture at both low[78,89] and high[87,90] frequencies. In addition, a decrease in the moisture sensitivity below about 5% moisture has been reported for low[10,25,26,78] and high[9] frequency room temperature modulus data. Even though one low frequency study[84] failed to document this modulus plateau at low moistures, it is believed to be a real phenomenon as it coincides with what is expected from the secondary relaxation behavior of cellulose. At low frequency the γ and β relaxation are complete at room temperature. Therefore, the conversion of the γ relaxation to the β relaxation by initial moisture addition has little effect on low frequency measurements. As moisture content is increased further, however, the onset of the α transition protrudes into the low frequency, room temperature domain. This results in an increase in loss tangent and a greater sensitivity of modulus to moisture. Ultrasonic measurements also

reveal a deviation from linearity at room temperature and low moisture content (see Fig. 55). However, the action is more complex at high frequency. Here the β and γ transitions are not complete at room temperature, and initial moisture increments can have an antiplasticizing effect. This, along with the shift of the α transition onset to a somewhat higher temperature, augments the difference between high and low frequency data at low and moderate moisture contents. This phenomenon did not cause deviations from linearity in the oven measurements, since dry data were all taken above room temperature where β was nearly complete and α was more dominant.

An examination of moisture sensitivity parameters from Table 4 brings out some interesting points. First of all, with one exception, the normalized values of β_M or β_{M1} in each regime are fairly consistent. Like measurements are of roughly the same value, and the CD longitudinal and shear slopes are more negative than the MD longitudinal values from the same sample. The one exception to the consistency of results, sample XVI, is reported as having such a low slope that its validity is called into question. Notice also that the relative moisture sensitivity is significantly lower at ultrasonic frequencies. However, if β_{M1} is converted to β_M by a density multiplication, and if sensitivity is compared on an absolute basis, results are similar. For example, the β_M value for sample XIV data is 0.30 $km^2/sec^2/\%$ when measured at low frequencies and 0.28 $km^2/sec^2/\%$ at ultrasonic frequencies.

The results in Table 4 can be interpreted in terms of the thermal relaxation model. At room temperature, the α transition plays a dominant role in the environmental sensitivity of the physical properties of cellulose. In Fig. 58, the α transition is idealized as a standard linear solid. Notice that this idealization produces a large linear regime in the plot of log frequency vs.

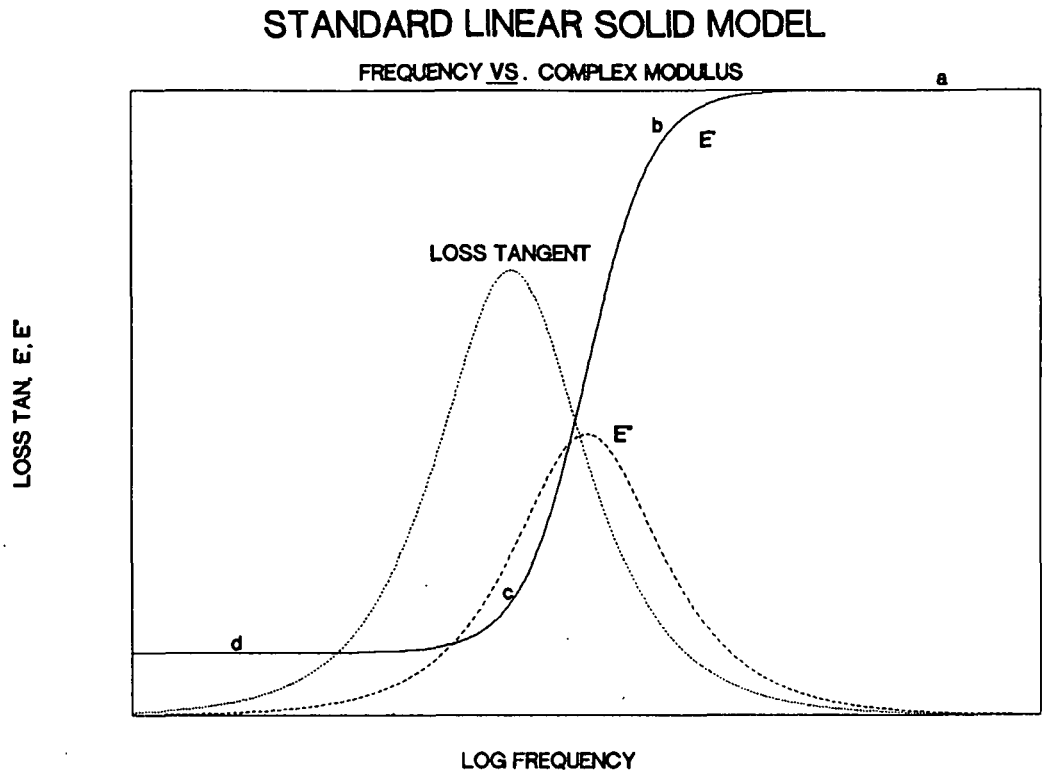

Figure 58. Loss tangent, loss modulus, and storage modulus-log frequency relations showing a single thermal relaxation for a viscoelastic material modeled as a standard linear solid.

modulus. The established principle of time-temperature superposition in polymeric materials[91] demonstrates that the changes produced by a shift in inverse temperature are often equivalent to a proportional change in the logarithm of the frequency. If the α transition is assumed to obey an Arrhenius relationship and moisture is assumed to have a linear effect on the activation energy, then a moisture-log frequency equivalence also results. Although the above analysis relies on some admittedly tenuous assumptions, it does rationalize many of the observed results. At low test frequencies, initial moisture addition would be roughly equivalent to moving along the storage modulus, E', curve from a to b (see Fig. 58) resulting in only minimal modulus changes. This would explain the reported low moisture sensitivity of modulus at low moistures. The more complex room temperature, moisture-ultrasonic mass specific modulus response

seen at low moistures is due to the closer spacing of transitions at these frequencies. Therefore, unlike the low frequency case where other transitions are complete and the path from a to b is affected only by the α transition response, the ultrasonic modulus is also affected by the completion of the β and γ transitions. With continued moisture addition, a regime is encountered where moisture and modulus are related nearly linearly (b to c). This helps explain the equivalence of low and high frequency β_{M1} and β_M values in Table 4. Ultrasonic data in this table would just be obtained higher along the line (closer to b) than low frequency data resulting in higher V_o^2 (and E_o^2) values. At even higher moisture addition levels, the relaxation nears completion and modulus begins to decrease at a decreasing rate (c to d), explaining the logarithmic modulus-moisture response reported at high moistures.

TRANSIENT

Even though a completely satisfactory explanation for the accelerated creep accompanying cyclic humidity conditions has not been proposed to date, the characteristics of this phenomenon are fairly well understood and good reviews on the subject exist. In a comprehensive review of data obtained under nonequilibrium moisture conditions, Back, Salmen, and Richardson[27] consider accelerated creep and transient decreases in modulus without distinction from one another. However, because of the wide range in reported results, the importance and/or even the existence of transient decreases in modulus (increases in loss tangent) accompanying sorption and desorption is still debatable. The present study, although adding to the base of knowledge in this area, did not clarify the picture completely. Therefore, the question of whether the accelerated creep phenomenon is related to nonequilibrium-equilibrium modulus differences remains unanswered. It is easy to imagine that a transient decrease in modulus

would lead to an increased creep rate over an extended period of time. However, reasonable explanations for accelerated creep may not have to incorporate a transient decrease of modulus in their solution.

As indicated in the results section, little or no transient increase in loss tangent and no transient decrease in mass specific modulus were found to accompany moisture changes when measured using ultrasonic techniques. Also, when samples were tested using the low frequency cyclic loading technique, mass specific modulus minima on sorption and desorption were not observed. Transient maxima in loss factor were, however, encountered with the low frequency technique. Therefore, data from the present study don't appear to be self consistent. It is also very difficult to combine these data with previously published results and make any definite statements regarding the transient modulus and loss tangent changes that accompany sorption and desorption. Possible reasons for the seemingly contradictory results are that various techniques have been used to test various materials in various loading modes and under various sorptive and desorptive conditions. Although the many differences complicate the analysis, a more detailed discussion of the studies comprising the body of evidence favoring transient decreases in modulus and/or increases in loss tangent enables a clearer picture to be drawn.

The magnitude of the transient effects observed varies between published studies; however, two studies stand out as being considerably different with regard to modulus changes occurring during sorption and desorption. First, far larger transient minima in the torsional rigidity of wool fibers accompanying sorption were found by Mackay and Downes (30-60%) than by Nordon (< 5%) in a subsequent study. Nordon found that the smaller minima obtained in his study were due to the smaller angular shear strain amplitudes (0.03% vs. 2%) and

larger fiber diameters (45 μm vs. 30 μm) used. The diameter is important in affecting sorption rate which, in turn, is responsible for the stress gradients built up within the fiber. Fiber diameter is also important in affecting the angular shear strain amplitude. At a given oscillation amplitude, doubling the diameter will result in a maximum shear strain that is twice as large. The fact that transient minima become greater as oscillation amplitude is increased indicates that nonlinear effects may play a role in the transient modulus decreases. It could be that most of the transient modulus decrease (loss tangent increase) is due to nonlinear effects. However, the abovementioned fact that larger transient modulus decreases occur in smaller diameter fibers where maximum angular shear strains are lower, sheds some doubt on the importance of sample linearity.

If they are important, nonlinear effects may help to explain the second seemingly inconsistent modulus study, that of Back, Salmen, and Richardson. Their sorption results (Fig. 16) are similar to the bulk of the data, exhibiting a slight minimum before increasing to a final equilibrium value. However, the desorption results obtained by these researchers (Fig. 17) show an initial minimum in stiffness which is inconsistent with all other data, including the present low and high frequency results. In other studies[58,65] (present low and high frequency data), modulus continuously increases with time as desorption proceeds. Ideally, the low frequency technique used in the present study has several advantages over the one employed by Back, Salmen, and Richardson. These include the possibility of using a variety of frequencies and strain amplitudes and the utilization of single sample testing. Testing at a variety of strain amplitudes should allow nonlinear-linear differences to be clarified, while the use of a single sample at all moisture contents decreases the scatter in the data and increases the confidence in the resulting trends. Unfortunately the practical frequency range was very small (0.5-1 Hz). Also, strain amplitude

could not be increased much above 0.1% before work hardening effects became dominant, and strain amplitudes below 0.025-0.05% were not possible. Therefore, the questions of the importance of test frequency and strain amplitude remain unanswered. The stiffness curves obtained by Back, Salmen, and Richardson shown in Fig. 16 and 17 are averages comprised from many load-elongation tests, and are therefore inherently higher in variability than the present low frequency data. Also, Back's tensile stiffness calculations are affected by the way secants to the load-elongation curves are drawn. The location of the secant is probably quite critical in determining whether a "true" linear tensile stiffness or a "nonlinear" tensile stiffness is obtained. Other than these noted differences, it is difficult to speculate about the reasons for the inconsistencies between the results obtained by Back, Salmen, and Richardson, and all others. In any case, if the bulk of the transient modulus data are assumed correct (excluding ultrasonic data), the typical transient result is a continuous modulus increase during desorption and a decrease (possibly passing through a slight minimum) with sorption.

Unfortunately, most of the studies don't verify whether transient modulus decreases relative to equilibrium values exist. The reason for this uncertainty is the fact that sample moisture content and temperature are not measured. Comparisons with equilibrium values are therefore impossible. Nevertheless, the reported minima seen with sorption are strong indications of transient-equilibrium differences. They don't, however, give a quantifiable estimate of these differences. For example, Fig. 16, which is typical of sorption results, shows little or no transient minimum in modulus but a 10-15% transient decrease. The two studies that do show direct differences between equilibrium and nonequilibrium modulus data, that of Mackay and Downes and Back,

Salmen, and Richardson, are ones that have previously been indicated as different from all others and are therefore, somewhat in question.

Transient maxima in loss tangent have been seen in several sorption[47,58,64,66] and desorption[66] (present low frequency work) studies. Increases appear to be larger when samples are tested in torsion[47,58,66] rather than in a longitudinal mode[64] (present low frequency work). The size of the transient maxima and the fact that they are produced under sorptive as well as desorptive conditions rules out the possibility of moisture induced temperature changes as a total explanation for the phenomenon. The major questions, then, are "why were these transient increases not found in the present ultrasonic study, why are they larger in torsion, and are the increases a real phenomenon?"

The ultrasonic techniques differ from those used previously in two important ways, namely, test frequency and strain amplitude. It is difficult to rationalize that test frequency is the critical difference. Frequency might become important if significant changes in samples can occur while the measurements are being made. This would possibly result in a "lack of loop closure" type effect. However, transient loss tangent changes occur for several minutes and sometimes several hours, whereas the lowest frequency test used to measure transient loss tangent maxima had a period of only $\approx$ 20 seconds. It seems, therefore, that the frequencies employed should have been more than adequate in following the transient phenomenon. Nevertheless, a situation could be supposed wherein the slow relaxations responsible for the transient effect allow secondary relaxations to occur over an extended period of time. These relaxations might then be seen at low frequencies and not at ultrasonic frequencies. The importance of strain amplitude has already been discussed. Nonlinear effects may play an important role in the differences found between ultrasonic and low

frequency data. Even though considerable loads were applied to ultrasonically tested strip resonance samples and found to produce no noticeable transient modulus decrease or loss tangent increase, the ultrasonic response in these cases is still linear.

As is the case with the accelerated creep phenomenon, the size of transient loss tangent maxima is dependent upon the direction and mode of testing. Crystalline regions in wool and cotton are aligned primarily along the fiber axis. Because water is unable to penetrate into these regions, they are unaffected by moisture change. Noncrystalline regions, on the other hand, are influenced considerably by moisture. Therefore, moisture sensitivity and transient moisture effects are expected to be larger in tests more heavily influenced by the noncrystalline regions. A series-parallel argument can be used to better explain the differences in test mode and direction. Paper and individual fibers can be idealized as two component systems. One component, A, representing the crystalline regions, has a very high modulus, E_A, and a very low loss tangent, Tan_A, while the other component, B, representing the noncrystalline regions, has a low modulus, E_B, and a high loss tangent, Tan_B. Figure 59 shows these components in parallel and in series configurations. Suppose an axial compressive stress is applied as shown in case I. Here the resulting strain is equal to the strains in each of the components. Because $E_A >> E_B$, most of the stress will reside in A, and strain and loss tangent will be small. In models II and III, on the other hand, the components are in series and the stresses are equal. In these cases, the fact that $E_A >> E_B$ results in the strain being concentrated in component B and the loss tangent being high. Of course, in an actual situation, ideal parallel and series cases don't exist and materials fall somewhere between these two extremes. Such concepts give at least a qualitative feeling for the differences in test modes and directions.

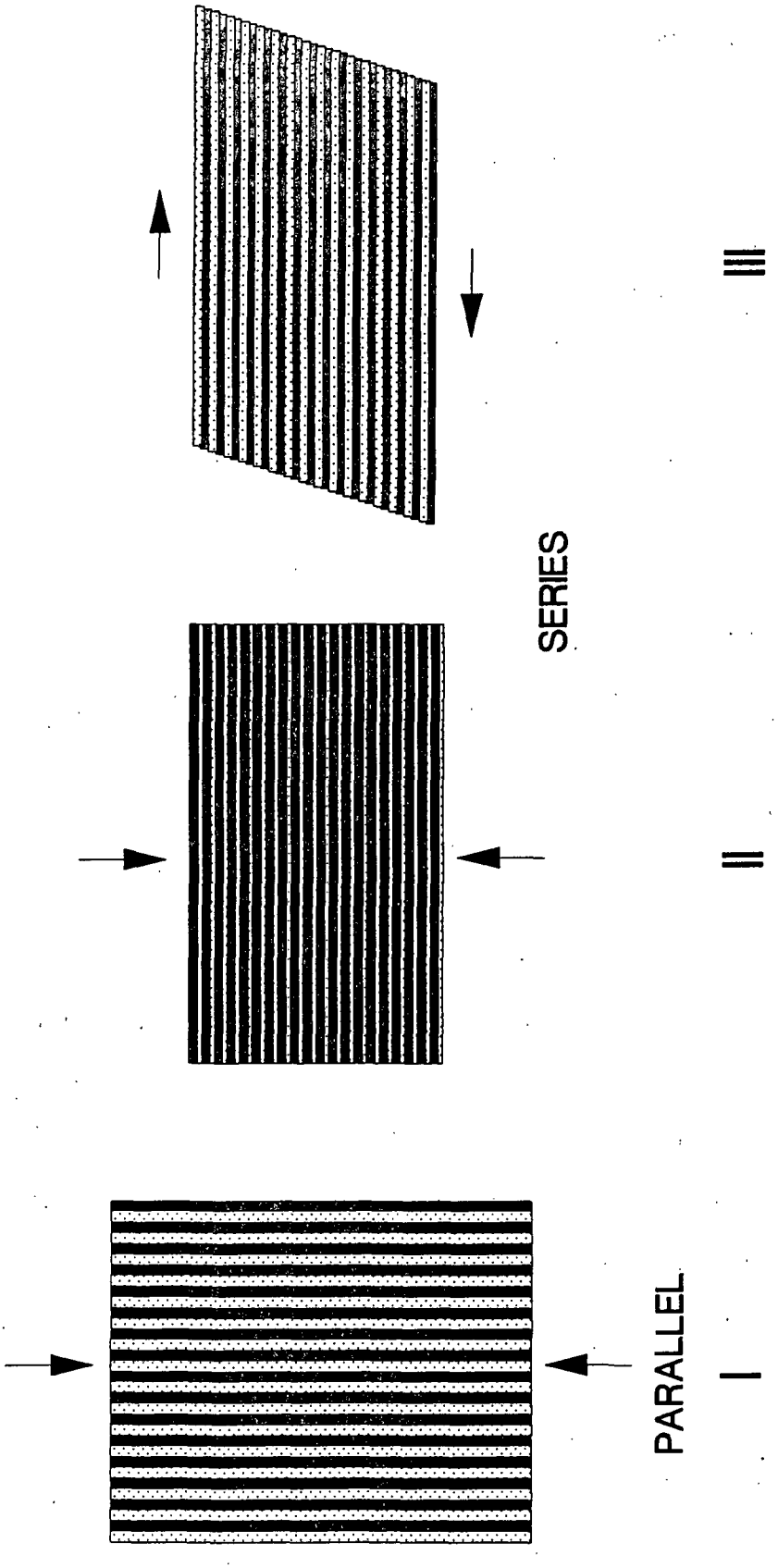

Figure 59. A model of a two component system where one component has a much higher modulus and a much lower loss tangent.

Fiber axial moduli are expected to be closer to the parallel case than fiber transverse moduli. Also, MD longitudinal moduli are assumed nearer to the parallel case than CD longitudinal and in-plane shear moduli which, in turn, are assumed closer than ZD longitudinal and out-of-plane shear moduli. Therefore, moisture is expected to affect transverse fiber moduli and in-plane shear moduli more than longitudinal moduli, and torsional loss tangent maxima of fibers and sheets are expected to be larger than those found in longitudinal tension. This conclusion appears to be substantiated by most of the experimental data. The transient loss tangent maxima measured in torsion of fibers by Mackay and Downes (100%) and De Ruvo, Lundberg, Martin-Lof, and Soremark (25%) and in torsion of paper strips by Kubat and Lindbergson (100%) were generally larger than those found in tension by Danilatos and Postle (20%) and in the present study (25%). The largest transient minima in modulus also come from a torsion study (Mackay and Downes) as is expected from the above arguments. Surprisingly, the large loss tangent maxima found by Kubat and Lindbergson were not accompanied by modulus minima.

If the ideas concerning the influence of test direction on transient loss tangent maxima and modulus minima are correct, larger effects are expected in the thickness direction (ZD) of paper than in the MD or CD. To test this hypothesis, a few experiments were performed on linerboard and blotter stock where mass specific moduli in the ZD were measured during sorption and desorption. However, no transient minima in ZD moduli occurred. Figures 60 and 61 show typical data.

Finally, the question of transient temperature changes needs to be addressed. As seen in the ultrasonic data from the present study (Fig. 37 and 38) as well as in conductivity data,[82] corrections for temperature must be made

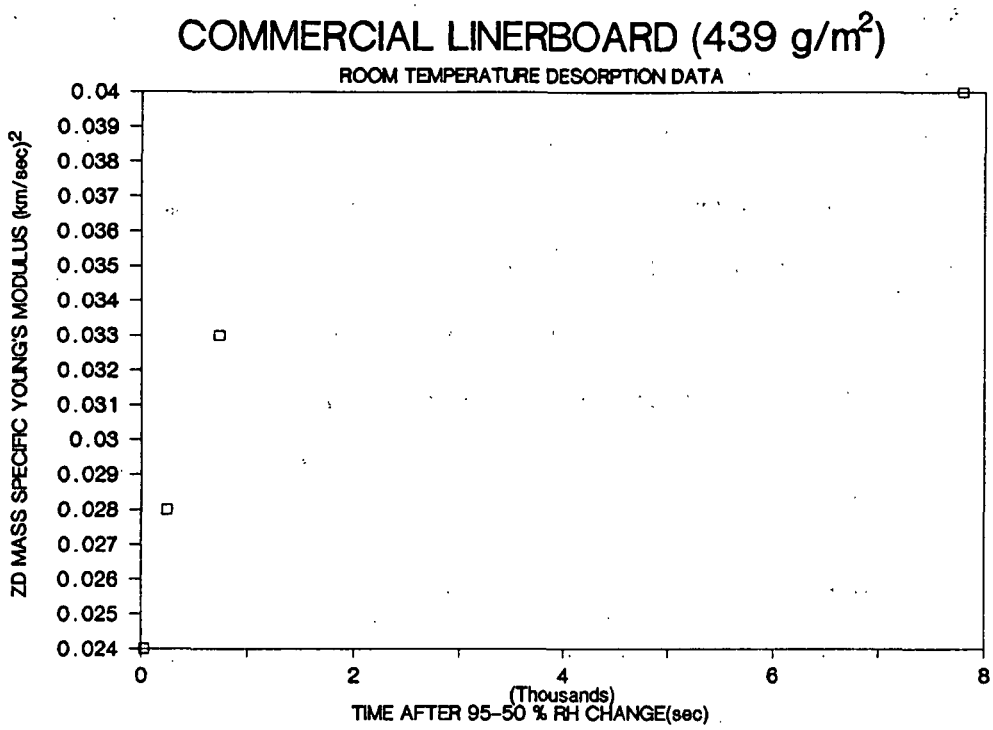

Figure 60. Ultrasonic ZD mass specific Young's modulus-time data for commercial linerboard undergoing desorption.

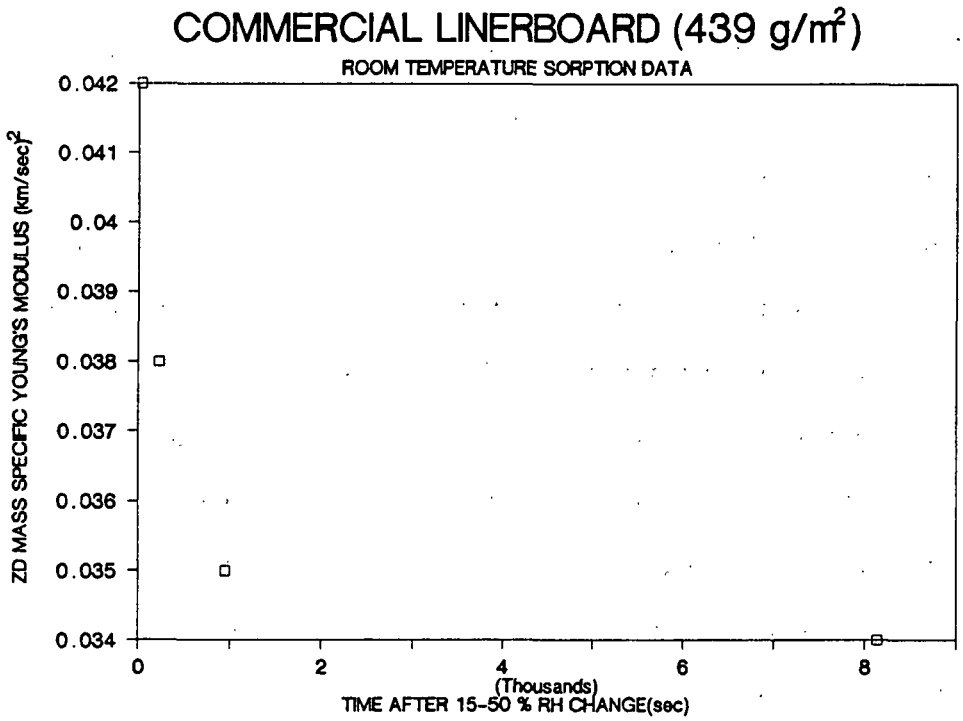

Figure 61. Ultrasonic ZD mass specific Young's modulus-time data for commercial linerboard undergoing sorption.

to ensure that all data are compared on a common basis. Moisture induced temperature changes cause sorptive modulus data to be lower and desorptive data higher than equilibrium values. It is possible, therefore, that the reported modulus minima accompanying sorption are due to the increased temperature of samples. This would help to explain why transient changes are more dramatic at low moisture contents where the heat of sorption is the greatest.[59,68] However, due to the lack of pertinent moisture and temperature data, it is not possible to determine whether or not temperature effects can explain the total sorptive-equilibrium differences. Of course, temperature corrections affect desorption data in the opposite way. That is, if a transient decrease in modulus is observed in data uncorrected for evaporative cooling effects, the decrease will be even larger when corrections are made. Therefore, temperature changes certainly aren't responsible for the initial decrease in stiffness found by Back, Salmen, and Richardson in samples undergoing desorption.

It is also unlikely that transient temperature changes can explain the loss tangent maxima. At room temperature and low test frequencies, increases in temperature are expected to increase loss tangent values. Sorptive heating might therefore cause loss tangent maxima to occur. However, maxima were also found accompanying desorption where temperatures fall initially and loss tangents are expected to be lower. Also, inordinately large temperature increases are required to explain observed sorptive loss tangent maxima. Finally, changes in loss tangents occur long after moisture induced temperature transients are complete. For example, loss tangents shown in Fig. 15 are still decreasing hours after a vacuum is drawn, even though sample temperature excursions are complete after only a few minutes.

CONCLUSIONS

A considerable amount of work must be completed before a comprehensive understanding of the moisture-temperature-frequency-modulus relationships in cellulose is obtained. Transient moisture conditions only compound the complexity of the picture. The present study has hopefully increased our knowledge in this area and added some insight regarding ultrasonic-low frequency differences. Thermal relaxation concepts have been shown to be quite useful in helping to explain the equilibrium differences. Under conditions commonly encountered during the manufacture and use of paper, temperature and moisture are believed to affect modulus primarily through their influence on the α transition. This relaxation is a result of the motion of large chain segments in the noncrystalline regions of cellulose. As frequencies become higher and/or temperatures lower, the secondary γ and β transitions become increasingly important in affecting modulus. The γ relaxation is believed to be due to the motion of methylol side groups and the β relaxation to the motion of methylol-water complexes. Under the conditions prevalent at the reel of a paper machine, where ultrasonic velocity measurements are made, these thermal relaxations combine to produce linear moisture-mass specific modulus and temperature-mass specific modulus relationships. This greatly simplifies the calculations required to adjust modulus values to a standard temperature-moisture condition. The linear relations are coincidental, however, and do not persist if moisture and temperature ranges are extended.

Transient effects of moisture on modulus and loss tangent are still not well understood. Transient decreases in mass specific modulus have not been found at ultrasonic frequencies and nonequilibrium moisture correction of on-machine data is therefore unnecessary. However, results from the present low

frequency study as well as those from several other studies indicate that a transient increase in loss tangent accompanies both sorption and desorption. The transient decrease in modulus during moisture change suggested by several studies could not be reproduced in the present study. Additional work is required in this area before more definite conclusions can be drawn.

RECOMMENDATIONS

Many questions concerning the effects that moisture, temperature, and frequency have on the viscoelastic parameters of cellulosic materials remain unanswered. When moisture sorption and desorption are added to the picture, things become even more complicated. The development of a suitable experimental setup would go a long way in solving some of these questions. Requirements for such a setup would include the ability to make modulus and loss tangent measurements over a wide range of temperatures, humidities, frequencies, and sorptive and desorptive conditions. Dynamic mechanical instruments are presently available that can sinusoidally load samples at frequencies up to 1 kHz, while ultrasonic techniques can test from about 10 to 100 kHz. Dielectric and NMR techniques can be used at even higher frequencies. If these instruments were all located in one lab, a comprehensive moisture-temperature-frequency-modulus study could be undertaken without encountering the problems inherent when trying to make comparisons of data from different studies. A dynamic mechanical instrument, capable of making tests over a wider range of frequencies and strain amplitudes than was possible with the present low frequency technique, would also be helpful in determining the importance of linear vs. nonlinear considerations with regard to transient modulus decreases and/or loss tangent increases.

ACKNOWLEDGMENTS

Without the assistance of many individuals this thesis would not have become a reality. I would especially like to thank Mark Van Zummeren for writing the majority of the computer programs found in Appendixes III and IV and Will Wink for his help with the original oven-ultrasonic setup. Their help was greatly appreciated. I would also like to thank members of my thesis committee, Dr. Robert Stratton and John Waterhouse. Their knowledge was invaluable and was always imparted freely.

Finally, my deepest gratitude goes to my major advisor, Dr. Charles Habeger. He made the pursuit of a Ph.D. a rewarding and enjoyable experience. I can't imagine having a better advisor either academically or personally. I will miss him.

LITERATURE CITED

1. Craver, J. K.; Taylor, D. L., Tappi 48(3):142-7(March, 1965).

2. Habeger, C. C.; Whitsitt, W. J., Fibre Sci. Technol. (19):215-39(1983).

3. Habeger, C. C.; Baum, G. A., Tappi J. 69(6):106-11(1986).

4. Ward, I. M. Mechanical Properties of Solid Polymers. New York, NY, Wiley-Interscience, 1971:Chapter 7.

5. Hill, T. L. Introduction to Statistical Thermodynamics. Reading, MA, Addison-Wesley, 1960:Chapter 11.

6. Kolarik, J.; Janacek, J., J. Polymer Sci. (16):441-9(1967).

7. Bradley, S. A.; Carr, S. H., J. Polymer Sci. Polymer Phys. Ed. (14):111-24(1976).

8. Jackson, W. J.; Caldwell, J. R., Adv. Chem. Ser. (48):185-95(1965); J. Appl. Polymer Sci. (11):211-44(1967).

9. Pankonin, B. M.; Habeger, C. C., J. Polymer Sci. Polymer Phys. Ed. (26):339-52(1988).

10. Stratton, R. A., J. Polymer Sci. Polymer Chem. Ed. (11):535-44(1973).

11. Kimura, M.; Nakano, J., J. Polymer Sci. Polymer Lett. Ed. (14):741-5 (1976).

12. Klason, C.; Kubat, J., Svensk Papperstid. 79(15):494-500(1976).

13. Nishinari, K.; Fukada, E., J. Polymer Sci. Polymer Phys. Ed. (18): 1609-19(1980).

14. Mikhailov, G. P.; Artukhov, A. I.; Shevlev, V. A., Vysokomol. Soed. (A11):553-63(1969).

15. Seidman, R.; Mason, S. G., Can. J. Chem. (32):744-62(1954).

16. Abdel Moteleb, M. M.; Naoum, M. M.; Shinouda, H. G.; Rizk, H. A., J. Polymer Sci. Polymer Chem. Ed. (20):765-74(1982).

17. Norimoto, M.; Yamada, T., J. Wood Res. (52):31-43(1971).

18. Ishida, Y.; Yoshino, M.; Takayanagi, M., J. Appl. Polymer Sci. 1(2): 227-35(1959).

19. Handa, T.; Fukuoka, M.; Yoshizawa, S.; Kanamoto, T., J. Appl. Polymer Sci. (27):439-53(1982).

20. Mikhailov, G. P.; Artukhov, A. I.; Borisova, T. I., Vysokomol. Soed. 9B(2):138-41(1967).

21. Goring, D. A. I., Pulp Paper Mag. Can. 64(12):T517-27(Dec., 1963).

22. Salmen, N. L.; Back, E. L., Svensk Papperstid. 80(6):178-83(1977).

23. Yano, S.; Hatakeyama, H.; Hatakeyama, T., J. Appl. Polymer Sci. (20):3221-31(1976).

24. Salmen, N. L., Doctoral Dissertation, Stockholm, Sweden, The Royal Institute of Technology, 1980.

25. Nissan, A. H., Tappi 60(10):98-101(Oct. 1977).

26. Salmen, L.; Back, E., Tappi 63(6):117-20(1980).

27. Back, E. L.; Salmen, N. L.; Richardson, G., Svensk Papperstid. 86(6): R61-71(April 13, 1983).

28. Armstrong, L. D.; Kingston, R. S. T., Nature (185):862-3(March 19, 1960).

29. Armstrong, L. D.; Kingston, R. S. T., Austral. J. Applied Sci. 13(4): 257-76(Dec., 1962).

30. Armstrong, L. D.; Christensen, G. N., Nature (191):869-70(Aug. 26, 1961).

31. Hearmon, R. F. S.; Paton, J. M., Forest Prod. J. 14(8):357-9(Aug., 1964).

32. Bazant, Z. P.; Meiri, S., Wood Sci. Technol. (19):179-82(1985).

33. Armstrong, L. D., Wood Sci. 5(2):81-6(Oct., 1972).

34. Arima, T.; Grossman, P. U. A., J. Inst. Wood Sci. 8(2):47-52(Dec., 1978).

35. Arima, T., J. Japan Wood Sci. 25(7):469-75(1979).

36. Gibson, E. J., Nature (206):213-15(April 10, 1965).

37. Takemura, T., Memoirs College of Agriculture, Kyoto Univ. 88:31-48(1966).

38. Armstrong, L. D.; Grossman, P. U. A., Wood Sci. Technol. (6):128-37 (1972).

39. Sauer, D. J.; Haygreen, J. G., Forest Prod. J. 18(10):57-63(Oct., 1968).

40. Haygreen, J.; Hall, H.; Yang, K.; Sawicki, R., Wood and Fiber 7(2): 74-90(Summer, 1975).

41. McNatt, J. D.; Hunt, M. O., Forest Prod. J. 32(5):49-54(May, 1982).

42. Byrd, V. L., Tappi 55(2):247-52(Feb., 1972).

43. Byrd, V. L., Tappi 55(11):1612-13(Nov., 1972).

44. Gunderson, D. E.; Considine, J. M., Proc. TAPPI Intl. Process Materials Quality Evaluation Conf. 1986:246-51.

45. Gunderson, D. E., Tappi 64(11):67-76(Nov., 1981).

46. Byrd, V. L.; Koning, J. W., Tappi 61(6):35-7(June, 1978).

47. De Ruvo, A.; Lundberg, R.; Martin-Lof, S.; Soremark, C. The Fundamental Properties of Paper (2). Ernest Bonn Limited, London 1976:797-9.

48. Schniewind, A. P., Wood Sci. Technol. (2):188-206(1968).

49. Grossman, P. U. A., Wood Sci. Technol. (10):163-8(1976).

50. Byrd, V. L., Tappi J. 67(7):86-90(July, 1984).

51. Erickson, R. W.; Sauer, D. J., Forest. Prod. J. 19(12):45-51(Dec., 1969).

52. Chen, M. M., Wood Sci. 7(1):34-42(July, 1974).

53. Feughelman, M., Text. Res. J. 32(9):788-9(Sept., 1962).

54. Bazant, Z. P., Mechanics Today. Vol. 2. New York, NY, Pergamon Press, 1975: 1-93.

55. Gardner, R.; Gibson, E. J.; Laidlaw, R. A., Forest Prod. J. 17(4):50-1 (April, 1967).

56. Schaffer, E. L., Wood and Fiber (3):232-5(1972).

57. Bazant, Z. P., Wood Sci. Technol. (19):159-77(1985).

58. Mackay, B. H.; Downes, J. G., J. Appl. Polymer Sci. 2(4):32-8(1959).

59. Nordon, P., Text. Res. J. 32(7):560-8(July, 1962).

60. Feughelman, M.; Robinson, M. S. M., J. Appl. Polymer Sci. 1(3):371-2 (1959).

61. Haly, A.; Feughelman, M., J. Text. Inst. 51(12):T573-88(Dec., 1960).

62. Haly, A.; Feughelman, M., Text. Res. J. 31(2):131-40(Feb., 1961).

63. Feughelman, M.; Nordon, P., J. Appl. Polymer Sci. 6(24):670-3(1962).

64. Danilatos, G. D.; Postle, R., J. Macromol. Sci. Phys. Ed. B19(1):153-65(1981).

65. Danilatos, G. D.; Postle, R., J. Appl. Polymer Sci. (26):193-200(1981).

66. Kubat, J.; Lindbergson, B., J. Appl. Polymer Sci. (9):2651-4(1965).

67. Kubat, J.; Lindbergson, B., Svensk Papperstid. 68(21):743-56(Nov. 15, 1965).

68. Algie, J. E., Text. Res. J. 34(6):477-86(June, 1964).

69. Shishoo, R.; Lundell, M., Text. Res. J. 42(5):285-91(May, 1972).

70. Hearl, J. W. S.; Peters, R. H. Moisture in Textiles. New York, NY, Interscience, 1960:Chapter 8.

71. Kubat, J.; Martin-Lof, S.; Soremark, C., Svensk Papperstid. 72(23): 763-7(1969).

72. Van den Akker, J. A.; Root, C.; Wink, W. A., Paper Trade J. 115(24): 33-6(Dec. 10, 1942).

73. Wink, W. A., Tappi 44(6):171A-80A(June, 1961).

74. Van Zummeren, M. L.; Young, D. J.; Habeger, C. C.; Baum, G. A.; Treleven, R. A., Ultrasonics (25):288-94(1987).

75. Wink, W. A.; Hardacker, K. W.; Van Eperen, R. H., Tappi 47(1):13-15(Jan., 1964).

76. Kubat, J.; Nyborg, L.; Steenberg, B., Svensk Papperstid. 66(19):754-64 (1963).

77. Rigdahl, M.; Salmen, N. L., J. Mat. Sci. (19):2955-61(1984).

78. Htun, M.; De Ruvo, A.; Fellers, C., J. Appl. Polymer Sci. (30):1597-604(1985).

79. Higgins, H. G., Appita 12(1):1-17(1958).

80. Dusoiu, N., C. R. Acad. Sci. B280(24):777-9(1975).

81. Aberg, R., Svensk Papperstid. 76(16):602-6(1973).

82. Sapieha, S.; Inoue, M.; Lepoutre, P., J. Appl. Polymer Sci. (30): 1257-66(1985).

83. Benson, R. E., Tappi 54(5):699-703(May, 1971).

84. Riemen, W. P.; Kurath, S. F., Tappi 47(10):629-33(Oct., 1964).

85. Brezinski, J. P., Doctoral Thesis. Appleton, WI, The Institute of Paper Chemistry, 1955.

86. Austin, J. N., Master's Thesis, Appleton, WI, The Institute of Paper Chemistry, 1978.

87. Caulfield, D. F.; Weatherwax, R. C., Trans. from Fibre-Water Interactions in Paper-Making, Oxford (2):741-58(1977).

88. Baum, G. A.; Brennan, D. C.; Habeger, C. C., Tappi 64(8):97-101(Aug., 1981).

89. Pierce, F. T., J. Text. Inst. (20):T133-50(1929).

90. Byl, C. C., Master's Thesis. Appleton, WI, The Institute of Paper Chemistry, 1983.

91. Ferry, J. D., Viscoelastic Properties of Polymers, (Chapt. 11), John Wiley and Sons, New York, 1980.

APPENDIX I

STRIP RESONANCE CALCULATIONS

In order to find the strip resonance frequencies, the assumption is first made that the traveling wave solutions in the strip are,

$$\sigma = e^{i\omega(t-x/c)-\alpha x}$$

to the right and,

$$\sigma = e^{i\omega(t+x/c)+\alpha x}$$

to the left, where σ is the displacement along the x direction at time, t, ω is the angular frequency, c is the phase velocity, and α is the attenuation coefficient. These equations are solutions to the equation of motion,

$$E(\partial^2\sigma/\partial x^2) = \rho(\partial^2\sigma/\partial t^2)$$

if,

$$(\alpha+i\omega/c)^2 = -\omega^2\rho/E$$

This means that E is complex (i.e., $E = E' + E''$) and E' and E'' can be found in terms of c, α, ω, and ρ:

$$-\omega^2/\rho = (E' + E'')(\alpha^2 + 2\alpha i\omega/c - \omega^2/c^2)$$
$$= E'(\alpha^2 - \omega^2/c^2) - 2\alpha E''\omega/c + i[E''(\alpha^2 - \omega^2/c^2) + 2\alpha E'\omega/c]$$

Assuming $\alpha \ll \omega/c$,

$$\begin{aligned} E' &\approx \rho c^2 \\ E'' &\approx 2\alpha\rho c^3/\omega \\ \tan\delta \equiv E''/E' &\approx 2\alpha c/\omega \end{aligned} \qquad (21)$$

Now a solution of the form,

$$\sigma = A_1 e^{i\omega(t-x/c)-\alpha x} + A_2 e^{i\omega(t+x/c)+\alpha x} \qquad (22)$$

which satisfies the boundary conditions of the strip resonance can be found:

$\sigma = \varepsilon^{i\omega t}$	$\sigma = 0$
Transmitter	Receiver
$x = 0$	$x = \ell_s$

At $x = 0$ Eq. (22) $\rightarrow 1 = A_1/Z - A_2/Z$

At $x = \ell$ Eq. (22) $\rightarrow 0 = (A_1/Z)e^{-\alpha\ell - i\omega\ell/c} - (A_2/Z)e^{\alpha\ell + i\omega\ell/c}$

where Z is the mechanical impedance of the system ($\sqrt{\rho E'}$). Solving for A_1 and A_2 gives:

$$A_1 = (Ze^{\alpha\ell+i\omega\ell/c})/\ (e^{\alpha\ell+i\omega\ell/c} - e^{-\alpha\ell-i\omega\ell/c})$$

$$A_2 = (Ze^{-\alpha\ell-i\omega\ell/c})/(e^{\alpha\ell+i\omega\ell/c} - e^{-\alpha l-i\omega\ell/c})$$

The signal at the receiver is proportional to,

$$P(\ell)/Z = e^{i\omega t}(A_1 e^{-\alpha x - i\omega x/c} + A_2 e^{\alpha x + i\omega x/c})$$

and,

$$P(\ell)/Z = 2e^{i\omega t}/(e^{\alpha\ell+i\omega\ell/c} - e^{-\alpha\ell-i\omega\ell/c})$$

$$\left| P(\ell)/Z \right|^2 = 2/(e^{2\alpha\ell} + e^{-2\alpha\ell} - e^{-2i\omega\ell/c} - e^{2i\omega\ell/c})$$

$$\left| P(\ell)/Z \right|^2 = 1/[\cosh(2\alpha\ell) - \cos(2\omega\ell/c)]$$

Assuming $2\alpha\ell \ll 1$ and using a Taylor series to expand to the second order:

$$\cosh(2\alpha\ell) \approx 1 + 2\alpha^2\ell^2$$

The derivative of $\left| P(\ell)/Z \right|^2$ is then taken in order to find the location of the resonance peak:

$$\partial \left| P(\ell)/Z \right|^2/\partial\omega = -[(2\ell/c)\sin(2\omega\ell/c)]/[\cosh(2\alpha\ell) - \cos(2\omega\ell/c)]^2 = 0$$

This equation is satisfied whenever $2\omega\ell/c = n\pi$. However, only those solutions with an even n give maximums. Therefore,

$$\underline{\omega = cn\pi/\ell} \tag{23}$$

where ℓ, n, and ω are equivalent to ℓ_s, m+1, and f given in the text (pg. 45).

The loss tangent can then be calculated to ensure that the width of the resonance peak at $1/\sqrt{2}$ of the maximum amplitude is, in fact, the correct width to use in loss tangent determinations. This width is found where $|P(\ell)/Z|^2$ is equal to $1/2\,|P(\ell)/Z|^2_{max}$ which is equal to $1/[\cosh(2\alpha\ell) - 1]$ and approximately equal to $1/(2\alpha^2\ell^2)$. So when,

$$|P(\ell)/Z|^2 = 1/[\cosh(2\alpha\ell) - \cos(2\omega\ell/c)] = 1/(4\alpha^2\ell^2)$$

the $1/\sqrt{2}$ height criterion is satisfied. The cosine term in the above equation can be estimated as,

$$\cos(2\omega\ell/c) \approx 1 - 2\ell^2\,(\omega - \omega_o)^2/c^2$$

where ω_o is the resonant frequency. Therefore,

$$4\alpha^2\ell^2 \approx 1 + 2\alpha^2\ell^2 - [1 - 2\ell^2(\omega^2 - \omega o)^2/c^2]$$

and,

$$\alpha^2c^2 \approx (\omega - \omega_o)^2$$

The $1/\sqrt{2}$ height width, $\Delta\omega$ is equal to $2(\omega - \omega_o)$ so:

$$\Delta\omega/\omega_o \approx 2\alpha c/\omega_o$$

The right-hand side of this final equation is approximately equal to the loss tangent [as calculated in Eq. (21)] indicating that width at the $1/\sqrt{2}$ peak height is, in fact, the proper one to use for loss tangent calculations.

APPENDIX II

TI9900 PROGRAM

This program systematically prompts the user for several required input parameters including; the lock-in sensitivity setting, the sample name and length, the harmonic to evaluate, the approximate frequency of this harmonic, the approximate voltage amplitude, and the approximate loss tangent. The last three parameters are obtained from the X-Y recorder plot of the sample. As soon as the loss tangent is input, data acquisition and analysis begin. Several keys on the keyboard can then be pressed at any time to direct the flow of the program (lines 705-718).

```
1   REM.....STRIP RESONANCE TECHNIQUE.....
2   REM.....PANKONIN & BERGER.....
3   REM.....8/10/87.....
10   DIM DA[3],F[2],FR[13],APL[13],SP[5],SB[20],DUM[2],TI[3],DS[6]
15   DIM STD[3],D[256]
20   F=0:: NN=10000:: P=1:: DYN=.9:: LEA=0:: CN=0:: PB=0:: OFR=0:: CO=5:: DL=1
30   INPUT "SENSITIVITY (MV)"SNS
40   INPUT "SAMPLE"$SB[0]"  LENGTH(CM)"LGT
45   INPUT "   WAVE  0=FUNDAMENTAL 1=1ST HARMONIC ETC"WAV
50   INPUT "FREQUENCY(HZ)"FS"    AMPLITUDE(MV)"AMP"    LOSS TANGENT"TGD
60   STD[1]=TGD*FS/4
61   STD[2]=500:: STD[3]=500
115   $M="1":: GOSUB 2000  !SET HP TO LISTEN
120   $F[0]=INP[AMP]:: GOSUB 5920
130   FR[2]=FS
140   T=TIC[0]
160   IN NN/2<>INP[NN/2] THEN GOTO 400
200   FR[5]=FR[2]-FR[2]/2/(WAV+1)  !.....FIND MIN-1
210   L=5:: DEL=STD[2]:: GOSUB 5000:: GOSUB 4300
220   FR[8]=FR[2]+FR[2]/2/(WAV+1)  !FIND MIN-2
230   L=8:: DEL=STD[3]:: GOSUB 5000:: GOSUB 4300
240   ABA=(APL[8]-APL[5])/(FR[8]-FR[5]):: BBA=APL[5]-ABA*FR[5]
250   IF NN/2<>INP[NN/2] THEN GOTO 417
400   L=2:: DEL=STD[1]:: GOSUB 4900:: GOSUB 4000  !.....FIND MAX
410   TGT=APL[2]*0.707
413   IN NN/2<>INP[NN/2] THEN GOTO 200
417   IF LEA=2 THEN GOSUB 8000:: GOTO 602
420   FR[10]=FR[2]-1250:: FR[11]=FR[2]-750  !.....FIND 1/2-
430   L=10:: DEL=FR[10]-FR[11]:: GOSUB 5160:: GOSUB 4600
440   FR[12]=FR[2]+1250:: FR[13]=FR[2]+750  !.....FIND 1/2+
450   L=12:: DEL=FR[13]-FR[12]:: GOSUB 5160:: GOSUB 4600
601   TGD=((FR[12]+FR[13])-(FR[10]+FR[11]))/2/FR[2]
602   MOD=(FR[2]*LGT*2/(WAV+1))^2/10000000000
603   FS=FR[2]
604   TIME $TI[0]
610   $SB[0]=#"99999",NN
640   $DUM[0]=#" 999.00",MOD:: $SB[0]=$SB[0]+$DUM[0]
650   $DUM[0]=#"9.0000 ",TGD:: $SB[0]=$SB[0]+$DUM[0]+" "+$TI[0]
693   IF LEA<>2 THEN GOTO 696
694   IF NN/P=INP[NN/P] THEN PRINT $SB[0];#"SSSSS"APL[10];APL[11];APL[13];APL[12];TGT;APL[2];INP[AMP]
696   IF NN/P=INP[NN/P] AND LEA=0 THEN PRINT $SB[0];FR[2];#SSSSSS"APL[2];INP[AMP]
697   IF F=0 THEN GOTO 702
698   IF LEA=2 AND TGT<APL[11] AND TGT<APL[13] AND TGT>APL[10] AND TGT>APL[12] THEN GOTO 701
699    ELSE GOTO 702
```

APPENDIX II (Continued)

```
701   IF NN/PB=INP[NN/PB] THEN GOSUB 6000
702   NN=NN+1
703   AMP=AMP*OFFFH/(APL[2]+ABA*FR[2]+BBA)*DYN
704   IF AMP>10000 THEN AMP=10000
705   IF NKY[045H] THEN GOTO 900  !E FOR EXIT
706   IF NKY[053H] THEN GOTO 40   !S FOR NEW SAMPLE
708   IF NKY[043H] THEN N=1:: GOTO 900  !C TO CLEAR IEEE-488
709   IF NKY[042H] THEN INPUT "FREQ. TO B6900"PB:: GOSUB 6100  !B FOR B6900 COMMUNICATION
710   IF NKY[052H] THEN INPUT "RESEQUENCED NUMBER"NN  !R FOR NEW SEQUENCE NUMBER
711   IF NKY[050H] THEN INPUT "PRINT FREQUENCY"P  !P FOR PRINT FREQUENCY
712   IF NKY[044H] THEN INPUT "VALUE FOR DELAY"DL  !D FOR LOCK-IN DELAY
713   IF NKY[046H] THEN INPUT "DYNAMIC RANGE"DYN  !F FOR NEW LOCK-IN RANGE
714   IF NKY[054H] THEN Z=SNS:: INPUT "SENSITIVITY (MV)"SNS:: GOTO 830  !T FOR THIS
716   IF NKY[04FH] THEN LEA=0:: PRINT "OLD(<11/15/83) METHOD"  !O FOR THIS
717   IF NKY[057H] THEN INPUT "VALUE FOR CO"CO  !W FOR THIS
718   IF NKY[04EH] THEN LEA=2:: CN=1:: PRINT "NEW METHOD(4/14/86)"  !N FOR THIS
760   GOTO 120
830   AMP=AMP*SNS/Z:: GOTO 714
900   $M="?":: GOSUB 2000  !HP TO UNLISTEN
905   CRB[-24]=1:: CRB[-9]=0:: CRB[-24]=0
906   IF  (NN-1)/P=INP[(NN-1)/P] THEN GOTO 910
907   IF N=1 THEN PRINT $SB[0]
910   IF N=1 THEN N=0:: INPUT "SCAN #"$Y:: $M="1":: GOSUB 2000:: GOTO 708
990   STOP
1000   BASE 0130H  !.....HP DATA
1016   FOR I=0 TO 2
1018    FOR J=1 TO 6
1020     IF CRB[-7]=0 THEN GOTO 1020  !IS NRFD LOW ?
1030     $D=$DA[I;J],1
1040     IF $D="*" THEN GOTO 1100
1050     CRF[8]=255-ASC[$D]:: CRB[-8]=0  !DAV LOW
1060     IF CRB[-6]=0 THEN GOTO 1060  !IS NDAC HIGH ?
1070     CRB[-8]=1  ! DAV HIGH
1080    NEXT J
1090   NEXT I
1100   RETURN
1999   REM.....HP MANAGEMENT
2000   BASE 0130H:: CRB[-2]=0:: CRB[-4]=0  !REN TRUE, ATN FALSE
2010   CRF[8]=255-ASC[$M]:: CRB[-8]=0  !DAV LOW
2020   IF CRB[-6]=0 THEN GOTO 2020  !IS NDAC LOW ?
2030   CRB[-8]=1:: CRB[-4]=1:: RETURN   !DAV HIGH,ATN FALSE
2999   REM.....A/D CONVERSION
3000   MWD[04FF8H]=0:: AA=0:: T3=TIC[0]
3002   IF TIC[T3]<>DL THEN GOTO 3002
3004   FOR J=1 TO CO
3010    MWD[04FFAH]=0  !CONV COMMAND
3020    IF MWD[04FFCH]>0 THEN GOTO 3020  !EOC FLAG
3030    AA=AA+MWD[04FFEH]  !READ DATA
3032   NEXT J
3036   AA=AA/CO
3040   RETURN
4000   M=L-1:: N=L+1  !.....FIND MAX
4010   IF APL[M]>APL[N] THEN GOTO 4050
4020   IF APL[L]>APL[N] THEN GOTO 4130
4030   APL[M]=APL[L]:: FR[M]=FR[L]:: APL[L]=APL[N]:: FR[L]=FR[N]
4040   X=N:: FR[X]=INP[FR[X]+DEL]:: GOTO 4090
4050   IF APL[L]<APL[N] AND APL[M]<APL[N] THEN GOTO 4030  !....FOUND MIN
4060   APL[N]=APL[L]:: FR[N]=FR[L]:: APL[L]=APL[M]:: FR[L]=FR[M]
4080   X=M:: FR[X]=INP[FR[X]-DEL]
4090   $F[0]=FR[X]
4110   GOSUB 5900:: APL[X]=AA-(ABA*FR[X]+BBA)
4120   GOTO 4010
4130   IF DEL<25 THEN GOTO 4210  !CONVERGENCE
4135   DEL=INP[DEL/2]
4140   GOSUB 4900
4200   GOTO 4010
4210   STD[1]=10*DEL:: RETURN
4300   M=L-1:: N=L+1  !.....FIND MIN
4310   IF APL[M]<APL[L] THEN GOTO 4350
4320   IF APL[L]<APL[N] THEN GOTO 4430  !F2 MIN DECREASE DEL
4330   APL[M]=APL[L]:: FR[M]=FR[L]:: APL[L]=APL[N]:: FR[L]=FR[N]
4340   X=N:: FR[X]=INP[FR[X]+DEL]:: GOTO 4390
4350   IF APL[L]>APL[N] AND APL[M]>APL[N] THEN GOTO 4330  !....FOUND MAX
```

APPENDIX II (Continued)

```
4360  APL[N]=APL[L]:: FR[N]=FR[L]:: APL[L]=APL[M]:: FR[L]=FR[M]
4380  X=M:: FR[X]=INP[FR[X]-DEL]
4390  $F[0]=FR[X]
4410  GOSUB 5900:: APL[X]=AA
4420  GOTO 4310
4430  STD[(L+1)/3]=DEL
4450  RETURN
4600  A=TGT-APL[L]:: B=TGT-APL[L+1]  !.....FIND 1/2 WIDTH
4620  IF TGT>APL[L] THEN GOTO 4650
4630  IF TGT>APL[L+1] THEN GOTO 4710  !L,L+1 BRACKET TARGET
4640  IF APL[L]<APL[L+1] THEN GOTO 4670
4645  GOTO 4690
4650  IF TGT<APL[L+1] THEN GOTO 4710  !L,L+1 BRACKET TARGET
4660  IF APL[L]<APL[L+1] THEN GOTO 4690
4670  FR[L+1]=FR[L]:: APL[L+1]=APL[L]
4680  FR[L]=FR[L]-DEL:: T=L:: GOTO 4750
4690  FR[L]=FR[L+1]:: APL[L]=APL[L+1]
4700  FR[L+1]=FR[L+1]+DEL:: T=L+1:: GOTO 4750
4710  IF ABS[FR[L]-FR[L+1]}<20 THEN GOTO 4790  !CONVERGENCE
4720  DEL=DEL/2
4730  IF ABS[A]>ABS[B] THEN FR[L]=(FR[L]+FR[L+1])/2:: T=L:: GOTO 4750
4740  FR{L+1]=(FR[L]+FR[L+1])/2:: T=L+1
4750  $F[0]=INP[FR[T]]
4755  GOSUB 5900:: APL[T]=AA-(ABA*FR[T]+BBA)
4760  GOTO 4600
4790  RETURN
4900  FR[L-1]=FR[L]-DEL:: FR[L+1]=FR[L]+DEL  !....INITIALIZE MAX
4910  FOR K=L-1 TO L+1
4920  $F[0]=INP[FR[K]]:: GOSUB 5900:: APL[K]]=AA-(ABA*FR[K]+BBA)
4930  NEXT K:: RETURN
5000  FR[L-1]=FR[L]-DEL:: FR[L+1]=FR[L]+DEL  !....INITIALIZE MIN
5010  FOR K=L-1 TO L+1
5020  $F[0]=INP[FR[K]]:: GOSUB 5900:: APL[K]=AA
5030  NEXT K:: RETURN
5160  FOR K=L TO L+1  !INITIALIZE 1/2 +/-
5180   $F[0]=INP[FR[K]]:: GOSUB 5900:: APL[K]=AA-(ABA*FR[K]+BBA)
5190  NEXT K
5200  RETURN
5899  REM.....DATA FORMAT TO HP
5900  $DA[0]="FRHZ*":: $DA[0;3]=/$F[0]:: GOSUB 1000:: GOSUB 3000
5910  RETURN
5920  $DA[0]="AMMV*":: $DA[0;3]=/$F[0]:: GOSUB 1000
5930  RETURN
5999  REM.....B6900 COMMUNICATION LINK
6000  BAUD 2,4:: BASE 0180H:: CRB[14]=1:: CRB[5]=0:: CRB[0]=0::CRB[14]=0
6010  CRB[16]=1:: $CRT=%0DH
6020  UNIT 2:: PRINT $SB[0];$CRT;:: CRB[16]=0:: UNIT 1
6030  RETURN
6100  IMASK 6:: TRAP 6 TO 6230
6120  BASE 0180H:: CRB[-58]=1
6130  INPUT $SB[0];
6140  IF $SB[0]="E" THEN F=0:: PRINT :: GOTO 6220  !DON'T SEND TO B6900
6150  IF $SP[0]="P1" THEN F=1:: PRINT :: GOTO 6220  !SEND TO B6900
6155  PRINT "  -INT.6 TO READ MSG-"
6160  Q=256:: I=1:: Y=0:: GOSUB 6000
6170  CRB[15]=1:: CRB[15]=0
6180  FOR W=1 TO Q
6190   IF CRB[21]=1 THEN GOTO 6210
6200   ON I THEN GOTO 6190,6130
6210   D[W]=CRF[8]:: CRB[18]=1:: NEXT W:: Y=1:: GOTO 6230
6220  RETURN
6230  FOR Q=1 TO W-1
6240   IF D[Q-1]=020H AND D[Q]=020H THEN GOTO 6290
6250   IF D[Q]=023H THEN PRINT
6260   IF D[Q]<020H THEN GOTO 6290
6280   $R=%D[Q]:: PRINT $R;
6290  NEXT Q
6300  PRINT :: I=2:: IF Y=1 THEN GOTO 6130
6310  CRB[-27]=0:: CRB[-53]=1
6320  IRTN
6400  DIM SB[20],D[256]
6410  GOSUB 6100:: STOP
8000  REM.....NEW METHOD.....(4/14/86)
```

APPENDIX II (Continued)

```
8010   CN=CN+1
8100   IF NN/2=INP[NN/2] THEN GOTO 8440
8420   IF CN=2 THEN FR[10]=FR[2]-1100:: FR[11]=FR[2]-600:: OFR=FR[2]  !FIND 1/2-
8421   FR[10]=FR[10]+FR[2]-OFR:: FR[11]=FR[11]+FR[2]-OFR
8422   IF TGT<APL[11] AND FR[11]-FR[10]>249 THEN FR[11]=FR[11]-50
8424   IF TGT>APL[10] AND FR[11]-FR[10]>249 THEN FR[10]=FR[10]+50
8425   IF FR[11]-FR[10]<201 AND APL[11]-TGT>TGT-APL[10] THEN FR[11]=FR[11]-25:: FR[10]=FR[10]-25
8426    ELSE FR[11]=FR[11]+25:: FR[10]=FR[10]+25
8427   IF TGT>APL[11] THEN FR[11]=FR[11]+50
8428   IF TGT<APL[10] THEN FR[10]=FR[10]-50
8430   L=10:: GOSUB 5160:: GOSUB 8700:: LFT=Z
8435   IF NN/2=INP[NN/2] THEN GOTO 8500
8440   IF CN=2 THEN FR[13]=FR[2]+700:: FR[12]=FR[2]+1200:: OFR=FR[2]  !....FIND 1/2+
8441   FR[12]=FR[12]+FR[2]-OFR:: FR[13]=FR[13]+FR[2]-OFR
8442   IF TGT<APL[13] AND FR[12]-FR[13]>249 THEN FR[13]=FR[13]+50
8444   IF TGT>APL[12] AND FR[12]-FR[13]>249 THEN FR[12]=FR[12]-50
8445   IF FR[12]-FR[13]<201 AND APL[13]-TGT>TGT-APL[12] THEN FR[13]+25:: FR[12]=FR[12]+25
8446    ELSE FR[13]=FR[13]-25:: FR[12]=FR[12]-25
8447   IF TGT>APL[13] THEN FR[13]=FR[13]-50
8448   IF TGT<APL[12] THEN FR[12]=FR[12]+50
8450   L=12:: GOSUB 5160:: GOSUB 8700::: RIT=Z
8455   IF NN/2=INP[NN/2] THEN GOTO 8420
8500   TGD=(RIT-LFT)/FR[2]
8545   OFR=FR[2]
8550   RETURN
8700   Z=FR[L+1]-((APL[L+1]-TGT)/(APL[L+1]-APL[L]))*(FR[L+1]-FR[L])
8750   RETURN
```

APPENDIX III

APPLE PROGRAM

This program uses several menus to allow the operator to choose the desired input parameters and the type of test run. The main menu displays the five options shown in lines 5240-5300. Choice No. 3 allows the operator to see the quality of the ultrasonic signals. Once these signals are satisfactory, the test parameters can be set using option No. 4 to call up the parameter menu. All choices in this menu are clearly outlined and may lead to additional menus. After the desired parameters have been input, an equilibrium or transient run can be started by going back to the main menu and choosing options No. 1 or No. 2. Once data have been acquired, they can be saved using option No. 5.

```
900  REM  COPYRIGHT (C) 1983 BY THE INSTITUTE OF PAPER CHEMISTRY
1020  GOSUB 40000: REM  PROGRAM INITIALIZATION
1040  GOSUB 5000: REM  INVOKE MAIN MENU
1060  STOP
2000  REM  ****
2010  REM  FIND DELAY
2100 CD = 0: VTAB (24)
2120 RIGHT = 01
2140 LEFT = ZERO
2160 OF = OM
2180  GOSUB 3000
2200 MAX = IN
2240 OM = OM + 01:OF = OM
2260  GOSUB 3000
2280 MTEST = IN
2300  IF MTEST >  = MAX THEN DI = 01
2320  IF MTEST < MAX THEN DI = ZERO
2340 MAX = MTEST
2360  IF DI = ZERO AND RIGHT = 01 THEN RIGHT = ZERO:LEFT = 01:CD = CD + 01:GOTO 2400
2380  IF DI = ZERO AND LEFT = 01 THEN LEFT = ZERO:RIGHT = 01:CD = CD + 01
2400  HTAB (01): PRINT "MTEST= ";MTEST;"  OM=";OM
2410 MH(3) = MH(2):MH(2) = MH(1):MH(1) = MTEST
2420 OM = OM + RIGHT - LEFT
2440 OF = OM
2460  IF CD = TWO THEN  GOTO 2540
2480 P =  PEEK ( - 16384): POKE  - 16368,0: REM   CHECK FOR PANIC BUTTON
2500  IF P = 208 THEN  RETURN
2520  GOTO 2260
2540 OF = OM: VTAB (24): PRINT ""
2550  GOSUB 3500
2560  GOSUB 11500
2580  RETURN
3000  REM  ****
3010  REM  INTEGRATE
3100  POKE MM(13), INT (OF / T5)
3120  POKE MM(12),OF -  INT (OF / T5) * T5
3140  CALL MM(8): REM CROSCOR
3160 IN =  PEEK (MM(21)) * 65536 +  PEEK (MM(20)) * T5 +  PEEK (MM(19))
3180  IF IN > 8388608 THEN IN = IN - 16777216
3200  RETURN
3500  REM  ****
3510  REM  PERFORM QUADATIC FIT
3520  REM  USING THE LAST THREE OFFSETS
3530 YP = 3:YM = 1
```

APPENDIX III (Continued)

```
3550 AQ = (MH(YM) - 2 * MH(2) + MH(YP)) / 2
3560 BQ = MH(2) - MH(YM) - AQ * (2 * OM - 1)
3570 NQ =  - BQ / (2 * AQ)
3590  PRINT "OM = ";OM;"      NQ = ";NQ
3670  RETURN
5000  REM  ****
5010  REM  MAIN MENU
5100  TEXT : HOME
5160  VTAB (1)
5180  HTAB (10): PRINT "MAIN CONTROL MENU"
5200  PRINT
5240  HTAB (4): PRINT "1=EQUILIBRIUM DATA ACQUISITION"
5260  HTAB (4): PRINT "2=TRANSIENT DATA ACQUISITION"
5270  HTAB (4): PRINT "3=CHECKOUT"
5290  HTAB (4): PRINT "4=SET TEST PARAMETERS"
5300  HTAB (4): PRINT "5=SAVE DATA ON DISK"
5460  INPUT "ENTER YOUR CHOICE  ";CH
5500  IF CH = 3 THEN  GOSUB 10000
5510  IF CH = 4 THEN  GOSUB 16000
5540  IF CH = 2 THEN O$ = "T":E = 0: GOSUB 41620: GOSUB 54000
5550  IF CH = 1 THEN O$ = "E":D = 0: GOSUB 41620: GOSUB 54000
5555  IF CH = 5 THEN  PRINT "IS THIS THE SAMPLE'S FIRST RUN: Y OR N ?"
5557  PRINT : INPUT Y$
5558  IF Y$ = "Y" THEN Q = 0
5559  IF Y$ = "N" THEN Q = 1
5560  IF CH = 5 AND Q = 1 THEN  GOSUB 22300
5570  IF CH = 5 AND Q = 0 THEN  GOSUB 22000
5680  GOTO 5100
5700  RETURN
6500  REM ****POKE THE BASELINE LENGTH
6580 XX =  INT (OH(TT) * 0.75)
6600  IF XX > 127 THEN XX = 127
6620  POKE MM(35),XX
6630  RETURN
9000  REM  ***********
9010  REM **INPUT SAMPLE NAME
9030  TEXT : HOME
9040  PRINT "ENTER THE SAMPLE NAME"
9050  PRINT "": INPUT SN$
9060  RETURN
10000  REM  ****
10020  REM  CHECKOUT
10120  PRINT D$;"PR#0"
10140  HOME : VTAB (23):TT = 1: GOSUB 6500
10150  PRINT "PRESS 'S' TO STOP CHECKOUT"
10160  PRINT "D = SAMPLE DATA      : SIG AVER  = ";AS
10180  PRINT "T = CHANGE TIME BASE : TIME BASE = ";DWELL
10200  IF (OL < 1) THEN  PRINT ": NUM TESTS = ";NS;
10220  GET A$
10230  PRINT
10240  IF  LEFT$ (A$,1) = "S" THEN  GOTO 10400
10260  IF  LEFT$ (A$,1) = "D" THEN  GOTO 10320
10270  IF  LEFT$ (A$,1) = "X" THEN ER = 1: RETURN
10275  IF  LEFT$ (A$,1) = "T" THEN  GOSUB 21000
10280  GOTO 10140
10320 OF = 0: GOSUB 11500
10340  CALL MM(5): REM CHECKOUT
10360  GOTO 10140
10400  TEXT : RETURN
10700  REM  ****
10710  REM  CHANGE SIGNAL AVERAGING
10750  TEXT : HOME
10760  PRINT "CURRENT NO. OF AVERAGED SIGNALS=";AS
10770  INPUT "PLEASE ENTER THE NEW VALUE ";AS
10780  IF AS = 0 THEN  GOTO 10750
10782  PRINT "CURRENT AVERAGING LENGTH = ";AL
10784  INPUT "ENTER THE NEW LENGTH ";AL
10786  IF AL = 0 THEN  GOTO 10782
10790  GOSUB 10820
10800  RETURN
10820  POKE MM(2),AS
10825  POKE MM(4),AL / 256
10830  POKE MM(3),AL -  INT (AL / 256) * 256
```

APPENDIX III (Continued)

```
10835  RETURN
11500  REM  **********
11520  REM   POKE 2ND SPAN OFFSET
11760  POKE MM(13), INT (OF / 256)
11780  POKE MM(12),OF -  INT (OF / 256) * 256
11800  REM
11820  RETURN
12500  REM  **********
12510  REM  INIT SPANS
12540  TEXT : HOME
12545  PRINT ""
12550  PRINT "THE DEFAULT WIDTH FOR SPAN1 = ";D1
12560  PRINT "THE DEFAULT WIDTH FOR SPAN2 = ";D2: PRINT : PRINT
12565  PRINT "THE CURRENT WIDTH FOR SPAN1 = ";S1
12570  PRINT "THE CURRENT WIDTH FOR SPAN2 = ";S2
12580  PRINT "ARE THE DEFAULTS ACCEPTABLE? (Y OR N)"
12590  PRINT "": GET A$
12600  IF  LEFT$ (A$,1) = "Y" THEN  GOTO 12630
12610  PRINT "": INPUT "ENTER THE WIDTH FOR SPAN1  ";S1
12620  PRINT "": INPUT "ENTER THE WIDTH FOR SPAN2  ";S2
12630 DE = S2 - S1
12640  RETURN
15200  TEXT : HOME
15220  VTAB (2): HTAB (9): PRINT "CORRECTIVE ACTION MENU"
15250  HTAB (5): PRINT "1 = CHANGE SIGNAL AVERAGING"
15260  HTAB (5): PRINT "2 = CHANGE THE STARTING OFFSET"
15280  HTAB (5): PRINT "3 = RETURN TO DATA COLLECTION"
15290  HTAB (5): PRINT "4 = RETURN TO MAIN MENU"
15300  PRINT "": HTAB (5): INPUT "ENTER 1,2,3,OR 4 ";CR
15340  IF CR = 1 THEN  GOSUB 10700
15360  IF CR = 2 THEN  GOSUB 15500
15380  IF CR = 3 THEN  RETURN
15400  IF CR = 4 THEN ER = 0: GOTO 16000
15410  GOTO 15200
15440  RETURN
15500  REM  **********
15520  REM  QUESS OFFSET
15560  HOME
15580  VTAB (2): HTAB (1): PRINT "PRESENT DEFAULT OFFSET = ";OM
15590  PRINT : PRINT "IS THIS ACCEPTABLE? (Y OR N) "
15592  PRINT : GET A$
15600  IF  LEFT$ (A$,1) = "Y" THEN OH(TT) = OM: RETURN
15620  HTAB (1): PRINT "": INPUT "ENTER YOUR ESTIMATE  ";EO
15640  IF EO = 0 THEN  GOTO 15560
15660 OH(TT) = EO:OM = EO
15680  RETURN
16000  REM ****
16010  REM CHANGE TEST PARAMS
16100  TEXT : HOME
16110  HTAB (6): PRINT "TEST PARAMETER MENU": PRINT
16140  HTAB (4): PRINT "1=CHANGE SIGNAL AVERAGING"
16160  HTAB (4): PRINT "2=SAMPLE WEIGHING OPTION"
16180  HTAB (4): PRINT "3=CHANGE TRANSDUCER SEPERATIONS"
16220  HTAB (4): PRINT "4=CHANGE OPERATOR NAME"
16240  HTAB (4): PRINT "5=CHANGE OFFSETS"
16260  HTAB (4): PRINT "6=CHANGE NUM REPS FOR REGRESSION"
16270  HTAB (4): PRINT "7=CHANGE V0^2"
16280  HTAB (4): PRINT "8=SPECIFY MEASUREMENTS"
16290  HTAB (4): PRINT "9=CHANGE A/D DWELL"
16300  HTAB (4): PRINT "10=CHANGE SAMPLING DELAYS"
16310  HTAB (4): PRINT "11=CHANGE TOLERANCES"
16320  HTAB (4): PRINT "12=CHANGE STEPPER TRAVEL"
16325  HTAB (4): PRINT "13=INPUT ORIGINAL WT. AND M.C."
16327  HTAB (4): PRINT "14=MOVE TRANSDUCERS OUT"
16330  HTAB (4): PRINT "15=CONTINUE"
16335  HTAB (4): PRINT "16=RETURN TO MAIN MENU"
16440  INPUT "ENTER YOUR CHOICE ";CR
16460  IF CR = 1 THEN  GOSUB 10700
16480  IF CR = 2 THEN  GOSUB 49000
16500  IF CR = 3 THEN  GOSUB 12500
16540  IF CR = 4 THEN  GOSUB 9700
16560  IF CR = 5 THEN  GOSUB 15500
16580  IF CR = 6 THEN  GOSUB 43500
```

APPENDIX III (Continued)

```
16600  IF CR = 7 THEN  GOSUB 43000
16620  IF CR = 8 THEN  GOSUB 44000
16640  IF CR = 9 THEN  GOSUB 21000
16660  IF CR = 10 THEN  GOSUB 47000
16680  IF CR = 11 THEN  GOSUB 46000
16700  IF CR = 12 THEN  GOSUB 48800
16705  IF CR = 13 THEN  GOSUB 53000
16707  IF CR = 14 THEN  GOSUB 24000
16710  IF CR = 15 THEN  RETURN
16715  IF CR = 16 THEN  GOTO 5100
16798  GOTO 16100
16800  RETURN
17000  REM  **********
17010  REM  FORMATTING ROUTINE
17100 AA$ = "":I1 = 0
17120 X =  INT (X * 10 ^ DP + 0.5)
17130 A1$ =  STR$ (X)
17140 LT =  LEN (A1$)
17150  IF LT >  = DP THEN  GOTO 17210
17160 LP = DP - LT
17170  FOR KK = 1 TO LP
17180 A1$ = "0" + A1$
17190  NEXT KK
17195 LT = DP
17210  FOR KK = LT TO 1 STEP  - 1
17220 AA$ =  MID$ (A1$,KK,1) + AA$
17230 I1 = I1 + 1
17240  IF I1 = DP THEN AA$ = "." + AA$
17250  NEXT KK
17260  RETURN
21000  REM  ********
21010  REM  CHANGE THE DWELL TIME
21015  VTAB (24)
21020  PRINT "THE PRESET DWELL TIME = ";DWELL;" MICRO SEC."
21030  PRINT : PRINT "ENTER THE NEW DWELL TIME IN MICRO SEC. "
21035  INPUT DWELL
21040  RETURN
22000  REM  **********
22020  REM  DATA TO DISK
22052  IF O$ = "T" THEN SN$ = "T" + SN$
22055  REM
22060  PRINT D$;"OPEN ";SN$;",D2"
22080  PRINT D$;"WRITE ";SN$
22100  FOR D = 1 TO 75
22115  IF FR$(1,D) = "ZERO" THEN  GOTO 22150
22120  IF O$ = "E" THEN  PRINT FR$(1,D); SPC( 1);FR$(2,D); SPC( 1);FR$(3,D);SPC( 1);FR$(4,D)
22125  IF O$ = "T" AND D = 1 THEN  PRINT FR$(1,D): GOTO 22140
22130  IF O$ = "T" THEN  PRINT FR$(1,D); SPC( 6 -  LEN (FR$(1,D)));FR$(2,D);SPC( 1);FR$(3,D); SPC( 1);FR$(4,D); SPC( 1);FR$(5,D)
22140  NEXT D
22150  REM
22160  PRINT D$;"CLOSE ";SN$
22176  REM
22177  PRINT D$;"OPEN ";"GETBACK";",D1"
22178  PRINT D$;"CLOSE ";"GETBACK";
22180  RETURN
22300  REM   **********
22320  REM   DATA TO DISK
22355  REM
22357  IF O$ = "T" THEN SN$ = "T" + SN$
22360  PRINT D$;"APPEND ";SN$;",D2"
22380  PRINT D$;"WRITE ";SN$
22400  FOR D = 1 TO 75
22415  IF FR$(1,D) = "ZERO" THEN  GOTO 22450
22420  IF O$ = "E" THEN  PRINT FR$(1,D); SPC( 1);FR$(2,D); SPC( 1);FR$(3,D);SPC( 1);FR$(4,D)
22425  IF O$ = "T" AND D = 1 THEN  PRINT FR$(1,D): GOTO 22440
22430  IF O$ = "T" THEN  PRINT FR$(1,D); SPC( 6 -  LEN (FR$(1,D)));FR$(2,D);SPC( 1);FR$(3,D); SPC( 1);FR$(4,D); SPC( 1);FR$(5,D)
22440  NEXT D
22450  REM
22460  PRINT D$;"CLOSE ";SN$
22465  PRINT D$;"APPEND ";"GETBACK";",D1"
22470  PRINT D$;"CLOSE ";"GETBACK"
22500  RETURN
23000  REM **GET WEIGHT FROM METTLER
```

APPENDIX III (Continued)

```
23010  REM  SLOT 2
23050  PRINT D$;"IN#2"
23100  PRINT D$;"PR#2"
23120  PRINT  CHR$ (1);"E D"
23130  REM
23140  PRINT  CHR$ (1);"F D"
23180  INPUT A$
23200 A1$ =  LEFT$ (A$,1)
23220 A2$ =  MID$ (A$,2,1)
23240  IF A1$ = "S" AND A2$ = " " THEN WT$ =  MID$ (A$,4,9):WT =  VAL (WT$)
23260  IF A2$ = "D" THEN  GOTO 23120
23265  IF WT = 0.0 THEN  GOTO 23120
23267 S = S + 1
23269 MC = 100 - 100 * (WO - 37.834) * (1 - GM / 100) / (WT - 37.834)
23270  IF O$ = "E" THEN MF = MC: GOTO 23275
23271  IF S = 1 THEN MF = MC: GOTO 23275
23273 MF = MC - (12 / 31) * (ML - MC)
23275 X = MF:DP = 2: GOSUB 17000:MF$ = AA$
23276 X = MC:DP = 2: GOSUB 17000:MC$ = AA$
23277 ML = MC
23280  REM :PRINT D$;"IN#0"
23290  PRINT D$;"PR#0"
23295  PRINT MF; SPC( 2);MC
23300  RETURN
23500  REM **GET TEMP FROM FLUKE
23550 TS = OP(9): GOSUB 27500
23600 XS = 0: CALL MM(51)
23620  FOR I = 1 TO 5
23640 X =  PEEK (MM(40 + I))
23660 XS = XS * 10 + X * 0.1
23680  NEXT I
23700 TP = XS
23710 X = TP:DP = 1: GOSUB 17000:TP$ = AA$
23720  RETURN
24000  REM **RAISE PROBES
24100  POKE MM(37),OP(11): CALL MM(48)
24110  RETURN
24500  REM **LOWER PROBES
24600  POKE MM(37),OP(11): CALL MM(47)
24610  RETURN
25000  REM **TURN FAN ON
25100  CALL MM(49)
25110  RETURN
25500  REM **TURN FAN OFF
25600  CALL MM(50)
25610  RETURN
27000  REM **GET TIME
27010 P =  PEEK ( - 16384): POKE  - 16368,0: REM    CHECK FOR PANIC BUTTON
27011  IF P = 208 THEN  GOTO 16000
27020 SL = 7
27040  PRINT D$;"IN#";SL
27060  PRINT D$;"PR#";SL
27080  INPUT ":";CL$
27100  PRINT D$;"IN#0"
27120  PRINT D$;"PR#0"
27140  RETURN
27500  REM  **TIME DELAY
27520  GOSUB 27000:XS$ =  RIGHT$ (CL$,2):XM$ =  MID$ (CL$,15,2):XH$ + MID$ (CL$,12,2):XD$ = MID$ (CL$,6,2)
27530 XS =  VAL (XS$):XM =  VAL (XM$):XH =  VAL (XH$):XD =  VAL (XD$)
27540 XT = XD * 24 * 60 ^ 2 + XH * 60 ^ 2 + XM * 60 + XS
27560  GOSUB 27000:YS$ =  RIGHT$ (CL$,2):YM$ =  MID$ (CL$,15,2):YH$ = MID$ (CL$,12,2):YD$ = MID$ (CL$,6,2)
27570 YS =  VAL (YS$):YM =  VAL (YM$):YD =  VAL (YD$):YH =  VAL (YH$)
27580 YT = YD * 24 * 60 ^ 2 + YH * 60 ^ 2 + YM * 60 + YS
27590  IF (YT - XT) < TS THEN  GOTO 27560
27600  RETURN
32000  REM  **********
32020  REM  ON LINE RECORD LOOP
32100 I = 1:ER = 0
32120 OF = 0: GOSUB 11500
32130  CALL MM(6): REM TAKE SIGNALS
32140  GOSUB 2000: REM   CALC OFFSET
32160  CALL MM(24): REM PLOTBOTH
32180  IF P = 208 THEN OM = OH(TT):RJ = 1: GOSUB 15200
```

APPENDIX III (Continued)

```
32200  IF ER = 1 THEN ER = 0: RETURN
32220  IF RJ = 1 THEN RJ = 0: GOTO 32120
32230 VE = DE / (DWELL * NQ):V2 = VE ^ 2
32240 VE =  INT (VE * 1000 + 0.5) / 1000:V2 =  INT (V2 * 1000 + 0.5) / 1000
32245 R = V2 / VO
32247 X = R:DP = 3: GOSUB 17000:R$ = AA$
32250 WL =  PEEK (MM(15)) * 256 +  PEEK (MM(14))
32260  GOSUB 33550
32263 E = E + 1
32265  IF O$ = "T" THEN FR$(1,E) = CL$:FR$(2,E) = R$:FR$(3,E) = TP$:FR$(4,E) + MF$:FR$(5,E) = MC$
32275  PRINT : PRINT "VELOCITY = ";VE: PRINT E
32280 I = I + 1
32282 HO =  PEEK ( - 16384): POKE  - 16368,0: REM   CHECK FOR HOLD
32284  IF P = 200 THEN  GOSUB 11000:HO = 0
32286  IF HO = 200 THEN  GOSUB 11000
32320  RETURN
33000  REM  **********
33010  REM  WRITE ON LINE HEADINGS
33020  POKE 33,33: REM
33030  PRINT D$;"PR#1"
33050  PRINT "OPERATOR : ";NA$
33070  PRINT : PRINT "SAMPLE : ";SN$
33080  IF O$ = "E" THEN  PRINT : PRINT  SPC( 10);"TIME"; SPC( 10);"R";SPC( 6);"MOIST.";SPC( 4);"TEMP"; SPC( 3);"SIG AV": PRINT
33085  IF O$ = "T" THEN  PRINT : PRINT "TIME"; SPC( 3);"R"; SPC( 6);"MOIST.";SPC( 4);"TEMP" SPC( 3);"SIG AV" :PRINT
33090  PRINT D$;"PR#0": POKE 33,40
33100  RETURN
33550  REM   ** WRITE RESULTS FIRST TIME
33560  POKE 33,33
33565  IF O$ = "T" THEN CL$ = TI$
33570  PRINT : PRINT D$;"PR#1"
33580  PRINT  SPC( 1);CL$; SPC( 2);R$; SPC( 5);MF$; SPC( 4);TP$; SPC( 5);AS
33590  PRINT D$;"PR#0"
33600  RETURN
38000  REM **COLLECT DATA
38020 P =  PEEK ( - 16384): POKE  - 16368,0: IF P = 208 THEN ER = 1: RETURN
38060 R = 0:WT = 0:TP = 0
38100  IF OP(6) = 0 THEN  GOTO 38300
38120  GOSUB 23500
38300  IF OP(5) = 0 THEN  GOTO 38390
38320  GOSUB 25500
38340 TS = OP(8): GOSUB 27500
38360  GOSUB 23000
38380  IF ER = 1 THEN  GOSUB 5000
38390  IF OP(4) = 0 THEN R$ = "99": GOTO 61000
38400  IF O$ = "E" THEN  GOTO 38526
38420 J = 1:TS = 0
38425  IF K = 1 THEN  GOSUB 27500:FT = XT:TI$ = CL$
38450  IF K > 1 THEN  GOSUB 27560:TI$ =  STR$ (YT - FT)
38510  IF OP(12) = 1 THEN  GOSUB 24500: GOSUB 25000:TS = OP(7): GOSUB 27500
38520  IF OP(12) = 0 THEN  GOSUB 25000:TS = OP(7): GOSUB 27500
38525  GOSUB 32000: GOTO 38530
38526  IF OP(12) = 1 THEN  GOSUB 24500: GOSUB 25000:TS = OP(7): GOSUB 27500:GOSUB 27000: GOSUB 32000
38527  IF OP(12) = 0 THEN  GOSUB 25000:TS = OP(7): GOSUB 27500: GOSUB 27000:GOSUB 32000
38528  IF O = 0 THEN  GOSUB 60000
38530  IF ER = 1 THEN  RETURN
38550  IF OP(12) = 1 THEN  GOSUB 24000: RETURN
38560  IF OP(12) = 0 THEN  RETURN
38600  GOSUB 25000:TS = OP(7): GOSUB 27500: RETURN
40000  REM  **********
40010  REM  VARIABLE INITIALIZATION
40030  DIM FR$(5,75)
40040  DIM OH(4),OP(13),MM(51)
40100 MTEST = 0:IN = 0:OM = 45:CD = 0
40110 DI = 0:RIGHT = 0:LEFT = 0:OF = 0
40115 T5 = 256:VO = 1.0:
40120 ZERO = 0:O1 = 1:C = 0:TWO = 2
40140 V2 = 0::VE = 0
40170  GOSUB 41000
40260 D$ =  CHR$ (4)
40270  PRINT D$;"BLOAD GRAPH5/A$1000,A$1000"
40280  PRINT D$;"BLOAD SOURCE11/A$1200,A$1200"
40290  PRINT D$;"BLOAD AVERAGE6/A$1600,A$1600"
40292  PRINT D$;"BLOAD BOX4/A$1C00,A$1C00"
```

APPENDIX III (Continued)

```
40300  GOSUB 42000: REM SET TEST PARAMS
40320  PRINT "TURN ON PRINTER"
40330  PRINT : PRINT D$;"PR#1": PRINT
40340  PRINT D$;"PR#0":FF = 2
40400  POKE MM(1),128: REM SET AUTOFIND TO AUTOMATIC  WINDOW FIND
40420 ZF = 0: HCOLOR= 3
40430  GOSUB 42500: REM  INIT OFFSETS
40440  CALL MM(46): REM INIT BOX
40450  RETURN
41000  REM  ***** INIT MACHINE LANGUAGE POINTERS
41110 MM(1) = 772: REM $0304 AUTOFIND
41120 MM(2) = 769: REM $0301 AV
41130 MM(3) = 770: REM $0302 AVWINDOL
41140 MM(4) = 771: REM $0303 AVWINDOH
41150 MM(5) = 5641: REM $1609 CHECKOUT
41160 MM(6) = 5635: REM $1603 CONTROL2
41170 MM(7) = 5632: REM $1600 CONTROL1
41180 MM(8) = 4608: REM $1200 CROSCOR
41190 MM(9) = 0
41200 MM(10) = 0
41210 MM(11) = 0
41220 MM(12) = 782: REM $030E LOOFFSET
41230 MM(13) = 783: REM $030F HIOFFSET
41240 MM(14) = 780: REM $030C LOWINDOW
41250 MM(15) = 781: REM $030D HIWINDOW
41260 MM(16) = 0
41270 MM(17) = 792: REM $318 STEP COUNT
41280 MM(18) = 0
41290 MM(19) = 784: REM $0310 LOWSUM
41300 MM(20) = 785: REM $0311 LOWSUM1
41310 MM(21) = 786: REM $0312 LOWSUM2
41320 MM(22) = 787: REM $0313 LOWSUM3
41330 MM(23) = 0
41340 MM(24) = 4096: REM $1000 PLOTBOTH
41350 MM(25) = 0
41360 MM(26) = 0
41370 MM(27) = 0
41380 MM(28) = 0
41390 MM(29) = 0
41400 MM(30) = 0
41410 MM(31) = 0
41420 MM(32) = 4108: REM $100C WINLINE
41430 MM(33) = 0
41440 MM(34) = 0
41450 MM(35) = 790: REM $316 BASESPN1
41460 MM(36) = 0
41470 MM(37) = 792: REM $318 STEPPER COUNT
41480 MM(38) = 0
41490 MM(39) = 0
41500 MM(40) = 0
41510 MM(41) = 784: REM $310 FLUKE 1MSD
41520 MM(42) = 785: REM $311 FLUKE 2MSD
41530 MM(43) = 786: REM $312 FLUKE 3MSD
41540 MM(44) = 787: REM   $313 FLUKE 4MSD
41550 MM(45) = 788: REM   $314 FLUKE 5MSD
41560 MM(46) = 7168: REM $1C00 INIT BOX
41570 MM(47) = 7171: REM $1C03 STEPCLOCK
41580 MM(48) = 7174: REM $1C06 STEPCOUN
41590 MM(49) = 7177: REM $1C09 TFANON
41600 MM(50) = 7180: REM $1C0C TFANOFF
41610 MM(51) = 7183: REM $1C0F FLUKE
41615  RETURN
41620  FOR C = 1 TO 5
41640  FOR D = 1 TO 75
41660 FR$(C,D) = "ZERO"
41680  NEXT D
41700  NEXT C
41710 D = 0
41720  RETURN
42000  REM **SET TEST DEFAULTS
42100 DWELL = .2
42120 AS = 25:AL = 300: GOSUB 10820: REM  SIG AV
42160 S1 = 28.0:S2 = 59.7: REM  SET SPANS
```

APPENDIX III (Continued)

```
42180 D1 = S1:D2 = S2: REM SAVE DEFAULTS
42190 DE = S2 - S1
42210 OP(1) = .020: REM  R TOL
42220 OP(2) = 1.0: REM  T TOL
42230 OP(3) = .100: REM  M TOL
42240 OP(4) = 1: REM TAKE VEL IF 1
42250 OP(5) = 1: REM TAKE WT IF 1
42260 OP(6) = 1: REM TAKE TEMP IF 1
42270 OP(7) = 3: REM  VELOCITY WAIT AFTER FAN ON
42280 OP(8) = 4: REM      WT WAIT AFTER FANOFF
42300 OP(10) = 5: REM  SAMPLES PER REGRESSION
42305 OP(12) = 0: REM   RAISE AND LOWER PROBES IF 1
42310 OP(11) = 50: REM  STEPPER COUNT
42330 OP(13) = 0: REM  EQUIL WAIT
42400  RETURN
42500  REM ****RESET INITIAL OFFSETS
42530 OH(1) = 45
42540 OH(2) = 65
42550 OH(3) = 94
42560 OH(4) = 94
42570  RETURN
43000  REM **ENTER V0^2
43100  HOME : PRINT "ENTER V0 SQUARED": PRINT
43110  INPUT V0
43120  RETURN
43500  REM **NUM REPS FOR REGRESSION
43510  HOME : PRINT "CURRENT NUMBER OF REPS FOR REGRESSION IS ";OP(10)
43520  PRINT : PRINT "ENTER NEW VALUE": PRINT
43540  INPUT OP(10)
43550  RETURN
44000  REM **SPECIFY MEASUREMENTS
44100  HOME : PRINT "DO YOU WANT R?"
44120  PRINT "": GET A$
44140 OP(4) = 0: IF  LEFT$ (A$,1) = "Y" THEN OP(4) = 1
44180  HOME : PRINT "DO YOU WANT WEIGHT?"
44200  PRINT "": GET A$
44220 OP(5) = 0: IF  LEFT$ (A$,1) = "Y" THEN OP(5) = 1
44260  HOME : PRINT "DO YOU WANT TEMPERATURE?"
44280  PRINT "": GET A$
44300 OP(6) = 0: IF  LEFT$ (A$,1) = "Y" THEN OP(6) = 1
44400  RETURN
44500  REM **VEL TOLERANCE
44600  HOME : PRINT "CURRENT VELOCITY TOLERANCE IS ";OP(1)
44610  PRINT : INPUT "ENTER NEW VALUE ";OP(1)
44620  RETURN
45000  REM **TEMP TOL
45100  HOME : PRINT "CURRENT TEMP TOLERANCE IS ";OP(2)
45110  PRINT : INPUT "ENTER NEW VALUE";OP(2)
45130  RETURN
45500  REM **WEIGHT TOL
45600  HOME : PRINT "CURRENT WEIGHT TOLERANCE IS ";OP(3)
45610  PRINT : INPUT "ENTER NEW VALUE";OP(3)
45630  RETURN
46000  REM **CHANGE TOLERANCES
46100  HOME : HTAB (10): PRINT "TOLERANCE MENU": PRINT
46120  HTAB (4): PRINT "1. CHANGE VEL TOL"
46140  HTAB (4): PRINT "2. CHANGE TEMP TOL"
46160  HTAB (4): PRINT "3. CHANGE WT TOL"
46180  HTAB (4): PRINT "4. EXIT"
46200  PRINT : HTAB (4): INPUT "ENTER YOUR CHOICE";CH
46220  IF CH = 1 THEN  GOSUB 44500
46240  IF CH = 2 THEN  GOSUB 45000
46260  IF CH = 3 THEN  GOSUB 45500
46280  IF CH = 4 THEN  RETURN
46300  GOTO 46100
46310  RETURN
47000  REM **CHANGE DELAYS
47100  HOME : HTAB (10): PRINT "DELAY MENU": PRINT
47120  HTAB (4): PRINT "1. VEL DELAY AFTER FAN ON"
47140  HTAB (4): PRINT "2. WT DELAY AFTER FAN OFF,PROBES UP"
47165  HTAB (4): PRINT "3. TIME BETWEEN RUNS"
47170  HTAB (4): PRINT "4. EXIT"
47180  PRINT : HTAB (4): INPUT "ENTER YOUR CHOICE";CH
```

APPENDIX III (Continued)

```
47200  IF CH = 1 THEN  GOSUB 47500
47220  IF CH = 2 THEN  GOSUB 48000
47240  IF CH = 3 THEN  GOSUB 50000
47250  IF CH = 4 THEN  RETURN
47280  GOTO 47100
47300  RETURN
47500  REM **VEL DELAY
47520  HOME : PRINT "CURRENT VEL DELAY AFTER PROBES DOWN = ";OP(7)
47530  INPUT "ENTER NEW DELAY";OP(7)
47540  RETURN
48000  REM **WT DELAY
48020  HOME : PRINT "CURRENT WT DELAY AFTER PROBES OFF,FAN OFF = ";OP(8)
48040  INPUT "ENTER NEW DELAY ";OP(8)
48060  RETURN
48800  REM **STEPPER TRAVEL
48810  HOME : PRINT "CURRENT STEPPER TRAVEL = ";OP(11)
48820  INPUT "ENTER NEW VALUE ";OP(11)
48840  RETURN
49000  REM   **WEIGHING AN IDENTICAL SAMPLE
49100  HOME : PRINT "DO YOU WANT TRANSDUCERS RAISED AND LOWERED?"
49200  PRINT "": GET A$
49300 OP(12) = 1: IF  LEFT$ (A$,1) = "N" THEN OP(12) = 0
49500  RETURN
50000  REM  **EQUILIBRIUM DELAY
50010  HOME : PRINT "CURRENT TIME TO REACH EQUILIBRIUM = ";OP(13)
50020  INPUT "ENTER NEW TIME ";OP(13)
50030  RETURN
53000  REM  **INPUT ORIGINAL MOISTURE AND WEIGHT OF SAMPLE
53010  HOME : PRINT "ENTER THE ORIGINAL MOISTURE CONTENT"
53020  INPUT GM
53030  PRINT "ENTER THE ORIGINAL SAMPLE WEIGHT"
53040  INPUT WO
53050  RETURN
54000  REM  ** TRANSIENT DATA LOGGER
54020 NT = OP(10):ER = 0:RJ = 0
54040  GOSUB 25000
54060  GOSUB 9000
54080  GOSUB 33000
54100 TS = OP(13): GOSUB 27500
54110 R1 = 0:R2 = 0:R3 = 0:T1 = 0:T2 = 00:T3 = 0:W1 = 0:W2 = 0:W3 = 0
54120  FOR K = 1 TO NT
54130  GOSUB 38000
54145  NEXT K
54147  IF O$ = "T" THEN CH = 5: GOTO 5555
54150  PRINT D$;"PR#1"
54160  PRINT : PRINT  SPC( 5);"R =   ";AR$;" +- ";SR$
54170  PRINT  SPC( 2);"TEMP = ";TA$;" +- ";ST$
54180  PRINT "MOIST. =  ";AW$;" +- ";SW$: PRINT : PRINT : PRINT
54195  PRINT D$;"PR#0"
54200  IF SR > OP(1) OR ST > OP(2) OR SW > OP(3) THEN  GOTO 54110
55000  REM  ****CREATING DATA FOR STORAGE ON DISK
55100 D = D + 1
55105  PRINT D
55110 FR$(1,D) = CL$:FR$(2,D) = AR$:FR$(3,D) = TA$:FR$(4,D) = AW$
55120  IF D > 40 THEN OP(13) = 3600
55130  IF D > 60 THEN OP(13) = 7200
55140  IF D > 70 THEN OP(13) = 21600
55200  GOTO 54100
60000  REM  **TRANSIENT STATS
60020 R1 = R1 + R ^ 2:R2 = R2 + R:R3 = R2 ^ 2
60025 T1 = T1 + TP ^ 2:T2 = T2 + TP:T3 = T2 ^ 2
60030 W1 = W1 + MC ^ 2:W2 = W2 + MC:W3 = W2 ^ 2
60035 SR = ( ABS (R1 - R3 / NT) / (NT - 1)) ^ .5:AR = R2 / NT
60040 ST = ( ABS (T1 - T3 / NT) / (NT - 1)) ^ .5:TA = T2 / NT
60045 SW = ( ABS (W1 - W3 / NT) / (NT - 1)) ^ .5:AW = W2 / NT
60050 X = AR:DP = 3: GOSUB 17000:AR$ = AA$
60060 X = SR:DP = 3: GOSUB 17000:SR$ = AA$
60070 X = AW:DP = 3: GOSUB 17000:AW$ = AA$
60080 X = SW:DP = 3: GOSUB 17000:SW$ = AA$
60090 X = ST:DP = 3: GOSUB 17000:ST$ = AA$
60100 X = TA:DP = 3: GOSUB 17000:TA$ = AA$
60110 TP = 0:WT = 0:MC = 0
60200  RETURN
```

APPENDIX III (Continued)

```
61000  IF O$ = "E" THEN  GOSUB 27000: GOSUB 60000: GOSUB 38600: RETURN
61010 J = 1:TS = 0
61012  IF K = 1 THEN  GOSUB 27500:FT = XT
61014  IF K > 1 THEN  GOSUB 27560:CL$ =  STR$ (YT - FT)
61020 E = E + 1:FR$(1,E) = CL$:FR$(2,E) = R$:FR$(3,E) = TP$:FR$(4,E) = MF$:FR$(5,E) = MC$
61040  GOSUB 38600: RETURN
```

APPENDIX IV

INSTRON PROGRAM

This program also uses menus to prompt the user for the required input parameters. The quality of the stress-strain loop can be seen by using the checkout(1) option located in the main menu section. Several parameters can be adjusted within this option to obtain the desired loop shape. Once the loop is deemed satisfactory, a transient run can be started by choosing option 1, do_test, located in the main menu.

```
PROGRAM bern1;
{$R+ }

{$I d:typedef.mod }
{$I d:graphix.sys }  (* call this e:graphix.sys when not compiling on epson *)
{$I d:kernel.mod }

  CONST
    max_screen_fields = 30;
    max_reps = 30;
    max_error_code=30;
    max_time_intervals =  10000;
    max_buffer =  10000;
    max_sorbtion_points = 20;
    disk_io_trigger = 9;
    board = 0;
    dma_level = 1;
    int_level = 2;
    base_adr = $300;


  TYPE
    stringtype = string[80];
    bufftype   = array[1..max_screen_fields] of stringtype;
    codetype   = array[1..max_error_code] of boolean;
    sampletype = RECORD
                   samplename       : stringtype;
                   seriesname       : stringtype;
                   length           : real;
                   basis_weight     : real;
                   width            : real;
                   fs_load          : real;
                   fs_strain        : real;
                   crosshead_speed  : real;
                   est_elongation   : real;
                   total_crosshead_cycles      : integer;
                   total_sorbtion_points     :integer;
                   gain             : real;
                   points_per_cycle : integer;
                   count            : integer;
                   rate             : integer;
                   save_to_disk     : char;
                 END;

    resultstype = RECORD
                    start_time:real;
                    time_elapsed_since_start:real;
                    first_low_point_location:integer;
```

APPENDIX IV (Continued)

```
                    test_cycle_start_time:real;
                    test_cycle_end_time:real;
                    sampletime      : stringtype;
                    sampledate      : stringtype;
                    time_mid        : array[0..max_sorbtion_points] of real;
                    modulus         : array[0..max_sorbtion_points] of real;
                    loss_tan        : array[0..max_sorbtion_points] of real;
                    freq            : array[0..max_sorbtion_points] of real;
                    e_mid           : array[0..max_sorbtion_points] of real;
                    e_delta         : array[0..max_sorbtion_points] of real;
                  END;

{$I tdash16.mod }
(* {$I fakedash.pas }  *)


  VAR
    drivename:stringtype;
    displayname:stringtype;
    data_drivename:stringtype;
    error_code:codetype;
       scrbuffer:bufftype;
    hold_scrbuffer:bufftype;
    sampleparms:sampletype;
    results:resultstype;
    rawdata:long_int_vector;
    sorbtion_point:integer;
    abort:boolean;


{$I d:video4.pas}
{$I d:doscrn4.pas}
{$I d:domenu4.pas}
{$I d:aux4.pas }
{$I d:date.pas }
{$I d:time.pas }
{$I d:timer.pas }
{$I getdata1.pas }
{$I output1.pas }
{$I parm1.pas }


(*****************************************************************************)
(* crunch_data                                                               *)
(*                                                                           *)
(*****************************************************************************)
 PROCEDURE crunch_data(var abort:boolean);

  VAR
    stress_low,stress_high:integer;
    strain_low,strain_high:integer;
    n_pnt:integer;
    n_real:real;
    ns:integer;
    n_start:integer;
    n_last:integer;
    eh_point:integer;
    el_point:integer;
    cycle :integer;
    el : real; (* elongation at the low point in the cycle *)
    eh : real; (* elongation at the high point in the cycle *)
    ll : real; (* load at the low point in the cycle *)
    lh : real; (* load at the high point in the cycle *)
    area : real; (* area of stress strain curve  *)
    tl : real;
    th : real;
    cycle_finished :boolean;
    gmin_strain,gmax_strain:integer;
    gmin_stress,gmax_stress:integer;
    mid_point:integer;
    looking:boolean;
    i_start:integer;
```

APPENDIX IV (Continued)

```
  ipt:integer;
  high_trigger:integer;
  ratio:real;
  found:boolean;

{-------------------------------------------------------------------}
 PROCEDURE convert(var value,fullscale,gain:real;
                   a_d_range:real);
  { Converts an a/d conversion into a meaningful number.
    Value = value to be converted.
    fullscale = full scale range of the instrument amplifier
    gain = gain of a/d
    a_d_range = maximum digital value from a/d                    }
  BEGIN
    value := (value * fullscale) / (a_d_range * gain);
  END;


{-------------------------------------------------------------------------}
 FUNCTION not_enough_points(point:integer):boolean;
  BEGIN
       not_enough_points := false;
    IF point > sampleparms.count THEN
      BEGIN
        clrscr;
        write_text_in_box(6,0,0,'NOT ENOUGH DATA POINTS');
        press_space_bar_to_continue(1);
        abort := true;
        not_enough_points := true;
      END;
  END;

{-------------------------------------------------------------------}
 FUNCTION raw(point:integer):real;
  BEGIN
    raw :=  rawdata[point];
  END;

{-------------------------------------------------------------------}
 PROCEDURE start_looking(point:integer;var look:boolean);
  BEGIN
      IF(rawdata[point] > high_trigger) THEN look := true;
    END;

{-------------------------------------------------------------------}
 FUNCTION crossover(point:integer;
                    looking:boolean):boolean;

  BEGIN
    crossover := false;
    IF not looking THEN exit;
        IF (rawdata[point] < rawdata[point - 4]) and
                (rawdata[point] < mid_point) THEN crossover:= true;
    END;

 BEGIN
  i_start := 4;
  area := 0;
  el := 0;
  eh := 0;
  ll := 0;
  lh := 0;
  tl := 0;
  th := 0;
  abort := false;
  gmin_stress := 10000;
  gmax_stress := 0;
  n_pnt := i_start;
  REPEAT
    IF (rawdata[n_pnt+1] >= 4095) or
       (rawdata[n_pnt+1] <= 0   ) THEN
      BEGIN
        abort := true;
```

APPENDIX IV (Continued)

```
      exit;
    END;

  IF rawdata[n_pnt] > gmax_stress THEN
    BEGIN
      gmax_stress := rawdata[n_pnt];
      gmax_strain := rawdata[n_pnt + 1];
    END;
  IF rawdata[n_pnt] < gmin_stress THEN
    BEGIN
      gmin_stress := rawdata[n_pnt];
      gmin_strain := rawdata[n_pnt + 1];
    END;
  n_pnt := n_pnt + 2;
UNTIL n_pnt >= (sampleparms.count - 4);

mid_point := trunc( (gmax_stress + gmin_stress) / 2.0);
high_trigger := gmin_stress + trunc(0.75 * (gmax_stress - gmin_stress));

n_pnt := i_start;
found := false;
  REPEAT
  IF rawdata[n_pnt] >= high_trigger THEN
    BEGIN
      found := true;
    END;
  IF not found THEN n_pnt := n_pnt + 2;
UNTIL found;

i_start := n_pnt;
looking := true;
REPEAT
  n_pnt := n_pnt + 2;
UNTIL crossover(n_pnt,looking);
mid_point := rawdata[n_pnt];
n_start := n_pnt + 1;   (* point to strain *)
n_real := n_start;
n_pnt := n_start;


WITH sampleparms,results DO
  BEGIN
    test_cycle_start_time:=time_elapsed_since_start + n_real/(rate);
    cycle_finished := false;

    FOR cycle := 1 to total_crosshead_cycles DO
      BEGIN
        looking := false;
        REPEAT
          area := area + raw(n_pnt-1)*(raw(n_pnt)-raw(n_pnt-2));
          n_pnt := n_pnt + 2;
          IF not_enough_points(n_pnt + 2) THEN exit;
          IF not looking THEN start_looking(n_pnt+1,looking);
        UNTIL crossover(n_pnt-1,looking);
     END;

    n_last := n_pnt;
       area := area + (raw(n_start-2)-raw(n_last-2))*(mid_point);

    el := 4000;
    eh := 0;
    eh_point := 0;
    el_point := 0;


    ipt := n_start;
    REPEAT
      ipt := ipt + 2;
      IF rawdata[ipt] > eh THEN
        BEGIN
          eh_point := ipt;
          eh := rawdata[ipt];
        END;
```

APPENDIX IV (Continued)

```
          IF rawdata[ipt] < el THEN
            BEGIN
              el_point := ipt;
              el := rawdata[ipt];
            END;
        UNTIL ipt >= n_last;


        eh := (rawdata[eh_point-2]+rawdata[eh_point]+rawdata[eh_point+2])/3.0;
        lh := (rawdata[eh_point-1]+rawdata[eh_point+1])/2.0;
        el := (rawdata[el_point-2]+rawdata[el_point]+rawdata[el_point+2])/3.0;
        ll := (rawdata[el_point-1]+rawdata[el_point+1])/2.0;
        area := area / total_crosshead_cycles;

        loss_tan[sorbtion_point] :=
          4.0 * (area)/(pi * (lh-ll)*(eh-el));


        convert(lh,fs_load,gain,4095.0);
        convert(ll,fs_load,gain,4095.0);
        convert(eh,fs_strain,gain,4095.0);
             convert(el,fs_strain,gain,4095.0);

        e_mid[sorbtion_point]   := 50.0*(lh+ll)*(eh-el)/((lh-ll)*(length));
        e_delta[sorbtion_point] := 100.0 * (eh - el) / length;

        n_real :=  (n_last - n_start);
        test_cycle_end_time:=test_cycle_start_time + n_real/(rate);

        freq[sorbtion_point] :=
          total_crosshead_cycles/(test_cycle_end_time-test_cycle_start_time);
        time_mid[sorbtion_point] := test_cycle_start_time +
          (test_cycle_end_time - test_cycle_start_time) / 2.0;
        modulus[sorbtion_point] :=
          ( (lh-ll)*length)/(width*basis_weight*(eh-el));
        est_elongation   := eh - el;
        set_rate_and_count;

      END;
  END;


(*************************************************************************)
(* checkout;                                                             *)
(*                                                                       *)
(*************************************************************************)
PROCEDURE checkout(mode:integer);
  VAR
    abort :boolean;

  BEGIN
    get_parameters(abort);
    IF abort THEN exit;
    sorbtion_point := 0;
    results.time_elapsed_since_start := 0.0;
    CASE mode OF
      1: BEGIN    (* get new data and display  *)
           write_text_in_box(6,0,0,'TAKING DATA ');cursor(24,1);
           take_data(abort);
         END;
      2: BEGIN   (* read previously acquired data from disk *)
           read_dump;
           sound(200);delay(1000);nosound;
         END;
    END;
    IF abort THEN exit;
    IF not abort THEN  graph1(true);
    crunch_data(abort);
    IF abort THEN exit;
    WITH results DO
      BEGIN
        writeln(space(27),' time     = ',  time_mid[0] :10:0 );
        writeln(space(27),' modulus  = ',  modulus[0]  :10:0 );
```

APPENDIX IV (Continued)

```
      writeln(space(27),' loss_tan = ',  loss_tan[0] :10:4 );
      writeln(space(27),' freq     = ',  freq[0]     :10:4 );
      writeln(space(27),' e_mid    = ',  e_mid[0]    :10:4 );
      writeln(space(27),' e_delta  = ',  e_delta[0]  :10:4 );
    END;
  press_space_bar_to_continue(1);
  IF mode = 1 THEN dump; (* save newly acquired data to disk *)
END;


(*************************************************************************)
(* do_test                                                               *)
(*                                                                       *)
(*************************************************************************)
PROCEDURE do_test;

  VAR
    ch:char;
    spacebar,panic,abort,abort1,abort2,abort3:boolean;

 {-----------------------------------------------------------------------}
   PROCEDURE corrective_action_menu(var abort_test:boolean);
   VAR
     exit_corrective_action:boolean;
     correction_choice:integer;
     filename:stringtype;
     esc_pressed:boolean;

   BEGIN    (* procedure corrective_action_menu *)
     abort_test := false;
     exit_corrective_action := false;
     correction_choice := 1;
     WHILE not exit_corrective_action DO
       BEGIN
          filename := drivename + 'inmenu3.men';
          domenu4(correction_choice, filename);
          CASE correction_choice OF
             1: BEGIN
                  exit_corrective_action := true;
                  abort_test := false;
                END;
             2: BEGIN
                  get_parameters(esc_pressed);
                END;
             3: BEGIN
                  exit_corrective_action := true;
                  abort_test := true;
                END;
          END;
       END;

  END;     (* procedure corrective_action_menu *)

 {-----------------------------------------------------------------}
  PROCEDURE screen_template;
    CONST
      toprow=6;
      botrow=14;
      leftcol=28;
      rightcol=52;

    BEGIN
      clrscr;
      draw_text_box(toprow,leftcol,botrow,rightcol);
      cursor(toprow+2,leftcol+2);
      write('START TIME  =',results.start_time:8:0);
      cursor(toprow+3,leftcol+2);
      write('ELAPSED     =');
      cursor(toprow+4,leftcol+2);
      write('TEST POINT  =',sorbtion_point-1:8);
      cursor(toprow+5,leftcol+2);
      write('MODULUS     =',results.modulus[sorbtion_point-1]:8:0);
      cursor(toprow+6,leftcol+2);
```

APPENDIX IV (Continued)

```
    write('LOSS TAN    =',results.loss_tan[sorbtion_point-1]:8:4);
  END;


{-------------------------------------------------------------------}
 PROCEDURE get_time(var total_min:real);
  VAR
    hours,min,sec,frac:integer;
  BEGIN
    timer(hours,min,sec,frac);
    total_min := hours*3600.0 + min*60.0 + sec;
    cursor(1,1);write(hours,' ',min,' ',sec);
  END;

{-------------------------------------------------------------------}
 FUNCTION elapsed_time:real;
  VAR
    current_time:real;

  BEGIN
    get_time(current_time);
        elapsed_time := current_time - results.start_time;
  END;

{-------------------------------------------------------------------}
 PROCEDURE start_sorbtion;
  BEGIN
    clrscr;
    write_text_in_box(6,0,0,'START SORBTION ');hide_cursor;
    sound(500);delay(700);nosound;
    get_time(results.start_time);
  END;

{-------------------------------------------------------------------}
 PROCEDURE wait_for_next_test(var abort:boolean);
  VAR
    criteria : real;

  BEGIN
    abort := false;
    criteria := exp(1.0 + 0.5 * sorbtion_point);
    clrscr;
    screen_template;
    REPEAT
      IF sorbtion_point > 4 THEN
        delay(200)
      ELSE
        delay(30);
      look_for_panic(spacebar,panic);
      IF panic THEN
        BEGIN
          abort := true;
          exit;
        END;
      results.time_elapsed_since_start  := elapsed_time;
      cursor( 9,43);write(results.time_elapsed_since_start:8:0);hide_cursor;
    UNTIL results.time_elapsed_since_start > criteria;
  END;

{-------------------------------------------------------------------}
 FUNCTION do_not_continue_with_test(var found_abort, abort:boolean):boolean;
  BEGIN
    do_not_continue_with_test := false;
    look_for_panic(spacebar,panic);
    IF (not found_abort) and (not panic) THEN exit;
    corrective_action_menu(abort);
    IF abort THEN
      BEGIN
        do_not_continue_with_test := true;
      END
    ELSE
      BEGIN
        IF sampleparms.total_sorbtion_points < sorbtion_point THEN
```

APPENDIX IV (Continued)

```
            BEGIN    (* kick out if user changes points required to less *)
                     (* than you already have taken                       *)
              sampleparms.total_sorbtion_points := sorbtion_point;
              abort := true;
              do_not_continue_with_test := true;
              exit;
            END;
          screen_template;
          results.time_elapsed_since_start  := elapsed_time;
          cursor( 9,43);write(results.time_elapsed_since_start:8:0);hide_cursor;
        END;
    END;

  BEGIN
    get_parameters(abort);
    IF abort THEN exit;
    sorbtion_point := 0;
    write_text_in_box(6,0,0,'TAKING TIME ZERO DATA ');cursor(24,1);
    get_time(results.start_time);     (* need this for getting freq *)
    results.time_elapsed_since_start := elapsed_time;
    take_data(abort);
       IF abort THEN exit;
    crunch_data(abort);
    IF abort THEN exit;
    results.sampledate := date;
    results.sampletime := time;
    sorbtion_point := 1;
    look_for_panic(spacebar,abort);
    IF abort THEN exit;
    clrscr;
    write_text_in_box(6,0,0,'START IN 5 SECS ');
    delay(5000);
    start_sorbtion;
    REPEAT
      wait_for_next_test(abort1);
      IF do_not_continue_with_test(abort1,abort) THEN exit;
      results.time_elapsed_since_start  := elapsed_time;
      take_data(abort1);
      IF (not abort1) THEN crunch_data(abort2);
      abort3 := abort1 or abort2;
      IF do_not_continue_with_test(abort3, abort) THEN exit;
      IF sorbtion_point >= disk_io_trigger THEN results_to_disk;
      IF sorbtion_point >= disk_io_trigger THEN graph1(false);
      sorbtion_point := sorbtion_point + 1;

    UNTIL sorbtion_point > sampleparms.total_sorbtion_points;
    sorbtion_point := sorbtion_point - 1;
    IF sorbtion_point < disk_io_trigger THEN results_to_disk;

  END;

(*************************************************************************)
(* main_menu;                                                            *)
(*                                                                       *)
(*************************************************************************)
PROCEDURE main_menu;
  VAR
    menuchoice:integer;
    exitprogram:boolean;
    mainmenufile:stringtype;
    aborttest:boolean;

  BEGIN
    menuchoice := 2;
    exitprogram := false;
    mainmenufile := drivename + 'inmenu1.men';
    WHILE not exitprogram DO
      BEGIN
        domenu4(menuchoice,mainmenufile);
        CASE menuchoice OF
          1: do_test;
          2: checkout(1);
          3: checkout(2);
```

APPENDIX IV (Continued)

```
        4: exit;
      END;
    END;
  END;

(*****************************************************************************)
(*                                                                           *)
(* main program                                                              *)
(*                                                                           *)
(*****************************************************************************)
BEGIN

  IF paramcount > 0 THEN
    drivename := paramstr(1)
  ELSE
    drivename := 'c:';

  IF paramcount > 1 THEN
    displayname := paramstr(2)
  ELSE
    displayname := 'hgc';

    IF paramcount > 2 THEN
    data_drivename := paramstr(3).
  ELSE
    data_drivename := 'c:';

  initgraphic;delay(200);
  leavegraphic;delay(500);
  definewindow(1,0,0,xmaxglb,ymaxglb);
  set_default_params;
  init_dash(abort);
  IF not abort THEN
    BEGIN
      main_menu;
      clrscr;
    END;
END.
```

APPENDIX V

ANALYSIS OF LACK OF LOOP CLOSURE (see Fig. 62)

As previously mentioned (see Fig. 2), the parameters L and S can be used to determine the loss tangent in cyclic loading tests. Problems arise, however, when these cyclic tests are conducted under sorptive or desorptive conditions. Changes in modulus that occur as well as hygroexpansivity effects cause the shape, location, and slope of the stress-strain loop to be altered. This usually results in the loop being unclosed. In other words, the initial stress-strain value does not equal the value obtained at the completion of a load cycle. Fortunately, L and S, and hence $\tan\delta$ can be defined in such a way as to minimize the anomalous results caused by a lack of loop closure. The following relations are assumed for stress and strain:

$$\sigma(t) = \sigma_o \sin(\omega t+\delta) + \sigma_s \tag{24}$$

$$\varepsilon(t) = (\sigma_o/E_c)\sin\omega t + \sigma_s/E_s + \alpha_H t \tag{25}$$

$$E_c = E_{co}(1-\alpha_c t)$$

$$E_s = E_{so}(1-\alpha_s t)$$

where, α_c is the time rate of change of cyclic modulus, α_s is the time rate of change of static modulus, α_H is the increase in strain due to hygroexpansivity, σ_s is the static stress, σ_o is the cyclic stress amplitude, E_{co} is the initial cyclic modulus, and E_{so} is the initial static modulus. To simplify the analysis, α values are assumed to be constant within a loop.

The loss tangent obtained under transient moisture conditions is defined as $\mathrm{Tan}\delta_T$ and is again equal to $2L/\pi S$. L' is defined as an area inside the loop when going around a full cycle from t=0 to $t=2\pi$ and using the above definitions for stress and strain. Because the loop is unclosed in a transient moisture

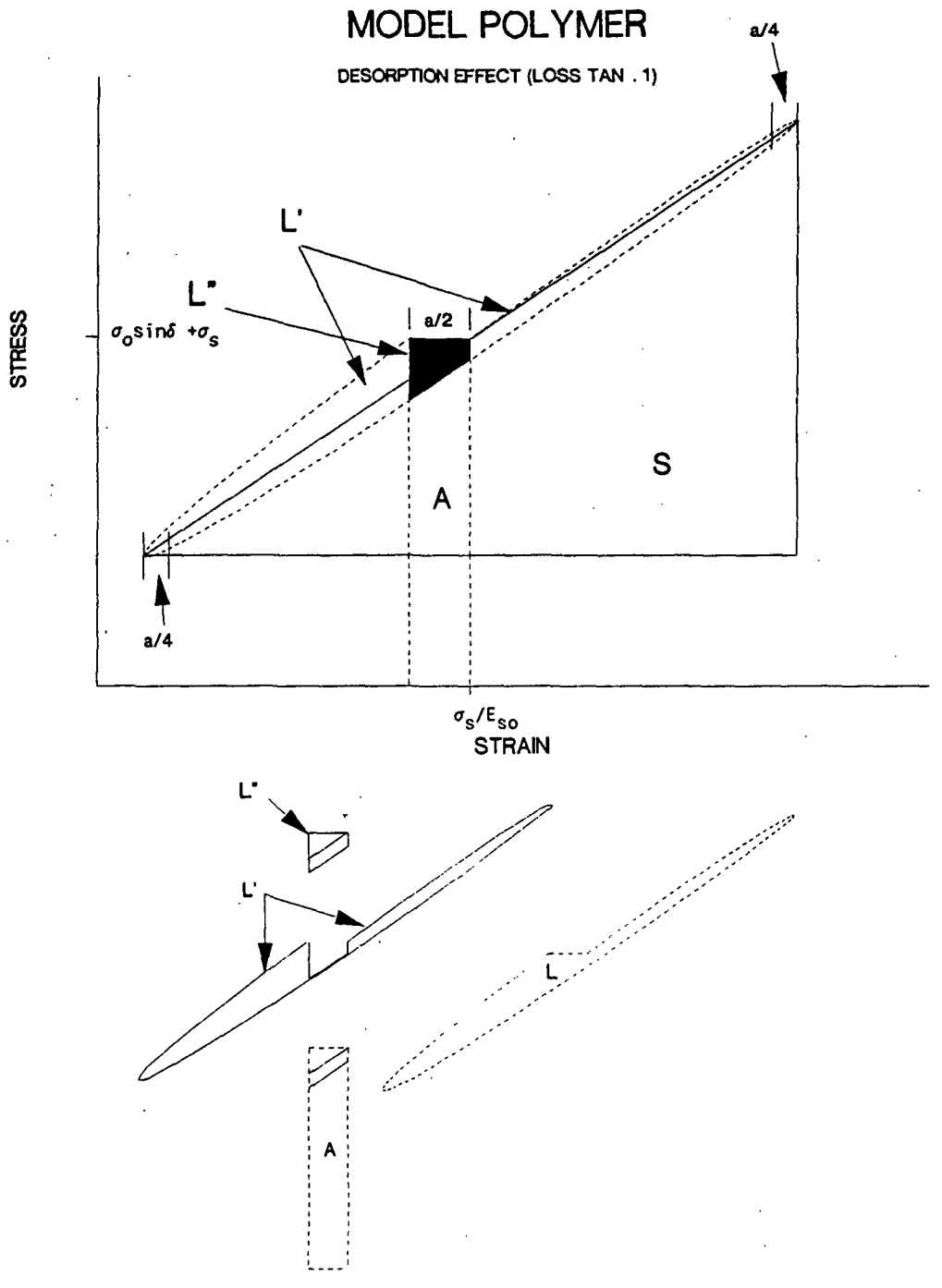

Figure 62. A model of a stress-strain cycle in a viscoelastic material loaded sinusoidally and undergoing desorption.

case, an area L" must be added to (or subtracted from) L' to close the loop and obtain L (see Fig. 62). Starting at t=0 (i.e., in the middle of the loop) simplifies the calculations. If $\alpha_c t \ll 1$ and $\alpha_s t \ll 1$ then:

$$1/[E_{co}(1-\alpha_c t)] \approx (1+\alpha_c t)/E_{co}$$

$$1/[E_{so}(1-\alpha_s t)] \approx (1+\alpha_s t)/E_{so}$$

and

$$\varepsilon(t) = (\sigma_o/E_{co})\sin\omega t(1+\alpha_c t) + (\sigma_s/E_{so})(1+\alpha_s t) + \alpha_H t$$

Taking the derivative with respect to t:

$$d\varepsilon/dt = \sigma_o\omega\cos\omega t(1+\alpha_c t)/E_{co} + \sigma_o\alpha_c\sin\omega t/E_{co} + \sigma_s\alpha_s/E_{so} + \alpha_H$$

An integration around the stress-strain loop from t=0 to $t=2\pi/\omega$ results in the area, L'-(A-L"):

$$L-(A-L") = \int_0^{2\pi/\omega} [\sigma_o\omega\cos\omega t(1+\alpha_c t)/E_{co} + \sigma_o\alpha_c\sin\omega t/E_{co} + \sigma_s\alpha_s/E_{so} + \alpha_H]\,[\sigma_o\sin(\omega t+\delta) + \sigma_s]dt$$

$$= \int_0^{2\pi/\omega} \sigma_o^2\alpha_c\omega t(\sin\omega t\cos\omega t\cos\delta + \cos^2\omega t\sin\delta)dt + (2\pi/\omega)(\sigma_o^2\alpha_c\cos\delta/2E_{co} + \sigma_o^2\omega\sin\delta/2E_{co} + \sigma_s^2\alpha_s/E_{so} + \alpha_H\sigma_s)$$

The terms in the brackets to the right of the integral sign can then be integrated by parts:

$$\int_0^{2\pi/\omega} t\sin\omega t\cos\omega t\,dt = (t\sin^2\omega t)/2\omega\Big|_0^{2\pi/\omega} - \int_0^{2\pi/\omega}[(\sin^2\omega t)/2\omega]dt = -\pi/2\omega^2$$

$$\int_0^{2\pi/\omega} t\cos^2\omega t\,dt = \int_0^{2\pi/\omega}(t/2)(1+\cos 2\omega t)dt$$

$$= \pi^2/\omega^2 + (t\sin 2\omega t)/4\omega\Big|_0^{2\pi/\omega} - \int_0^{2\pi/\omega}[(\sin 2\omega t)/4\omega]dt = \pi^2/\omega^2$$

Therefore:

$$L'-(A-L'') = -\sigma_o^2\alpha_c\pi\cos\delta/2\omega - \sigma_o^2\alpha_c\pi^2\sin\delta/\omega + (2\pi/\omega)(\sigma_o^2\alpha_c\cos\delta/2E_{co} + \sigma_o^2\omega\sin\delta/2E_{co} + \sigma_s^2\alpha_s/E_{so} + \alpha_H\sigma_s)$$

$$= (\sigma_o^2\pi/E_{co})(\sin\delta + \alpha_c\pi\sin\delta/\omega + \alpha_c\cos\delta/2\omega + 2\sigma_s^2\alpha_sE_{co}/\sigma_o^2\omega E_{so} + 2\sigma_sE_{co}\alpha_H/\sigma_o^2\omega)$$

This is the solution obtained by cycling back to the same stress. Due to the lack of loop closure, the area A in Fig. 62 has not yet been accounted for. This area is:

$$A = (\varepsilon_{t=0}-\varepsilon_{t=2\pi})(\sigma_{t=0,2\pi})$$

$$= \{\sigma_s/E_{so} - [(\sigma_s/E_{so})(1+\alpha_s 2\pi/\omega) + \alpha_H 2\pi/\omega]\}(\sigma_o\sin\delta + \sigma_s)$$

$$= (\sigma_o^2\pi/E_{co})(-2\sigma_sE_{co}\alpha_s\sin\delta/E_{so}\omega\sigma_o - 2\sigma_s^2\alpha_sE_{co}/\sigma_o^2\omega E_{so} - 2\alpha_HE_{co}\sin\delta/\sigma_o\omega - 2\sigma_s\alpha_HE_{co}/\sigma_o^2\omega$$

Adding A to the previously determined quantity, L'-(A-L'') results in:

$$L' + L'' = L = (\sigma_o^2\pi/E_{co})(\sin\delta + \alpha_c\pi\sin\delta/\omega + \alpha_c\cos\delta/2\omega - 2\sigma_sE_{co}\alpha_s\sin\delta/\sigma_o\omega E_{so} - 2E_{co}\alpha_H\sin\delta/\alpha_o\omega)$$

In paper δ is usually small and $\cos\delta >> \sin\delta$. Also, α's are assumed to be $<<$ 1. Therefore, the quantities inside the second set of brackets containing both an α parameter and a $\sin\delta$ are considered to be second order terms. If these terms are neglected:

$$L = (\sigma_o^2\pi/E_{co})(\sin\delta + \alpha_c\cos\delta/2\omega)$$

When cyclic tests are employed under transient moisture conditions the parameter, S can be defined as:

$$S = 1/2(\varepsilon_{max}-\varepsilon_{min}-a/4)(\sigma_{\varepsilon max}-\sigma_{\varepsilon min})$$

where ε_{max} occurs at approximately $t=\pi/2\omega$ and ε_{min} at $t=3\pi/2\omega$. Notice that S

contains the term a/4 which was not present in the previously defined S. The reason for including this term stems from the fact that the slope of the stress-strain loop is changing over the time period in which S is being calculated. Ideally, S should be obtained when this slope is not changing. In an equilibrium moisture situation this is the case, and S can be calculated without problems. However, the drift in ε accompanying moisture change causes S to be artificially high during desorption and low during sorption. As previously stated, α's are assumed to be constant within a cycle. Therefore, at a given stress, strain changes linearly over the time frame of a cycle. The midpoint of a cycle is approximately at a time $t=\pi/\omega$. The maximum ε is obtained at $\pi/2\omega$ before this time and ε_{min} at $\pi/2\omega$ after this time. The drift in ε over the period of one cycle is equal to a/2 (Fig. 62). The drift occurring while S is being measured is therefore a/4. By correcting for this drift, an average S can be calculated at $t=\pi/\omega$, and differences between sorption and desorption results can be eliminated:

$$
\begin{aligned}
S &= 1/2\{[\varepsilon_{max}]-[\varepsilon_{min}]-1/2[a/2]\}[(\sigma_{\varepsilon max})-(\sigma_{\varepsilon min})] \\
&= 1/2\{[(\sigma_o/E_{co})(1+\alpha_c\pi/2\omega) + (\sigma_s/E_{so})(1+\alpha_s\pi/2\omega) + \alpha_H\pi/2\omega] - \\
&\qquad [-(\sigma_o/E_{co})(1+\alpha_c 3\pi/2\omega) + (\sigma_s/E_{so})(1+\alpha_s 3\pi/2\omega) + \alpha_H 3\pi/2\omega] - \\
&\qquad [1/2[\sigma_s/E_{so} - (1+\alpha_s 2\pi/\omega)\sigma_s/E_{so} + \alpha_H 2\pi/\omega]\}[(\sigma_o\cos\delta + \sigma_s) - \\
&\qquad (-\sigma_o\cos\delta + \sigma_s)] \\
&= (2\sigma_o^2\cos\delta/E_{co})(1+\alpha_c\pi/\omega)
\end{aligned}
$$

The loss tangent can then be calculated:

$$
\begin{aligned}
\mathrm{Tan}\delta_T &= 2L/\pi S \\
&\approx (2\sigma_o^2\pi/E_{co})(\sin\delta+\alpha_c\cos\delta/2\omega)/[(\pi 2\sigma_o^2\cos\delta/E_{co})(1+\alpha_c\pi/\omega)] \\
&\approx (\tan\delta+\alpha_c/2\omega)/(1+\alpha_c\pi/\omega) \qquad (26)
\end{aligned}
$$

So a lack of loop closure causes $\tan\delta_T$ to be artificially high on sorption and low on desorption. As α_c/ω decreases, the loop closes and $\tan\delta_T \rightarrow \tan\delta$ as is expected. Notice that, σ_s, σ_o, E_{co}, E_{so}, α_s, and α_H have no effect on $\tan\delta_T$ to the first order.

In order to test the validity of Eq. (26), it was compared to the numeric approach that is outlined in Appendix IV and employed during actual cyclic tests on the Instron. Numeric data were fabricated from Eq. (24) and (25) using a total of 250 stress-strain points per cycle, this being the same number as that utilized in a typical cyclic test. Also, to be consistent with actual tests, the assumptions that $E_{co} \approx E_{so}$, $\sigma_o \approx \sigma_s$, and $\alpha_c \approx \alpha_s$ were made. In order to make reasonable comparisons, approximations for α_c and α_H must first be made. Values for α_c in samples undergoing sorption or desorption can be calculated from the slope of modulus vs. time graphs (see Fig. 44-47). However, obtaining the initial slope (α_{cmax}) can sometimes be difficult. Calculating α_H is even more difficult and requires an understanding of the moisture-length relationship as well as the rate of moisture change as a function of time. With the present test technique these data are unknown. Nevertheless, good approximations of α_c and α_H can be made using the shapes of actual data loops. Figure 63 shows the changes in the location, size, and slope of a hysteresis loop obtained from a sample undergoing desorption. Typing paper was chosen as the example because its moisture changed the most rapidly relative to other samples and its lack of loop closure was therefore the most extreme. Loops similar to those shown in this figure can also be fabricated using known values of σ_o, σ_s, E_{co}, E_{so}, and ω and assuming various values for α_c and α_H. By comparing fabricated loops to actual loops approximations of α_c and α_H can be obtained. The effects that varying α_s and α_H have on $\tan\delta_T$ can then be investigated. It was found that

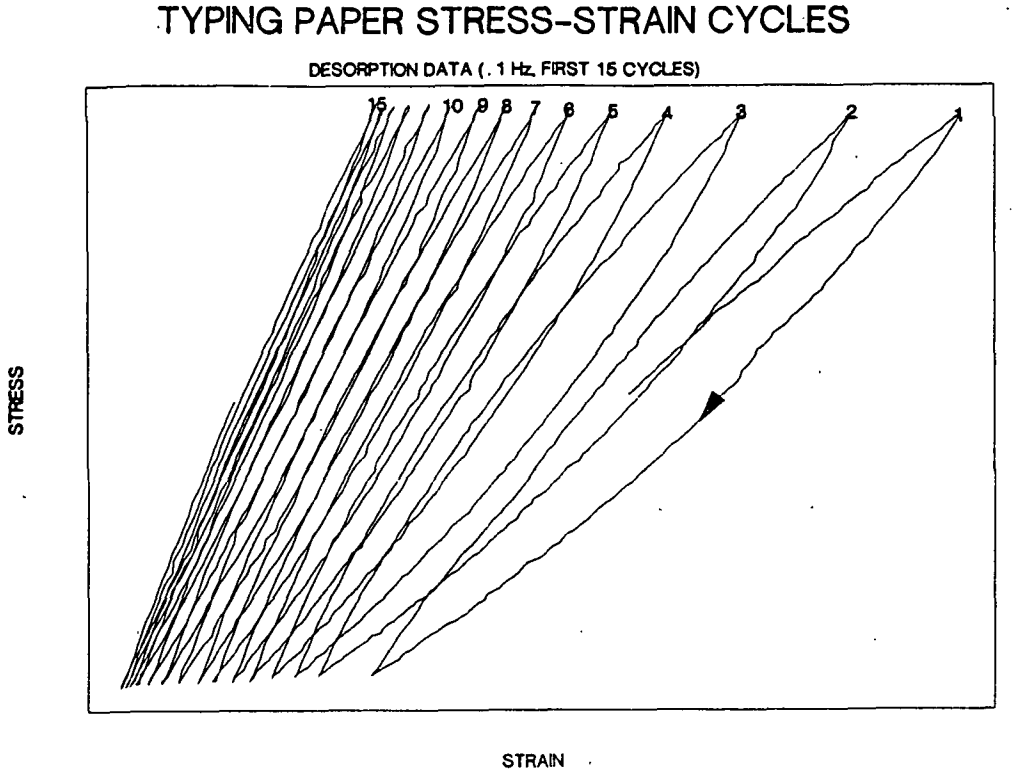

Figure 63. Actual stress-strain cycles for commercial typing paper undergoing desorption.

increases in α_S and/or α_H of over an order of magnitude caused no significant changes in the numerically calculated $\tan\delta_T$ even though extreme lack of loop closure resulted. This indicates that the simplifying assumptions made in the analytic approach were reasonable. Changes in α_c are more critical to $\tan\delta_T$ values, however. Figure 64 shows cyclic data obtained at 0.1 and 1 Hz for typing paper samples at the maximum desorption rate. As is expected, the lack of loop closure is most extreme at the lower frequency. Similar loops can be fabricated using reasonable α's as shown in Fig. 65. Sorption loops as well as $\tan\delta_T$ values calculated using the numeric and analytic methods are also shown in this figure. Notice that the lack of loop closure obtained at 0.1 Hz leads to a decrease in $\tan\delta$ of approximately 12% when measured using the numeric approach, while the more perfectly closed loop obtained at 1 Hz results in a decrease of

only 2%. Note also that the analytic approach gives even better results. Numeric results can be improved by increasing the number of data points analyzed per cycle. Considering the variability in measuring the loss tangent, lack of loop closure is certainly not an important factor in the present study if a test frequency of 1 Hz is employed. However, at lower frequencies and maximum sorption or desorption rates it can become important.

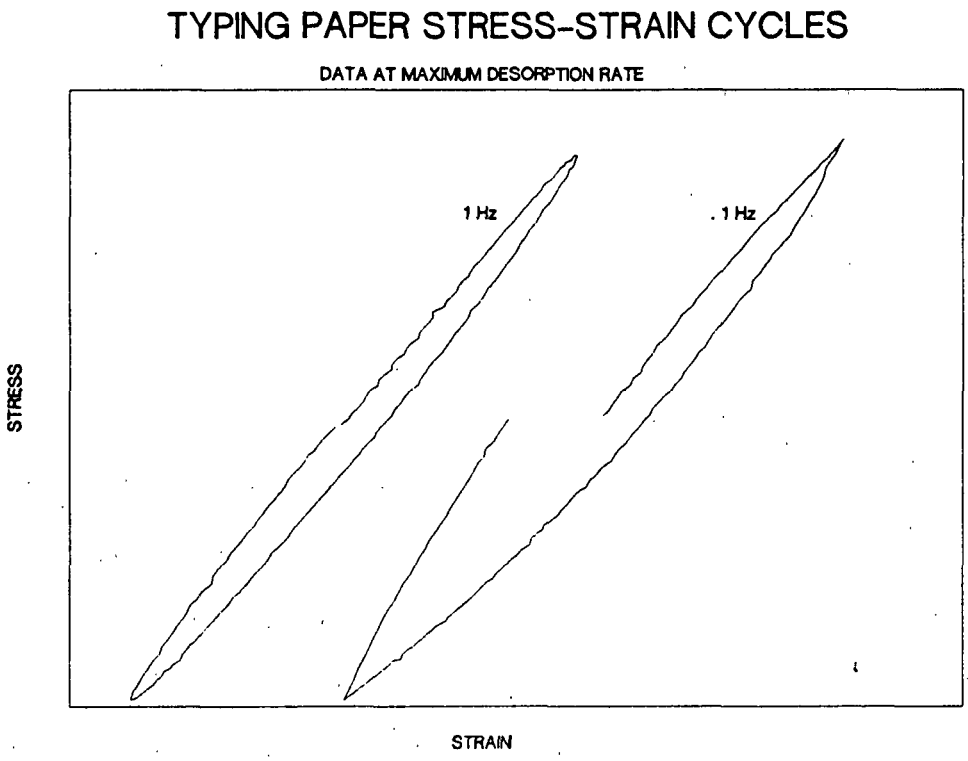

Figure 64. Typical stress-strain cycles at 0.1 and 1 Hz for commercial typing paper under maximum desorption rate conditions.

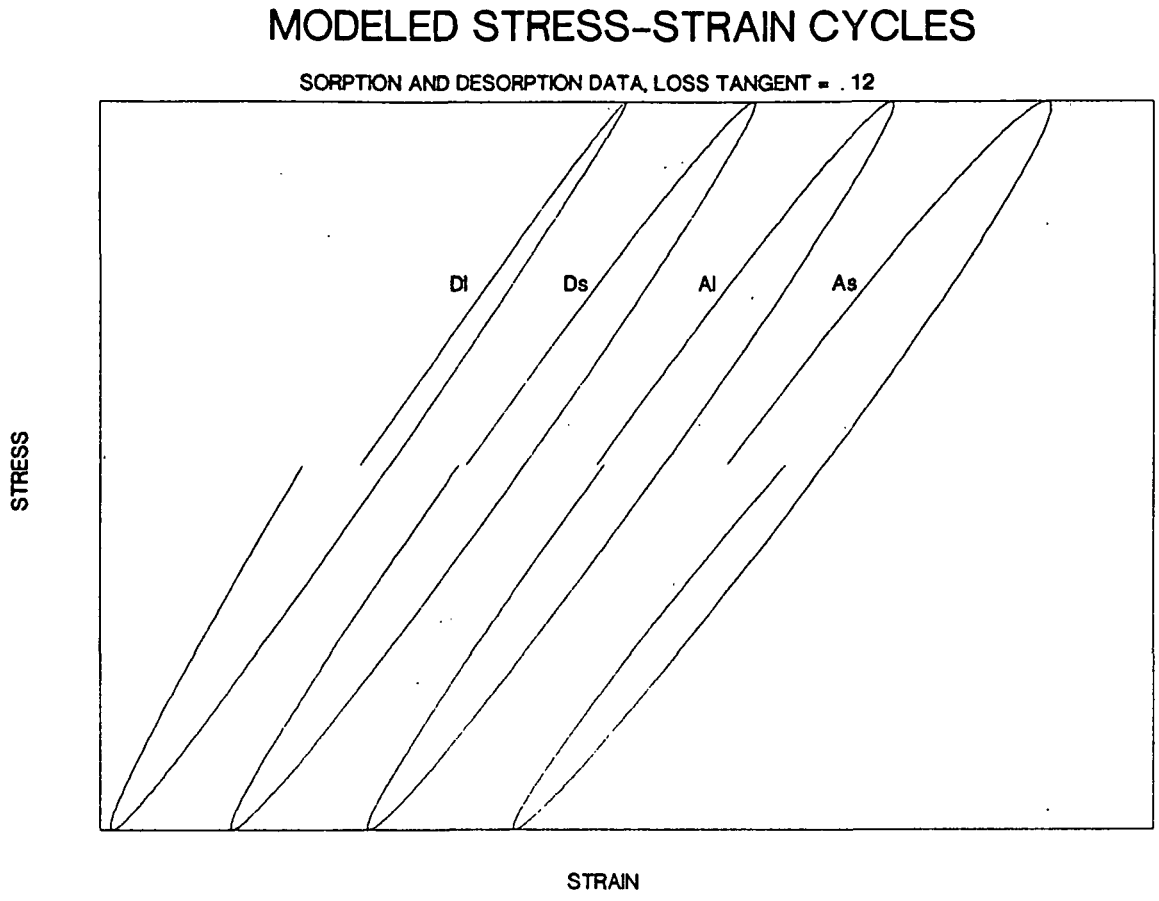

LOSS TANGENT VALUES FOR ABOVE CURVES

Curve ID	Analytic Method	Numeric Method	Actual Value	% Difference Num vs. Actual
Dl	.117	.106	.121	-12.4
Ds	.120	.118	.121	-2.1
As	.121	.121	.121	0.6
Al	.123	.131	.121	9.0

Figure 65. Modeled stress-strain cycles for various values of α_c.

APPENDIX VI

ANALYSIS OF RESPONSE TIME DIFFERENCE BETWEEN LOAD CELL AND STRAIN GAGE

Figure 66 shows changes in the loss factor as a function of frequency when measured on several brass foil strips. Notice that loss factor increases with test frequency and that this relation appears quite linear up to a frequency of around 2 Hz. At higher frequencies a slight deviation from linearity appears to occur, possibly due to the onset of inertial effects as described in Appendix VII. A least squares regression equation of the form:

$$\text{Tan}\delta = 0.0052 + 0.0173f + 0.0026f^2 \qquad (27)$$

fits the data quite nicely with an r^2 value of around 0.98. It can also be noted that the regression line doesn't pass through the origin as is expected for an elastic solid. This might be due to the slight scatter in the data, the fact that the brass strips are not completely elastic, or to some unexplained artifact of the experimental setup. In any case, the small loss tangent of 0.0052 is close to the expected value of zero.

The reason for the increase in loss factor with frequency is not known for certain, but is believed to be due to a difference in the response times of the stress and strain signals. If the dc strain signal were to lag that from the load cell by a constant amount, a linear increase in loss tangent with frequency would result. The magnitude of the loss tangent change is modeled in Fig. 67 at three different offset times. Notice the similarity between Fig. 66 and 67. The increase in loss tangent of approximately 0.02 at 1 Hz obtained from Eq. (27) would seem to indicate a response lag of just over 0.003 second in the strain signal relative to that from the load cell.

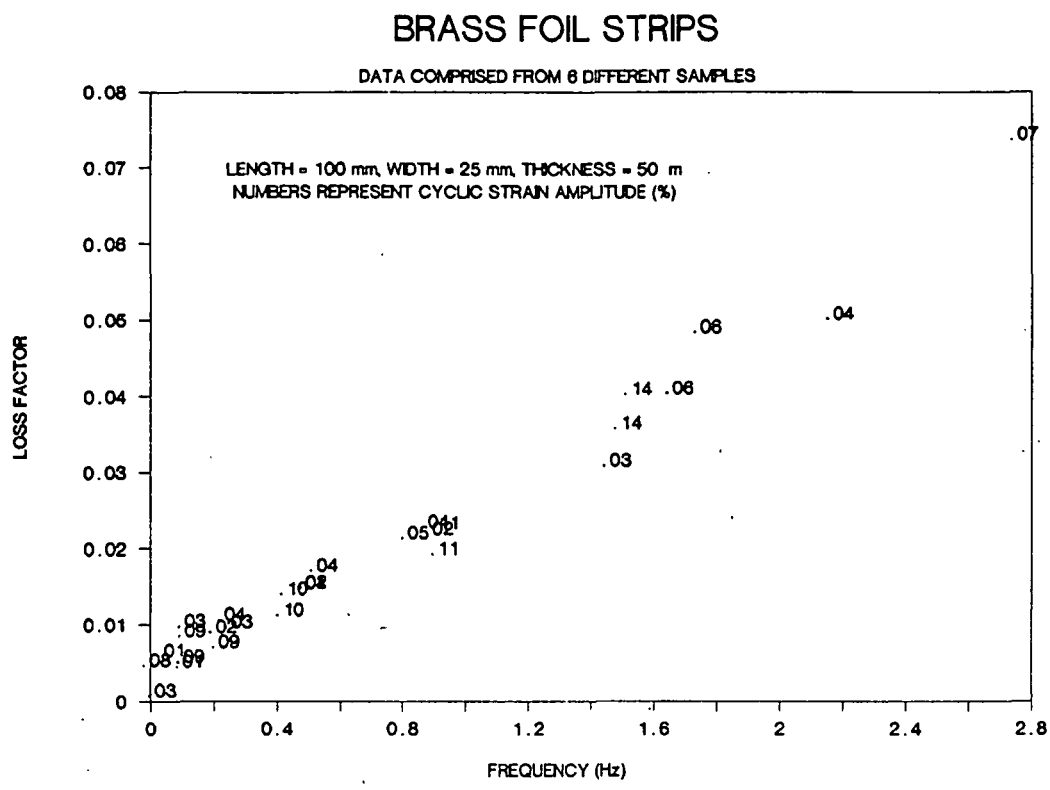

Figure 66. Loss factor-frequency data for brass foil strips.

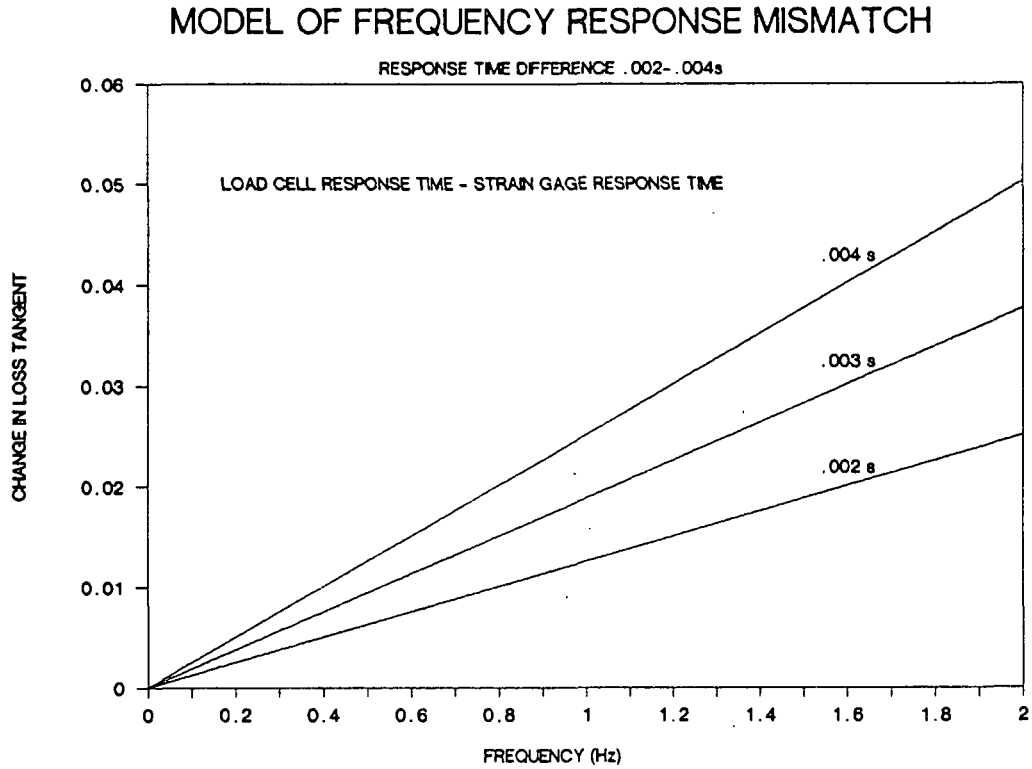

Figure 67. A model of the expected changes in loss tangent with test frequency at various load cell-strain gage frequency response mismatch values.

Figure 68 gives loss factor vs. frequency data for a commercial typing paper. Note the similar effect that frequency has on the uncorrected data in this figure and data obtained with the brass foil (Fig. 66). Figure 68 also contains data which have been corrected for frequency using Eq. (27) but neglecting the offset term:

$$\mathrm{Tan}\delta_c = \mathrm{Tan}\delta_{uc} - 0.0173f - 0.0026f^2$$

$\mathrm{Tan}\delta_c$ and $\tan\delta_{uc}$ are the corrected and uncorrected loss tangents, respectively. The offset was not used in this correction because it was felt that it might be the result of a real loss tangent in the brass. Corrected data are seen to become much more stable with frequency, with a slight decrease occurring at higher frequencies. This decrease may be due to the use of a slightly erroneous correction factor or could possibly be a real change in loss tangent with frequency. Regardless of whether the proposed explanation for the loss factor increase is valid, corrections to data at increased frequencies should be made. The empirical correction factor obtained from the brass foil strips appears to work quite well and was therefore applied to all cyclic data reported in this thesis.

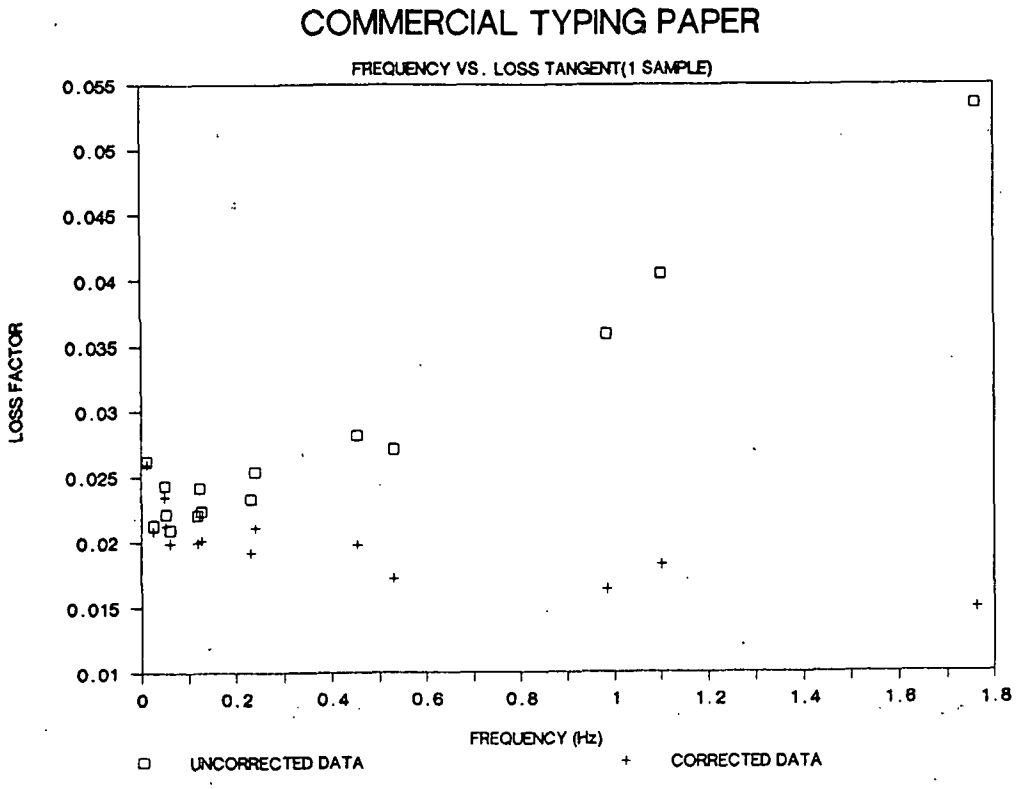

Figure 68. Loss factor-frequency data for commercial typing paper.

APPENDIX VII

ANALYSIS OF INERTIAL EFFECT WITH INSTRON

As the frequency of a cyclic test increases, the inertial effects due to the acceleration and deceleration of the clamp assembly begin to have an appreciable influence in the measured loss tangent and modulus values. The mass of the sample is insignificant compared to that of the clamp assembly and its inertial effects are ignored. The total force, F_T, on the load cell is therefore a sum consisting of the force due to the sample, F_s, and a force resulting from the inertial effects of the moving clamp assembly, F_i. If sinusoidal loading is assumed then the previously described equations for stress and strain are:

$$\varepsilon(t) = \varepsilon_o \sin\omega t, \quad \sigma(t) = \sigma_o \sin(\omega t+\delta)$$

Using sample length, l, and cross-sectional area, A, these equations can be rewritten:

$$e(t) = \varepsilon_o l \sin\omega t, \quad \sigma(t) = (F_s/A)\sin(\omega t+\delta)$$

where e(t) is the elongation in the sample as a function of time. This elongation is also a measure of the clamp assembly movement and can be differentiated twice to obtain the acceleration, a, in the clamp:

$$a(t) = -\omega^2 \varepsilon_o l \sin\omega t$$

F_i can then be calculated using this acceleration:

$$F_i = ma = -m\omega^2 \varepsilon_o l \sin\omega t$$

It is easy to show that inertial effects don't influence the energy dissipated per cycle, L:

$$L = \oint \sigma d\varepsilon = \int_0^{2\pi/\omega} [(F_s/A)(\sin\omega t\cos\delta + \cos\omega t\sin\delta) - m\omega^2\varepsilon_o l\sin\omega t/A][\omega\varepsilon_o\cos\omega t]dt$$

$$= \pi E''\varepsilon_o^2$$

Any change in loss tangent will therefore be due to changes in S. If the inertial term is accounted for, an S_i can be calculated:

$$S_i = 1/2(\varepsilon_{max} - \varepsilon_{min})(\sigma_{\varepsilon max} - \sigma_{\varepsilon min})$$

$$= 2\varepsilon_o\cos\delta(F_s - m\omega^2\varepsilon_o l)/A$$

Inertial effects therefore decrease S:

$$\% \text{ dec. in } S = 100(S - S_i)/S$$

$$= 100[2F_s\varepsilon_o\cos\delta/A - 2\varepsilon_o\cos\delta(F_s - m\omega^2\varepsilon_o l)/A]/(2F_s\varepsilon_o\cos\delta/A)$$

$$= 100m\omega^2\varepsilon_o l/F_s$$

$$= \frac{400\pi^2 l f^2}{E'A} \qquad (28)$$

Because of the relationships between S, E' and tanδ and the fact that inertia does not change L, the % decrease in S is equal to the % decrease in E' as well as the % increase in tanδ:

$$(S - S_i)/S_i = (E' - E_i')/E' = (\tan\delta_i - \tan\delta)/\tan\delta_i$$

where E_i' and $\tan\delta_i$ are the respective storage modulus and loss tangent including the inertial effects, and $\tan\delta_i$ is crosshead frequency in cycles per second.

An example of the expected effects of frequency when testing typing paper using the Instron system is as follows:

m = 2720 gms
l = 10 cm
A = 101 μm
E' = 7E10 dynes/cm^2

% Tanδ inc. (E' dec.) = 0.06% @ 1 Hz
= 1. % @ 4 Hz
= 6. % @ 10 Hz

Therefore, changes in loss tangent due to inertia in the clamps are minimal below a frequency of 4 Hz. From Eq. (28) it can be seen that inertial effects are expected to become greater as test frequency or sample length increase or as modulus or cross-sectional area become smaller. However, within the frequency, modulus, area, and length ranges covered in this study, inertial effects were insignificant. Notice that the changes in loss tangent with frequency discussed in Appendix VI are far greater than the those encountered from inertial effects.